ALTERATIONS OF FIBRONECTIN AND LAMININ AND EXPRESSION OF MATRIX METALLOPROTEINASES FOLLOWING SKELETAL MUSCLE ISCHEMIA - REPERFUSION INJURY

Bulang He

December 2002

THE THESIS SUBMITTED TO THE ADELAIDE UNIVERSITY FOR THE DEGREE OF MASTER OF SURGERY

THE WORK DESCRIBED WAS PERFORMED WITHIN THE DEPARTMENT OF SURGERY, THE QUEEN ELIZABETH HOSPITAL, THE UNIVERSITY OF ADELAIDE

CONTENTS

STATEMENT OF ORIGINALITY

This work contains no material which has been accepted for the award of any other degree or diploma in any university or other tertiary institution and, to the best of my knowledge and belief, contains no material previously published or written by another person, except where due reference has been made in the text. I give my consent to this copy of the thesis, when deposited in the Adelaide University Library, being available for loan and photocopying.

Bulang He

December 2002

ABSTRACT

Aims: To investigate alterations in fibronectin (FN) and laminin (LN) levels, and the expression of associated caseinolytic MMPs in tissues following skeletal muscle (SM) ischemia and reperfusion (I/R).

Materials and Methods: The rats were subjected to 4 h hindlimb ischemia, followed by reperfusion for 0, 4, 24 or 72 h. Two further groups was administered doxycycline before ischemia was induced. The rats were then sacrificed and samples were processed. ELISA, Immunohistochemical techniques, Zymography and Western blotting were employed.

Results: Plasma FN (pFN) decreased following hindlimb ischemia and subsequently increased with reperfusion. FN accumulated in the basement membrane (BM) of SM, whereas degradation occurred in the lungs and kidneys after SM I/R. FN decreased in the liver after SM ischemia and then increased with reperfusion. However, LN was degraded in all BM. Following doxycycline treatment, levels of FN increased in lungs, kidneys, and liver. Degradation of LN was inhibited in all tissues by doxycycline. In addition, a 20 kDa caseinolytic species was identified in lung tissues, which was inhibited by EDTA and 1,10-phenanthroline, but not inhibited by PMSF. This species was down-regulated by anesthesia only and then up-regulated immediately following bilateral hindlimb I/R. An increased production of this MMP was also found after treatment of the rats with doxycycline.

Conclusions: FN has a specific affinity to injured tissue, as was mirrored by rapid depletion of pFN, which was secreted by the liver. Moreover, the degradation of FN in lungs and kidneys and LN in all BM was suggested to be due to the effects of MMPs. In addition, doxycycline reduced the degradation of FN in lungs and kidneys and LN in all tissues studied by inhibiting the activity of MMPs. However, degradation of FN was not evident in SM, because there was an over deposition of FN in SM following I/R. Furthermore, a caseinolytic MMP, rather than a serine protease, was involved in lung injury following SM I/R. Doxycycline increased the production of this MMP. Although it has not been identified, this MMP was suggested to be a lower molecular weight MMP, possibly MMP-7 or MMP-12. Further study is needed for confirmation of its identity.

ACKNOWLEDGEMENTS

This research was undertaken in the Department of Surgery, at The Queen Elizabeth Hospital, The Adelaide University, Adelaide, Australia under the guidance of Dr. Prudence A.Cowled PhD, Mr. Robert A.Fitridge, MBBS, FRACS, and Prof. Guy. Maddern, FRACS, PhD. I am indebted to all three supervisors for their patience, dedication, support and encouragement throughout my research. Mr. Fitridge and Dr Cowled contributed endless patient hours assisting me in all aspects in the laboratory work and thesis writing, for which I will always be grateful.

I would like to express my gratitude to Professor G. Maddern for his assistance of allowing me the great opportunity to undertake the research project and clinical work in the Department of Surgery at The Queen Elizabeth Hospital.

The invaluable assistance of the laboratory staff, J. Carter, Ms S. Millard, BSc, for teaching me the immunohistochemical techniques, A. Varelias, PhD, P. Laws for teaching me zymography and western blot procedures, R. Knowling for helping with ELISA analysis and statistical assistance. I am grateful for their continued support through the research project.

I would like to thank the staff of the Animal House at The Queen Elizabeth Hospital for their help and care of my animals.

Special thanks to P. Laws and D. Roach for their contributions to the establishment of the animal model and allowing me to share some groups of experimental animals.

Finally, I owe many thanks to Prof. Juzhong Gao, the president of Beijing Chaoyang Hospital, and Prof. Delin Guan, the director of Urology Institue, Capital University of Medical Sciences for their support, understanding and allowing me the time to undertake the postgraduate study overseas.

Last but not least, many thanks to my family, in particular to my wife Ying Han and my daughter Phoebee He for their understanding, love, support and patience throughout my research.

CONFERENCE PRESENTATIONS AND PUBLICATIONS

1.**B. He**, P. Cowled, R. Fitridge and G. Maddern. Alterations of fibronectin and laminin in tissues following skeletal muscle ischemia and reperfusion. Research Day, North Western Adelaide Health Service (Oct 5, 2001 oral presentation).

2 **B. He**, P.E. Laws, R. Knowling, P.A. Cowled, R.A. Fitridge. Alterations of fibronectin and laminin in the basement membrane after skeletal muscle ischemia and reperfusion. The combined meeting of The Australia & New Zealand Society for Vascular Surgery (Aug 31-Sept 4, 2002, Queensland, Australia. Poster).

3 **B. He**, P.E. Laws, R. Knowling, P.A. Cowled, R.A. Fitridge. Alterations of fibronectin and laminin in the basement membranes following skeletal muscle ischemia and reperfusion (manuscript in preparation for publication).

4. **B. He**, P.E. Laws, R. Knowling, P.A. Cowled, R.A. Fitridge. The role of MMPs in the remote lung injury following skeletal muscle ischemia and reperfusion (manuscript in preparation for publication).

TABLE OF CONTENTS

CHAPTER 1

INTRODUCTION

AND

LITERATURE REVIEW

OF

ISCHEMIA AND REPERFUSION INJURY

AND

MATRIX METALLOPROTEINASES

1.1 Introduction

Ischemia and reperfusion (I/R) is a common clinical event, which occurs in ischemic heart disease, stroke, shock, following cardiopulmonary resuscitation, vascular surgery and organ transplantation. Ischemic heart disease and stroke are two of three major causes of death in western society. Reperfusion during vascular surgery includes by-pass of arterial occlusion, thrombectomy of arteries and repair of abdominal aortic aneurysm (AAA), in which tissue ischemia and reperfusion is unavoidable. AAA is a potentially fatal disease that occurs in 2-9% of the over 65 year old population (1). Organ transplantation is an effective procedure for improving quality and length of life of patients with organ failure, such as end stage chronic renal failure and hepatic failure, cardiomyopathy, pulmonary insuficiency and short bowel syndrome. More than 200,000 kidney transplants have been performed in the United States since 1964 with best 5-year graft survival rates of 90% (2). The number of liver transplant performed annually in the United States more than doubled from 1,713-4,689 between 1988-1999 with one-year and 10- year patient survival rates 85% and 78 % respectively (3). Obviously, the allograft will suffer an inevitable ischemia and reperfusion insult during organ retrival, preservation and implantation.

1.2 Mechanisms of Ischemia / Reperfusion (I/R) Injury

I/R injury is a very multi-factorial process involving complex biochemical reactions, production of oxygen free radicals, release of cytokines, activation of neutrophils with adhesion to the endothelium and migration, increase in microvascular permeability, cellular apoptosis and necrosis.

1.2.1 Generation of Reactive oxygen species (ROS)

Under normal conditions, intracellular energy is stored in the form of adenosine 5'-triphosphate (ATP) which is dephosphorylated to adenosine 5'-diphosphate (ADP) and adenosine 5'-monophosphate (AMP), simultaneously accompanied by the release of energy

during cellular metabolism. During ischemia, the blood supply to the tissue is interrupted and oxygen is lacking, leading to anaerobic metabolism with an increase in local concentration of lactic acid and changes to protease kinetics. Breakdown of ATP occurs resulting in the formation of adenine nucleotides, hypoxanthine, xanthine, inosine and adenosine. Normally, hypoxanthine is oxidized to uric acid by the enzyme xanthine dehydrogenase, even though it can also be oxidized by xanthine oxidase, an isoform of xanthine dehydrogenase, and in the process, transfers an electron to O_2 forming O_2^- (4). It has been determined that ischemia results in conversion of xanthine dehydrogenase to xanthine oxidase within endothelial cells. The outcome of all these events will lead to endothelial cell damage and release of xanthine oxidase into the plasma of the reperfused tissue (5). Increased xanthine oxidase uses molecular oxygen introduced during reperfusion to convert hypoxanthine to xanthine, releasing superoxide during this process (6). Hypoxanthine and xanthine serve as oxidizable purine substrates for xanthine dehydrogenase or xanthine oxidase. Therefore, a burst of superoxide radicals and hydrogen peroxide is produced following reperfusion. On the other hand, the depletion of the cellular ATP results in increase in intracellular calcium concentration due to the dysfunction of ATP-dependent membrane ion pumps. The elevation of intracellular calcium may activate proteases, which are capable of converting the dehydrogenase to the oxidase (7). The mechanisms of production of superoxide radicals and hydrogen peroxide are illustrated in Fig 1.1

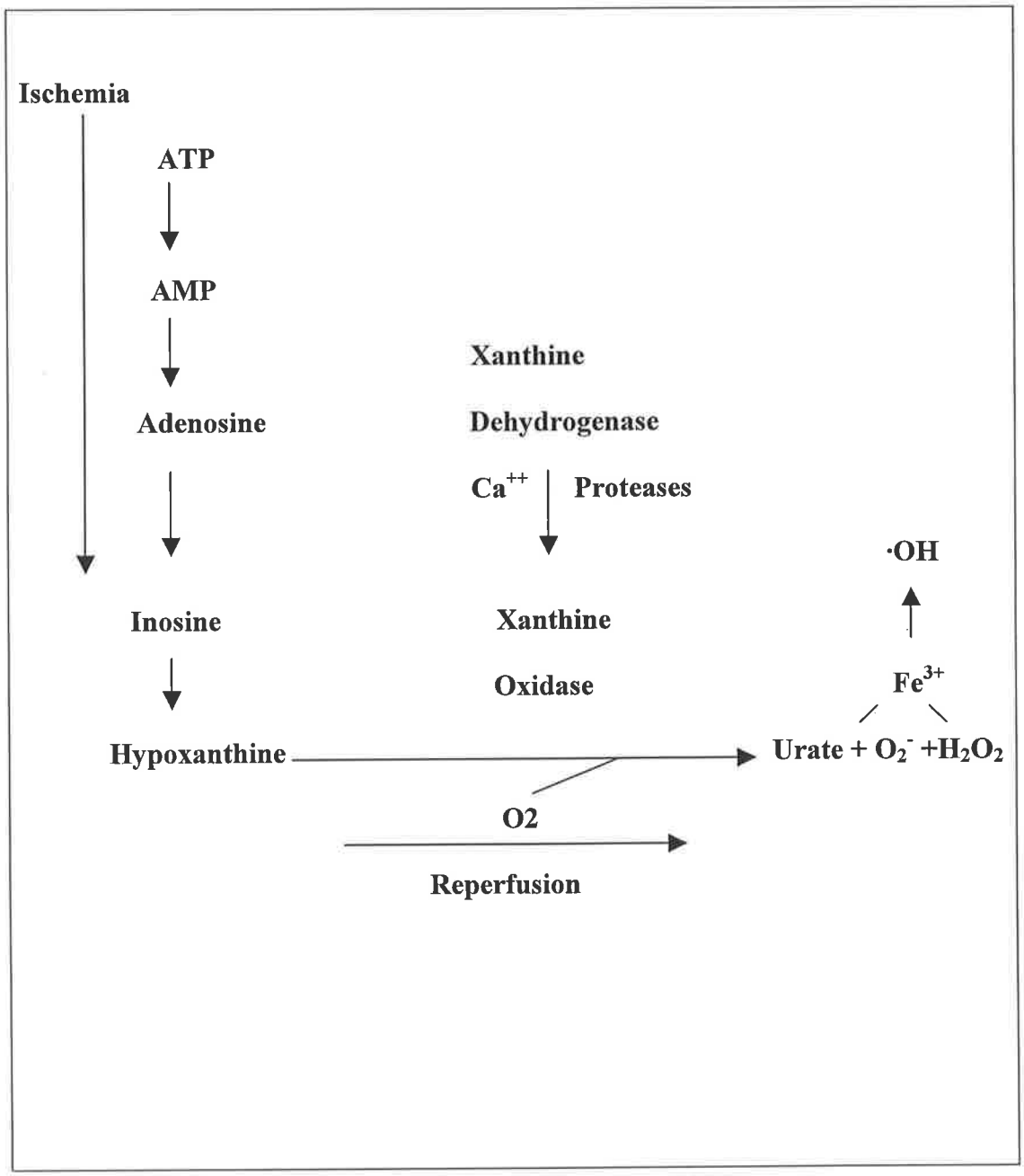

Fig 1.1. The mechanisms of ischemia/reperfusion-induced production of ROS (8).

The activity of xanthine dehydrogenase is different in various tissues. Therefore, the duration of ischemia required for conversion of xanthine dehydrogenase to oxidase is variable. For example, in rat ileum, about 90% of total activity is present as xanthine dehydrogenase. If ileum is completely ischemic even for very short periods, there is a rapid conversion from xanthine dehydrogenase to xanthine oxidase within 10 seconds, resulting in generation of superoxide or hydrogen peroxide. The content of xanthine oxidase in the heart doubles after 8 minutes of ischemia, and in the liver, spleen, lungs and kidney, the same increase requires about 30 minutes (6). In contrast, skeletal muscle contains less xanthine dehydrogenase and there is no conversion of xanthine dehydrogenase to xanthine oxidase during ischemia. This observation is consistent with the clinical findings in which the skeletal muscle is capable of resistance to longer periods of ischemia (up to 4 hours) (9).

The oxygen free radicals that are produced during ischemia-reperfusion of the tissues are highly reactive, initiating peroxidation of cellular lipid membrane and resulting in structural and functional cellular damage (10). In addition, lipid peroxidation of polyunsaturated fatty acids produces lipid peroxyl radicals that may propagate a chain reaction in adjacent fatty acid molecules. Moreover, hydroxyl radical (·OH) may cause direct oxidation of proteins and DNA, ensuing enzyme inactivity and DNA strand breakage (11), (12).

1.2.2 Lipid peroxidation

Arachidonic acid is released during I/R following activation of phospholipase A2 due to increased intracellular calcium and lipid peroxidation of cell membranes. The metabolites of arachidonic acid are thromboxane A2 (Tx A2), leukotriene B4 (LTB4) and prostaglandins, which have been demonstrated to have an important role in the pathogenesis of reperfusion injury.

TxA2 is a powerful chemoattractant that induces neutrophil adhesion to endothelium during ischemia-reperfusion. TxA2 will also stimulate platelet aggregation and induce

vasoconstriction (13), (14). In addition, TxA2 has been shown to have direct effects on endothelium, increasing the permeability of the endothelial monolayer (15).

LTB4 is another potent chemotactic agent and plays an important role in endothelial dysfunction. It binds to specific receptors on the surface of neutrophils and elicits a variety of responses. LTB4 stimulates neutrophil degranulation and enhances the expression of cell surface adhesion molecules, improving neutrophil binding to endothelial cells and migration, increasing microvascular permeability (16). Moreover, LTB4 and TxA2 depend on each other to exert their biological effects. The effects of LTB4 on vascular permeability require the presence of TxA2 (15). It has been observed that administration of a LTB4 receptor antagonist before reperfusion significantly reduced the interstitial edema and prevented skeletal muscle necrosis (17).

The ischemia-induced oxidative burst of neutrophils is also thromboxane-dependent. The initial neutrophil activation manifest by the oxidative burst is a graded response to stimulation by thromboxane and is not an "all or none" event after ischemia. Thromboxane not only increases the oxidative metabolism of the neutrophils but also primes the cell for enhanced responses to other stimuli (18).

The prostaglandin endoperoxides (prostaglandin H2) are generated from arachidonic acid by cyclo-oxygenase and converted to prostacyclin by the action of prostacyclin synthase (13). Prostacyclin may result in relaxation of vascular smooth muscle and prevent platelet aggregates binding to the endothelium. The analogue of prostacyclin, iloprost, was determined to be useful in the treatment of peripheral vascular diseases, such as thromboangiitis obliterans (19). Furthermore, some exogenous agents have been produced to reduce I/R-induced injury. U74500, an inhibitor of lipid peroxidation, SC4 1930, a LTB4 receptor antagonist, and GR32191, a TxA2 receptor antagonist, have all been demonstrated to

be able to increase muscle blood perfusion and preserve muscle viability after ischemia and reperfusion (20), (21).

Platelet activating factor (PAF) is also produced by the endothelium through the action of phospholipase A_2 during lipid peroxidation of cellular membranes. It is a potent inflammatory chemoattractant, promoting leukocyte adhesion to endothelial monolayers and increasing the microvascular permeability and albumin extravasation. It has been demonstrated that administration of PAF antagonists was able to attenuate leukocyte adhesion and emigration, and therefore reducing microvascular permeability (22), (23), (24).

Lipid peroxidation and the production of chemoattractants such as TxA2 and PAF are considered to contribute to the activation of neutrophils and the release of cytokines (such as TNF-α). The activated neutrophils that may subsequently be sequestered into the inflammatory tissue have been implicated in playing a key role during the ischemia and reperfusion injury.

1.2.3 Role of Neutrophils in ischemia/reperfusion injury

Considerable evidence supports an important role for neutrophils in the pathogenesis of ischemia and reperfusion injury in various organs and tissues such as brain, heart, intestine, liver, kidney, lung and skeletal muscle (25), (26), (27), (28), (29), (30). Several studies in animal models have shown that depletion of neutrophils by vinblastine or inhibition of neutrophil infiltration by selectin antibodies reduced the severity of ischemia and reperfusion injury (31), (32), (33).

A prerequisite for neutrophil-mediated injury is the adhesion of the neutrophils to microvascular endothelium followed by transendothelial migration, which occurs by a receptor-ligand mechanism. Many molecules and cytokines have been demonstrated to be

involved in this process, including the neutrophil adhesion molecules, which are members of CD11/CD18 membrane glycoprotein complex. Related molecules on the endothelium are the endothelial leukocyte adhesion molecules (ELAM-1) (34) and the intercellular adhesion molecule (ICAM-1) (35). ICAM-1 is a potent neutrophil adhesion receptor whose expression is increased on the surface of endothelial cells following ischemia (36) and mediates firm neutrophil attachment to activated endothelial cells by binding to $ß_2$–integrins, heterodimeric adhesion receptor glycoproteins which are expressed on the neutrophil surface. CD18, located on the neutrophil surface is the common $ß_2$-subunit for both LFA-1 (CD11a/CD18) and Mac-1 (CD11b/CD18) and is responsible for ICAM-1-mediated leukocyte adhesion to endothelial cells (37), (38). Antibody blockade of the CD11/CD18 complex will abolish leukocyte adhesion to the endothelium, thus protecting against ischemia/reperfusion-induced injury and also decreasing microvascular permeability (39), (40), (41). Similarly, other studies have confirmed the importance of CD18 adhesion molecules in neutrophil influx into the heart (29), Lung (42), and skeletal muscle (43) following I/R of these organs. In addition, the binding of neutrophil CD18 to endothelium appears to be the signal required for the neutrophil to release H_2O_2 and proteases into the extracellular matrix (44). The former inversely promotes leukocyte adhesion to endothelium (22), while the latter may facilitate the migration of leukocytes and increase of vascular permeability.

The selectin family, including L-selectin, P-selectin, and E-selectin have been found to play an essential role in initiating neutrophil adhesion to endothelium, (45), (46). L-selectin is constitutively expressed on leukocytes, while P-selectin is stored in preformed Weibel-Palade bodies before constitutive or inducible translocation to the surface of activated platelets and endothelial cells. However, the expression of E-selectin is slower than L-selectin on activated endothelium (34). Neutrophil rolling initiated by L-selectin seems to be the primary step before the firm adhesion (47), (48). P-selectin and E-selectin contribute to the firm adhesion of neutrophils to endothelium and emigration (49). Expression of P- and E-selectin is also

upregulated in the vascular endothelium after ischemia and reperfusion, which contributes to leukocyte recruitment and subsequent tissue injury (50), (51). Local production of IL-1ß and /or TNF-a by these leukocytes induces P-and E-selectin expression on endothelium that continues the cascade of events that increase cell adherence and infiltration of neutrophils into the injured tissues (52), (53). Blockade of selectins shows a beneficial effect in I/R injury, which has been well documented in various organs, including the heart (54), lung (55), kidney (56), Liver (57), and skeletal muscles (48).

Moreover, activation of the complement cascade, whether via the classical or alternative pathway, finally leads to the cleaving of C3, which plays a role in the adhesion of neutrophils and monocyte/macrophages to endothelium (58). Complement may also result in tissue damage after I/R that is independent of neutrophil infiltration (59), (60). Inhibition or blockade of complement could ameliorate I/R-induced inflammation and necrosis. These protective effects could be attributed in part to reduced neutrophil infiltration, and decreased $C_{5b\text{-}9}$ deposition as well (61), (62); (63), (64).

Sequestration of activated neutrophils into the tissues during I/R may lead to local toxic effects as well as remote organ injury (65), (66) by producing free oxygen radicals and cytokines, releasing proteinases and peroxidases; increasing microvascular permeability and albumin extravasation, and resulting in "no flow" phenomenon (67), (68), (69). Neutrophils are known to produce O_2^- and H_2O_2 and to secrete myeloperoxidase, an enzyme that catalyses the formation of hypochlorous acid from H_2O_2 and chloride ions (8). Activated neutrophils are also able to produce nitric oxide (70). Of the 20 or more enzymes contained within the polymorphonuclear cell (PMN) granules, which are released after PMN activation, elastase is especially destructive. These enzymes are capable of degrading virtually all components of the endothelial basment membrane as well as junctional proteins that maintain endothelial barrier function (43), (71).

Obstruction of capillaries may ensue, leading to "no flow" phenomenon. Plugging of capillaries by neutrophils (72), microvascular constriction induced by prostaglandins and endothelin-1 (73), endothelial swelling (74), platelet aggregates (75), and compression of extravasated albumin are considered to be factors in the development of "no reflow". Tissue ischemia not only induces leukocyte activation and adhesion molecule expression, but also renders remote organ such as lung, more vulnerable to vascular injury (71). Blockade of leukocyte activation, adhesion, and infiltration (using monoclonal antibody to ICAM-1 and /or LFA-1, ICAM-1 antisense oligonucleotides) have demonstrated protection of the organ function against I/R injury (76), (77).

In conclusion, activation of neutrophils and consequently their sequestration into the tissues plays a crucial role during the process of I/R injury. Adhesion molecules CD11/CD18 on neutrophils, ICAM-1 on endothelia and the selectin family are considered to contribute to neutrophil adhesion and emigration. In addition, activated neutrophils can produce free oxygen radicals and cytokines, release proteinases, leading to the increase in microvascular permeability and albumin extravasation. Plugging of neutrophils and platelet aggregates in capillaries; endothelial swelling and compression by extravasated albumin combine to result in blood "no flow" phenomena and tissue injury.

1.2.4 Nitric oxide (NO)

Nitric oxide is an endothelium-derived vasodilator. It was initially named endothelium-derived relaxing factor (EDRF) and later identified as nitric oxide (NO) (78), (79). Under normal conditions, NO is synthesized from the amino acid L-arginine by nitric oxide synthase (NOS) which exists in the endothelium in four isoforms, NOS I, NOS II, NOS III and NOS IV. NOS I and NOS III are constitutive enzymes which are calcium and calmodulin dependent, whereas the others are inducible and depend on transcription (80), (81).

NO stimulates soluble guanylate cyclase activity and increase intracellular guanosine 3'-cyclic monophosphate (cGMP) production in vascular smooth muscle cells and platelets (70). Elevated cGMP promotes relaxation of vascular smooth muscle and inhibits not only platelet aggregation, but also platelet adhesion to the endothelium (82). Moreover, NO may protect the vascular wall against the vasoconstrictive effects of endothelin (83). In addition, it was suggested that NO is an important factor in the maintenance of normal diuresis and natriuresis, as well as glomerular filtration rate (84).

During ischemia and reperfusion, the production of NO is dependent on the availability of the substrates O_2 and L-arginine. Depletion of L-arginine may lead to the disarrangement of the domains of constitutive nitric oxide synthase, reduction of NO concentration, and an increase in superoxide. NO relaxes the endothelial cells and thereby narrows the endothelial junctions. Therefore, inhibition of NO production has been shown to increase microvascular permeability and protein extravasation. Treatment with L-arginine can prevent the excessive release of superoxide, preserve NO concentration, and thus inhibit microvascular constriction in skeletal muscle subjected to ischemia and reperfusion, significantly reducing muscule reperfusion edema (85). Furthermore, it was also observed that administration of NO donors effectively attenuates ischemia/reperfusion-induced leukocyte adherence, emigration and albumin leakage in postcapillary venules. This is consistent with *in vivo* studies indicating that NO is also an antiadhesive molecule (86) The mechanism of the effects is probably due to NO donors inactivating superoxide, preventing neutrophil activation and expression of adhesive molecules, and increasing vascular shear rate. Moreover, the NO donors can effectively prevent the platelet-leukocyte aggregation and degranulation of mast cells elicited by I/R. Mast cells have already been shown to release a variety of substances that could induce the leukocyte-endothelium adhesion, leukocyte-platelet aggregation and microvascular protein extravasation (87).

On the other hand, nitric oxide may react with superoxide to yield secondary cytotoxic species via the peroxynitrite anion ($ONOO^-$). The production of peroxynitrite depends on the product of superoxide and nitric oxide concentrations, relatively small increases of superoxide and nitric oxide products lead to greatly increased peroxynitrite formation, up to potentially cytotoxic levels (88). Peroxynitrite or its decomposition products can induce lipid peroxidation without a requirment for iron (89). The protective effects of scavengers of superoxide may be due to preventing the decomposition of nitric oxide by scavenging superoxide, maintaining normal nitric oxide concentration and vasodilatation. Under normal physiological conditions, the flux of NO exceeds the rate of superoxide production to allow NO to scavenge the low levels of intracellular superoxide, reducing arteriolar tone, maintaining vasodilation, preventing platelet aggregates and thrombosis, minimizing leukocyte adhesion to the endothelium. However, during ischemia and reperfusion, the balance between NO and superoxide is tipped in favour of superoxide production. This is because of a great increase in the production of superoxide by endothelial cells and activated leukocytes with concomitant decline in the synthesis of nitric oxide from endothelial cells. The decreased NO levels are unable to maintain vasodilation. The accumulation of superoxide elicits the production of platelet-activating factor (PAF), enhances the activation and deposition of complement on the endothelial cell surface and promotes the leukocyte-endothilial adhesion.

In summary, NO is an endothelium-derived vasodilator, capable of protecting the vascular wall against vasoconstrictive effects of endothelin. The production of NO is dependent on the availability of substrates O_2 and L-arginine. During ischemia and reperfusion, the balance between NO and superoxide is tipped in favour of superoxide production. The decreased NO is unable to maintain vasodilation, resulting in microvascular constriction and increase in vascular permeability. Administration of L-arginine effectively ameliorates I/R injury by

inactivating superoxide, preventing neutrophil activation and microvascular protein extravasation.

1.2.5 Endothelium and endothelin

Endothelium is enriched in xanthine oxidase, which is capable of generating superoxide (O_2^-) and H_2O_2 in response to an ischemia and reperfusion insult. It has been demonstrated that plasma xanthine oxidase activity increased dramatically following aortic occlusion and reperfusion, as well as during hepatic and intestinal I/R (90), (91), (92). Endothelial cells not only release superoxide and hydrogen peroxide by the enzymic activity of xanthine oxidase, but also gives rise to many chemoattractants and cytokines including intercellular adhesion molecule-1 (ICAM-1), endothelins, P-selectin and tumor necrosis factor alpha. In the presence of these chemical substances, activated endothelium can promote leukocyte-endothelial adhesion, leukocytes transendothelial migration, leukocyte-platelet aggregates and finally enhance microvascular permeability and albumin extravasation (26), (93).

Endothelin-1 (ET-1) is a 21-amino acid peptide, which was discovered in 1988 and has been determined to be the most potent known vasoconstrictor (94), (95). It is released from endothelial cells under the stimulation of ischemia and reperfusion, thrombin, transforming TGF- ß, noradrenaline, phorbol ester and the calcium ionophore A23187 (96), (94), (97), (98), (99). Endothelin can initiate smooth muscle contraction by promoting an influx of calcium ions and release of calcium from intracellular stores (100), (101). Furthermore, endothelin is a potent mitogen and may stimulate DNA synthesis in vascular smooth muscle cells and stimulate neutrophil adhesion to endothelial cells (102), (103).

Further studies have demonstrated that ischemia alone increases the expression of ET-1 mRNA, and that ET-1 peptide was clearly elevated in the cortical peritubular capillary network (PTCN) in the kidney following ischemia without any reperfusion. Reperfusion may

continue to stimulate ET-1 mRNA expression and therefore play a fundamental role in the injury cascade (96).

Endothelin-1 is a very important agent in the pathophysiology of acute renal failure (ARF) due to its intense vasoconstrictive properties in the kidney. ET-1 has been shown to result in vasoconstriction in both the afferent and efferent arterioles of the glomerular tuft when added exogeneously. This effect has been postulated to be the cause of ET-1-induced ARF that ET-1 initiates vasoconstriction in the glomerular tuft along with the arcuate and interlobular arteries (104), (105). Similarly, the endogenous sites of ET-1 peptide expression in the kidney after ischemia are in the endothelium of the cortical PTCN, which represents a continuation of the efferent arteriole of the glomerulus into a capillary bed that surrounds the convoluted tubules. ET-1 would cause hypoxia to the adjacent cells lining the tubules by restricting blood flow in the PTCN. The ongoing vasoconstriction in this area may prolong hypoxia and lead to cell death and to the typical tubular epithelial sloughing which occurrs in acute tubular necrosis (ATN). Therefore, the localization of ET-1 to the PTCN further supports the hypothesis of ET-1 being a possible pathophysiological factor in ATN (96).

The evidence for ET-1 action in the PTCN leading to ATN has been supported in other studies by administration of a receptor antagonist. The administration of the ET_A receptor antagonist BQ123 in isolated perfused kidney models as well as *in vivo* models of renal ischemia improved the renal blood flow, promoted glomerular filtration rate (GFR) and ameliorated the proximal tubular necrosis (106), (107). The ET-1 peptide, once released, is easily bound with high affinity to ET receptors that have also been up-regulated, or at least increased in affinity for ET, following ischemia. Thus, the most optimal time to administer ET receptor antagonists should be prior to the ischemic insult (108).

In liver, endothelin-1 (ET-1) has been indicated to play a role in the development of hepatic I/R injury by causing deterioration of the hepatic microcirculation. Endothelin is released from vascular and sinusoidal endothelial cells, as well as macrophages. Hepatic stellate cells are nonparenchymal liver cells which are abundant in ET receptors and induce microcirculatory disturbance. ET-1 has the strongest vasoconstrictive effects among the three isotypes and with a high affinity for ET receptors. Release of ET-1 and binding to the receptors on the stellate cells may result in its contraction and sinusoidal constriction, thus promoting microcirculatory disturbance and leading to hepatic ischemia reperfusion injury. The administration of nonselective ET receptor antagonist, such as TAK–044, ameliorates hepatic ischemia reperfusion injury through improvement of hepatic microcirculation and oxygenation along with reduced hepatic neutrophil infiltration (109).

There is an interaction between oxygen radicals and ET-1 by which the exogenous reactive oxygen species increase ET-1 release and expression of ET-1mRNA in cultured human mesangial cells. There is evidence that oxygen radical scavengers reduce basal ET-1 production, indicating that endogenous oxygen radicals may also stimulate ET-1 production. The mechanisms of this effect are probably due to reduction in NO levels, disruption of the cell membrane with release of stored ET-1 and through augmentation of thromboxane levels, as well as of the transcription factor, NF-KB (110), (111), (112).

Under normal conditions, there is a balance between the production of endothelin (ET) and nitric oxide (NO) to maintain the well-established tissue microcirculation. After I/R, the release of NO is damaged due to the action of the reactive oxygen species, in favour of the production of endothelin, resulting in inhibition of vasodilation and an increase in vasoconstriction. This has been suggested to be a major determinant in the regulation of regional and systemic haemodynamic function and cellular proliferation (113).

In summary, endothelin is a most potent vasoconstrictor, which is released from endothelium under the stimulation of ischemia and reperfusion. Free oxygen radicals could furthur increase the expression and production of ET-1. Endothelin is also able to stimulate neutrophil adhesion to endothelium and restrict blood flow, prolonging hypoxia and leading to cell death.

1.2.6 Cell death by apoptosis and necrosis

Apoptosis has been well known to play an important regulatory role in various disease processes including cancer (114), (115), autoimmune disease (116); (117), ventricular dysplasia (118)) and renal cystic disease (119). Recently, apoptosis has been recognised to be present in various tissues after ischemia/reperfusion injury, including brain, heart, lung, kidney and liver (120), (121), (122), (123). Inhibition of apoptosis often leads to improved function in many organ systems (124), (125), (126). Fischer et al (127) have found that with shorter periods of ischemia, the mode of cell death in lung tissues after reperfusion is primarily apoptototic, while with longer periods of ischemia, cell death after reperfusion is primarily necrotic. Increased necrosis was associated with a significant deterioration of transplanted organ function. Therefore, it was suggested that the mild to moderate ATP depletion triggers apoptosis, while severe depletion of ATP results in necrosis (128). It is likely that many features of the cell signalling process leading to the apoptotic form of cell death is shared with those associated with necrotic form of cell death. The pathway that is followed by the cell is dependent on both the nature and severity of insults, evolving from apoptotic to necrotic form of cell death.

Apoptosis is a process of programmed cell death, morphologically characterized by overall cellular condensation, shrinkage, and plasma membrane blebbing, with nuclear chromatin margination and condensation followed by segmentation and DNA fragmentation. Consequently, the apoptotic cell is broken up into smaller membrane-bound apoptotic bodies

that are usually phagocytosed by macrophages without initiating an inflammatory response (129), (130). The absence of inflammation is a crucial feature of apoptosis, thus it permits cell death without destruction of adjacent cells, and therefore is advantageous for normal cellular turnover, development and homeostasis of organs under physiological and pathological conditions. In contrast, necrosis is a form of irreversible cell death accompanied by the loss of cell membrane integrity and ion pump damage, leading to cell swelling, lysis, and release of intracellular enzymes and lysozyme, followed by neutrophil migration, inflammatory reactions and edema (131), (132). Moreover, the kinetics of apoptosis has been demonstrated to include shrinkage and retraction of the cell, with an active phase of pseudopod formation around the periphery of the cell, and a quiescent spherical phase with mitochondrial matrix swelling, followed by a necrotic phase (133).

The apoptotic cascade is initiated either by death receptor ligation and activation of caspase-8 or by mitochondrial damage and activation of caspase-9 (134). Caspases are a family of intracellular cysteine proteases, which cleave their substrates at aspartic acid residues (135). These proteases are present as inactive zymogens in essentially all animal cells, but can be triggered to assume active states, generally involving their proteolytic processing at conserved aspartic acid (Asp) residues (136)). In humans and mice, approximately 14 caspases have been identified, which are subgrouped according to either their amino acid sequence similarities or their protease specificities. Functionally, it is useful to classify caspases into upstream (initiator) caspases and downstream (effector) caspases (137). There are two pathways for caspase activation, extrinsic and intrinsic. The extrinsic pathway can be induced by members of the TNF family of cytokine receptors, such as TNFR1 and Fas (138). The intrinsic pathway can be induced by release of cytochrome c into the cytosol, thereby triggering apoptosis (139). In addition, it has been demonstrated that caspases participate in hypoxic injury to renal tubular cells and I/R injury to the kidney (140), (141).

Mitochondria become susceptible to damage during ischemia and reperfusion. Long periods of ischemia can alter the electron transport complexes in mitochondria. All of the complexes show a reduction in their activity with structural damage to the subunits after 60 min of warm ischemia (142). Damaged complexes of the electron transport chain may be more prone to electron leakage and this may continue for an extended period after reperfusion (143). ATP hydrolysis during ischemia causes a rise in free inorganic phosphate, which increases membrane permeability (144). Extended warm ischemia causes progressive reduction of the iron-sulfur proteins associated with complex I (NADH dehydrogenase) or complex II (succinate dehydrogenase) of the electron transport chain and results in liberation of the ferrous iron that can be critical in reperfusion by reducing H_20_2 and forming ROS (145). In addition, ischemia also results in the impairment of mitochondrial antioxidant defenses, and renders cells more susceptible to oxidative stress (146), (147). After reperfusion, ROS produced by mitochondria may play a significant role in reperfusion injury although xanthine oxidase and polymorphonuclear leukocytes are a source of ROS. A burst of O_2^- production occurs from the mitochondria electron transport chain when oxygen is reintroduced to the cell. With the introduction of O_2 during reperfusion, the electron transport chain complexes may be damaged, resulting in a leak of electrons that react with oxygen to generate O_2^- which leads to an oxidative burst (148), (149), (143). The change in the mitochondrial membrane, which consists of disruption of the electrochemical gradient of the inner membrane, development of permeability transition, production of ROS, and release of apoptotic factors into the cytosol could trigger apoptosis (150), (151). Moreover, mitochondria contain the members of the anti-apoptotic Bcl-2 family at the external membrane, which prevents permeability transition in cells and the release of mitochondrial apoptogenic factors (152), (153). Together with pro-apoptotic molecules, such as Bax and Bid, Bcl-2 plays an important role in regulating apoptosis (153). Also, cytochrome c release into the cytosol has been implicated as an intermediate event in the initiation of apoptosis after a variety of toxic and other stimuli and injury in several cell types (154), (155), (156) Mitochondrial damage is

associated with the release of cytochrome c and apoptosis-inducing factor (AIF) from the mitochondrial intermembrane space. Current evidence suggests that cytochrome c release activates caspases, which result in typical apoptotic cell death (139).

On the other hand, oxidative stress and the production of reactive oxygen intermediates are also considered as mediators for apoptosis (157), (158). Reactive oxygen species and metabolites may induce apoptosis by direct DNA damage, oxidation of lipid membranes, or upregulation of regulatory "apoptosis genes" (157). It is generally accepted that hydrogen peroxide can gain access to the DNA, and in the presence of iron in the DNA, results in the site-specific generation of hydroxyl radicals that cause the DNA damage. Furthermore, endonuclease activation occurs as an early event leading to DNA fragmentation and thus inhibition of endonuclease prevents hydrogen peroxide-induced DNA strand breaks, DNA fragmentation, and cell death (159), (160). Other studies also support the idea that reactive oxygen metabolites may be important in endonuclease activation and subsequently apoptosis (161). Feldenberg et al (162) have shown that apoptosis induced by partial ATP depletion is accompanied by increased activity of caspase-8 and is ameliorated by pretreatment with inhibitor of caspase-8. Intracellular ATP concentration, which has been shown to be required for apoptosis signal transduction, both upstream and downstream of caspase activation, plays a crucial role in the determination of cell death fate by apoptosis or necrosis (163), (164).

It has been suggested that excessive cell loss through apoptosis can cause acute and chronic organ insufficiency. Jo et al (165) have demonstrated that apoptosis clearly contributes to tubular cell loss in renal I/R injury and hence subsequent renal failure. Suzuki et al (166) found that apoptosis of mycardium is related to infarct size after ischemia and reperfusion. Similar studies have also provided evidence for apoptotic effects in organ function in liver, intestine and lung graft (167), (168), (127). However, other studies (169), (170) have found that apoptotic cell death makes a minor contribution to ischemia/reperfusion injury in skeletal

muscles. These results suggest that although apoptosis occurs in a range of tissues under ischemia and reperfusion insult, it is probably tissue specific.

In summary, apoptosis play an important role in a variety of tissues after ischemia and reperfusion injury. The production of ROS, damage of mitochondria and depletion of ATP, subsequent release of cytochrome c and apoptosis-inducing factors, and activation of caspase family members all contribute to the process of apoptosis. The advantage of apoptosis is that it permits cell death without destruction of adjacent cells. However, excessive cell loss due to apoptosis can lead to the organ insufficiency, while inhibition of apoptosis improves organ function. It seems that apoptosis plays a key role in a variety of tissues after IR injury, but only a minor contribution in skeletal muscles.

1.2.7 Alterations of fibronectin (FN) after I/R

FN as a generally agreed name emerged in 1977. It was previously known as cold-insoluble globulin (CIg), antigelatin factor, cell attachment protein (c-CAP), cell spreading factor (CSF), cell surface protein (CSP), or surface fibroblast antigen (SFA). The structure of fibronectin is a large dimeric glycoprotein composed of a series of independently folding modular domains known as fibronectin repeats I, II, III (171). These repeating units contain regions of domains that interact with a number of other matrix molecules as well as different cells, mediating cell migration, differentiation, proliferation and matrix assembly (172), (173). Structural diversity in fibronectin arises by regulated alternative splicing of a single gene transcript in three segments, termed EIIIA, EIIIB, and V in rats, and ED-A, ED-B, and IIICS in humans (171). The EIIIA or ED-A and EIIIB or ED-B domains are either included or excluded as intact type III homology repeats. The V or IIICS may be excluded, partially included, or fully included. The latter form contains the connecting segment-1 (CS1) region, which is known to play a pivotal role in mediating leukocyte adhesion (174). FN variants which include the EIIIA and EIIIB segments are prominent in FN produced during

embryogenesis, and their expression in the adult tissues is minimal except when induced under certain pathological conditions (175), (176). Adult liver synthesizes the plasma form of FN, which excludes the EIIIA and EIIIB domains, whereas these domains are markedly increased during cutaneous wound healing (177), (178) and neointimal hyperplasia (179), (180). Alternative splicing of the FN gene allows for the generation of multiple isoforms with 20 isoforms possible in humans (181). FN has a molecular weight of 440 kDa.

FN is considered as a multifunctional protein that is now studied by many different types of biologists. It exists in two forms: plasma fibronectin and tissue (cellular) fibronectin. Plasma fibronectin is a soluble form of FN in blood and lymph fluids, which is mainly produced by hepatocytes and secreted into plasma. Macrophages, fibroblasts, endothelial cells, and smooth muscle cells produce tissue fibronectin that is one of the major components of the basement membrane of tissues. It plays an important role in cell to cell and cell to matrix interactions such as lymphocyte adhesion, migration and activation (171), (182), (183), (184). Fibronectin is also essential for embryonic development (185).

Plasma fibronectin (pFN) is an opsonic molecule that markedly enhances macrophage phagocytic clearance of blood-borne nonbacterial particulates (186), (187), (188). Clearance of such debris from blood by macrophages of the liver and spleen minimizes their deposition in extrahepatic beds such as the lungs and kidneys and is thought to ensure integrity of organ function by preventing microembolization of these particulates in organ vascular beds with subsequent organ failure (189). The depression in liver and spleen phagocytic function is associated with a significant increase in the deposition of particles in the lung (188). Acute depletion of pFN has been well documented after severe trauma, burns, infections and periphreal ischemia and reperfusion injury (190), (191), (192), (188). This acute depletion is attributed to its rapid binding to sites of tissue injury and as well, its consumption as an opsonic protein in the clearance of tissue debris circulating as a result of injury and wound

infection (191), (193). Some studies have shown that the loss of ^{125}I-labelled fibronectin from the plasma after injury is accompanied by its increased localization in the injured tissue as well as in the liver, the latter reflecting Kupffer cell phagocytic clearance of fibronectin opsonized blood-borne tissue debris (193), (188). The deposition pFN in tissue matrix suggests that it may play a crucial role in early wound healing and tissue repair by improving fibroblast, epithelial and endothelial cells adhesion and migration. In addition, rebound hyperfibronectinemia has been observed following the initial decline of plasma FN after thermal injury or skeletal muscle ischemic injury (193), (188). Whether the elevated pFN is a beneficial response that contributes to host defense and wound repair or a reflection of tissue injury without any protective role remains unclear. Elevated pFN may improve macrophage phagocytosis and wound healing and promote restoration of lung endothelial integrity after injury. The major source of rebound pFN elevation is from liver synthesis mediated by cytokine IL-6 (188).

Alterations in FN have also been identified in the basement membrane during organ I/R. In a small bowel transplant model, increased FN was observed in the basement membrane within the villi cores and crypt areas after reperfusion as well as during rejection (194). In heart allografts, FN accumulation in the cytoplasm of cardiomyocytes was positively correlated with the degree of cardiomyocyte coagulation necrosis. Labarrere et al (195) also found that there was a correlation between the deposition of FN and later development of chronic rejection or graft failure. Moreover, the increased FN deposition was observed in heart allograft biopsies (196).

FN accumulation has been observed in experimental myocardial infarct. It was localized in a patchy fashion in the cytoplasm and interstitial space of some myocytes in the infarct area. This accumulation continued to increase at 24 h, reached a maximum at 48 h and decreased thereafter (197). pFN and platelet-derived FN were considered to contribute to the

accumulation of FN observed in necrotic myocardium and interstitium (198), (199). It is likely that this FN acts both as a chemotactic stimulus for inflammatory cells to migrate into the areas of myocyte necrosis, and as a scaffold for endothelial cells and fibroblasts to grow and collagen assembly. Furthermore, the accumulation of FN may function as a template for the deposition of collagen during healing of the infarct. In addition, FN may improve platelet aggregation (200) and induce the release of platelet products such as TGF-$ß_1$ and platelet-derived endothelial cell growth factor (201), (202). Local synthesis of fibronectin by sprouting endothelial cells and connective tissue cells at the border zone of the infarct area appears to play a role in the angiogenesis that characterizes infarct healing (197). FN has been found to accumulate more rapidly in animal models of cardiac I/R than in hearts of animals with permanent ligation of a coronary artery (179), (203).

Similar phenomena were observed in the kidney following ischemia and reperfusion injury. The concentration of fibronectin rapidly increased in all areas of the kidney as early as 3 h after ischemia, reached a maximum at day 5, and declined thereafter (204), (205). In particular, there was a marked accumulation of FN in the distal tubular lumen (205). It is unclear whether the source of fibronectin is from plasma, the tubular epithelial cells or a combination of both. It is possible that the pFN escapes into the peritubular space and tubular basement membrane during the congestion and hyperemia associated with early ischemia and reperfusion injury and with increased capillary permeability. At later stages, FN may be synthesized locally by tubular epithelium. Likewise, local synthesis of FN by injured epithelial cells has been observed in the restitution of skin wound, intestinal epithelium and cornea (178), (206), (207).

Furthermore, accumulation of FN has also been found in lung injury. In the lung, FN existed in the interstitial matrix as well as under both the alveolar epithelial and endothelial cell layers (208), (209). These cells can also synthesize FN and incorporate FN into the extra cellular

matrix via a cell-depencent polymerization process (210), (211). Thus, FN was considered to support attachment and survival of normal human bronchial epithelial cells and induce integrin clustering and focal adhesion, implicating FN plays a role in lung injury and repair (212), (213). It has been demonstrated that plasma FN escapes and incorporates into the lung extracellular matrix during lung acute injury in postsurgical bacteremia, and then attenuates the increase in lung endothelial protein permeability and stabilize the integrity of the lung vascular barrier (208), (214), (215), (216). Curtis and colleagues (217) have also found that purified human plasma FN was able to incorporate into subendothelial matrix and co-localized with endogenous bovine FN in the inflammation-induced lung injury and reduce the protein permeability. The mechanism of increased FN in the injured lung is possibly due to the interstitial and alveolar spaces being flooded with plasma and local synthesis by activated macrophages, fibroblasts, endothelial cells and type II alveolar epithelial cells in damaged pulmonary parenchyma (216). It could be postulated that fibronectin may function to organise the subsequent deposition of other matrices such as collagen in the extracellular matrix and improve repair of injury.

The effects of increased expression of fibronectin following ischemia and reperfusion are not well elucidated. Fibronectin as a multifunctional protein, contains multiple functional sites including cellular binding, spreading, proliferation and differentiation domains, all of which are of potential importance in cellular regeneration and recovery from injury after ischemia and reperfusion (171), (215). In one recent study, Sakai et al (218) found that deposition of plasma fibronectin in the infarcted area of the brain in control mice was related to the upregulation of the anti-apoptotic protein Bcl-2, thereby preventing caspase-3-mediated apoptosis. However, deposition of plasma fibronectin was not detected in the infarcted brains of plasma fibronectin-deficient (gene knockout) mice, which was accompanied by an increased number of caspase-3-positive apoptotic cells and greater infarction volumes. These

results suggest that plasma fibronectin incoporated into the tissue matrix may protect cells against ischemic injury by inhibiting cellular apoptosis.

Moreover, others found that synthetic fibronectin peptides could inhibit polymorphonuclear leukocyte (PMN) recruitment in ischemic tissue concomitant with reduced infarct volume and improve neurological outcome in rat cerebral ischemia / reperfusion (219), (220). The role of the synthetic FN peptides (FN-C/H-V) in mediating the adhesion of leukocytes to the endothelium is complex and poorly understood. Possibly, this may be attributed to its interaction with integrins on the cell surface and modification of leukocyte adhesion (220).

Not only is FN a target of I/R- induced injury, but it is also an active participant in the immune cascade leading to graft rejection (221), (194) In more recent studies, FN has been found to play a crucial role in allograft rejection. EIII A^+ FN expression by macrophages is a critical feature of graft rejection versus tolerance. The lack of EIII A^+ FN expression by infiltrating macrophages in the tolerant state was associated with marked depression of IL-2 and IFN-r at both mRNA and protein levels. The expression of $EIIIA^+$ FN may amplify the rejection cascade through upregulation of type 1 cytokines, IL-2 and IFN-r in allografts (222). The interaction between α4-integrin and FN may be important to leukocyte homing to the graft site (223). Pathologically, the most prominent feature of chronic rejection is expansion of extracellular matrix and widening of the basement membrane. Clinically, in patients with acute or chronic kidney allograft rejection, urinary FN levels are found to be significantly higher than those of patients with stable graft function. This enhanced urinary FN is likely to be derived from glomerular protein leakage and tubular cell secretion (224). The integrin family of cell surface receptors has long been known to play an essential role in the physical aspects of cellular adhesion. These molecules represent the principal receptors for extracellular matrix proteins such as FN but also participate in transduction of outside/inside signals and contribute to trigger a multitude of cellular events including activation and

differentiation (225). The adhesion of T cells to FN via α4-integrin and α5-integrin could up-regulate the levels of NF-KB (226) and promotes the activation of the p125 ^{FAK} /Zap-70 complex in human T cells (226).

FN exerts synergistic effects on T-cell activation by acting as a costimulator for both $CD4^+$ and $CD8^+$ T cells through the T cell receptor (227), (183) and cytokine release (228). The production of IL-2 and TNF-a is also stimulated by interactions between $CD4^+$ T cells and FN (228), (229). It was found that there were a molecular heterogeneity in FNs observed in cardiac allografts and that the incorporation of the EIIIA, EIIIB, and V domains in the FN had distinct temporal and spatial distribution patterns during rejection (230). In addition, FN was increased in cardiac allografts as early as 3 hours post transplant, and its preferential expression by day 4-6 before the actual rejection was accompanied by a concomitant rise of VLA-4^+ cells (231). Administration of fibronectin connective segment-1 (CS1) peptide could block CS1-α4ß1 interactions and decrease intragraft infiltration by $CD25^+$ cells, then interrupt the host immune cascade. CS1 peptide therapy is capable of abrogating acute rejection and prolongs cardiac allograft survival in rats. This effect was accompanied by decreased intragraft expression of total FN and cellular adhesion molecules, α4 ß1, VCAM-1 and ICAM-1, and reduced infiltration of $CD4^+$, CD^8, and $CD25^+$ cells with diminished expression of mRNA coding for Th1 (IL-2, IFN-r) and Th2 (IL-4, IL-6) cytokines. This immunosuppressive effect could be reversed and acute rejection recreated by adjunctive treatment with recombinant IL-2 in rats (232). Furthermore, the use of CS1 peptides effectively prevented progressive allograft failure associated with chronic rejection (233). The lack of FN in tolerant rats associated with infiltrating leukocytes plays an important role in the maintenance of tolerance by depressing local expression of Th1 cytokines that otherwise facilitate acute graft rejection in transplant recipients (234). It was also found that FN could augment T cell adhesion, proliferation and secretion of the cytokines IL-2 and IFN-r triggered by peptide-MHC complexes (235). Therefore, administration of CS1 peptide to attenuate

lymphocyte sequestration and cytokine dependent immune cascade in the allografts could be a novel therapeutic approach to modulate graft rejection. Others have found that CS1 peptides inhibite leukocyte recruitment and attenuate the acute inflammatory response with an almost complete blockade of chronic inflammation in an erosive model of polyarthritis (236). Moreover, in a murine contact hypersensitivity model, it was found that CS1 peptides could partially inhibit T-cell migration to skin inflammatory areas (237).

On the other hand, T–lymphocyte migration into tissues during allogragt rejection requires local degradation of the basement membrane. Transient adherence to fibronectin induces the production of activated forms of matrix metalloproteinase-2 (MMP-2) and MMP-9, as well as down regulation of tissue inhibitor of metalloproteinase-2 (TIMP-2) by T cell lines, facilitating the T cell migration into the extracellular matrix (238).

Furthermore, FN plays a key role in several stages of wound healing including platelet aggregation, epidermal cell migration and differentiation, collagen matrix assembly and wound contraction (239), (240). Macrophages are the first cells in healing wounds to express increased amounts of FN mRNA locally as early as 2 days after injury. Some of these FNs contain the EIIIA and EIIIB domains. At a later stage, granulation tissue fibroblasts assume the role of expressing FNs in both adult and embryonic forms (177). In some forms of wound healing, fibronectin splicing patterns resemble embryonic patterns, suggesting that specific types of fibronectin are important in wound healing (178).

A complex interaction between FN and members of the integrin family occurs on cell surface, by which the cellular function could be changed. The fibronectin fragments that bind to cells may help to regulate monocyte interactions with tissue matrix by acting upon the monocyte FN receptor VLA-5 (241). The interactions between VLA-5 and FN significantly enhance both spontaneous and monocyte chemoattractant protein-1 (MCP-1) driven monocyte

migration into a tissue matrix. It was also observed that VLA-5 – mediated adhesion of monocytes to native FN may induce cellular apoptosis (242). The adhesion of fibronectin to macrophages could augment macrophage phagocytosis of apoptotic neutrophils at inflammatory sites during the resolution of inflammatory responses. This observation suggest that the extracellular matrix enviroment may provide regulatory signals that act indirectly to alter the potential for removal of apoptotic cells and influence the process of resolution of inflammation (243). In addition, it has been shown that soluble fibronectin peptides trigger apoptosis of nontransformed fibroblasts in culture and in fibrin gels through disruption of an integrin-mediated survival-signalling pathway (244). Synthetic FN peptides (Trp-9-tyr) have been found to alter the progression of leukocyte-mediated tissue destruction after thermal injury (245). Moreover, FN–bound TNF-α has been observed to stimulate significantly the secretion of MMP-9 by monocytes. This interaction was suggested to limit the availability and bioactivity of TNF-α to target areas of inflammation (246).

The production of FN has considered to be influenced by cytokines due to their combined elevation during many pathological conditions. TNF-α was demonstrated to stimulate the expression of fibronectin in fibroblasts isolated from the heart (247). TGF-β is abundant in injured lungs and has profound effects on FN production by alveolar type II cells (248). TGF-beta and IL-1 were also known to promote FN synthesis in glomerular basement membrane in autoimmune glomerulonephritis (249).

In conclusion, FN is a multifunctional protein that exists as plasma and cellular FN. Plasma FN is an opsonic molecule that markedly enhances macrophage phagocytic clearance of blood-borne nonbacterial particulates. cFN is one of the major components of the basement membrane. Alterations of both pFN and cFN were observed during the process of ischemia and reperfusion. The rapid deposition of FN in the basement membrane during I/R was considered to attenuate tissue injury and, as well, to facilitate tissue repair. Moreover, there

are complex interactions between FN and members of integrin family on cell surface or cytokines by which cellular functions could be changed. FN was also found to be an active participant during the immunoreactive cascade in an allograft that undergoes I/R insult.

1.2.8 Alteration of laminins after I/R.

Laminins (LNs), discovered in 1979, are multifunctional glycoproteins and major components of extracellular matrix that contribute to the architecture of the basement membrane and play significant roles in adhesion, growth, migration, and differentiation of several cell types (250), (251). LN is composed of three subunit molecular chains: α, ß, and γ. Five α, 4 ß, and 3γ chains have been identified to date that combine to form 12 different isoforms which have tissue-specific and developmentally regulated expression patterns. The differential expression of LN isoforms under differential endothelial cell activation suggests a role for LN in inflammatory events (252), (253), (254). It has been demonstrated that the amount of LN in glomerular basement membrane (GBM) is significantly less than that in the tubular basement membrane (TBM), implying that the GBM is vulnerable to the damage in a multitude of renal diseases (254). The change in expression of LN chains in glomeruli may aggravate progressive immune injury in a mice model of lupus nephritis (255). Moreover, it was found that LN could protect mesangial cells from apoptosis induced by serum starvation and DNA damage in a *in vitro* rat model. This effect is not associated with changes in cellular levels of apoptosis regulatory proteins of the Bcl-2 family, suggesting that the glomerular mesangial cell survival is dependant on interactions with certain components of ECM (256). Furthermore, the occurrence of some diseases, such as epidermolysis bullosa and congenital muscular dystrophies are related to certain LN chain gene defects (257), (258). It has also been found that lack of the α3 ß1 chain causes defective kidneys and lungs (259).

Laminin-5, an isoform of LN, has been demonstrated to promote adhesion, migration, and scattering of several types of cultured cells more efficiently than all other ECM proteins. The extracellular deposition of laminin-5 is mediated by the short arm of the γ2-chain that steers intermolecular interactions with basement membrane components and promotes cellular adhesion (260). In addition, another LN isoform, laminin-8 is synthesized and secreted by blood lymphoid cells, and this LN isoform could promote chemokine-induced migration and proliferation of the cells (261). The laminin-8 and laminin-10 are able to improve T cell migration into the sites of inflammation (262).

Moreover, it has been found that anti-LN treatment significantly reduced the migration of peripheral lymphocytes into the allograft. This observation implies that LN may play a crucial role in lymphocyte traffic, involved in immunoreactivity of the allograft (263) and allograft rejection (264). In another study, LNs have been determined to be able to influence immunocompetent cells and possibly play an important role in overcoming the allograft acute rejection (265). Indeed, LNs have been observed to play a key role in T cell migration (263), (266) and T cell differentiation (267).

Recently, ECM including LNs, has been suggested to play an important role in I/R injury and organ allograft rejection. The level of LN in plasma was significantly increased after reperfusion and the anti-LN staining enhanced as well in the basement membrane of small bowel in a rat transplant model. This enhanced staining was also observed during the occurrence of graft rejection (194) In addition, it was found that elevated LN was correlated significantly with the extent of preservation and reperfusion injury in human liver transplants. These ongoing changes in basement membrane may increase the risk of subsequent early

allograft rejection (268). Thus, investigation of levels of LN may be of value for predicting the development of allograft rejection.

However, the change in patterns of LN in brain and kidney are different from those observed after ischemia and reperfusion in the gut or liver. The LN fluorescence intensity was found to decreased in the basal lamina components following cerebral I/R. The loss of LN and other components in basement membrane were considered to be responsible for the disruption of microvascular integrity and increased vascular permeability (269). In kidney I/R injury, LN in tubular basement membrane showed a dramatic decrease after 18 h of reperfusion, which persisted for 48 h. This was followed by a marked increase up until day 5 (204). These results imply that the alterations of LN is tissue specific and time dependent after I/R. Alterations of LN are also temperature dependent during ischemia. The changes in LN were more prominent during cold ischemia than those during warm ischemia in small bowel (270). LN in the basement membrane of skeletal muscle found to be degraded after moderate ischemia without reperfusion. This degradation is closely associated with the up-regulation of matrix metalloproteinases, MMP-2 and MMP-9 (271). Thereby, modulation of the expression of MMPs could provide a new therapeutic target for critical skeletal muscle ischemia injury.

Furthermore, it has been determined that there are some interactions between LN and cytokines. For example, TNF-α may function together with LN to strengthen cellular binding to the ECM and promote immune cell recruitment to inflammatory site (272).

In summary, LN is another multifunctional glycoprotein and major component of extracellular matrix. Different isoforms of LN were found to play a role in the development of certain disease. Alterations of LN were also observed during ischemia and reperfusion injury. The administration of LN peptide was demonstrated to ameliorate ischemia-induced tissue

injury. In addition, LN was found to participate in allograft immunoreactivity and graft rejection.

1.2.9 Remote organ lung injury after lower torso I/R.

Remote organ injury following lower torso I/R is associated with high rates of morbidity and mortality. This injury manifests as adult respiratory distress syndrome (ARDS), renal failure and liver dysfunction (273), (274), (275). Lung is the distant target organ most frequently affected. Lung injury is characterised by progressive hypoxemia, pulmonary hypertension, increased pulmonary vascular permeability, pulmonary edema and neutrophil sequestration (273), (276), (65).

Lower torso I/R is a common clinical event, which frequently occurs in vascular surgery, such as in elective and ruptured abdominal aortic aneurysm repair. A number of studies have been conducted to investigate the mechanisms of the remote lung injury associated with lower torso I/R, implicating humoral mediators during I/R in playing a pivotal role in pathogenesis of lung injury. The injury is neutrophil-mediated with the destruction of the endothelial basement membrane. Immuno-depletion of neutrophils before the ischemic insult was shown to moderate both the local and remote organ injury in animal models (277), (278). The basement membrane of the capillary endothelium and the alveolar epithelium is a complex of type IV collagen and other proteins. MMPs and serine proteases are the primary neutrophil products that may degrade the basement membrane. Oxygen free radicals are generated and released from the ischemic tissue and lead to peroxidation of lipid cellular membrane and production of Tx A2, LTB4 (279), (30), (66). Interleukins such as IL-10, TNF-α are also produced and released and complement activation also occurrs during ischemia and reperfusion (280). These chemoattractants and cytokines can activate the circulating neutrophils and facilitate the neutrophil-endothelial cell interaction via the selectin family of

adhesion molecules (281), (34), (282)) and result in the adherence, migration and sequestration of neutrophils into interstitium (283), therefore leading to an increase in microvascular permeability and extravasation of albumin (284).

Complement inhibition by using soluble recombinant form of complement receptor type 1 (sCR1) has been successfully shown to ameliorate local and remote organ injury after skeletal muscle and gut I/R (285), (286). Remote lung injury after hind limb I/R was also reported to be selectin dependent. Blockade of selectin using selectin antibodies or recombinant soluble selectin glycoprotein ligand 1, was demonstrated to reduce remote lung injury (287), (283). In addition, Harkin et al (288) have found that rBPI $_{21,}$ which is a recombinant amino-terminal fragment of the bactericidal/permeability-increasing protein (BPI), can reduce endotoxemia and cytokine production, therefore attenuating circulating neutrophil priming, and ameliorating the remote acute pulmonary dysfunction after lower limb ischemia-reperfusion. Furthermore, activated neutrophils can release oxygen free radicals and proteolytic enzymes, thereby degrading and remodelling the extracellular matrix, resulting in the destruction of broncho-alveolar basement membrane (283), (289), (290).

In recent studies, upregulation of MMPs was identified to contribute to acute lung injury in several pathological processes. Increased expression of MMP-1, MMP-2, and MMP-9 was detected in the lungs of patients with idiopathic pulmonary fibrosis and histocytosis X (291), (292). Increased MMP-9 activity and mRNA expression were observed in lung tissue following ischemia and reperfusion. This increased MMP-9 was contributed by leukocytes recruited into the pulmonary interstitum (293). In patients with adult respiratory distress syndrome and asthma, over-expression of MMP-9 and TIMP-1 were demonstrated in the bronchoalveolar lavage fluids (294), (295). In a model of airway injury, MMP-7 (matrilysin)

expression was up regulated in migrating epithelial cells and the activity of this proteinase is required for repair of airway wounds (296). The level of MMPs correlates directly with an increase in the concentration of degradation products of type IV collagen within the basement membrane (297). The effect of inhibition of matrix metalloproteinase by chemically modified tetracyclines in lung injury following cardiopulmonary bypass was investigated in a pig model (298). It was found following administration of tetracycline 3 (COL-3) that levels of both elastase and MMP-9 and MMP-2 activity were reduced, associated with decreased neutrophil infiltration into the pulmonary interstitium and decreased extracapillary extravasation of protein. This prevention of lung injury is due not only to inhibition of MMPs, but also to the reduction of neutrophil infiltration. Likewise, Tobias et al (299) demonstrated up-regulation of MMP-9 in lung tissue in acute pancreatitis and this increased expression was colocalized with transmigrated neutrophils. MMP inhibition by administration of batimastat (BB-94), was recognised to reduce neutrophil transmigration and alveolar capillary permeability in pancreatitis-associated lung injury. In abdominal sepsis induced lung injury, increased serine protease activity was demonstrated in circulating leukocytes and a substantial increase in the spontaneous release of oxygen radicals by circulating granulocytes was also observed, suggesting that systemic priming of granulocytes and increased production of toxic neutrophil products may be critical for the development of organ injury (300). The pro-inflammatory mediators IL-1ß and TNF-α were speculated to be potent stimulants for MMP-9 release from neutrophils (301). These results suggest that up-regulation of MMPs may play a central role in acute distant lung injury. This elevated activity of MMPs is induced by pro-inflammatory cytokines. Thus, inhibition of MMP activity may be a new therapeutic target to reduce the lung injury. Previous work in our laboratory has identified that the levels of MMP-2 and MMP-9 were elevated after 4 bilateral hind limb ischemia with shorter times reperfusion and returned to lower levels following 72 h reperfusion (302). This result implies that over production of MMPs may play a role in distant lung injury after lower torso I/R.

It is clear that lower torso I/R can initiate a systemic inflammatory response, which is characterised by the production of proinflammatory cytokines, release of free oxygen radicals and adhesion molecules, and activation of circulating neutrophils. These activated neutrophils can be sequestered into the lung tissue via activation of selectins and adhesion molecules. Following stimulation by cytokines, activated neutrophils produce matrix metalloproteinases and serine proteinase, which degrade the basement membrane. The progression of this damage will inevitably result in the increase of vascular permeability, the extravasation of albumin into the bronchi-alveoli and finally, causing pulmonary insufficiency.

1.2.10 Defence strategies for I/R injury

Based on the studies of the mechanisms of I/R injury, a number of therapeutic strategies have been introdued to ameliorate this unavoidable injury. Antioxidation and scavenging of ROS is one of the major targets for ameliorating I/R injury. Glycine infusion has been shown to have a cytoprotective effects on skeletal muscle I/R injury, leading to less muscular edema and necrosis (303). The mechanism of protective effect is that glycine can promote the formation of phosphocreatine (Pcr), which is an energy source for cells, and therefore preserve mitochondria integrity and maintain the oxidative-phosphorylation pathway, resulting in resistance against the effects of oxygen radicals, tumor necrosis factor and metabolic acidosis. These protective effects of glycine have also been observed in kidney undergoing I/R injury (304), (305). Protective effects were also observed in skeletal muscle I/R injury following administration of adenosine, resulting in overproduction of nitric oxide and down regulation of TNF-α (306). M40401, a highly active SOD mimetic, has a protective effects in splanchnic ischemia and reperfusion injury by reducing lipid peroxidaton and inhibiting of peroxynitrite production (307). The bioflavonoid quercetin was demonstrated to be useful in protecting skeletal muscle against I/R injury. It can prevent excessive accumulation of superoxide, preserve the concentration of nitric oxide at a sufficient level to maintain vasorelaxation in the surrounding smooth muscles and inhibit platelet aggregation and adhesion within the lumen.

Moreover, it may increase the total nitric oxide concentration by scavenging superoxide in the endothelial cells (308).

Vitamin E is a powerful antioxidant, which is able to reduce the extent of peroxidation-related I/R injury. Most studies have shown that vitamin E can enhance cardiac function and recovery after a period of experimental I/R or after coronary artery bypass (309), (310). It has also been found that there was a marked consumption of vitamin E in abdominal aortic surgery including cross clamping of the aorta. Supplementary administration of vitamin E to patients undergoing abdominal aortic repair was determined to have a protective effect against I/R. The mechanism of this effect is not only due to direct effects of the antioxidant, but also due to limiting neutrophil infiltration into the tissues during the period of ischemia and reperfusion (311), (312).

Furthermore, Allopurinol has been shown to protect skeletal muscle against I/R injury. This is related to the inhibition of free oxygen radical generation rather than interference with purine salvage (313). Pyruvate, is a 3-carbon compound physiologically present in tissues and used by the cells as energy substrate during anaerobic glycolysis. Pyruvate has been shown to act as an ROI scavenger by reacting with hydrogen peroxide to form water and carbon dioxide, thereby preventing the formation of the toxic hydroxyl ion and inhibiting superoxide formation (314). The protective role of Pyruvate after I/R injury has been shown in small bowel, kidney and liver (315), (316), (317). Propionyl-L-carnitine, an acyl derivative of carnitine involved in fatty acid oxidation pathway and adenosine 5'-triphosphate (ATP) generation of mitochondria, has been shown to lower lipid peroxidation and free radical generation and to be able to preserve tubular cell structure after renal I/R (318)). Guanosine was observed to protect against renal ischemic injury by replenishing GIP stores and preventing tubular apoptosis (319). In addition, L-arginine and glutathione have both been shown to be protective against oxygen radical-induced I/R injury (320), (321). Insulin has

been determined to reduce postischemic myocardial apoptotic death through phosphorylation of eNOS and the concurrent increase of NO production (321). Similarly, a protective effect of insulin was observed in kidney after I/R injury (322).

Iinhibition of the production and binding of proinflammatory cytokines should be another mechanism for reducing I/R injury. IL-1 receptor antagonist (IL-1ra) has been shown to inhibit the effects of IL-1α and IL-1β, leading to attenuated inflammatory injury during I/R, and to protect cells against IL-1-induced apoptosis. It has been observed that IL-1ra gene transfection protect myocardium from I/R injury shown as reduced inflammatory response and decreased apoptosis (166). Administration of C5a receptor antagonist or blockade of selectin has also been observed to significantly reduce ischemia and reperfusion injury (323), (324). IL-10, an anti-inflammatory cytokine has been found to ameliorate I/R injury to the lung (325), hind limb (326), kidney (327), and heart (328). This cytokine acts by inhibition of TNF-α, ICAM-1 and leukocyte activation.

Inhibition of caspase-3 has been observed to upregulate bcl-2 expression and down-regulate TNF-α, reducing cardiac allograft damage from I/R injury. This result may indicate a greater role for the direct antioxidant effects of bcl-2 (329). More interestingly, pretreatment with low-dose cyclosporine A (CsA) or tacrolimus (FK 506) was shown to prevent subsequent I/R injury in the liver, brain, heart, small bowel, lung and kidney (330), (331). The mechanism of these protective effects may involve the inhibition of NF-KB, a central transcription factor mediating inflammatory injury and also induction of hsp 70 expression (331), (330).

Having demonstrated the importance of MMPs in tissue ischemia and reperfusion injury, it is likely that inhibition of MMP activity may result in protective effects during ischemia and reperfusion. A few studies have emerged to show that inhibition of MMPs either by MMP antibody or doxycycline significantly decreased ischemic/reperfused organ injury and

improved organ function (332), (333)). A previous study in our laboratory has also shown that doxycycline could partially inhibit the activity of MMP-9 and MMP-2 and subsequently reduce the degradation of collagen IV in the basement membrane of skeletal muscle (302). Further studies are still needed to investigate the effects of inhibition of MMPs on ischemia and reperfusion injury.

In conclusion, ischemia and reperfusion injury is a very complicated pathological event. Although many agents have been shown to offer protective effects against I/R injury in experiment models, few have been observed to be clinically effective. Further investigations are still required to explore the mechanisms of I/R injury and identify effective strategies to modify or avoid this injury.

1.3. Matrix metalloproteinases (MMPs)

Matrix metalloproteinases (MMPs) are a family of zinc-dependent enzymes that have a crucial role in regulation of extracellular matrix. Previous studies have identified that these enzymes, together with tissue inhibitors of metalloproteinases (TIMPs), have been involved in many pathophysiological processes including embryonic development, cancer invasion and metastasis, vascular diseases, arthritis, wound healing, and I/R injury (334), (335), (333).

MMPs have many characters in common as follows; they are secreted in a latent form and activated by removal of the amino-terminal propeptide-sequence; they contain a zinc ion at the active site and thus are inhibited by the zinc chealtor, ethylenediamenetetraacetic acid (EDTA); they have proteolytic activity against components of the extracellular matrix, and their activity can be inhibited by tissue inhibitors of metalloproteinase (TIMPs) (336). In addition, it has been reported that some MMPs are involved in the processing of cytokines such as TNF-α (337). MMPs have been divided into four subfamilies according to their

substrates and structures, namely collagenases, gelatinases, stromelysins and membrane-type MMPs.

1.3.1 Role of Matrix Metalloproteinases (MMPs) in I/R injury

Among the consequences resulting from the exposure of tissue to ischemia and reperfusion is increased vascular permeability and edema, involving degradation of vascular basement membrane and extracellular matrix. MMPs have been suggested as participants in this process. It has been observed that the expression and production of MMP-2 by vascular endothelial cells is upregulated after prolonged hypoxia and reoxygenation further increases its expression (338). The up-regulation of MMP-2 gene expression and its protein activity indicate that MMP-2 is of prime importance in the reponse of endothelial cells to hypoxia/ischemia.

The expression of MMPs after ischemia and reperfusion has also been studied *in vivo*. Enhanced activity of MMPs, primarily MMP-2 and MMP-9 coupled with a reduction in TIMP expression, has been demonstrated in a variety of models of brain and heart ischemia. Some investigations have found that both pro-MMP-9 and pro-MMP-2 are markedly increased after focal cerebral ischemia and reperfusion and the peak of elevation is at different times (339), (340). The early appearance of activated MMP-2 and MMP-9 is associated with an increase in blood-brain barrier permeability and hemorrhagic transformation (341). The disruption of the blood-brain barrier during focal cerebral ischemia is also considered to be due to activation of metalloproteinases (342). The increased activity of MMPs contribute to degradation of vascular basement membrane and extracellular matrix, thus enhancing microvascular permeability and albumin extravasation, even subsequent hemorrhage (343), (269). Differential expression of MMPs during cerebral ischemia was observed by Rosenberg et al (344) in which MMP-9 and MMP-3 were produced, and MMP-3 may activate pro-MMP-9. Elevation of MMP-2 was detected early by Heo et al (341) in focal cerebral ischemia

and this elevation was highly correlated with the extent of neuronal injury. Furthermore, the role of MMP-9 in ischemic cerebral injury was demonstrated in a mouse model by Gursoy-Ozdemir and his colleagues (345). Mice treated with N-nitro-1-arginine (L-NA), an inhibitor of nonselective nitric oxide synthase (NOS) showed significantly reduced levels of vascular damage, correlating with decreased MMP-9 expression. Decreased expression of MMP-9 was consistent with better-preserved vascular integrity and reduced infarct volume. Moreover, up-regulation of MMPs was suggested to facilitate cell migration and angiogenesis after I/R injury (346).

In ischemic myocardium, it has been observed that increased activity of MMPs was accompanied by decreased levels of myocardial collagen (347), (348). Robert and colleagues (349) have found that endogenous procollagenase could be activated by the ischemic insult, leading to degradation of extracellular matrix and thus resulting in a decrease in cardiac collagen and enlargement of the heart. Accordingly, Etoh et al (350) demonstrated that myocardial MMP activation could occur within the myocardial infarction region during the early post ischemia period in the absence of reperfusion. The role of MMPs in myocardial dysfunction after I/R was further studied by Cheung et al (333). They found that the release of MMPs from the heart into the coronary effluent was immediately increased as a consequence of ischemia and reperfusion. The production of pro-MMP-2 and active MMP-2 peaked during the first and fifth minutes of reperfusion and the degree of elevation of MMP-2 correlatd with the duration of ischemia. The over-expression of MMP-2 was associated with impaired mechanical function of the heart. In contrast, inhibition of MMP-2 by MMP antibody or doxycycline was able to promote recovery of heart function following I/R

It has been found that reactive oxygen species can activate pro-MMP-2 in human smooth muscle cells and inactivate TIMP-1 *in vitro* (351), (352). Therefore, the increased biosynthsis of peroxynitrite and decreased TIMP-1 gene expression may contribute to the up-regulation of

MMP activity observed during heart ischemia and reperfusion (353), (354). Moreover, an elevation of MMP-9 was observed by Lindsey et al (355) both in lymph and reperfused myocardium, with MMP-9 localized to the perineutrophil area, suggesting activation might be initiated by neutrophils adhering to the extracellular matrix during the first hour of reperfusion. Potential beneficial effects of early MMP-9 activation include the removal of matrix and necrotic myocytes, releasing growth factors and cell surface receptors, remodeling of the extracellular matrix for scar formation, processing inflammatory mediators such as IL-1 and influencing angiogenesis (356), (357), (358), (346)). The more focused secretion and activation of MMP-9 might obviate the danger of inappropriate proteolytic degradation (355). During the healing phase, damaged collagen must first be degraded and removed before necrotic myocytes can be resorbed and new collagen generated to form a scar. Expression of MMP-9 could clearly play a role in monitoring the timing, localization, and levels of matrix degradation to optimize events of remodeling after I/R injury (359).

The alterations of MMPs in lung tissue after I/R were investigated by Soccal et al (289) and Yano et al (293). MMP-9 activity and gene expression were low during ischemia and then increased upon reperfusion, while no changes or only smaller increase for MMP-2 were observed during I/R. TIMP-1 gene expression was low during ischemia and during the early phase of reperfusion, then was dramaticlly increased at the late phase of reperfusion. Expression of MMPs contributes to the degradation of extracellular matrix, resulting in the increase in alveolar-capillary permeability and lung damage. The production of MMP-9 is most widely found in inflammatory cells especially neutrophils, monocytes/macrophages and T lymphocytes, while MMP-2 is constitutively expressed by fibroblasts, endothelial cells and vascular smooth muscle cells (360), (361). Bronchial and type II alveolar epithelial cells produce both gelatinases (362). Increased MMP-9 activity may be induced by the elevation of pro-inflammatory cytokines such as tumor necrosis factor TNF-α and IL-1ß (363). In recent studies, MMPs have been shown to facilitate shedding of molecules such as ICAM-1 and L-

selectin, from the cell surface, Their release might decrease the attachment of neutrophils to the endothelium and ameliorate I/R-induced injury (364), (365). The increase in TIMP-1 expression observed during the late phase of reperfusion may compensate for the MMP-9 activity and reduce the extent of lung injury (293).

MMP-2 has also been determined to play an important role in renal damage following I/R. It was found that gene expression of MMP-2 was significantly increased at an early stage of ischemia/reperfusion and then was decreased progressively, associated with increasing expression of TIMP-1, as well as an increase in gene expression of TGF-β. These changes may shift the balance of extracellular matrix towards accumulation, leading to fibrosis and development of proteinuria (366).

Apart from MMP-2, Meprin A has been determined to be another major matrix degrading enzyme in renal tubules, and is localized in the corticomedullary part of the proximal convoluted tubules in kidney (367). After I/R, meprin A undergoes translocation to reach and adhere to the tubular basement membrane, degrading the laminin-nidogen complex and destroying the tubular basement membrane. The increase in meprin A and destruction of tubular basement membrane may lead to acute renal failure following ischemia–reperfusion injury (367). Moreover, it has been demonstrated that mice with low levels of renal tubular meprin A have less ischemia induced renal damage than those with normal levels of meprin A (368). Therefore, it is suggested that meprin A play a crucial role in renal I/R injury.

The role of MMPs in the skeletal muscle I/R injury has been studied in our laboratory. Initial experiments have shown that ischemia and reperfusion of rat skeletal muscle resulted in upregulation of MMP-2 and MMP-9, both in local skeletal muscle and remote organs such as lung, correlating with degradation of interstitial collagen IV (302). The production of MMP-9 was attributed to infiltrating leukocytes, while the site of production of MMP-2 was not clear,

possibly from skeletal muscle satellite cells (369), (370). Doxycycline, an inhibitor of MMPs was able to reduce the activity of MMP-2 and MMP-9 and protect against collagen IV breakdown (302).

In general, it has been observed that MMPs together with TIMPs play a pivotal role during ischemia and reperfusion injury. Elevated expression of MMPs contributes to the disruption of basement membrane, increasing vascular permeability and tissue edema. In addition, upregulation of MMPs combined with adhesive molecules facilitates neutrophil adhesion to and transmigration through endothelial cells into the target site, improving tissue remodeling. It seems clear that production of MMP-9 can be attributed to infiltrating leukocytes. Alterations of MMPs and TIMPs result in the imbalance of degradation and synthesis of extracellular matrix, in favour of accumulation of extracellular matrix at the later stage of reperfusion, leading to tissue fibrosis. Inhibition of the activity of MMPs is able to diminish tissue injury after I/R. Therefore, modulation of the activity of MMPs following I/R could be a new therapeutic strategy for ameliorating tissue injury.

1.3.2 The role of MMPs in vascular diseases

The blood vessel wall is an integrated functional component of the circulatory system that is continually remodeling in response to hemodynamic changes and diseases. The endothelium releases active mediators, such as endothelin, cytokines and nitric oxide which have immediate vasoactive properties and longer-term trophic effects on the medial smooth muscle cells (SMCs) that actively control vessel wall tension and synthesize the major structural components: collagens type I, III, IV and V, elastin, proteoglycans and glycoproteins. These components interact to form a complex network, which gives the blood vessels elastic physical characteristics. The matrix therefore is a dynamic structure rather than being merely scaffolding for the surrounding cells. Matrix integrity involves the synthesis and degradation of these components under certain conditions.

The most striking histological feature of abdominal aortic aneurysms is the fragmentation and relative decrease in medial elastin and cellular inflammatory response (371), (372), suggesting those MMPs and their inhibitors, the TIMPs may play a key role during this process. A number of studies have determined that MMPs play an important role in the formation and expansion of abdominal aortic aneurysms (AAA). MMP-1, MMP-2 and MMP-9 have each been identified in aortic aneurysmal tissues proposed as etiologic agents for this disease (373), (374), (375). Natalia et al (376) have found that increased mRNA expression of MMP-1, MMP-9 and MMP/TIMP ratios in aneurysmal tissues as compared with normal aortas may shift the balance towards matrix degradation, leading to the formation of aortic aneurysms. In addition, MMP-9 was identified to be the predominant metalloproteinase expressed in aneurysms. MMP-9 mRNA levels have been shown to be 20 times and 2 times higher respectively than those of MMP-1 and MMP-2. These elevations in MMP and TIMP-1 mRNA are corresponded to the increases in protein levels and activity. Both mRNA and protein levels of MMP-2 and MMP-9 were also found to be elevated within aneurysmal tissues in other studies (377), (378), (379). Davis et al (335) found that the precursor of MMP-2 in AAA is largely activated locally and binds to the tissue matrix tightly, facilitating matrix degradation. Such activation may be mediated by recently characterised plasma membrane-anchored MT-MMPs (380), other proteases MMP-1 and MMP-7 (381) or reactive oxygen species (351).

In recent studies, it was identified that MT1-MMP and TIMP-2 are both present in the aneurysm and normal arterial wall in the same distribution as MMP-2, suggesting an effect of MT1-MMP complexing with TIMP-2 on the activation of MMP-2 in the media layer (382), (383). Nollendorfs et al (384) also demonstrated that both mRNA and protein of MT-1-MMP are increased in AAA tissue and suggested the importance of MT-1-MMP in AAA pathogenesis was through its ability to activate pro-MMP-2. MMP-2 was produced by

mesenchymal cells and production was most prominent when mesenchymal cells were surrounded by inflammatory cells, whereas MMP-9 was produced by macrophages infiltrating into the vessel wall (385), (386). Patel et al (387) found that aneurysm-derived SMCs had greater elastolytic activity than cells from age-matched normal aortic tissue.

Many cytokines that are identified within AAA tissue secreted from macrophages, have been shown to enhance MMP production by vascular smooth muscle cells (SMCs) (388), (389). Both MMP-9 and MMP-2 have potent elastolytic ability, implicating a major role in the remodeling that occurs with AAA. MMP-2 is a more active elastase than is MMP-9 and has the ability to degrade interstitial collagen (390). These observations support a role for MMP-2 in the medial elastolysis that accompanies aneurysm formation, causing fragmentation of elastin and the initiation of a proteolytic inflammatory reaction, leading to aneurysm degeneration. Moreover, Annabi et al (391) have demonstrated that chronic aortic wall inflammation was also mediated by macrophage infiltration and production of active MMP-1 and MMP-12. The altered MT1-MMP proteolytic turnover and differential regulation of TIMP-1 was also observed by Annabi et al (391), suggesting that tight regulatory mechanisms are involved in the molecular regulation of MMP activation in the pathogenesis of AAAs.

Carrell et al (392) have detected mRNA expression of 14 MMPs and 4 TIMPs in samples of aortic wall from the patients with AAA and aortic occlusive disease (AOD). They found that MMP-3 and TIMP-3 were significantly over-expressed in the AAA samples compared to AOD, while a wide range of other MMPs and MT-MMPs were found at similar levels in both AAA and AOD. This study suggests that MMP-3 (Stromelysin-1) may also be involved in aneurysm pathogenesis.

Based on the proteolytic effects of over-expressed MMPs, particularly MMP-2, MMP-9 and MMP-3 on formation of AAA, studies have been conducted to determine if MMP inhibition

could control the development and progression of AAA. Marimastat, an inhibitor of a range of MMPs, especially MMP-2 and MMP-9 (393), has been shown to inhibit elastin degradation and reduce levels of active MMP-2 within aortic tissue cultures (394). Batimastat, an anticancer agent and MMP inhibitor, has been demonstrated to restrict the expansion of AAA in a rat model (395). Clinically, doxycycline, an inhibitor of matrix metalloproteinases, reduced the growth rates of small abdominal aortic aneurysms. The aneurysm expansion rate in the doxycycline group was significantly lower than that in the placebo group during 18 months follow-up in a pilot study (396).

Moreover, matrix metalloproteinases are known to be expressed in human atherosclerotic plaques by both SMCs and foam cells (397), (388). Advanced human atherosclerotic plaques contain chronic inflammatory infiltrates of macrophages and T lymphocytes with a lipid core covered by a fibrous cap. These macrophages are certainly potent producers of MMP-1,-3 and –9 (398), (399). Plaque instability, such as ulceration of the fibrous cap, intraplaque hemorrhage or plaque rupture is responsible for the complications of atherosclerosis, resulting in the onset of heart ischemia or stroke (400). Recent studies have shown that plaque instability is related to the release of proteolytic enzymes, in particular matrix metalloproteinases (401), (402).

MMP-1 was found to be over-expressed by several cell types in human carotid atherosclerosis and this was correlated to the histopathological evidence of plaque instability. MMP-1 degrades the major structural collagens of the plaque, leading to plaque expansion, rupture, and hemorrhage (403). Henney et al (397) demonstrated the presence of mRNA for MMP-3 in coronary plaques. Loftus et al (404) found that the concentration, production and expression of MMP-9 was significantly higher in unstable carotid plaques compared with plaques from less symptomatic patients, while there were no differences in the levels of MMP-1, MMP-2 and MMP-3. In addition, a sharp but transient increase in plasma levels of

MMP-9 was detected in patients with acute coronary syndromes (405). These results suggest that MMP-9 may play an important role in acute plaque disruption, leading to the onset of symptoms. Furthermore, the expression of MMP-8 mRNA and protein were detected in human atheroma *in situ*. This MMP-8 colocalized with cleaved, but not intact, type 1 collagen within the shoulder region of the plaque, a frequent site of rupture (406). This evidence suggests that MMP-8 may also exert an effect in rupture of atherosclerotic plaques. Fu et al (407) also identified that hypochlorous acid (HOCl) generated by myeloperoxidase may activate MMP-7, which, with myeloperoxidase, was colocalized to lipid-laden macrophages in human atherosclerotic lesions in the artery wall, contributing to plaque rupture.

Vein graft stenosis appears to be associated with increased expression of MMP-9 and increased MMP-2 activation (408). In one study (409) MMPs were found to be critical for smooth muscle cells migration and proliferation, which serve as the cellular basis for neointimal proliferation *in vivo*. Recently, the TIMPs have also been implicated in the pathogenesis of vein graft disease. The expression of TIMP-1, -2, -3 was identified during neointima formation in organ cultures of human saphenous veins (410). This observation suggests that TIMPs may have a potential role in graft vein neointimal proliferation. Vein grafts transfected with the gene for TIMP-3 showed an 84% reduction in neointima at 14 days and a 58% reduction at 28 days (411). Transfer of the TIMP-1 gene inhibited smooth muscle cell migration and neointima formation in human saphenous vein (412). Gene therapy will possibly be a new approach to the vein graft restenosis.

The role of MMPs in iatrogenic vascular pathogenesis has also been investigated. An induction of collagenase and stromelysin gene expression was observed in response to mechanical injury in vascular SMCs (413). MMP-9 was induced at day 3 and MMP-2 at day 7 and both enzymes persisted at elevated levels for up to 21 days after angioplasty in a pig model (414). Other studies have also shown a transient increase in MMPs activity after injury

during balloon angioplasty injury (415), (416). These investigations suggest that MMPs play an important role in vascular tissue remodeling and neointima formation after balloon angioplasty. Therefore, MMP inhibition may prevent the vascular restenosis after angioplasty. Batimastat, an inhibitor of MMP activity, has been shown to reduce significantly late lumen loss significantly after balloon angioplasty (417).

1.3.3 Matrilysin (MMP-7)

Matrilysin (MMP-7) is a member of the matrix metalloproteinase (MMP) family, which is believed to play an important role in both physiologic and pathologic conditions. It was first discovered in the involuting rat uterus and has a molecular weight pro-form 28 kDa and active-form 19 kDa (418). It is the smallest known MMP and can degrade a wide range of gelatins, proteoglycans, and glycoproteins of the matrix (418), including fibronectin, collagen type IV, laminin and entactin (419), (420). MMP-7 unlike other MMPs that are expressed or released only in response to injury, disease, or inflammation, is expressed by non-injured, non-inflamed exocrine and mucosal epithelium in most adult tissues. The production of MMP-7 appears to be limited only to a few normal human cell types including glandular epithelium of the pancreas, liver, breast, intestine and urogenital tissues (421), (422) mononuclear phagocytes, and renal mesangial cells (423). Moreover, MMP-7 expression has only been demonstrated *in vivo* in glandular epithelium (424), (425) and in human endometrium (426). Its expression in exocrine epithelial cells suggested that it may participate in the normal function of exocrine glands by preventing glandular obstruction (421). It has also been demonstrated that MMP-7 can activate several other MMPs, such as collagenase and MMP-2 (418), (427).

Numerous studies have found that up-regulation of MMP-7 is related to tumour invasion and metastasis. Overexpression of MMP-7 mRNA was observed in 61% of gastric cancer specimens. Immunohistochemical studies revealed that MMP-7 was mainly expressed in

cancer cells but not expressed on other normal cells. In addition, expression of MMP-7 was shown significantly higher in the gastric cancers of subserosa or beyond than in those within the submucosal layer. These investigations suggested that MMP-7 may directly and strongly contribute to the invasion step of human gastric cancer. Furthermore, expression of MMP-7, which was increased in gastric cancer cells by DNA transfection, rendered the gastric cancer cell more invasive *in vitro* (428), (429). Honda and colleagues (430) also found that the enhanced production of MMP-7 and its activation in gastric cancinoma cells are implicated in invasion and metastasis of human carcinomas. Therefore, MMP-7 may be a useful marker for determining the biological aggressiveness of gastric carcinoma

Enhanced secretion and activation of MMP-7 have also been observed during colorectal carcinogenesis. The levels of MMP-7 correlated positively with invasiveness in an *in vitro* assay (431). Down-regulation of MMP-7 by the introduction of anti-sense MMP-7 in BM 314 colon cancer cells caused these cells to become less invasive (432). This observation implies that MMP-7 may contribute to invasiveness of colon cancer cells. MMP-7 mRNA has also been detected in tumor-positive lymph nodes. Ichikawa et al (433) found that all 10 histological–positive lymph nodes were positive using sensitive RT-PCR techniques for MMP-7, whereas only eight of 60 histological-negative lymph nodes were positive for MMP-7. Thus an RT-PCR assay for MMP-7 may be a sensitive method for screening occult metastases in patients with colon cancer and may complement histologic examination. Moreover, the expression of MMP-7 mRNA and protein was also detected in endothelial cells of arterioles and venules adjacent to MMP-7 positive tumors, while endothelial cell adjacent to MMP-7-negtive tumors and those in normal tissues were negative for MMP-7. This endothelial cell-derived MMP-7 may contribute to tumor angiogenesis and tumor metastasis (434). In addition, Mori et al (435) demonstrated that MMP-7 mRNA levels were greater in the colorectal carcinoma than in paired adjacent normal colonic or rectal mucosa. The expression of MMP-7 mRNA in tumor tissues was also increased with increasing Duke's

stage and was greatest in the metastatic liver lesions. These findings imply that the over-expression of MMP-7 in human colorectal carcinomas is a useful marker for biologic aggressiveness.

Furthermore, expression of MMP-7 has been found in other tumor cells including lung, prostate, leukaemia, and multiple myeloma. Expression of MMP-7 in tumor cells has been considered to be related to tumor progression and metastasis (436), (437), (438), (427).

MMP-7 has also been suggested to play an important role in the differentiation of organ development. Wilson (422) found that MMP-7 was expressed in the juvenile small intestine and reproductive organs during postnatal development. The accumulation of significant levels of MMP-7 appeared to correlate with organ maturation. It was shown that upregulation of MMP-7 altered the integrity of the extracellular matrix and thereby induced cellular differentiation and destruction in a tissue-specific manner (439).

The prodution of MMP-7 in normal epithelium implies that this enzyme serves a common homeostatic function among various types of epithelia. Some observations suggest a role of MMP-7 in innate immunity of epithelium. Tissues in which MMP-7 is expressed are open to the environment and therefore are vulnerable to bacterial exposure. It has been demonstrated that acute infection of human colon, bladder, and lung carcinoma cells, primary human tracheal epithelial cells and human tracheal explants with type1-piliated *Eschericha coli* mediated a marked and sustained induction of MMP-7 expression. Based on mRNA levels, MMP-7 expression increased as early as 2 hours after infection, continuing to rise 10 hours after bacteria were removed and remaining elevated at 48 hours after infection. Bacterial-mediated stimulation of MMP-7 is confined to mucosal epithelial cells. Bacterial exposure does not affect the expression of other MMPs and does not influence MMP-7 expression in other cell types such as macrophages, fibroblasts, and keratinocytes (296). In addition,

bacterial infection can cause activation of the zymogen form of MMP-7 that is selectively released at the apical surface (440). It was recently found that cryptdins are processed to their active forms by MMP-7 and a deficiency in this enzyme resulted in impaired bactericidal activity *in vi*tro and *in vivo*. It was observed that MMP-7-null mice cannot effectively kill pathogenic *E. coli* due to the lack of defensin activation by MMP-7 (441). It was therefore speculated that the expression of MMP-7 in epithelial cells, along with increasing display of epithelial defense molecules (defensins and cathelicidins) (442) may play a direct role in the first line of defense against infection.

Interestingly, MMP-7 was also expressed in the epithelium of peribronchial glands and conducting airways in normal lungs. It has been determined that MMP-7 was increased in migrating airway epithelial cells in wounded human and mouse trachea. The production of MMP-7 in conducting airways, its upregulation following injury, its induction by alveolar epithelium, and its secretion either apically or basally suggest that MMP-7 serves multiple functions in intact and injured lungs (443). Although MMP-7 is regulated by bacterial exposure, it is also likely that the production of MMP-7 is induced in response to injury. Infection can lead to injury that in turn provides an opportunity for infection. Dunsmore and co-workers (443) demonstrated that MMP-7 was expressed in injured trachea. In their study, they found epithelial cells migrated over the edge of the cut surface in an attempt to heal the wounded tissue. Low levels of MMP-7 protein were detected in airway epithelial cells and stronger staining was evident in ductal epithelial cells in fresh trachea. From days 1-5 of culture, airway epithelial cells at the margin of the tissue samples moved off the basement membrane and migrated progressively along the surface of the adjacent interstitial matrix. High levels of expression of MMP-7 were seen in all epithelial cells that had migrated away from the wound edge. A stronger signal for MMP-7 protein was seen in migrating cells in contact with the underlying interstitial matrix than in cells in the migratory front without obvious contact to the matrix. Moreover, MMP-7 was observed being released towards the

matrix from some of these strongly positive cells, suggesting MMP-7 may be acting on an extracellular protein to facilitate cell migration. The same pattern of MMP-7 expression was also identified in mouse tracheas following injury. These investigations support the idea that MMP-7 functions in repair of the airway epithelium and reepithelialization.

It has also been observed that both the gene expression and active form of MMP-7 protein were induced in animals exposed to combustion and ambient air particles. The alveolar macrophages and monocytes were the primary source of air pollution particle-induced MMP-7 expression (444). In addition, expression of MMP-7 was found to be involved the pathogenesis of idiopathic fibrosis and cystic fibrosis of the lungs (445).

Furthermore, the expression of MMP-7 has been observed in cerebral ischemic insult, with variable patterns of expression. MMP-7 expression was low up to 1 week after infarct, and then increased remarkably in conjunction with macrophages infiltration from 1 week up to 5 years. This finding suggested a role for MMP-7 as a mediator of blood-brain barrier breakdown and tissue destruction in cerebral ischaemic injury (446).

The biosynthesis of MMP-7 is modulated by a number of cytokines. It was found that IL-4, IL-10, and IFN-γ all inhibited the expression of MMP-7, while other cytokines such as IL-1, TNF-α, and IL-6 do not influence the production of MMP-7. Moreover, glucocorticoids and retinoids suppress MMP-7 biosynthesis (423), (447).

1.3.4 MMP-12

Human macrophage metalloelastase (HME, MMP-12) is another member of the stromelysin subgroup that was initially found in alveolar macrophages of cigarette smokers (448). Its molecule weight of pro-enzyme form is 54 kDa, while the active form of the enzyme is 22 kDa, with broad substrate specificity, being capable of degrading elastin, FN, vitronectin and

heparan, and chondroitin sulfates (449). It has been demonstrated that alveolar macrophages from rats produce a spectrum of MMPs, including MMP-12 that is similar to the spectrum of enzymes produced by human alveolar macrophages (450). However, the catalytic properties and natural substrate specificity of rat MMP-12 catalytic domain differ from those of human MMP-12. The purified rat MMP-12 catalytic domain was highly active in digesting substrates such as collagen-V, vitronectin and fibronectin, but not luaminin and albumin (451). The catalytic domain of human recombinant MMP-12 has been crystallised in complex with the broad-specificity inhibitor batimastat, revealing an overall fold similar to that of other MMPs. The active-site cleft of MMP-12 is well equipped to bind and efficiently cleave the AlaMetPheLeuGluAla sequence in the reactive-site loop of α1-proteinase inhibitor (α1-PI) (452). MMP-12 shares many substrates with matrilysin (MMP-7) due to similarities in contouring and in particular, a common surface hydrophobicity both inside and distant from the active site cleft (452). Ectopic or excessive MMP-12 proteolysis has been associated with several pathological conditions including vascular disease, cancer growth and metastasis, host defense against infection, chronic obstructive pulmonary disease, and gastrointestinal ulcerations.

Extensive remodeling of the extracellular matrix plays a critical role in the development, progression, and rupture in aneurysmal disease, which is characterised by chronic aortic wall inflammation and destruction of medial elastin. It has long been suspected that aneurysmal degeneration is mediated by one or more proteinases specifically capable of degrading insoluble elastin. It has been demonstrated that substantially greater amounts of MMP-12 are present in AAA tissue than in normal aorta, with high affinity to elastin fibers observed both *in vitro* and *in vivo* (453) (1). MMP-12 expression was localised to aneurysm- infiltrating macrophages within the degenerative media of the AAA. In contrast, it was not observed within the elastic media of either normal aorta or AOD tissues. These findings support the view that localised expression of elastolytic MMPs at the site of aortic tissue damage plays an

important role in the pathogenesis of aortic aneurysm disease. Inhibition of the activity of MMPs was observed to retard progression and limit expansion of experimental abdominal aortic aneurysms (453) (395). Similarly, it was observed that the expression and activity of MMP-12 was increased in AAA lesions from patients, which in turn, can also activate other MMPs such as pro-MMP-2. Therefore, the formation of AAA lesions could be considered to be due to a cascade of actions of MMPs including MMP-2, MMP-9 and MT1-MMP (391).

MMPs have also been identified in vulnerable areas of atherosclerotic lesions and may contribute to plaque instability through extracellular matrix degradation (454). Among MMPs identified in atherosclerotic lesions, human macrophage metalloelastase (MMP-12) is a major elastase, a macrophage-specific MMP with broad substrate specificity, which is able to degrade many components of extracellular matrix in atheromas. Increased expression of MMP-12 in atherosclerotic lesions is likely to be a critical step in the initiation and progression of the atherosclerotic cascade (455). In addition, it was observed that rupture frequently occurs over macrophage-rich areas near the shoulder of the plaque (456). Moreover, it has been found that MMP-12 was up regulated by several cytokines such as IL-1ß, TNF-α and GM-CSF and growth factors such as Platelet-derived growth factor-BB (PDGF-BB) and vascular endothelial growth factor (VEGF) (456), (457). On the other hand, the expression of MMP-12 mRNA has been observed to be inhibited by TGF-ß1 and this inhibition also occurs at the level of transcription (456).

It has been demonstrated that MMP-12 was an efficient angiostatin-producing enzyme that inhibits the proliferation of human microvascular endothelial cells and metastatic tumor cell growth. That is, MMP-12 is required for the production of angiostatin and the subsequent inhibition of endothelial cell proliferation and neovascularisation (458). Generally, tumor-derived MMPs have been well recognised as promoters of tumor growth both by degrading matrix barriers and by enhancing angiogenesis (459). The contribution of macrophages to

angiogenesis must then depend on the fine regulation and balance of pro-and anti-angiogenic factors. Moreover, Dong et al showed that MMP-12 was involved in the generation of the angiogenesis inhibitor, angiostatin from plasminogen (460). Tumor cell lines transfected with MMP-12 showed a reduced ability in growth and metastasis (461).

MMP-12 also appears to play a role in host defenses during a period of neutropenia. In the absence of MMP-12, mice subjected to radiation therapy followed by allogeneic mismatched bone marrow transplant (BMT) are prone to pulmonary hemorrhage, tissue necrosis, and bacterial infection. It has been determined that MMP-12 is also involved in macrophage-mediated killing of Gram-positive bacteria (462).

The proteolytic activity of MMP-12 is likely to contribute to the pathogenesis of pulmonary emphysema (463) (464). It has been found that mice without macrophage elastase failed to recruit macrophages to the lung tissues and did not develop lung destruction in response to cigarette smoke, while wild-type mice exposed to cigarette smoke developed inflammatory cell recruitment and dilatation and destruction of alveolar walls and alveolar ducts. These observations mirror the pathology of smoker's lungs, although human lungs also have destruction and dilatation of respiratory bronchioles. These findings suggest a primary role for macrophages and macrophage elastase in the development of emphysema induced by cigarette smoke (464). In addition, MMP-12 has been found to be an important mediator in immune complex-induced acute lung injury. It was observed that metalloelastase is necessary for the full development of acute alveolitis in this model of lung injury, whereas reduced injury was found in metalloelastase-deficient mice model (465). Moreover, the synthesis and secretion of MMP-12 by alveolar macrophages was stimulated by surfactant protein D (SP-D) (466).

The repair process after acute lung injury depends on the balance between deposition and breakdown of matrix molecules. MMP-12 has been found to be involved in this process. It has been shown that MMP-12 increased significantly during the acute phase of bleomycin-induced pulmonary fibrosis in animal experiment. MMP-12 is produced by activated macrophages and is capable of degrading elastin and collagen type IV, the components of the basement membrane. This activation appears to be associated with areas of hemorrhage (467) (468). In contrast, it has been observed that macrophages from MMP-12-deficient mice have a reduced capacity to degrade extracellular matrix protein, rendering them unable to penetrate basement membrane (468). Clinically, it was found that the secretion of MMP-12 by macrophages was associated with damaged areas in the lung (463).

The expression of MMPs has been demonstrated to be associated with gastrointestinal ulcerations, involving epithelial cell migration and remodeling of intestinal stroma (469). Macrophages are the major cell types known to express MMP-12 in adult tissues and these cells are crucial in the immune and inflammatory events ongoing in the intestinal mucosa. Abundant expression of MMP-12 was detected in macrophages of the inflamed lamina propria and the ulcer base just beneath the shedding epithelium of the intestinal wall particularly in samples of colitis ulcerosa. This result suggested that MMP-12 produced by macrophages might mainly cleave fibronectin or laminin, leading to epithelial cell shedding, because continuity of the basement membrane under the shedding epithelium was not disturbed based on type IV collagen staining (470).

In summary, MMP-12, also known as macrophage metalloelastase, is mainly produced by macrophages, facilitating the migration of macrophages during certain pathological conditions. Some studies have demonstrated that MMP-12 was involved in the pathogenesis of pulmonary emphysema, abdominal aortic aneurysms, and gastrointestinal ulcerations, through its ability to degrade basement membrane particularly elastin, fibronectin and

laminin. In addition, MMP-12 was determined to play a role in host defense systems, participating in the removal of Gram-positive bacteria. MMP-12 was also capable of inhibiting angiogenesis through the production of angiostatin and abolishing the tumor growth and metastasis.

1.4. Aims of the current studies

An animal model for ischemia and reperfusion has been established in our labarotory imitating the surgical procedure of abdominal aortic aneurysm repair. Previous work has demonstrated the degradation of collagen type IV in the basement membrane both in ischemic skeletal muscle and remote organs, associated with increased expression of MMP-9 and MMP-2 (511). To explore the further mechanisms of ischemia and reperfusion injury, the aims of present study are to investigate the alterations in fibronectin and laminin in the tissues and the expression of other caseinolytic MMPs after I/R injury.

CHAPTER 2

MATERIALS AND METHODS ESTABLISHMENT OF ANIMAL MODEL FOR ISCHEMIA AND REPERFUSION INJURY

2.1 Establishment of Rat model of bilateral hind limb ischemia and reperfusion.

Male Sprague-Dawley rats weighing 250-280 gram were used for the experiment. Anaesthesia was induced with 3.5% halothane (Zeneca Ltd. Cheshire, U.K.), 1L/min of nitrous oxide (Linde gas PTY. Ltd, Yennora, N.S.W. Australia) and 1L/min of oxygen (Linde gas PTY, Ltd) until the animal was asleep. Anaesthesia was maintained for 4hr using a Midget-3 anaesthetic apparatus, administering 1-1.5% halothane via a Fluotec-3 vaporizer (Cyprane Ltd, Keighley, U.K.), 0.6L/min of nitrous oxide and 1L/min of oxygen.

A rat model of skeletal muscle ischemia/reperfusion has been established in the surgical laboratory at The Queen Elizabeth Hospital (169), (302) and was employed in this study with minor modifications. Briefly, the lower limbs were shaved, taped to the table and bilateral pneumatic digital cuffs (size 3) applied to the proximal thighs. Ischemia was produced by inflation of the cuffs to the pressure between 220 mm Hg-240 mm Hg and monitored by means of bilateral photo-plethysmography probes attached to the skin, distal to the cuffs and over the femoral artery. A Doppler ultrasound machine (Parks Medical Electronics; Aloha, Oregon, U.S.A.) was used to confirm distal ischemia every 15 minutes by the presence of a flat trace. Animals were monitored with a rectal thermometer probe and the core temperature maintained at 37 °C with a heating lamp. In addition, the respiratory rate of rats was monitored clinically.

Ischemia was maintained for 4 h before the digital cuffs were released and the return of blood flow to the limb monitored by the return of the Doppler trace. The anaesthetic agents were ceased firstly and inhaled oxygen was continued until the rat was completely awake. The rat was then allowed to recover from anesthesia and returned to the holding facility.

To control for the effects of anesthesia, sham-operated rats were treated identically, except the

digital cuffs were left deflated. The Animal Ethics Committees of The Queen Elizabeth Hospital and The Adelaide University approved all experimental procedures used in this study. Animals were obtained from Central Animal House, University of Adelaide and housed at The Queen Elizabeth Hospital Animal House. All animals were fed on standard rat chow and water ad libitum.

Reperfusion was allowed to proceed for 0, 4, 24 or 72 h prior to the rats being sacrificed with an intraperitoneal injection of 0.8 ml pentobarbitone sodium (Nembutal 160 mg/kg, 60 mg/ml) and tissues harvested. A midline laparotomy was followed by a left nephrectomy and middle lobe hepatectomy. Continuation of the incision to a midline sternotomy allowed for the aspiration of 2 ml of blood by direct cardiocentesis and a bilateral pneumonectomy to be performed. Finally both medial gastrocnemii were excised below the site of the cuff. The left lung, the middle segment of middle liver lobe and middle third of kidney and both gastrocnemii were homogenized for later zymographic analysis. The upper lobe of the right lung, the lower segment of middle liver lobe, inferior pole of kidney and distal third of both gastrocnemii were frozen in liquid nitrogen for immunohistochemistry. The lower lobes of the right lung, upper part of middle liver lobe, superior pole of kidney and distal third of the gastrocnemii were fixed in paraffin and embedded.

2.2 Processing of tissue Samples

Blood was placed into an eppendorf tube containing 0.08 ml of sodium citrate (3.2%) and centrifuged at 300 × g for 5 minutes at 4°C. The plasma was collected, snap-frozen in liquid nitrogen and stored at - 80°C for later analysis. The histopathology samples were fixed in 10% buffered formalin prior to setting in paraffin blocks and the immunohistochemistry samples were snap-frozen directly in liquid nitrogen and stored at - 80°C until required.

Tissues for zymographic analysis were weighed, 10mls of homogenising buffer (2.3.2 Homoginising Buffer) added per gram of tissue and the tissue was then homogenised at 1500 rpm for ten min (B.Braun Melsungen AG). Homogenized tissue was then centrifuged for 60 minutes (4°C) at 8131 × g. The supernatant was aspirated, placed in previously boiled Visking dialysis tubing (14 kDa cut off) and dialysed for 18 hours at 4°C in dialysis buffer (2.3.3 Dialysis Buffer) on a magnetic stirrer to remove the urea used in the homogenising buffer. The dialysed supernatant was snap-frozen in liquid nitrogen and stored at – 80 °C for later analysis.

A total of 75 rats were used throughout the entire experiments. Thirty-five, which had been previously used in other projects in the laboratory (302), were employed for subsequent investigation of alterations in fibronectin and laminin in the basement membrane. The groups of rats are summarised in Table 2.1. At the initial stage of experiment, it was realised that fibronectin was rapidly accumulated in the basement membrane of skeletal muscle and as well, the alterations in fibronectin in the liver is significant at the first glance. The changes of plasma fibronectin were postulated to be significant after skeletal muscle ischemia and reperfusion. Therefor, another 40 rats were used in the experiment according to the protocol mainly for plasma fibronectin analysis and zymography investigation. These experimental groups of rats are summarised in Table 2.2.

Table 2.1: Rats Employed from DM.Roach

Group	Duration (Hours)			Rat number / group
	Anaesthesia	Ischemia	Reperfusion	
Sham-operated	4	nil	nil	5
Bilateral hindlimb I/R	4	4	nil	5
Bilateral hindlimb I/R	4	4	4	5
Bilateral hindlimb I/R	4	4	24	5
Bilateral hindlimb I/R	4	4	72	5
Bilateral hindlimb I/R + Low dose doxycycline	4	4	24	5
Bilateral hindlimb I/R + high dose doxycycline	4	4	24	5

I/R: Ischemia/reperfusion.

Low dose doxycycline was defined as 50 mg/kg twice daily for 7 days.

High dose doxycycline was defined as 200 mg/kg twice daily for 7 days.

Table 2.2. Rat Model Used in This Experiment

Group	Duration (Hours)			Rat number / group
	Anaesthesia	Ischemia	Reperfusion	
Sham-operated	4	nil	nil	5
Sham-operated	4	nil	4	5
Sham-operated	4	nil	24	5
Sham-operated	4	nil	72	5
Bilateral hindlimb I/R	4	4	nil	5
Bilateral hindlimb I/R	4	4	4	5
Bilateral hindlimb I/R	4	4	24	5
Bilateral hindlimb I/R	4	4	72	5

2.3 Buffers and Solutions Used in This Study

2.3.1. 0.1%Bovine Serum Albumin solution/Phosphate Buffer Solution (BSA/PBS)

NaCl	7.2 g /L	7.2 g
Na_2HPO_4	1.48 g /L	1.48 g
KH_2PO_4	0.43 g/L	0.43 g

Made up to 1000 ml with Mili Q water, pH 7.2 and then 1 g of bovine serum albumin added to the solution.

2.3.2. Homogenising buffer:

Urea	2M	60 g
Tris (Hydroxymethyl aminomethane) HCl	50mM	3.94 g
NaCl	1g/L	0.5 g
EDTA (Ethylene diamine tetra acetic acid)	1g/L	0.5 g

Made up to 500 ml solution, pH 7.6. This solution was then divided and filtered with 0.2 μm filter into 5 aliquots of 100 ml each. 330 ul of Brij 35 solution (0.1%) and 100 ul of phenylmethanesulfonyl fluoride (0.1 mM) were added into the solution immediately prior to homogenising. (0.871g PMSF in 50ml of ethanol stored under – 80 °C).

2.3.3. Dialysis buffer:

Tris (Hydroxymethyl aminomethane) Base	25 mM	19.7 g
$CaCl_2$	10 mM	7.35 g

Made up to 5 litres, pH 8.5. This solution was then divided into 5 individual of 1L and sterilised in the autoclave for 20 minutes.

0.1% Brij 35 3.3mls and 0.1mM PMSF 1ml were added to each 1L immediately before dialysis.

2.3.4 Resolving gel for zymography (constituents for one gel)

MQ H_2O	2.0 ml
30% Acrylamide mix	1.7 ml
1.5M Tris (pH 8.8)	1.3 ml
10% SDS	50 µl
10% APS	50 µl
TEMED	2 µl
Gelatin (for gelatinolytic zymography)	0.005 g
Casein (for caseinolytic zymography)	0.0075 g

2.3.5 Stacking gel for zymography (constituents for one gel)

MQ H_2O	1.4 ml
30% Acrylamide/Bis	0.33 ml
0.5 M Tris HCl (pH 6.8)	0.25 ml
10% SDS	20 µl
10% APS	20 µl
TEMED	2 µl

2.3.6 Solutions for zymography gel

1.5 M Tris-HCl pH 8.8

Made up 23.6 g of Tris-HCl in 100ml H_2O (236.4 g in 1L) (Autoclave).

10% SDS (Lauryl sulfate)

0.1g in 1000 ul of Mili Q H_2O.

10% APS (Ammonium persulfate)

0.1g in 1000ul Mili Q H_2O.

0.5M Tris-HCl pH 6.8

7.9g of Tris-HCl in 100 ml Mili Q H_2O (Autoclave).

1 M $CaCl_2$

54 g $CaCl_2$ was dissolved in 200 ml Mili Q H_2O (Autoclave).

5M NaCl

146.1 g NaCl was dissolved in 500 ml Mili Q H_2O (Autoclave).

2.3.7 2 ×SDS gel loading buffer

100mM Tris-HCl pH6.8	2 ml	0.5M Tris-HCl pH 6.8
4% SDS	4 ml	10% SDS
0.2% Bromophenol blue	0.4 ml	5% Bromophenol blue solution
20% glycerol	2.5 ml	80% glycerol

Plus H_2O to 10 ml

2.3.8 10 ×Laemmli Running Buffer

Tris Base	25 mM	15.15 g
Glycine	200 mM	72.1 g
SDS	3.5 mM	5 g

Made up to 500ml with H_2O. Dilute 10 ml in 100ml Mili Q H_2O when using.

2.3.9 2.5% Triton X-100

25 ml of Triton X-100 in 975 ml Mili Q H_2O and stir with magnetic stirrer.

2.3.10 Development Buffer

Tris-HCl pH 7.6	50 mM	33.3 ml	1.5M Tris-HCl pH 8.8
NaCl	200 mM	40 ml	5 M NaCl
$CaCl_2$	5 mM	5 ml	1M $CaCl_2$
Brij-35	0.2%	6.67 ml	30% Brij-35

Plus Mili Q H_2O to 1 L.

2.3.11 Coomassie Blue Staining solution

Acetic acid	10 %	50 ml	acetic acid
Methanol	50 %	250 ml	methanol
Coomassie Blue	0.25 %	25 ml	5% Coomassie Blue

Plus 175 ml Mili Q H_2O to 500 ml.

2.3.12 Destain solution

Acetic acid	10 %	50 ml	acetic acid
Methanol	50 %	250 ml	methanol

Plus 200ml Mili Q H_2O to 500 ml.

2.3.13 Western Transfer Buffer

Tris Base	6.06 g
Glycine	28.8 g
Methanol	400 ml

Made upto 2 liters with Milli Q H_2O and stored at 4°C.

2.3.14Non-fat Powdered milk Solution

Skim milk powder	5 g
Phosphate buffered saline	100 ml

Prepared fresh before use.

2.3.15 Tris Buffered Saline for Western Blots

Tris HCl	2.42 g
NaCl	29.22 g

Made up in 1 L of Milli Q H_2O, pH adjusted 7.5 and autoclaved.

2.3.16 Western Antibody Buffer

Phosphate buffered saline	45 ml
Foetal calf serum	5 ml
Tween-20	25 µl

2.3.17 Western Loading Buffer

Tris HCl	62.5 mM
SDS	1.4 M
Glycerol	45 %
Bromophenol Blue	0.025 %
β-mercaptoethanol	2 %

Made up to pH 6.8

CHAPTER 3

ELEVATED ACTIVITY OF A LOW MOLECULAR WEIGHT CASEINOLYTIC MATRIX METALLOPROTEINASE IN THE LUNG FOLLOWING SKELETAL MUSCLE ISCHEMIA/REPERFUSION INJURY

3.1 Introduction

Gelatinolytic matrix metalloproteinases (MMPs) have been investigated in ischemia/reperfusion injury, but the activity of caseinolytic MMPs has not yet been reported in the literature. The aims of this chapter were to investigate the changes in caseinolytic MMPs both in skeletal muscle following ischemia/reperfusion and in remote organs including lung, kidney, and liver. Zymography and western blotting were employed to conduct the investigation.

3.1.1 Matrix metalloproteinases (MMPs)

Matrix metalloproteinases (MMPs) are a family of Zinc-dependent endopeptidases targeting extracellular matrix (ECM) compounds as well as a number of other proteins. Their proteolytic activity acts as an effector mechanism of tissue remodeling in physiological and pathological conditions and as modulators of inflammation. MMPs are regulated at different levels. At the transcriptional level, MMP expression is precisely controlled by various cytokines acting through positive or negative regulatory elements in the MMP gene promotor sequences. In addition, MMP activity is regulated at the post-transcriptional level by proteolytic activation of the latent proenzymes and by interaction with specific tissue inhibitors of matrix metalloproteinases (TIMPs). Expression and secretion of both MMPs and TIMPs are also influenced by cytokines (471). There are more than 20 known MMPs, which have been defined having the following characteristics as: (1) they are proteinases that degrade at least one component of the extracellular matrices, (2) they contain a zinc ion and are inhibited by chelating agents, such as phenanthrolin, (3) they are secreted in a latent form, being activated for proteolytic activity, (4) they are inhibited by tissue inhibitors of metalloproteinases (TIMPs), and share common amino acid sequences (472), (473). The known members of the MMP family are listed in Table 3.1, together with their preferred substrates (473).

Table 3.1 Matrix metalloproteinases and their major substrates

MMP	Alternative nomenclature	Main substrate (s)
MMP-1	Collagenase	Fibrillar collagens
MMP-2	Gelatinase A (72 kDa)	Type IV and V collagens, fibronectin
MMP-3	Stromelysin 1	Laminin, fibronectin, non-fibrillar collagen
MMP-7	Matrilysin	Laminin, fibronectin, non-fibrillar collagen
MMP-8	PMN collagenase	Fibrillar collagens
MMP-9	Gelatinase B (92 kDa)	Type IV and V collagens
MMP-10	Stromelysin 2	Laminin, fibronectin, non-fibrillar collagen
MMP-11	Stromelysin 3	Serpin
MMP-12	Metalloelastase	Elastin
MMP-13	Collagenase-3	Fibrillar collagens
MMP-14	MT1-MMP	Pro-MMP-2, fibronectin
MMP-15	MT2-MMP	Progelatinase A
MMP-16	MT3-MMP	Fibronectin, gelatin, collagen III
MMP-17	MT4-MMP	Not clear
MMP-18	Xenopus MMP Collagenase -4	Collagen I
MMP-19	Unknown	Gelatin
MMP-20	Enamelysin	Amelogenin
MMP-21	Xenopus	Unknown
MMP-22	CMMP (Chicken)	Unknown
MMP-24	MT5-MMP	Unknown
MMP-25	MT6-MMP	Progelatinase A
MMP-26	Matrilysin	Unkown

MMP: matrix metalloproteinase. PMN: polymorphonuclear neutrophil. MT (1-6)-MMP: membrane-type (1-6) matrix metalloproteinase.

3.1.2 Inhibitors of MMPs-Doxycycline

With an understanding of the effects of MMPs during pathological conditions such as tumor invasion and progression and ischemic injury, attention has been drawn to the study of the effects of inhibitors of MMPs on inhibition of the pathological process. Doxycycline, one of tetracycline derivatives, has been investigated extensively for its properties of inhibition of MMPs. Clinical trials have commenced in patients with periodontal disease and abdominal aortic aneurysm (AAA). With good results (474), (475). The effects of doxycycline on the severity of ischemia /reperfusion injury has also been investigated by Roach and co-workers (302). It was shown that degradation of collagen IV in skeletal muscle after ischemia was attenuated after administration of doxycycline by inhibition of the activity of MMP-9 and MMP-2. Doxycycline, (6-deoxy-5-hydroxy tetracycline) interacts with the Zn^{2+} cation by binding to the active Zn site in the most of MMP enzyme to mediate its inhibitory effect (476). The dosage used in these *in vivo* studies was 50 mg/kg to rats twice daily or 200 mg/kg to rats twice daily by gavage. There was no evidence of toxicity of doxycycline in the rats in this experiment.

3.1.3 Methods for detection of MMPs-Zymography

MMPs can be detected by a variety of techniques, each with its own advantages and disadvantages. These methods include immunohistochemistry, enzyme-linked immunosorbent assay (ELISA), mRNA analysis and zymography. Zymography has the advantages of measuring enzymatic activity quantitatively and of distinguishing the active form from the inactive pro-enzyme. Immunohistochemistry and *in situ* RNA analysis are able to localise the MMPs and their TIMPs, thus determining the site of production (473). In studies of mechanisms of ischemia and reperfusion injury, zymography has been extensively employed

to investigate the activity of MMPs during the ischemic insult and following reperfusion (477), (478), (340), (293), (302).

Zymography is an electrophoretic technique used to identify proteolytic activity for enzymes separated in polyacrylamide gels embedded with target substrate under certain condition. Basically, the substrate gelatin has been used to investigate the activity of MMP-2 and MMP-9, whereas casein used to investigate the activity of stromelysin and matrilysin. In this experiment, the specific substrate gelatin or casein was embedded in the polyacrylamide gels. MMPs migrate through the gel according to their size, and then degrade the substrate at this point on the gel. To identify the proteolytic action, the gel is stained with Coomassie Brilliant Blue for a certain period and then washed in destain solution until the proteolytic band is clearly observed (479). The results of MMP activity were shown as white bands on a blue background.

3.1.4 Western blotting

Western blotting is also known as protein immuno-blotting, in which the protein of MMP's can be examined further using a specific antibody. Combined with zymography, Western blotting was used in this experiment for confirmation of MMPs detected on the caseinolytic zymography gels.

3.2 Materials and Methods

3.2.1 Bradford Protein Assay

The Bradford Protein Assay is a dye-binding assay, in which a differential colour change of a dye occurs in response to the concentrations of protein. The manufacturer's instructions for the microassay procedure were conducted to determine the level of protein in the tissue dialysate for each rat sample.

Using bovine serum albumin (BSA) standard concentration, The Bio-Rad Protein Assay Dye Reagent was mixed with various concentration of BSA. Five dilutions of BSA from 1-10 μg/ml were produced. Two hundred μl of Dye reagent was mixed with BSA at appropriate dilution and mili-Q water to make up to 1 ml. The solution was incubated at room temperature for at least five minutes and the absorbance measured at 595 nm. Each sample was duplicated in the same run and the average of absorbance was recorded. A graph was drawn from the result of these known standard protein concentrations, indicating the protein level versus absorbance at 595 nm (An example graph in Figure 3.1).

The tissue samples were diluted with Dye reagent and milli-Q water in the same run as above. Protein concentration of tissue samples was calculated according to the standard equation, which was displayed in the graph by Excel software.

Figure 3.1 The standard graph for protein concentration assay (Bradford assay, example)

X: Protein concentration in the samples. Y: Average absorbance measured at 595 nm.

$Y = 45.928x + 38.937$ is an equation displayed by Excel software.

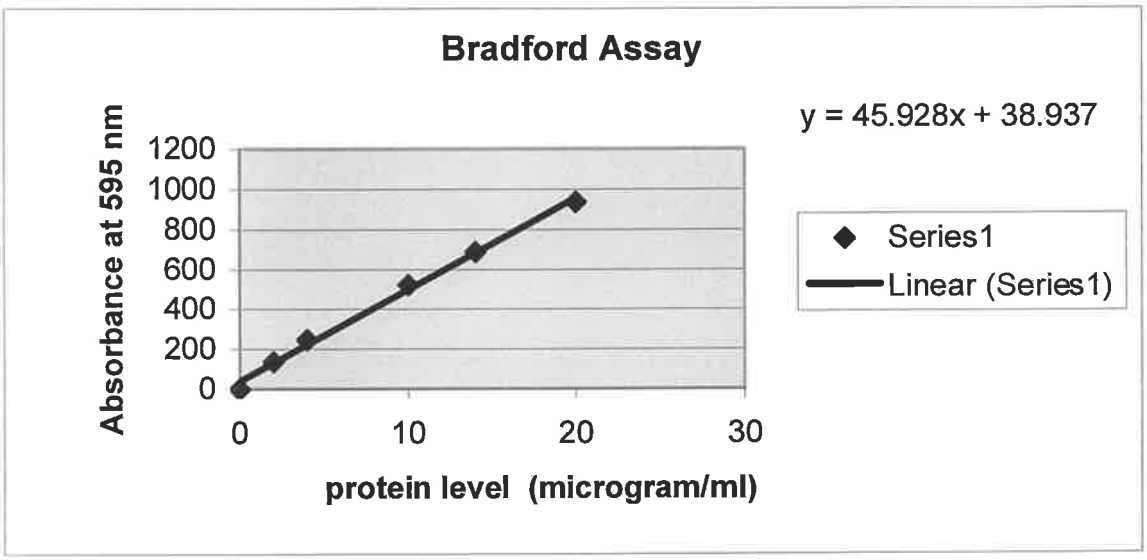
Bradford Assay
y = 45.928x + 38.937
Absorbance at 595 nm
1200
1000
800
600
400
200
0
0
10
20
30
protein level (microgram/ml)
Series1
Linear (Series1)

3.2.2 Sodium Dodecyl Sulfate Polyacrylamide Gel Electrophoresis (SDS-PAGE) Substrate-Embedded Zymography

The protein concentration of tissue samples was determined using a Bradford Assay method (BioRad, Hercules, CA, U.S.A). SDS-PAGE was performed using a modification of the procedure as described by Frisdal et al (271). Briefly, a 10 % polyacrylamide resolving gel (2.3.4) embedded with either 0.1 % gelatin or 0.15 % β-casein (Sigma Aldrich). A 5% stacking gel (2.3.5) was layered on top and allowed to set for 45 min. Wells were loaded with equal amounts of protein (80 μg/lane) diluted 1:1 in laemmli loading buffer (2.3.18). In order to identify the molecular weight of the proteolytic bands a standard protein molecular weight rainbow marker (Amersham) was loaded onto the gel. A standard MMP positive control (Sigma-Aldrich) was also loaded to allow for comparisons between gels. Gels were run for 40 min at 60 volts, followed by 90 min at 100 volts or until the dye front ran off the bottom of the gel. The gels were then washed 3 times in 2.5 % Triton X-100 solution 3 times for 15min, followed by 5 minutes wash in development buffer before incubation at 37 ^{o}C in development buffer for 18 h. Having allowed for the gelatinolytic or caseinolytic digestion to occur during the incubation period, the gels were stained with Coomassie Brilliant Blue Staining Solution (Sigma Aldrich, 2.3.11) for 30 min. De-staining was carried out with 40 % methanol and 10 % acetic acid (2.3.12) until the white bands of enzymic activity appeared clearly against the blue background. To confirm the identity of the proteolytic bands as MMPs, gels containing tissue samples were incubated either with 10 mM EDTA or 10 mM (1,10)-Phenanthroline added to the development buffer respectively, or with 1mM PMSF added to the samples for 18 h at 37 ^{o}C. Gels were photographed by digital camera and saved as Tagged Image File Format (TIFF files) using Kodak 1D image analysis software. Zymograms were assessed descriptively without any quantification of the bands.

3.2.3 Western blotting

Immuno-blotting was performed under reducing conditions. Briefly, stacking and resolving gels were assembled as described above without gelatin or casein. Protein samples (80 μg/lane) were loaded into each well with 2 % ß-mercaptoethanol in final volume of samples and Western loading buffer (2.3.17) and incubated at 100°C for 10 minutes. An MMP positive control (Sigma Aldrich) was included on all gels to verify the identity of the immunoreactive bands. The gels were electrophoresed as above, removed and allowed to equilibrate in transfer buffer (2.3.13) for 30 min at room temperature. Gels were then placed against a nitrocellulose membrane (Hybond ECL Amersham Biosciences, Little Chalfont, Buckinghamshire, U.K.) and transfer of proteins was performed at 400 mA for 60 min in transfer buffer (2.3.13). Non-specific binding to membrane was blocked with 5 % skimmed milk powder in phosphate-buffered saline (2.3.14) for 2 h prior to overnight incubation with polyclonal goat MMP-7 or MMP-13 antibody (Santa Cruz) in a 1/100 Western Antibody Dilution Buffer (2.3.16). Secondary detection was carried out for 1 h at room temperature with perioxdase-labelled rabbit anti-goat IgG antibody (Santa Cruz) in 1:1000 Western Antibody Dilution Buffer. The membrane was washed twice for 10 minutes with TBS solution (2.3.15) and placed on clean glass plate and the excess solution removed with tissue paper. ECL reagents (Amersham Biosciences) were prepared according to the manufacture's instructions and poured onto the membrane. A top glass plate was placed over the membrane and incubated for 1 minute before unbound reagents were removed by blotting with filter paper. The membrane was then exposed to a film (Amersham ECL) for 30 – 60 seconds before being developed in the radiology department at The Queen Elizabeth Hospital.

3.3 Results

3.3.1 Screening zymographic detection of caseinolytic activity in the tissues of rats following skeletal muscle I/R.

Referring to substrate gel zymography, MMP-3 (Stromelysin), MMP-7 (Matrilysin) and MMP-12 would be detectable more sensitively on casein gels.

Skeletal muscle

There were no proteolytically active bands detected on caseinolytic zymography in skeletal muscle tissue which was either subjected to 4 h ischemia with varying times of reperfusion or in sham-operated group (Figure 3.1 lane 2 and 6 in panel A, B, C and D).

Kidney

Two proteolytically active bands were observed on caseinolytic zymography in renal tissue both in all experimental groups and in sham-operated animals. No alterations of activity occurred in rats that underwent 4 h bilateral hindlimb ischemia and reperfusion, when compared with corresponding sham-operated group. The molecular weight of these active enzymes was between 80-90 kDa. The identity of these bands is unknown, but the investigation will be conducted in later on study. (Figure 3.1 lane 3 and 7 in panel A, B, C, and D).

Lung

An active caseinolytic band was detected on bottom of caseinolytic zymography gel in lung tissue of rats either in experimental group or sham-operated group. Compared to sham-operated group, the caseinolytic activity in the lung was increased immediately after skeletal muscle ischemia and during early reperfusion within 4 h, then decreased with reperfusion, to a lowest level (absent) at 24 hours of reperfusion, then recovered thereafter to baseline levels

Figure 3.1: Screening zymographic detection of caseinolytic activity in tissues following skeletal muscle ischemia and reperfusion

Rats were subjected to 4 h bilateral hindlimb ischemia or no ischemia followed by 0, 4, 24, or 72 h reperfusion before tissues were harvested. Lane 1: molecular weight marker and Lane 10: MMPs positive control. All experimental lanes (2-9) contain 80 μg of total protein. Bands corresponding to MMP-9, proMMP-2, active MMP-2 and a new caseinolytic MMP are shown (arrows).

Panel A: Rats were subjected to 4 h ischemia and no reperfusion (4/0) or no ischemia and no reperfusion (0/0).

Lane 2: Skeletal muscle, 4/0.
Lane 3: Kidney ,4/0.
Lane 4: Lung, 4/0.
Lane 5: Liver, 4/0.
Lane 6: Skeletal muscle, 0/0.
Lane 7: Kidney, 0/0.
Lane 8: Lung, 0/0.
Lane 9: Liver, 0/0.

Panel B: Rats were subjected to 4 h ischemia and 4 h reperfusion (4/4) or no ischemia and 4 h reperfusion (0/4).

Lane 2: Skeletal muscle, 4/4.
Lane 3: Kidney, 4/4.
Lane 4: Lung, 4/4.
Lane 5: Liver, 4/4.
Lane 6: Skeletal muscle, 0/4.
Lane 7: Kidney, 0/4.
Lane 8: Lung, 0/4.
Lane 9: Liver,0/4.

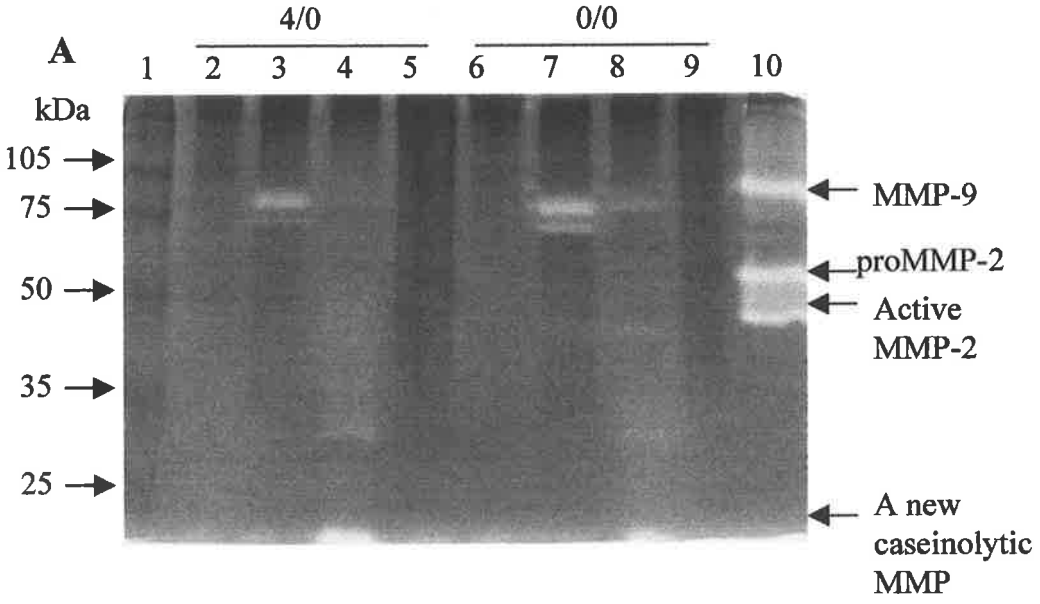
A
4/0
0/0
1
2
3
4
5
6
7
8
9
10
kDa
105
75
50
35
25
MMP-9
proMMP-2
Active
MMP-2
A new
caseinolytic
MMP

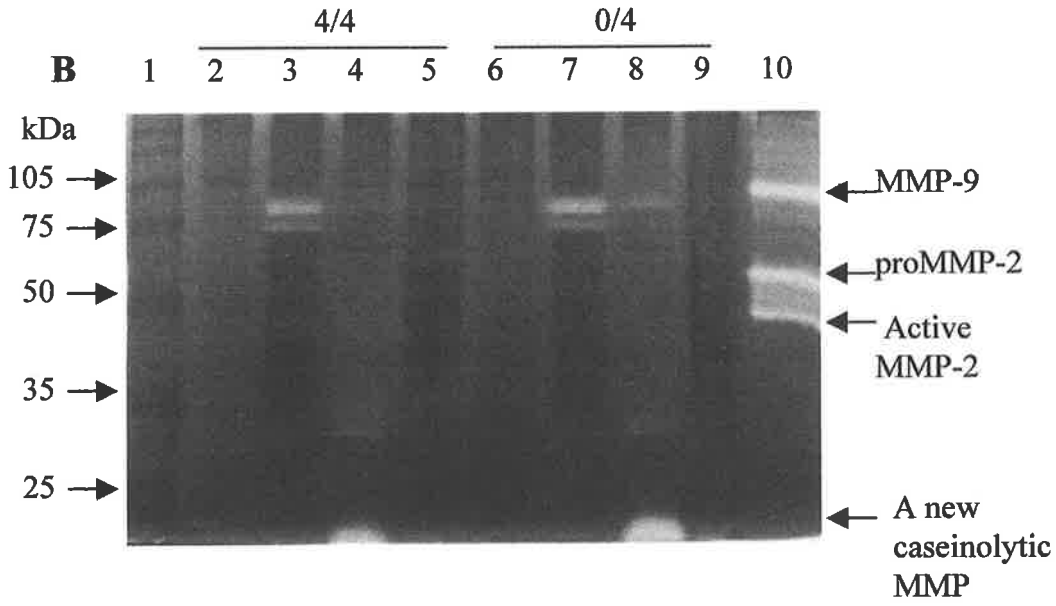
B
4/4
0/4
1
2
3
4
5
6
7
8
9
10
kDa
105
75
50
35
25
MMP-9
proMMP-2
Active
MMP-2
A new
caseinolytic
MMP

Figure 3.1 Continued

Panel C: Rats were subjected to 4 h ischemia and 24 h reperfusion (4/24) or no ischemia and 24 h reperfusion (0/24).

Lane 2: Skeletal muscle, 4/24.
Lane 3: Kidney, 4/24.
Lane 4: Lung, 4/24.
Lane 5: Liver, 4/24.
Lane 6: Skeletal muscle, 0/24.
Lane 7: Kidney, 0/24.
Lane 8: Lung, 0/24.
Lane 9: Liver,0/24.

Panel D: Rats were subjected to 4 h ischemia and 72 h reperfusion (4/72) or no ischemia and 72 h reperfusion (0/72).

Lane 2: Skeletal muscle, 4/72.
Lane 3: Kidney, 4/72.
Lane 4: Lung, 4/72.
Lane 5: Liver, 4/72.
Lane 6: Skeletal muscle, 0/72.
Lane 7: Kidney, 0/72.
Lane 8: Lung, 0/72.
Lane 9: Liver,0/72.

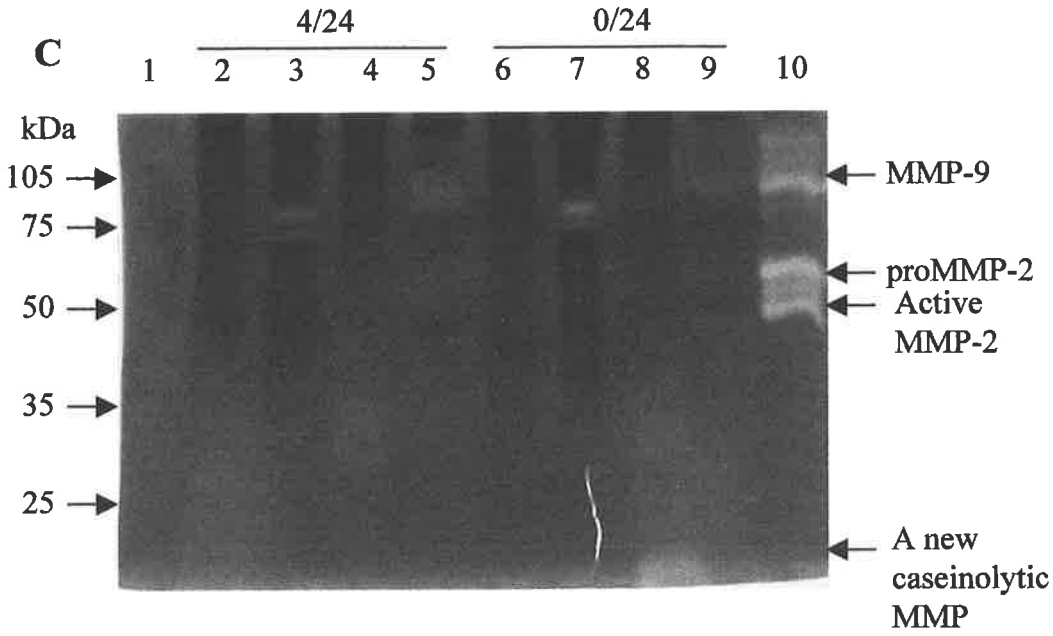
C
4/24
0/24
1
2
3
4
5
6
7
8
9
10
kDa
105
75
50
35
25
MMP-9
proMMP-2
Active
MMP-2
A new
caseinolytic
MMP

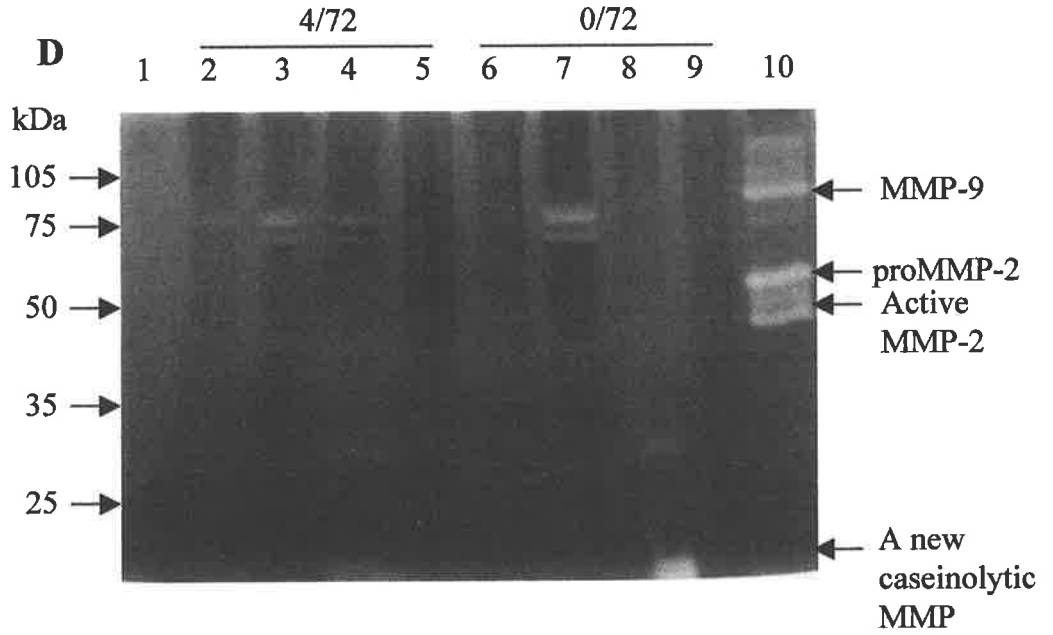
D
4/72
0/72
1
2
3
4
5
6
7
8
9
10
kDa
105
75
50
35
25
MMP-9
proMMP-2
Active
MMP-2
A new
caseinolytic
MMP

gradually. The molecular weight of this active species was approximately 20 kDa when compared with molecular weight standard. This species therefore needs to be investigated further (Figure 3.1 lane 4 and 8 in panel A, B, C, and D).

Liver

There was no active caseinolytic band detected in liver tissue of rats either in experimental or sham-operated groups (Figure 3.1 lane 5 and 9 in panel A, B, C, and D).

3.3.2 Zymographic detection of gelatinolytic MMP-2 and MMP-9 activity in skeletal muscle, kindey, lung and liver of the rats following bilateral hindlimb I/R for determining that the samples were harvested and processed properly and the present of activity of MMPs.

Figure 3.2 illustrates the zymographic analysis of gelatinolytic activity in skeletal muscle, kidney, lung and liver.

Skeletal muscle

ProMMP-2 was detected both in ischemic skeletal muscle with varying reperfusion time and sham-operated skeletal muscle, but there was no MMP-9 activity in skeletal muscle that underwent 4 h ischemia before reperfusion and in sham-operated group. However, MMP-9 activity was detected in the skeletal muscle that underwent 4 h ischemia followed by 4, 24 h, and 72 h reperfusion respectively. The production of proMMP-2 was also increased following skeletal muscle ischemia and reperfusion (Figure 3.2 lane 2 and 6 in panel A, B, C and D).

Kidney

ProMMP-2 was detected at baseline level in kidney of rats, both in experimental groups and in the sham-operated groups. There was no increase in proMMP-2 levels in kidney following

Figure 3.2: Zymographic detection of gelatinolytic activity in tissues following skeletal muscle ischemia and reperfusion

Rats were subjected to 4 h bilateral hindlimb ischemia or no ischemia followed by 0, 4, 24, or 72 h reperfusion before tissues were harvested. Lane 1: molecular weight marker and Lane 10: MMPs positive control. All experimental lanes (2-9) contain 80 μg of total protein. Bands corresponding to MMP-9, proMMP-2, active MMP-2 and are shown (arrows).

Panel A: rats were subjected to 4 h ischemia and no reperfusion (4/0) or no ischemia and no reperfusion (0/0).
Lane 2: Skeletal muscle, 4/0.
Lane 3: Kidney, 4/0.
Lane 4: Lung, 4/0.
Lane 5: Liver, 4/0.
Lane 6: Skeletal muscle, 0/0.
Lane 7: Kidney, 0/0.
Lane 8: Lung, 0/0.
Lane 9: Liver, 0/0.

Panel B: Rats were subjected to 4 h ischemia and 4 h reperfusion (4/4) or no ischemia and 4 h reperfusion (0/4).
Lane 2: Skeletal muscle, 4/4.
Lane 3: Kidney , 4/4.
Lane 4: Lung, 4/4.
Lane 5: Liver,4/4.
Lane 6: Skeletal muscle, 0/4.
Lane 7: Kidney, 0/4.
Lane 8: Lung, 0/4.
Lane 9: Liver, 0/4.

Panel C: Rats were subjected to 4 h ischemia and 24 h reperfusion (4/24) or no ischemia and 24 h reperfusion (0/24).
Lane 2: Skeletal muscle, 4/24.
Lane 3: Kidney , 4/24.
Lane 4: Lung, 4/24.
Lane 5: Liver,4/24.
Lane 6: Skeletal muscle, 0/24.
Lane 7: Kidney, 0/24.
Lane 8: Lung, 0/24.
Lane 9: Liver, 0/24.

Panel D : Rats were subjected to 4 h ischemia and 72 h reperfusion (4/72) or no ischemia and 72 h reperfusion (0/72).
Lane 2: Skeletal muscle, 4/72.
Lane 3: Kidney , 4/72.
Lane 4: Lung, 4/72.
Lane 5: Liver,4/72.
Lane 6: Skeletal muscle, 0/72.
Lane 7: Kidney, 0/72.
Lane 8: Lung, 0/72.
Lane 9: Liver, 0/72.

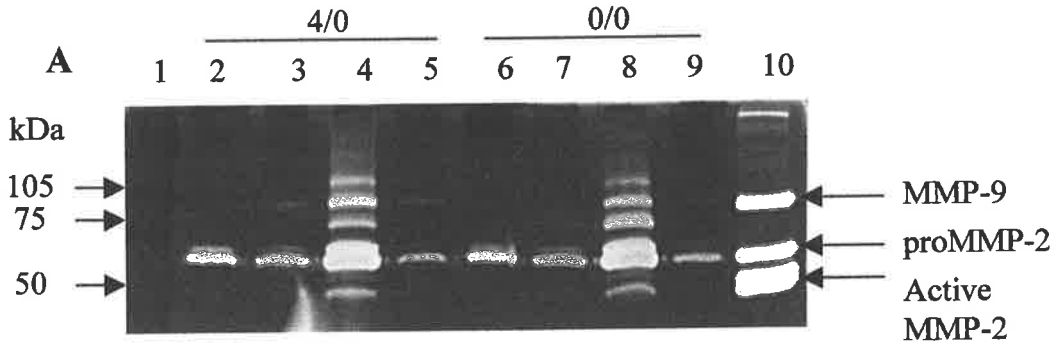
A
4/0
0/0
1 2 3 4 5 6 7 8 9 10
kDa
105
75
50
MMP-9
proMMP-2
Active
MMP-2

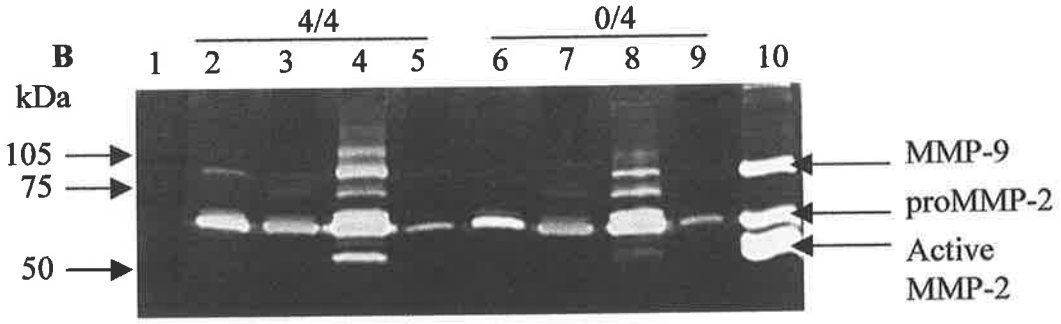
B
4/4
0/4
1 2 3 4 5 6 7 8 9 10
kDa
105
75
50
MMP-9
proMMP-2
Active
MMP-2

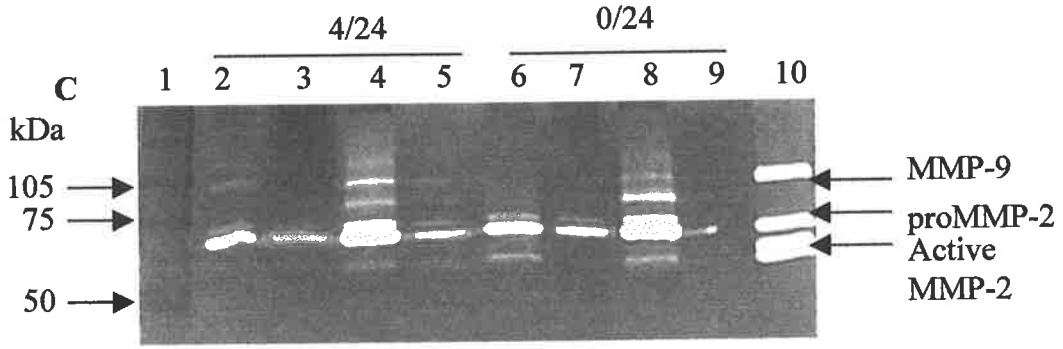
C
4/24
0/24
1 2 3 4 5 6 7 8 9 10
kDa
105
75
50
MMP-9
proMMP-2
Active
MMP-2

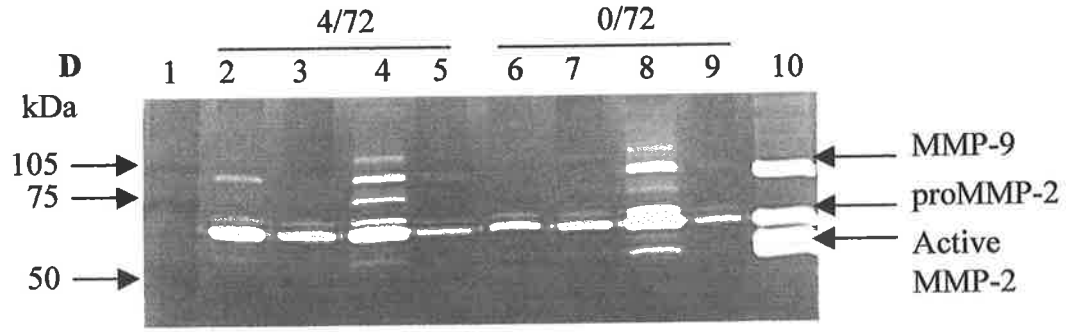
D
4/72
0/72
1 2 3 4 5 6 7 8 9 10
kDa
105
75
50
MMP-9
proMMP-2
Active
MMP-2

ischemia and reperfusion. There was no MMP-9 activity detected in renal tissue (Figure 3.2 lane 3 and 7 in panel A, B, C and D).

Lung

MMP-9, proMMP-2 and active MMP-2 were all detected in lung tissues both in all experimental groups and sham-operated groups. MMP-9 and active MMP-2 were increased in lung tissue of rats that underwent 4 h bilateral hindlimb ischemia and by 4 h reperfusion, compared with corresponding sham-operated group. Levels of MMP-9 and active MMP-2 then decreased with 24 h reperfusion, maintaining at lower level below the baseline upto 72 h (Figure 3.2 lane 4 and 8 in panel A, B, C, and D).

Liver

ProMMP-2, but not MMP-9 and active MMP-2, was detected in liver at a low level both in all experimental rats and sham-operated rats. There was no alterations observed after bilateral hindlimb ischemia and reperfusion (Figure 3.2 lane 5 and 9 in panel A, B, C, and D).

3.3.3 Further investigation if there is a caseinolytic MMP activity present in skeletal muscle following I/R.

Four individual skeletal muscle tissues of rats from each group that underwent 4 h ischemia followed by 24 h of reperfusion or in corresponding sham-operated group were used for detection. Skeletal muscle tissues following ischemia with different times of reperfusion were also used for detection of the change patterns of caseinolytic MMP if any.

There was no caseinolytic activity detected in skeletal muscle either in experimental groups where rats underwent 4 h bilateral hindlimb ischemia followed by reperfusion at varying times or in sham-operated rats that under 4 h anesthesia, no ischemia, no reperfusion (Figure 3.3 lane 2-9 in panel A and B).

Figure3.3: Further zymographic detection of caseinolytic activity in skeletal muscle following ischemia and reperfusion

Rats were subjected to 4 h bilateral hindlimb ischemia or no ischemia followed by 0, 4, 24, or 72 h reperfusion before skeletal muscle were harvested. Lane 1: molecular weight marker and Lane 10: MMPs positive control. All experimental lanes (2-9) contain 80 μg of total protein. Bands corresponding to MMP-9, proMMP-2 and active MMP-2 are shown (arrows).

Panel A: Skeletal muscle of rats that were subjected to 4 h ischemia and 24 h reperfusion (4/24) or no ischemia and 24 h reperfusion (0/24).

Lane 2-5: Individual skeletal muscle, 4/24.
Lane 6-9: Individual skeletal muscle, 0/24.

Panel B: Skeletal muscle of rats that were subjected to 4 h ischemia followed by 0, 4, 24, or 72 h reperfusion (4/0, 4/4, 4/24, 4/72) or no ischemia with 0, 4, 24, 72 h reperfusion (0/0, 0/4, 0/24, 0/72).

Lane 2: Skeletal muscle, 4/0.
Lane 3: Skeletal muscle, 4/4.
Lane 4: Skeletal muscle, 4/24.
Lane 5: Skeletal muscle, 4/72.
Lane 6: Skeletal muscle, 0/0.
Lane 7: Skeletal muscle, 0/4.
Lane 8: Skeletal muscle, 0/24.
Lane 9: Skeletal muscle, 0/72.

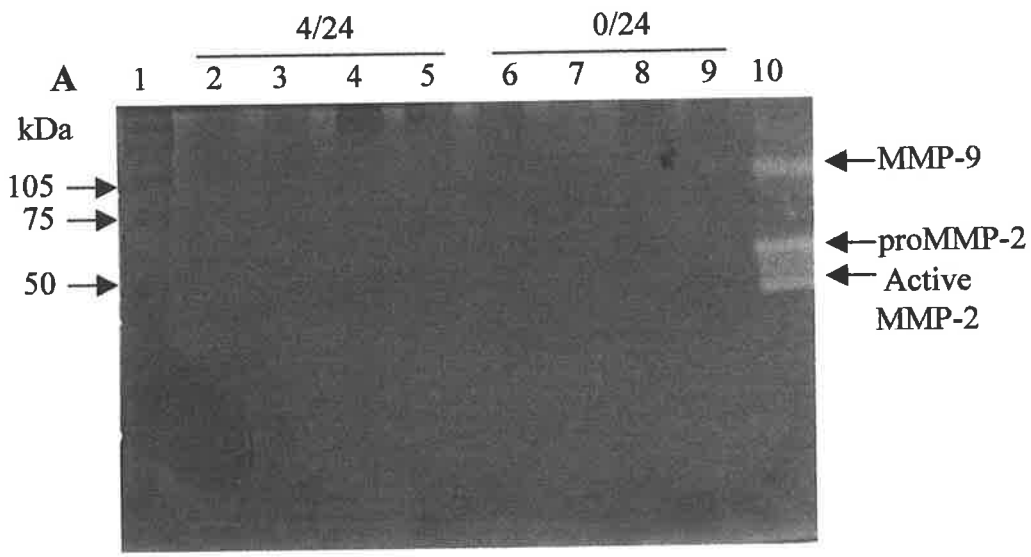
4/24
0/24
A
1
2
3
4
5
6
7
8
9
10
kDa
105
75
50
MMP-9
proMMP-2
Active
MMP-2

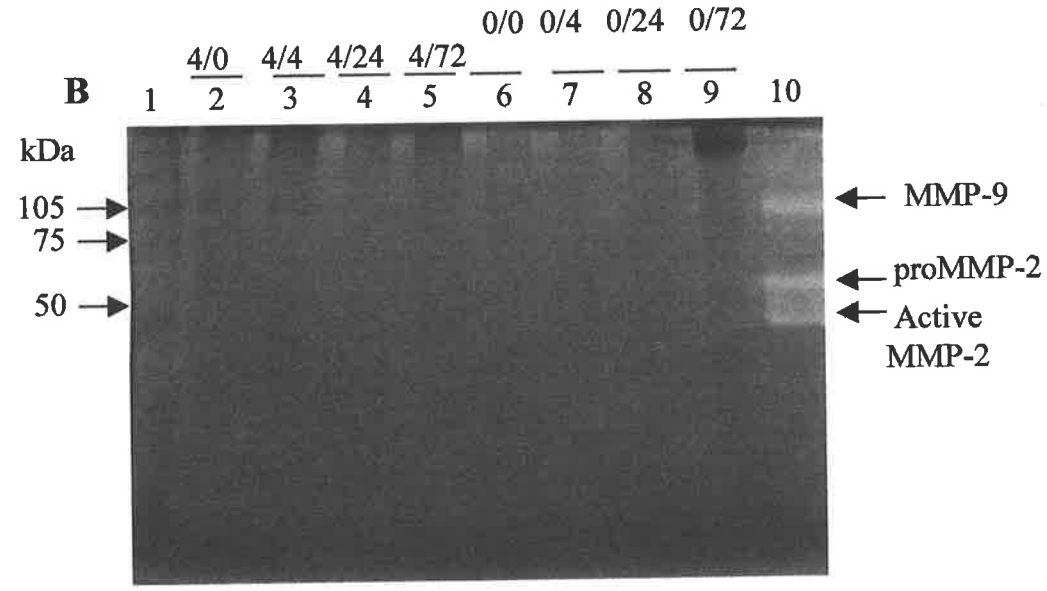
0/0
0/4
0/24
0/72
4/0
4/4
4/24
4/72
B
1
2
3
4
5
6
7
8
9
10
kDa
105
75
50
MMP-9
proMMP-2
Active
MMP-2

3.3.4 Zymographic detection of gelatinolytic activity in the same skeletal muscle tissues as above determining that the samples were harvested and processed properly with detectable MMP-2 and MMP-9 activity.

ProMMP-2 was detected both in ischemic skeletal muscle with varying reperfusion time and sham-operated skeletal muscle (Figure 3.4 lane 2-9 in panel A&B), but there was no MMP-9 activity detectable in skeletal muscle that underwent 4 h ischemia with early reperfusion and in sham-operated group (Figure 3.4 lane 2,3 in panel B). However, MMP-9 activity was detected in the skeletal muscle after 24 h or 72 h of reperfusion following ischemia (Figure 3.4 lane 4, 5 in panel A&B). In addition, the production of proMMP-2 increased in the skeletal muscle following 4h ischemia and 24 h or 72 h reperfusion respectively (Figure 3.4 lane 2-5 in panel A and lane 4-5 in panel B). There was no active MMP-2 detected in the skeletal muscle either in experimental group or in sham-operated group (Figure 3.4 panel A and B).

3.3.5 Effects of anesthesia on the production of caseinolytic activity in the lung tissues of rats (Sham-operated rats versus normal control rats).

There was a new caseinolytic active band detected in the normal lung tissues (Figure3.5 lane 6-9 in panel A, B, C, and D). The molecular weight of this proteolytically active species was approximately 20 kDa according to standard protein molecular weight in lane 1. This active band was absent in the lung tissues of rats that underwent 4 h anesthesia (Figure 3.5 lane 2-5 in panel A). This active species then increased gradually with time of recovery (Figure 3.5 lane 2-5 in panel b and c), reaching to the level observed in normal rats after 72 h of recovery from anesthesia (Figure 3.5 lane 2-5 in panel D). These results suggest that the activity of this new species is suppressed by anesthesia.

Figure3.4: Zymographic detection of gelatinolytic activity in skeletal muscle using the same samples as those in Figure 3.3 for determining the presence of emzymic activity of MMPs

Rats were subjected to 4 h bilateral hindlimb ischemia or no ischemia followed by 0, 4, 24, or 72 h reperfusion before skeletal muscle were harvested. Lane 1: molecular weight marker and Lane 10: MMPs positive control. All experimental lanes (2-9) contain 80 μg of total protein. Bands corresponding to MMP-9, proMMP-2 and active MMP-2 are shown (arrows).

Panel A: Skeletal muscle of rats that were subjected to 4 h ischemia and 24 h reperfusion (4/24) or no ischemia and 24 h reperfusion (0/24).

Lane 2-5: Individual skeletal muscle, 4/24.
Lane 6-9: Individual skeletal muscle, 0/24.

Panel B: Skeletal muscle of rats that were subjected to 4 h ischemia followed by 0, 4, 24, or 72 h reperfusion (4/0, 4/4, 4/24, 4/72) or no ischemia with 0, 4, 24, 72 h reperfusion (0/0, 0/4, 0/24, 0/72).

Lane 2: Skeletal muscle, 4/0.
Lane 3: Skeletal muscle, 4/4.
Lane 4: Skeletal muscle, 4/24.
Lane 5: Skeletal muscle, 4/72.
Lane 6: Skeletal muscle, 0/0.
Lane 7: Skeletal muscle, 0/4.
Lane 8: Skeletal muscle, 0/24.
Lane 9: Skeletal muscle, 0/72.

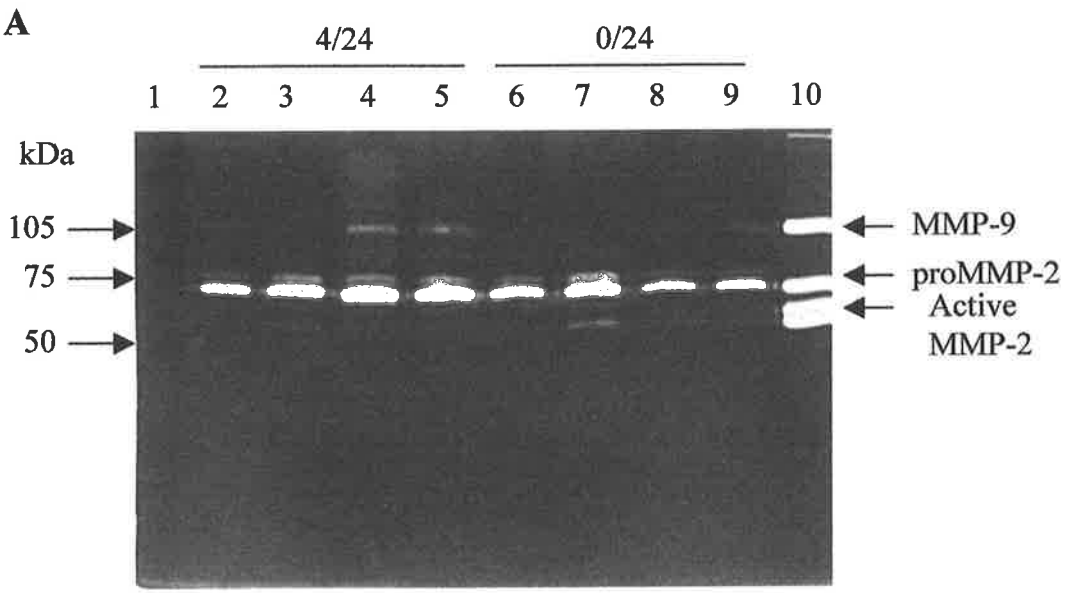
A
4/24
0/24
1 2 3 4 5 6 7 8 9 10
kDa
105
75
50
MMP-9
proMMP-2
Active
MMP-2


B
4/0 4/4 4/24 4/72 0/0 0/4 0/24 0/72
1 2 3 4 5 6 7 8 9 10
kDa
105
75
50
MMP-9
proMMP-2
Active
MMP-2

Figure 3.5: Zymographic detection of caseinolytic activity in the lung

Rats were subjected to 4 h anesthesia, no ischemia followed by 0, 4, 24, or 72 h recovery compared to normal control rats, no anesthesia, no ischemia. Lane 1: molecular weight marker and Lane 10: MMPs positive control. All experimental lanes (2-9) contain 80 μg of total protein. Bands corresponding to MMP-9, pro-MMP-2, active MMP-2 and new caseinolytic bands are shown (arrows).

Panel A: Lung tissue samples from 4 individual rats following 4 h anesthesia, no ischemia (0/0) compared to 4 individual rats in normal control group (Normal, no anesthesia, no ischemia, no reperfusion).

Lane 2-5: Lungs, 0/0.
Lane 6-9: Lungs, Normal.

Panel B: Lung tissue samples from 4 individual rats following 4 h anesthesia, no ischemia with 4 h recovery (0/4) compared to 4 individual rats in normal control group (Normal, no anesthesia, no ischemia, no reperfusion).

Lane 2-5: Lungs, 0/4.
Lane 6-9: Lungs, Normal.

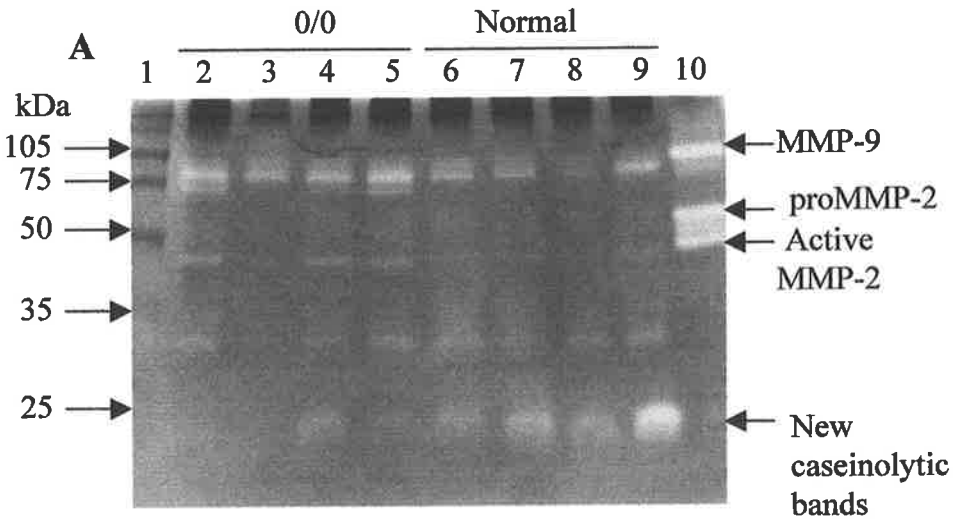
A
0/0
Normal
1 2 3 4 5 6 7 8 9 10
kDa
105
75
50
35
25
MMP-9
proMMP-2
Active
MMP-2
New
caseinolytic
bands

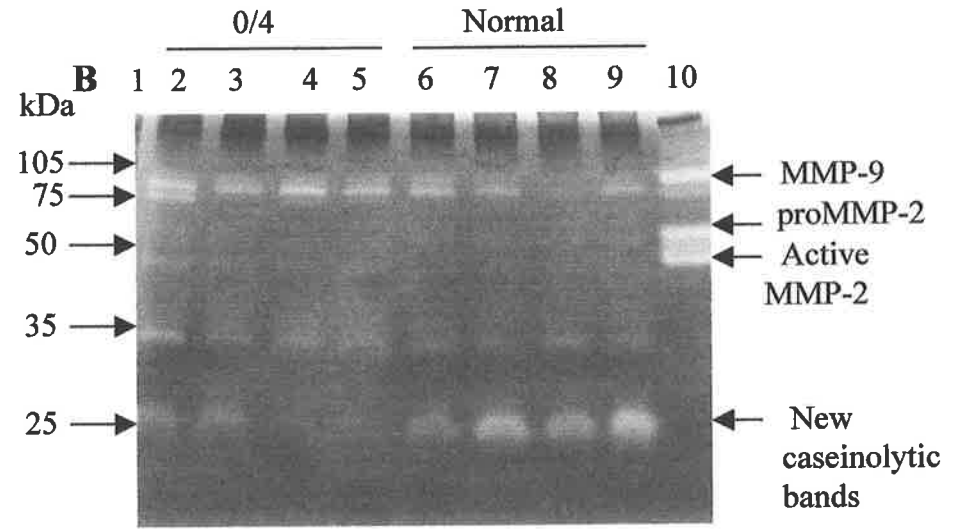
B
0/4
Normal
1 2 3 4 5 6 7 8 9 10
kDa
105
75
50
35
25
MMP-9
proMMP-2
Active
MMP-2
New
caseinolytic
bands

Figure 3.5 Continued

Panel C: Lung tissue samples from 4 individual rats following 4 h anesthesia, no ischemia with 24 h recovery (0/24) compared to 4 individual rats in normal control group (Normal, no anesthesia, no ischemia, no reperfusion).

Lane 2-5: Lungs, 0/24.
Lane 6-9: Lungs, Normal.

Panel D: Lung tissue samples from 4 individual rats following 4 h anesthesia, no ischemia with 72 h recovery (0/72) compared to 4 individual rats in normal control group (Normal, no anesthesia, no ischemia, no reperfusion).

Lane 2-5: Lungs, 0/72.
Lane 6-9: Lungs, Normal.

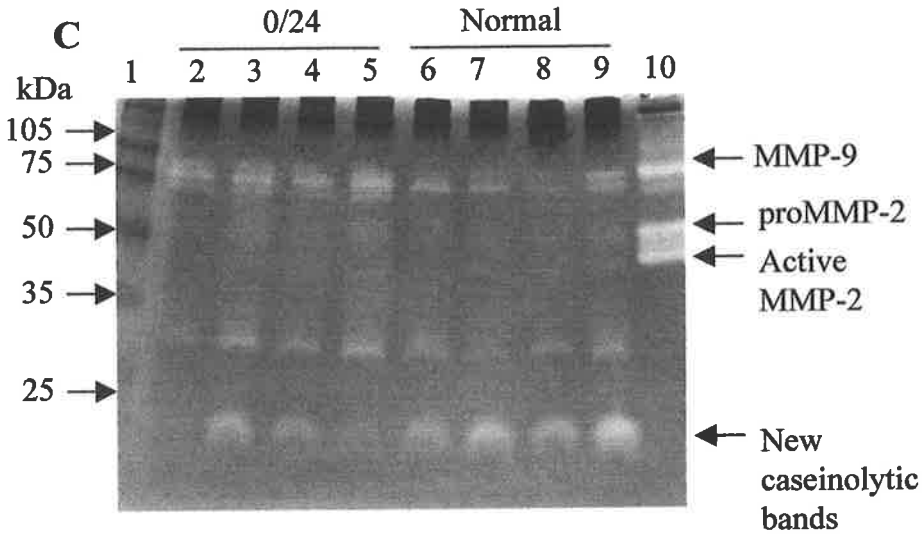
C
0/24
Normal
1 2 3 4 5 6 7 8 9 10
kDa
105
75
50
35
25
MMP-9
proMMP-2
Active MMP-2
New caseinolytic bands

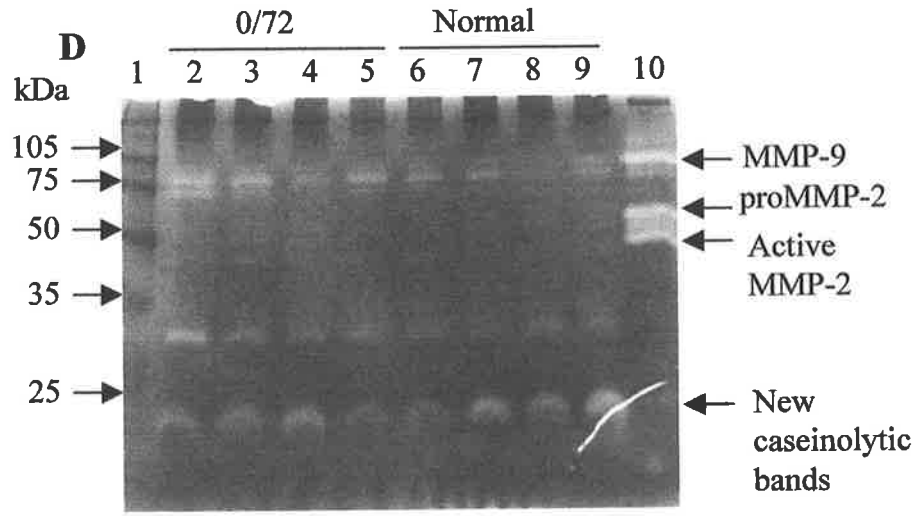
D
0/72
Normal
1 2 3 4 5 6 7 8 9 10
kDa
105
75
50
35
25
MMP-9
proMMP-2
Active MMP-2
New caseinolytic bands

3.3.6 Effects of anesthesia on production of gelatinolytic MMP-2 and MMP-9 in the lung tissues of rats using the same samples as above for determining that samples were harvested and processed properly and for the presence of activity of MMPs (Sham-operated rats versus normal control rats).

The gelatinolytic activity of MMP-9, proMMP-2 and active MMP-2 were detected in all lung tissues from sham-operated group or normal control group (Normal rats, no anesthesia, no ischemia, no reperfusion). There was an increased production of MMP-9 in the lung tissue of rats that underwent 4 h anesthesia and during early period of recovery (Figure 3.6 lane 2-5 in panel A&B). The elevated MMP-9 levels returned to baseline level after 24 h or 72 h of recovery (Figure 3.6 lane 2-5 in panel C&D). There were no alterations of proMMP-2 observed following 4 h anesthesia with varying times of recovery. The levels of active MMP-2 were increased immediately after 4 h anesthesia, and then returned to baseline level (Figure 3.6 lane 2-5 in panel A, B, C, and D).

3.3.7 Alterations of caseinolytic activity in the lung tissues following skeletal muscle I/R (Ischemic rats versus sham-operated rats).

The activity of the newly identified 20 kDa caseinolytic species was increased in the lung tissues of rats that underwent 4 h bilateral hindlimb ischemia only (I/R: 4/0, Figure 3.7 lane 2-5 in panel A). It then decreased with reperfusion (I/R: 4/4, Figure 3.8 lane 2-5 panel B), becoming undetectable (Figure 3.7 lane 2-5 in panel C) after 24 hours of reperfusion (I/R: 4/24), then a weak band was detected following 72 h of reperfusion (I/R: 4/72, Figure 3.7 lane 2-5 in panel D). In the sham-operated rats, this band was down-regulated in the lung tissues, presumably due to effects of anesthesia (Figure 3.7 lane 6-9 in panel A). It then increased gradually with recovery (Figure 3.7 lane 6-9 in panel B & C), reaching to the baseline level after 72 h (Figure 3.7 lane 6-9 in panel D).

Figure3.6: Zymographic detection of gelatinolytic activity in the lung using the same samples as those in Figure 3.5 for determining the presence of enzymic activity of MMPs

Rats were subjected to 4 h anesthesia, no ischemia followed by 0, 4, 24, or 72 h recovery compared to normal control rats, no anesthesia, no ischemia. Lane 1: molecular weight marker and Lane 10: MMPs positive control. All experimental lanes (2-9) contain 80 μg of total protein. Bands corresponding to MMP-9, pro-MMP-2 and active MMP-2 are shown (arrows).

Panel A: Lung tissue samples from 4 individual rats following 4 h anesthesia, no ischemia (0/0) compared to 4 individual rats in normal control group (Normal, no anesthesia, no ischemia, no reperfusion).

Lane 2-5: Lungs, 0/0.
Lane 6-9: Lungs, Normal.

Panel B: Lung tissue samples from 4 individual rats following 4 h anesthesia, no ischemia with 4 h recovery (0/4) compared to 4 individual rats in normal control group (Normal, no anesthesia, no ischemia, no reperfusion).

Lane 2-5: Lungs, 0/4.
Lane 6-9: Lungs, Normal.

Panel C: Lung tissue samples from 4 individual rats following 4 h anesthesia, no ischemia with 24 h recovery (0/24) compared to 4 individual rats in normal control group (Normal, no anesthesia, no ischemia, no reperfusion).

Lane 2-5: Lungs, 0/24.
Lane 6-9: Lungs, Normal.

Panel D: Lung tissue samples from 4 individual rats following 4 h anesthesia, no ischemia with 72 h recovery (0/72) compared to 4 individual rats in normal control group (Normal, no anesthesia, no ischemia, no reperfusion).

Lane 2-5: Lungs, 0/72.
Lane 6-9: Lungs, Normal.

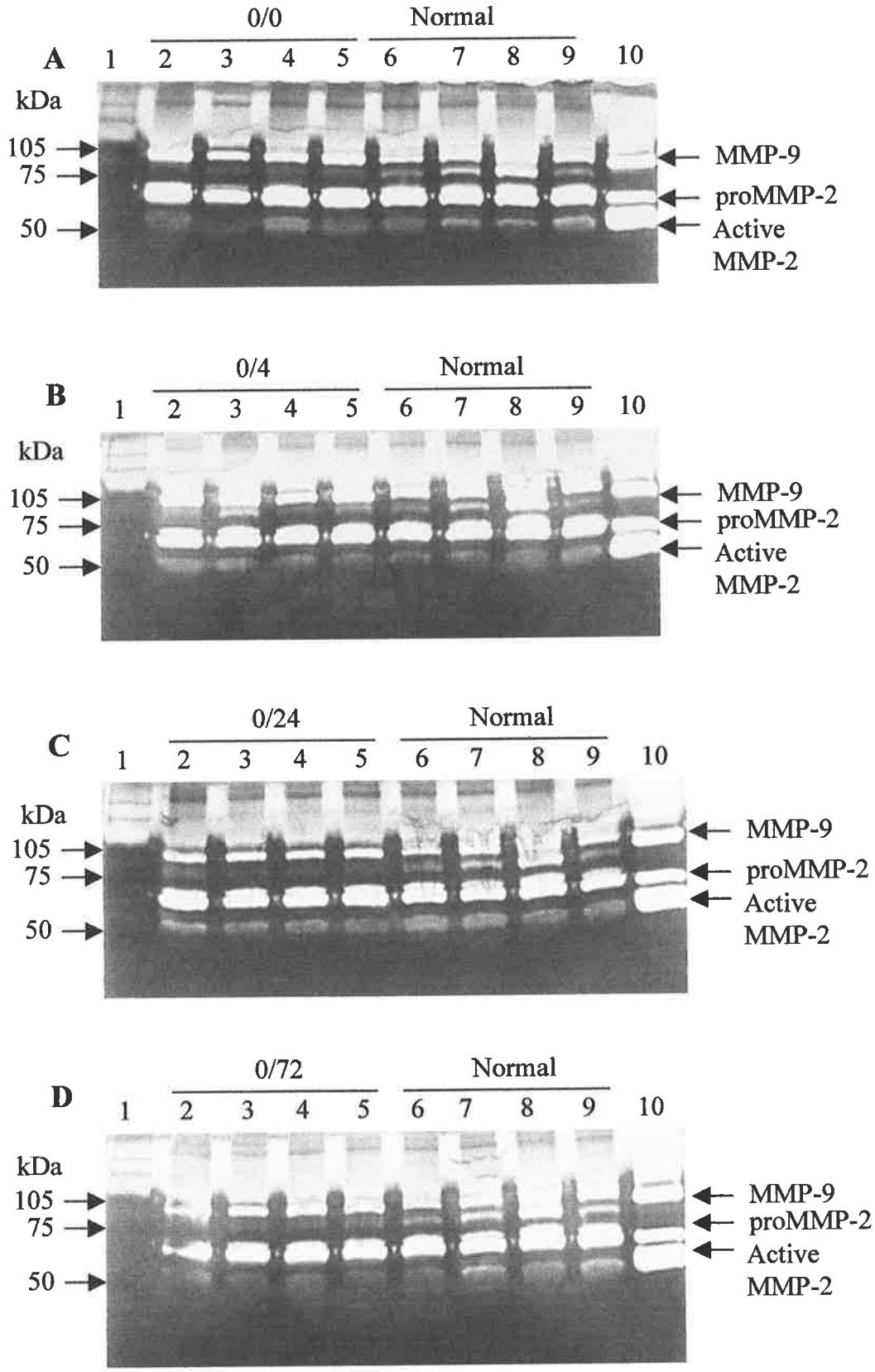
A
0/0
Normal
1 2 3 4 5 6 7 8 9 10
kDa
105
75
50
MMP-9
proMMP-2
Active MMP-2
B
0/4
Normal
1 2 3 4 5 6 7 8 9 10
kDa
105
75
50
MMP-9
proMMP-2
Active MMP-2
C
0/24
Normal
1 2 3 4 5 6 7 8 9 10
kDa
105
75
50
MMP-9
proMMP-2
Active MMP-2
D
0/72
Normal
1 2 3 4 5 6 7 8 9 10
kDa
105
75
50
MMP-9
proMMP-2
Active MMP-2

Figure 3.7: Zymographic detection of caseinolytic activity in the lung

Rats were subjected to 4 h bilateral hindlimb ischemia followed by 0, 4, 24, or 72 h reperfusion before tissues were harvested compared to sham-operated rats with 4 h anesthesia, no ischemia followed by 0, 4, 24, or 72 h recovery. Lane 1: molecular weight marker and Lane 10: MMPs positive control. All experimental lanes (2-9) contain 80 μg of total protein. Bands corresponding to MMP-9, pro-MMP-2, active MMP-2 and new caseinolytic bands are shown (arrows).

Panel A: Lung tissue samples from 4 individual rats following 4 h ischemia and no reperfusion (4/0) compared to those from 4 individual rats following 4 h anesthesia, no ischemia (0/0).

Lane 2-5: Lungs, 4/0.
Lane 6-9: Lungs, 0/0.

Panel B: Lung tissue samples from 4 individual rats following 4 h ischemia and 4h reperfusion (4/4) compared to those from 4 individual rats following 4 h anesthesia with 4 h recovery, no ischemia (0/4).

Lane 2-5: Lungs, 4/4.
Lane 6-9: Lungs, 0/4.

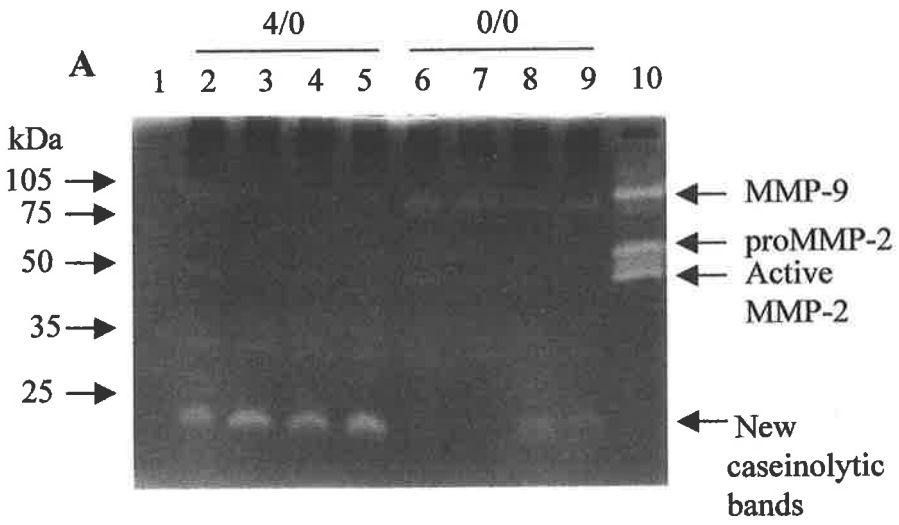
A
4/0
0/0
1 2 3 4 5 6 7 8 9 10
kDa
105
75
50
35
25
MMP-9
proMMP-2
Active
MMP-2
New
caseinolytic
bands

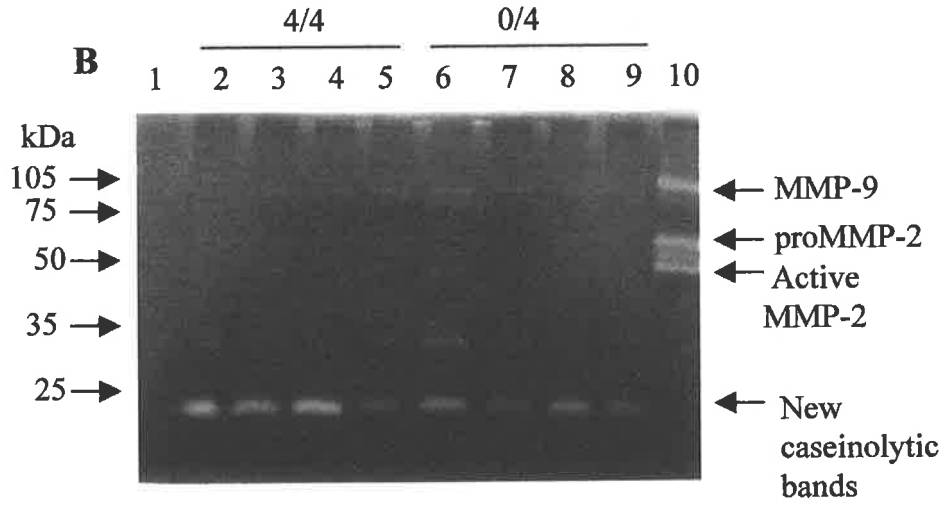
B
4/4
0/4
1 2 3 4 5 6 7 8 9 10
kDa
105
75
50
35
25
MMP-9
proMMP-2
Active
MMP-2
New
caseinolytic
bands

Figure 3.7 Continued

Panel C: Lung tissue samples from 4 individual rats following 4 h ischemia and 24 h reperfusion (4/24) compared to those from 4 individual rats following 4 h anesthesia with 24 h recovery, no ischemia (0/24).

Lane 2-5: Lungs, 4/24.
Lane 6-9: Lungs, 0/24.

Panel D: Lung tissue samples from 4 individual rats following 4 h ischemia and 72 h reperfusion (4/72) compared to those from 4 individual rats following 4 h anesthesia with 72 h recovery, no ischemia (0/72).

Lane 2-5: Lungs, 4/72.
Lane 6-9: Lungs, 0/72.

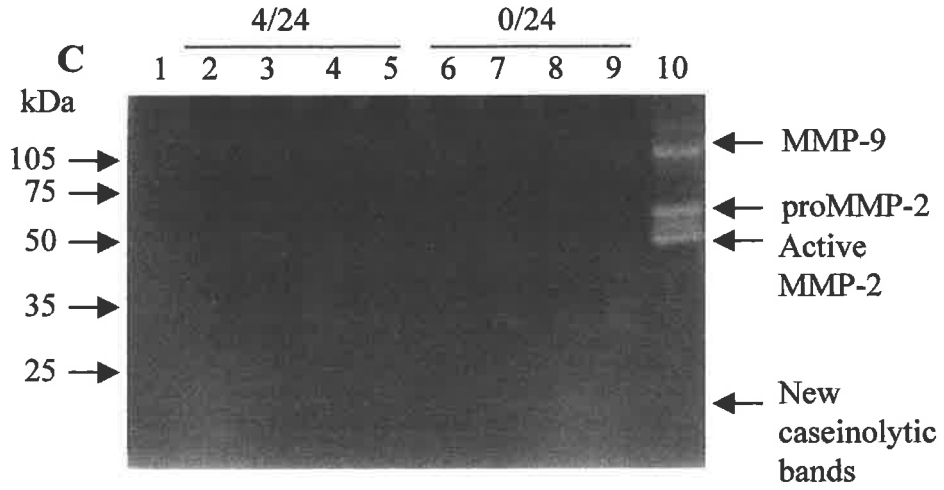
C
4/24
0/24
1 2 3 4 5 6 7 8 9 10
kDa
105
75
50
35
25
MMP-9
proMMP-2
Active MMP-2
New caseinolytic bands

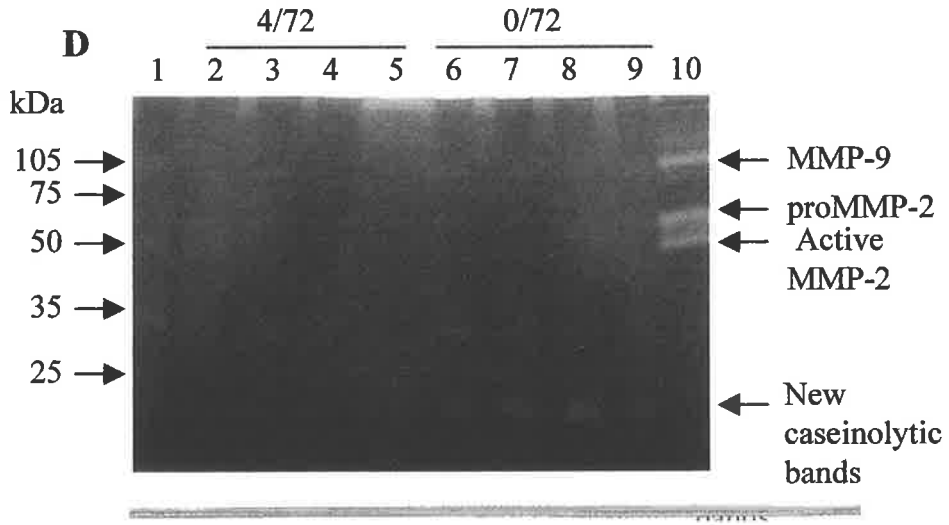
D
4/72
0/72
1 2 3 4 5 6 7 8 9 10
kDa
105
75
50
35
25
MMP-9
proMMP-2
Active MMP-2
New caseinolytic bands

3.3.8 Alterations of gelatinolytic MMP-2 and MMP-9 in the lung tissues following skeletal muscle I/R using the same samples as above for determining that the samples were harvested and processed properly and the presence of activity of MMPs (Ischemic rats versus sham-operated rats).

The activity of proMMP-9, active MMP-9, proMMP-2, and active MMP-2 were detected in the lung tissues of rats. The proMMP-9 and active MMP-9 were elevated in the lung tissues of rats that underwent 4 h bilateral hindlimb ischemia either with no reperfusion or 4 h, 24 h, and 72 h reperfusion respectively (Figure 3.8 lane 2-5 in panel A, B, C, and D), compared with those in correspondent sham-operated group (Figure 3.8 lane 6-9 in panel A, B, C, and D). There was no difference of MMP-2 activity between ischemic rats and sham-operated rats (Figure 3.8 panel A, B, C, and D).

3.3.9 Zymographic identification of the newly-detected active caseinolytic species in the lung tissues.

To identify if this newly-detected active caseinolytic species is an MMP or another protease, samples were incubated with EDTA, an inhibitor of MMPs, phenanthroline, a zinc chelator, and PMSF, an inhibitor of serine proteinase respectively. This new active caseinolytic species was completely inhibited by EDTA and phenanthroline (bands absent, Figure 3.9 panel B and panel C), but it was not inhibited by PMSF (bands present, Figure 3.9 panel D). This implies that the newly-identified active caseinolytic species in the lung was considered as one of MMPs rather than serine proteinase.

3.3.10 Confirmation of this newly-detected active caseinolytic MMP by Western Blot in the lung tissues.

This new active caseinolytic MMP in the lung tissues was considered to be a low molecular weight MMP according to the standard protein molecular weight. Therefore, MMP-7, whose molecular weight is 28/19 kDa (latent/active), was considered as a candidate. However, there

Figure 3.8: Zymographic detection of gelatinolytic activity in the lung using the same samples as those in Figure 3.7 for determining the presence of enzymic activity of MMPs

Rats were subjected to 4 h bilateral hindlimb ischemia followed by 0, 4, 24, or 72 h reperfusion before tissues were harvested compared to sham-operated rats with 4 h anesthesia, no ischemia followed by 0, 4, 24, or 72 h recovery. Lane 1: molecular weight marker and Lane 10: MMPs positive control. All experimental lanes (2-9) contain 80 μg of total protein. Bands corresponding to MMP-9, pro-MMP-2 and active MMP-2 are shown (arrows).

Panel A: Lung tissue samples from 4 individual rats following 4 h ischemia and no reperfusion (4/0) compared to those from 4 individual rats following 4 h anesthesia, no ischemia (0/0).

Lane 2-5: Lungs, 4/0.
Lane 6-9: Lungs, 0/0.

Panel B: Lung tissue samples from 4 individual rats following 4 h ischemia and 4 h reperfusion (4/4) compared to those from 4 individual rats following 4 h anesthesia with 4 h recovery, no ischemia (0/4).

Lane 2-5: Lungs, 4/4.
Lane 6-9: Lungs, 0/4.

Panel C: Lung tissue samples from 4 individual rats following 4 h ischemia and 24 h reperfusion (4/24) compared to those from 4 individual rats following 4 h anesthesia with 24 h recovery, no ischemia (0/24).

Lane 2-5: Lungs, 4/24.
Lane 6-9: Lungs, 0/24.

Panel D: Lung tissue samples from 4 individual rats following 4 h ischemia and 72 h reperfusion (4/72) compared to those from 4 individual rats following 4 h anesthesia with 72 h recovery, no ischemia (0/72).

Lane 2-5: Lungs, 4/72.
Lane 6-9: Lungs, 0/72.

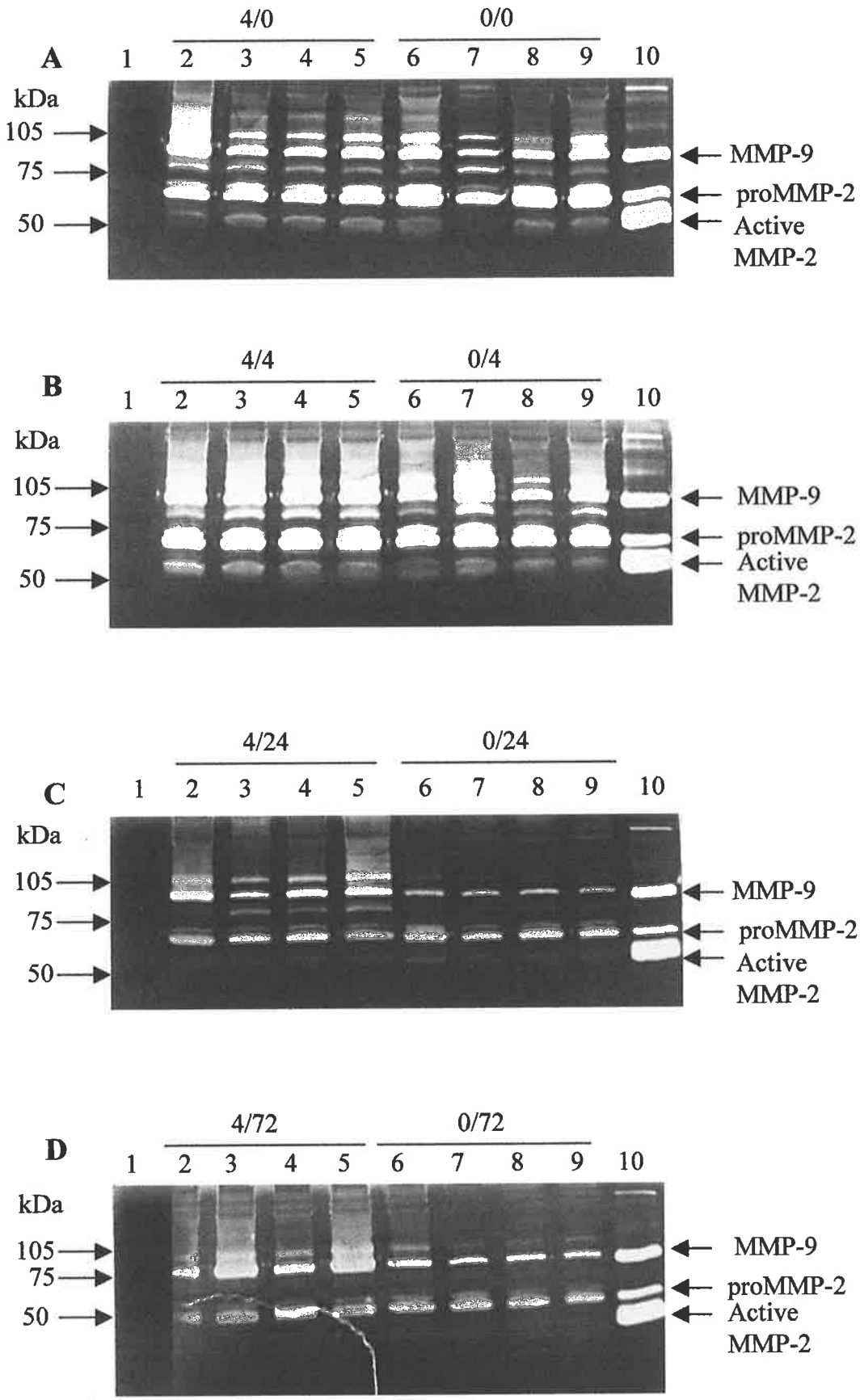
A
4/0
0/0
1 2 3 4 5 6 7 8 9 10
kDa
105
75
50
MMP-9
proMMP-2
Active
MMP-2
B
4/4
0/4
1 2 3 4 5 6 7 8 9 10
kDa
105
75
50
MMP-9
proMMP-2
Active
MMP-2
C
4/24
0/24
1 2 3 4 5 6 7 8 9 10
kDa
105
75
50
MMP-9
proMMP-2
Active
MMP-2
D
4/72
0/72
1 2 3 4 5 6 7 8 9 10
kDa
105
75
50
MMP-9
proMMP-2
Active
MMP-2

Figure3.9: Caseinolytic zymography to identify nature of the new matrix metalloproteinase bands observed in lung tissue samples

For each panel: Lane 1: molecular weight marker and Lane 10: MMPs positive control. All experimental lanes (2-9) contain 80 μg of total protein. Bands corresponding to MMP-9, pro-MMP-2, active MMP-2, MMP-13 and new caseinolytic MMP are shown (arrows).

Panel A: Casein zymography showing the new caseinolytic bands in lung tissue as positive control panel.

Lane 2-5 are 4 individual lung tissue samples from rats following 4 h bilateral hindlimb ischemia without reperfusion (4/0).

Lane 6,7 are 2 individual lung tissue samples of rats in correspondent sham-operated group that underwent 4 h anesthesia, no ischemia (0/0).

Lane 8.9 are 2 individual wounded skin samples which have been demonstrated to produce MMP-13 as positive control (Wound Healing Laboratory at The Queen Elizabeth Hospital) (Skin).

Panel B: Casein zymographic identification of the nature of new caseinolytc bands in lung tissue.

The lane structure is the same as panel A. The samples were incubated with 10 mM of EDTA in the development buffer.

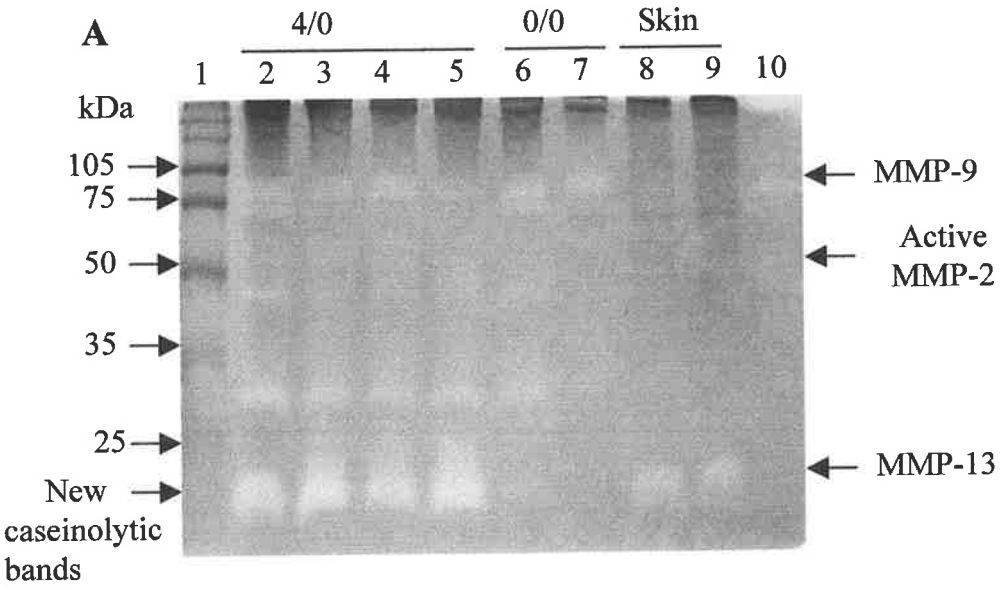
A
4/0
0/0
Skin
1
2
3
4
5
6
7
8
9
10
kDa
105
75
50
35
25
New caseinolytic bands
MMP-9
Active MMP-2
MMP-13

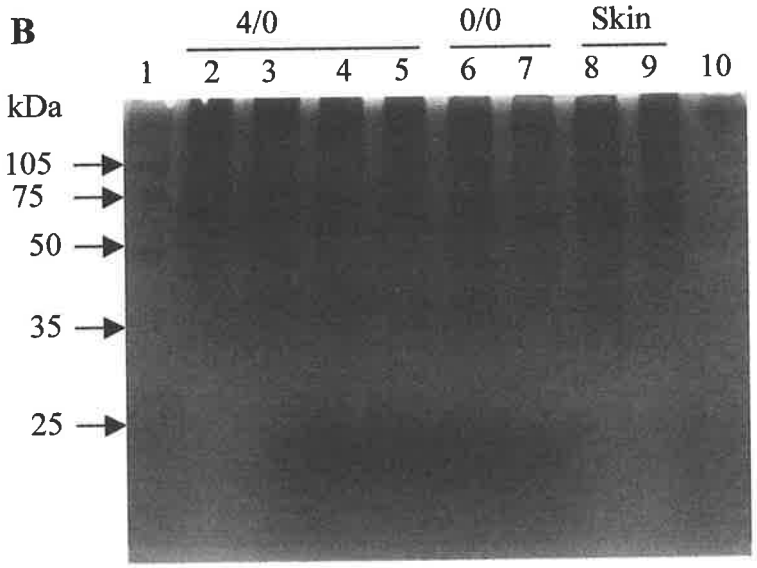
B
4/0
0/0
Skin
1
2
3
4
5
6
7
8
9
10
kDa
105
75
50
35
25

Figure 3.9 Continued

Panel C: Casein zymographic identification of the nature of new caseinolytic bands in lung tissue.

The lane structure is the same as panel A. The samples were incubated with 10 mM of phenanthroline in the development buffer.

Panel D: Casein zymographic identification of the nature of new caseinolytic bands in lung tissue.

The lane structure is the same as panel A. The samples were incubated with 0.1 mM of PMSF.

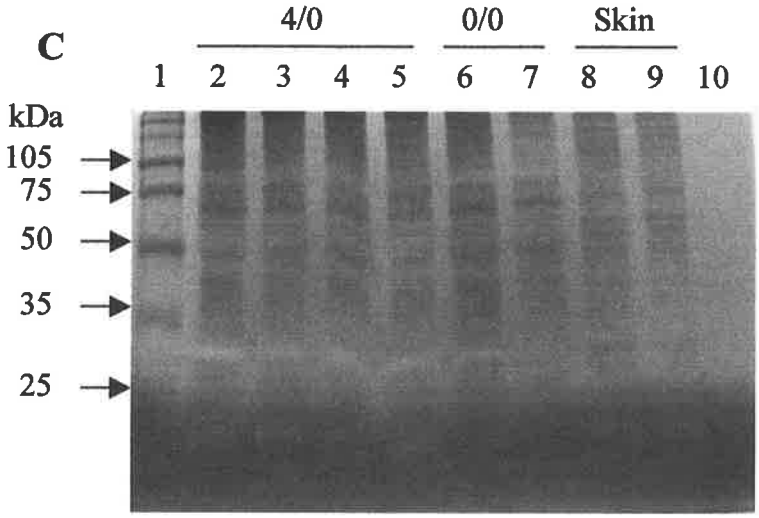
C
4/0
0/0
Skin
1 2 3 4 5 6 7 8 9 10
kDa
105
75
50
35
25

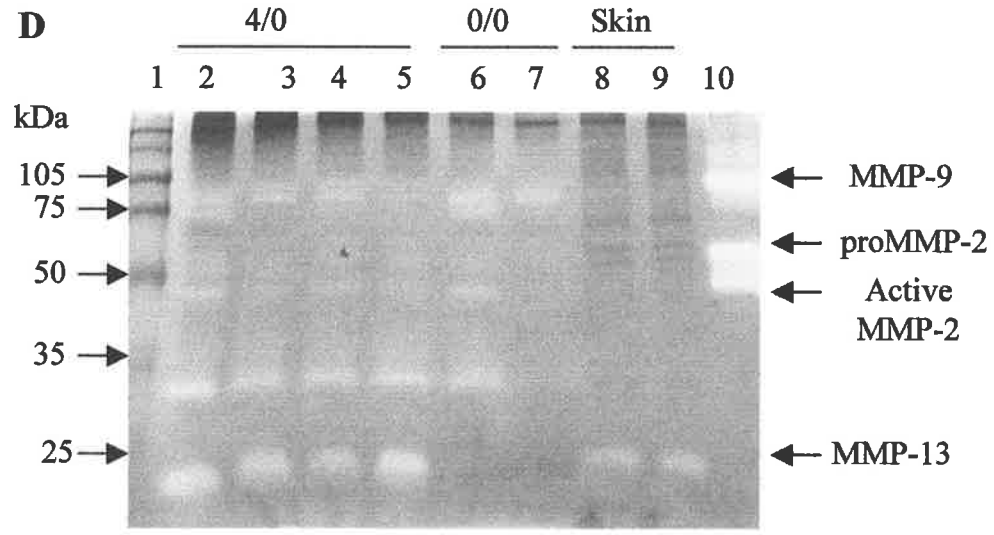
D
4/0
0/0
Skin
1 2 3 4 5 6 7 8 9 10
kDa
105
75
50
35
25
MMP-9
proMMP-2
Active MMP-2
MMP-13

Figure 3.10: Western blotting analysis for confirmation of the new active caseinolytic MMP bands detected in the lung

For each panel: Lane 1: molecular weight marker and Lane 10: MMPs positive control. All experimental lanes (2-9) contain 80 μg of total protein. Bands corresponding to MMP-9, pro-MMP-2, active MMP-2, MMP-13 and new caseinolytic MMP are shown (arrows).

Panel A: Confirmation of the active caseinolytic MMP bands in the lung using the anti-MMP-7 affinity-purified goat polyclonal antibody (Santa Cruz).

Lane 2-5 are 4 individual lung tissue samples from rats following 4 h bilateral hindlimb ischemia without reperfusion (4/0).

Lane 6,7 are 2 individual lung tissue samples of rats in correspondent sham-operated group that underwent 4 h anesthesia, no ischemia (0/0).

Lane 8.9 are 2 individual wounded skin samples which have been demonstrated to produce MMP-13 as positive control (Wound healing laboratory at The Queen Elizabeth Hospital) (Skin).

Panel B: Confirmation of the active caseinolytic MMP bands in lung tissue using anti-MMP-13 affinity-purified goat polyclonal antibody (Santa Cruz).

The lane structure is the same as panel A.

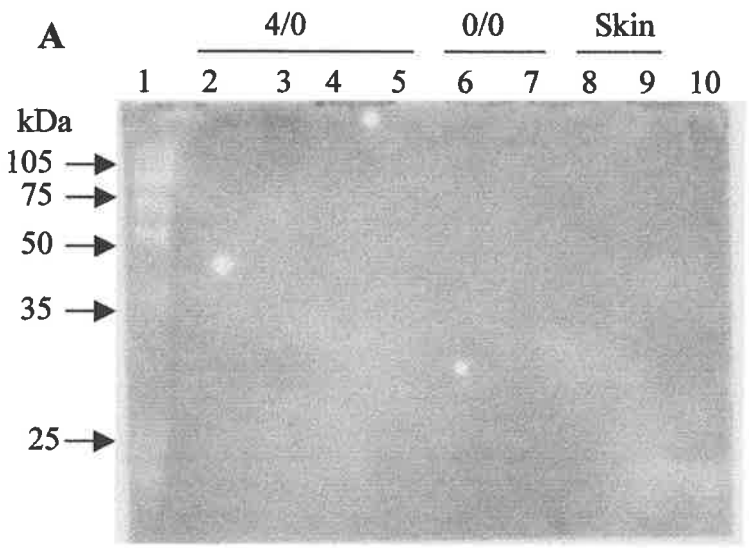
A
4/0
0/0
Skin
1 2 3 4 5 6 7 8 9 10
kDa
105
75
50
35
25

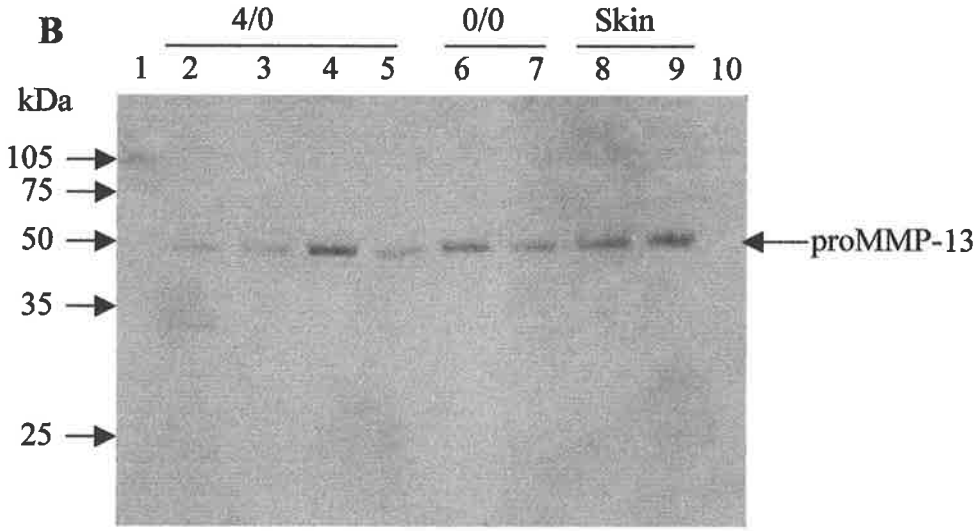
B
4/0
0/0
Skin
1 2 3 4 5 6 7 8 9 10
kDa
105
75
50
35
25
proMMP-13

was no positive band shown on western blot following exposure of blot to anti-MMP-7 polyclonal antibody (Figure 3.10 panel A). Furthermore, MMP-13 (52/42 kDa) was considered as another candidate based on experiments conducted in the wound-healing laboratory at The Queen Elizabeth Hospital (MMP-13 band was shown near the bottom of the casein gel for wounded skin samples). The samples from skin wound were employed in this experiment as a positive control. Once again, there was no positive signal shown on the western blotting film. This result suggests that the positive control was not working (Figure 3.10 panel B). Therefore, the possibility could not be excluded if this active casenolytic species is MMP-7 or MMP-13, due to the lack of positive control signal on Western blotting film.

3.3.11 Effects of doxycycline on activity of this newly-recognised caseinolytic MMP in the lung tissues.

There was an increased production of this active caseinolytic MMP in the lung tissues with administration of doxycycline (Figure 3.11 lane 6-9 in panel A&B) prior to bilateral hind limb 4 h ischemia and 24 h of reperfusion compared with untreated corresponding group (Figure 3.11 lane 2-5 in panel B), but it had not reached to the level in sham-operated group (Figure 3.11 lane 2-5 in panel A).

Figure3.11: Effects of doxycycline on the activity of this caseinolytic MMP in the lung

Rats were classified as 4 groups: (1) 4 h bilateral hindlimb ischemia followed by 24 h reperfusion before tissues were harvested (4/24), (2) 4 h anesthesia followed by 24 h recovery (0/24), (3) 4 h bilateral hindlimb ischemia followed by 24 h reperfusion with low dose doxycycline treatment (4/24 Doxy L.D), (4) 4 h bilateral hindlimb ischemia followed by 24 h reperfusion with high dose doxycycline treatment (4/24 Doxy H.D). Lane 1: molecular weitht marker. Lane 10: supernatant of HT29 colon cancer cell line, which was expected to produce MMP-7, but in fact no active MMP present. All experimental lanes (2-9) contain 80 μg of total protein.

Panel A: Effects of low dose doxycycline on the activity of this caseinolytic MMP in the lung.

Lane 2-5 are 4 individual lung tissues, 0/24.
Lane 6-9 are 4 individual lung tissues, 4/24 Doxy L. D.

Panel B: Effects of high dose doxycycline on the activity of this caseinolytic MMP in the lung.

Lane 2-5 are 4 individual lung tissues, 4/24.
Lane 6-9 are 4 individual lung tissues, 4/24 Doxy H. D.

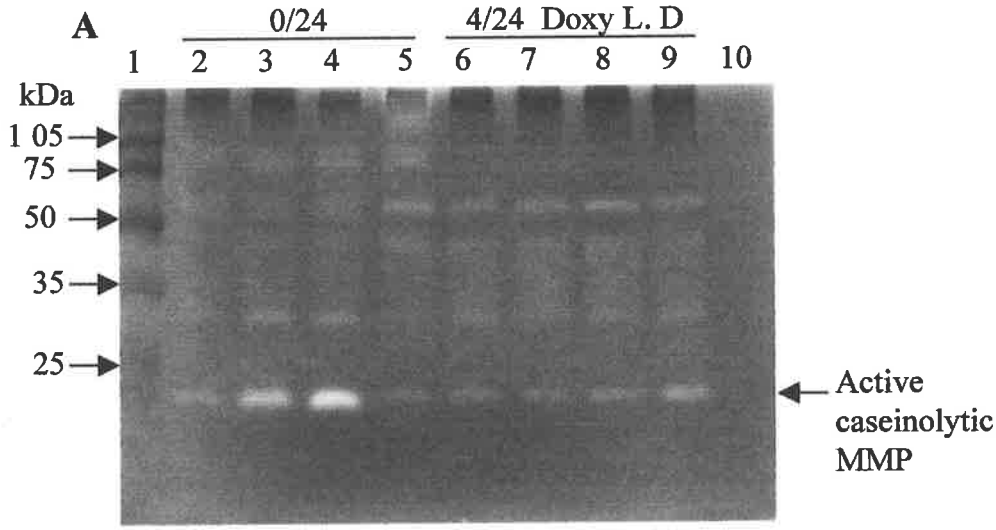
A
0/24
4/24 Doxy L. D
1 2 3 4 5 6 7 8 9 10
kDa
1 05
75
50
35
25
Active caseinolytic MMP

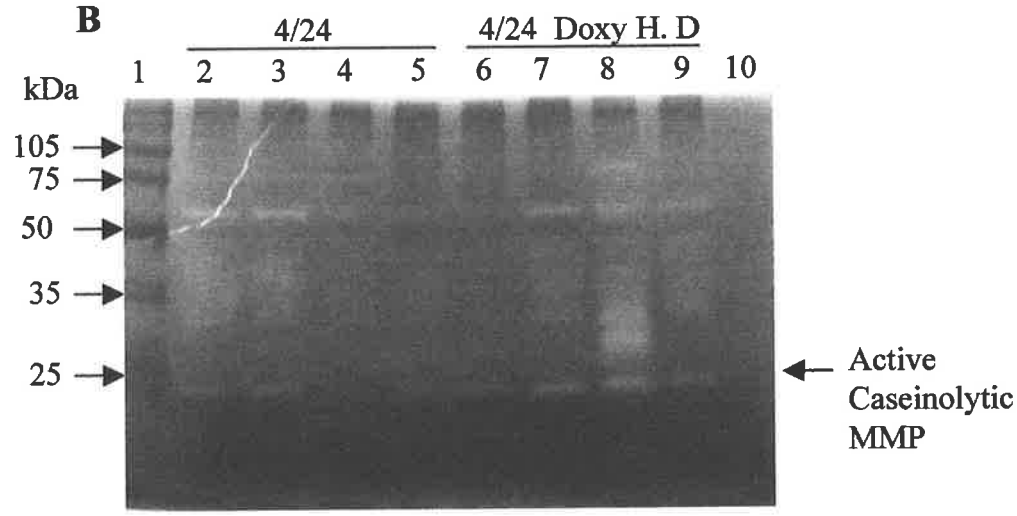
B
4/24
4/24 Doxy H. D
1 2 3 4 5 6 7 8 9 10
kDa
105
75
50
35
25
Active Caseinolytic MMP

3.4 Discussion

According to the specificity of substrate proteolysis, the MMP family is currently divided into 4 subclasses, which include collagenases such as MMP-1 and MMP-8, gelatinases (MMP-2 and MMP-9), stromelysin (MMP-3 and MMP-11) and matrilysin (MMP-7 and MMP-26). To facilitate investigation of the activity of MMPs, gelatin, collagen III, and casein have all been used as zymographic substrates in previous studies (480), (481). In the current study, gelatin or casein were embedded in SDS-PAGE gel to study the proteolytic activity of MMPs in tissues of rats that have undergone bilateral hindlimb ischemia and reperfusion.

Using caseinolytic zymography, a newly-identified caseinolytic species was detected in the lung tissues. It was demonstrated to be an MMP with low molecular weight, but the identity has not been confirmed by western blotting due to the lack of suitable positive control. This newly-identified MMP was expressed in normal lung tissues. It was less strongly expressed under anaesthesia, but it was up-regulated in the lung tissues while skeletal muscle was subjected to 4 h ischemia. The activity of this MMP was becoming weak again with reperfusion, it then recovered to the baseline level after 72 h of reperfusion. There was no caseinolytic activity detected both in skeletal muscle and the liver. In addition, two caseinolytic activity bands were detected in the kidney with molecular weight 80-90 kDa. However, no changes of the activity were observed following skeletal muscle ischemia and reperfusion. Therefore, no further investigations were conducted in the kidney.

On gelatinolytic zymography, there was detectable pro-MMP-2 at baseline level in normal skeletal muscle, whereas there was no detectable MMP-9 present in normal skeletal muscle. However, MMP-9 was induced dramatically by ischemia and reperfusion in skeletal muscle. ProMMP-2 was also increased in skeletal muscle after ischemia followed by reperfusion. These alterations in MMP-2 and MMP-9 in skeletal muscle are consistent with those observed by Roach et al and have been discussed in their report (302). In kidney, a baseline level of

proMMP-2 detected and maintained at the same level under all conditions. Moreover, there was no detectable MMP-9 in kidney under all conditions. In liver, there was a detectable low baseline level of both MMP-9 and ProMMP-2, which was remained under all conditions. Therefore, the expression of MMP-2 and MMP-9 was considered less important in the kidney and liver following skeletal muscle ischemia and reperfusion because of their low baseline level and lack of change with I/R. In normal lung tissue, and as well as experimental lung tissue, gelatinolytic activity corresponding to proMMP-9, active MMP-9, proMMP-2, and active MMP-2 was all detected on zymography. ProMMP-9 and active MMP-9 were up-regulated in the lung tissues of rats following 4 h bilateral hindlimb ischemia either before reperfusion or after 4 h, 24 h, or 72 h of reperfusion respectively, while there was no significant change in MMP-2 observed.

The current investigation suggested that MMP-9 and MMP-2 are involved in remote lung injury after skeletal muscle ischemia and reperfusion. Recently, it has been reported that expression of MMP-2 and MMP-9 correlated with altered alveolar-capillary permeability and increased with severity of ischemia/reperfusion-induced lung injury in a porcine model (289). The increased alveolar permeability was considered to be the result of capillary basal membrane disruption, occurring as a result of degradation of collagen IV, an important constituent of the lung basement membrane by MMP-2 and MMP-9. The role of MMP-9 activity in pulmonary ischemia/reperfusion injury has also been emphasised by Yano et al (293). In addition, a higher concentration of MMP-9 has been found in lung edema fluid of patients with adult respiratory distress syndrome (ARDS) (297). Although the primary causes of pulmonary injury vary, the basic undergoing pathological condition is in common, that is pulmonary edema due to disruption of alveolar-capillary basal membrane disruption. MMPs have been suggested to play a crucial role during this pathological progression. Furthermore, the important role of MMP-2 and MMP-9 in I/R injury in other organs such as brain and heart has been investigated in other studies (341), (348).

In the lung, MMP-2 is expressed by fibroblasts, endothelial cells and vascular smooth muscle cells, while MMP-9 was widely found in inflammatory cells, especially in neutrophils. Bronchial and type II alveolar epithelial cells produce both MMP-2 and MMP-9 (360), (361), (362). The production of MMP-2 and MMP-9 may also be regulated by pro-inflammatory cytokines. Gottschall et al (363) have demonstrated that TNF-α and IL-1β induced MMP-9 production in rat astrocytes. High levels of MMP-9, TNF-α, and IL-1β were found in the bronchoalveolar lavage fluid from the patients with acute respiratory distress syndrome (ARDS) (301). IL-1β was found to elevate MMP-2 production in human dental pulp cell cultures (482). Inhibition of these cytokines could be another option to ameliorate pulmonary injury following ischemia/reperfusion.

In order to investigate further the role of MMPs in I/R injury both in ischemic organ and remote organs, caseinolytic zymography was conducted to detect caseinolytic MMP activity in the tissues. Matrilysin and stromelysin are caseinolytic MMPs that are detectable on casein gel zymography. Caseinolytic MMPs were not detected either in normal skeletal muscle or in skeletal muscle after 4 h ischemia followed by reperfusion. However, a significant active species was identified in the lung tissues on caseinolytic zymography. The molecular weight of this active species was approximately 20 kDa according to the standard protein molecular weight marker. This active enzyme was recognised as one of the matrix metalloproteinases since its activity was completely inhibited by EDTA and 1,10-phenanthroline respectively, but was not inhibited by PMSF, an inhibitor of serine proteases. Among the MMPs, MMP-7 and MMP-12 are of lower molecular weight, suggesting this new casenolytic MMP may be MMP-7 or MMP-12. The molecular weight of the pro-form of MMP-7 is 28 kDa and its active form is 19 kDa, while the pro-enzyme of MMP-12 is 54 kDa and the active form is 20 kDa (418); (449). To confirm if this active species is MMP-7, a polyclonal MMP-7 antibody was used in western blotting. However, there was no positive signal detected. Even so, the

active enzyme could not be excluded as MMP-7, because there was no suitable MMP-7 positive control available in this experiment. A previous study in wound healing laboratory in our hospital has found that there was an over-expression of MMP-13 in wounded skin (T. Rayner, personal communication). These active bands were also detected at a similar size on casein gels to those observed in the current study. To confirm if the active enzyme was MMP-13, positive control samples from wounded skin and MMP-13 antibody were used in the western blot. Again, no positive signal was detected at the predicted 20 kDa position. So could it be concluded that this active enzyme is not active MMP-13. The question was raised if this active caseinolytic species were MMP-12 due to its lower molecular weight, active form 20 kDa. Because a suitable MMP-12 positive control was not available for this study, further study is therefore still needed to determine the identity of this caseinolytic species.

A number of studies have shown that lower torso I/R can lead to multiple-organ injury with local events including permeability edema, compartment syndrome, and muscle necrosis. (302), (285). Remote organ pulmonary insufficiency is the most frequent adverse event following lower torso I/R, characterised by neutrophil sequestration and increased pulmonary vascular permeability (285) (483). Kyriakides and coworkers have shown that neutrophil sequestration in lung tissue is the major pathological event in the development of distant lung injury (280). It was determined that neutrophil sequestration was dependent upon L-selectin and E-selectin with lung injury reduced by infusion of anti-selectin antibodies in a rat model (287). Moreover, remote lung injury was also related to complement activation, with a 94% of reduction in lung permeability when animals were treated with sCR1 (soluble complement receptor-1), even though pulmonary neutrophil sequestration was not abolished (285) (280) (286). The adhesion of neutrophils to activated microvascular endothelium is a key step in the remote organ injury, leading to the release of oxygen free radicals and cytotoxic proteinases, and facilitating neutrophil diapedesis, resulting in increased vascular permeability (278); (484).

In recent studies, disruption of the alveolar extracellular matrix and protein exudate into the alveolar space with hyalinisation of the alveolar membranes have been elucidated as key pathologic changes of adult respiratory distress syndrome (485). MMPs were implicated to play an important role in the degradation and remodelling of extracellular matrix. Increased expression of MMP-9 was detected in the bronchoalveolar lavage fluid (BALF) of patients with adult respiratory distress syndrome and asthma, suggesting over-expression of MMP-9 may play a key role in the lung injury (295), (294). The administration of MMP inhibitors have been shown to abolish both elastase and MMP activity, reducing neutrophil infiltration, decreasing capillary extravasation and therefore preventing lung dysfunction secondary to cardiopulmonary bypass (298). Up-regulation of MMP-9 and MMP-2 was also observed in the lungs following hind limb or lung I/R injury, associated with leukocyte infiltration into the tissues (302), (289), (293). Moreover, MMPs have been demonstrated to be involved in the recruitment of inflammatory cells into the lung tissues. Metalloelastase-deficient animals had less neutrophil infiltration into the lung tissues as compared with the wild-type control animals (298). Stromelysin-1 was identified to be associated with modulation of leukocyte infiltration into inflamed tissues (486). So was MMP-9 found to be necessary for neutrophil migration into the lung tissues in necrotizing pancreatitis-induced lung injury (299).

The expression of caseinolytic MMPs in the lung tissues following remote organ I/R has not been reported in the literature. In this study, we therefore for the first time have detected the over-expression of caseinolytic MMP in the lung tissues following bilateral hind limb I/R injury. Although the identity of this casenolytic MMP has not been confirmed, it was shown to be a lower molecular weight MMP. Matrilysin (MMP-7), one of low molecular MMPs has found to be expressed in the epithelium of peribronchial glands and conducting airways in normal lungs. The expression of MMP-7 was increased in migrating airway epithelial cells in wounded human and mouse trachea. Its up-regulation following injury, its induction by

alveolar epithelium, and its secretion either apically or basally suggested that MMP-7 serves multiple functions such as reepithelialization in intact and injured lungs (443), (296).

MMP-12 is another candidate for the identity of lower molecular weight caseinolytic MMP, especially in its active 20 kDa form. It has been demonstrated that alveolar macrophages from rats produce a spectrum of MMPs, including MMP-12 that is similar to the spectrum of enzymes produced by human alveolar macrophages (450). MMP-12 shares many substrates such as collagen V, FN and vitronectin with MMP-7 due to their close structural similarities (452), (451). Ectopic or excessive expression of MMP-12 has been associated with several pathological conditions including aortic aneurysm, cancer growth and metastasis, host defense of infection, chronic obstructive pulmonary disease, and gastrointestinal ulcerations. Moreover, it has been determined that the activity of MMP-12 contributes to the pathogenesis of pulmonary emphysema (463) (464). Mice without macrophage elastase (MME) failed to recruit macrophages and did not develop lung destruction in response to cigarette smoke, whereas the lungs of wild-type mice exposed to cigarette smoke demonstrated inflammatory cell recruitment and dilatation and destruction of alveolar walls and alveolar ducts. These observations mirror the pathology of smoker's lungs, although human lungs also have destruction and dilatation of respiratory bronchioles. These findings suggest a primary role for macrophages and macrophage elastase in the development of emphysema induced by cigarette smoking (464). In addition, MMP-12 has been found to be an important mediator in immune complex-induced acute lung injury. It was observed that MMP-12 is necessary for the full development of acute alveolitis in this model of lung injury, while reduced injury was found in MMP-12-deficient mice model (465). Furthermore, the synthesis and secretion of MMP-12 by alveolar macrophages was stimulated by surfactant protein D (SP-D) (466).

The repair of acute lung injury depends on the balance between deposition and breakdown of matrix molecules. MMP-12 has been implicated to be involved in this process. It has been

shown that MMP-12 increased significantly during the acute phase of bleomycin-induced pulmonary fibrosis in animal experiment, which is produced by activated macrophages and is capable of degrading elastin and collagen type IV, the components of the basement membrane. This activation appears to be associated with areas of hemorrhage (467) (468). In contrast, it was observed that macrophages from MMP-12 knockout mice have a reduced capacity to degrade extracellular matrix protein, rendering them unable to penetrate basement membrane (468). Clinically, it was found that the secretion of MMP-12 by macrophages was associated with damaged areas in the lungs (463).

In this study, the identity of the cells producing the caseinolytic MMP is not clear. Most likely, the elevated activity of this MMP is expressed by lung epithelial cells or macrophages following hind limb I/R and the over-expression may be mediated by cytokines. Interestingly, halothane anesthesia suppressed the expression of this MMP in the lung; however, the mechanism of the suppression is unknown. It has been found that increased expression of MMP-2 and MMP-9 was observed in the lung tissues during acute exposure to 100 % oxygen and in rat lungs by subacute hyperoxia (487) (488). The levels of MMP-9 were also elevated in the lung after halothane anesthesia of rats in this study.

Doxycycline is a broad-spectrum MMP inhibitor, which has been demonstrated in a number of studies (302), (396), (489), (490). However, there was an up-regulation of this active caseinolytic MMP in lung tissues after skeletal muscle I/R with administration of doxycycline. It is unclear whether doxycycline directly stimulates expression of this MMP or that doxycycline increases the net expression of this MMP by inhibiting the activity of other MMPs.

Taken together, no single mechanism is responsible for the remote lung injury after bilateral hind limb I/R. Previous and present studies have demonstrated that over-production of MMPs

play an important role in the acute lung injury following hind limb I/R (302). MMPs (both gelatinolytic and caseinolytic MMPs) participate in the degradation of extracellular matrix, facilitate the migration of neutrophils, enhance the vascular permeability and increase albumin extravasation. Moreover, there might be some complicated interactions between MMPs and /or MMPs and cytokines, such as activation of MMP-2 by MMP-7 or MMP-12 (427) (391) and elevation of MMP2 and MMP-9 by IL-1β (482), (301).

CHAPTER 4

ALTERATIONS OF FIBRONECTIN AND LAMININ IN BASEMENT MEMBRANES DURING SKELETAL MUSCLE ISCHEMIA/REPERFUSION INJURY

4. 1 Introduction

Fibronectin (FN) and laminin (LN), major components of the basement membrane (BM) have not yet been investigated in the tissues following skeletal muscle I/R. The studies in this chapter aimed to investigate the alterations in FN and LN in basement membrane and the levels of FN in plasma after rat bilateral hindlimb I/R. To achieve the investigation, both immunohistochemical techniques and ELISA were employed to quantify the levels of FN and LN.

4.1.1 Basement Membrane (BM)

Basement membranes (BM) are thin, sheet like structures found in many locations in the body, usually in close vicinity to the cells, which produce these extracellular matrices. Basement membranes may be deposited in a polarised fashion beneath such cells (epithelium and endothelium) or completely surround cells (muscle, fat and nerve cells) (491). Generally, basement membranes possess three main functions, which include participation in the maintenance and compartmentalisation of tissue architecture, control of fluid and substrate exchange, regulation of cell growth and differentiation and regulation of cell adhesion and migration (492). Basement membrane contains various glycoproteins. Although the number of components in any particular basement membrane is unknown, collagen IV, FN and LN are considered to be the major components. Collagen IV is a ubiquitous constituent in the BM, providing mechanical strength. Its loss will lead to cystic tissue transformation as was evidenced by analysis of polycystic nephropathies (492). FN and LN are another two of the most abundant extracellular matrix proteins and share many biological properties with each other. FN consists of two very similar polypeptide chains connected to each other by disulfide bonds at their C-terminal ends, whereas LN consists of a rodlike long arm (length 77nm) and three morphologically indistinguishable short arms (length 37nm) The components of

basement membranes for cell proliferation, migration and differentiation implies that their composition is more complex than their structure suggests. The molecular orientation of the individual components varies in the basement membrane according to biological needs (493). The differences in ultra-structure of basement membrane suggested to be related to the physiologic functions (494). The importance of basement membranes in adult tissue function has also been directly determined by the identification of genetic diseases caused by mutations in the genes of components in structural basement membrane, such as Alport syndrome and junctional epidermolysis bullosa (495). In addition, pathological damage is often observed in basement membranes in various diseases such as diabetic nephropathy (496), and Crohn's disease (497). Moreover, MMPs together with TIMPs have been found to play a crucial role in the balance between degradation and synthesis of extracellular matrices (498). The ability of MMPs to degrade basement membrane is also essential for the diverse invasive processes of angiogenesis and tumor metastasis (393), (419).

4.1.2 Plasma Fibronectin (pFN)

In recent studies, pFN has been implicated in playing an important role in ischemia-induced tissue injury. It has been demonstrated that levels of pFN were significantly higher in patients with acute myocardial infarction (AMI) than control subjects (499), (500). Accumulation of circulating pFN in sclerotic lesions has been implicated to be the major process of glomerulosclerosis in immunologically mediated kidney diseases and in chronic graft-versus-host disease (501). In rat models of kidney ischemia and reperfusion injury, a major change in glycoprotein levels in plasma and the extracellular matrix was observed. FN, which originated in the plasma, accumulated in tubular lumens, contributing to obstruction and subsequent renal failure. It was suggested that pFN might play a pivotal role in the pathogenesis of acute renal failure and repair of the ischemia-induced kidney injury (502). Moreover, pFN has been determined to be able to reduce brain injury following transient focal cerebral ischemia. This

is because pFN provides a matrix for adherence, migration and proliferation of white blood cells to repair the tissue damage. On the other hand, pFN also protects neuronal and non-neuronal cells from cell death by interacting with integrins to increase Bcl-2 expression, inhibiting apoptosis (218).

4.1.3 Immunohistochemistry

The components of basement membrane can be detected by immunohistochemical methods using labelled antibodies, to localise specific tissue antigen constituents. Antibodies are not visible with standard microscopy and must be labelled in a manner that does not interfere with their binding specificity. The marker must be of sufficient intensity to be detected and include fluorescent compounds, such as fluorescein and rhodamine and compounds used for light microscopy including horseradish peroxidase, glucose oxidase and intestinal alkaline phosphatase (503). A specific antibody reacts with the desired antigen (fibronectin or laminin) and the remaining constituents of the reagent are removed by washing. Biotinylated anti-rabbit IgG then binds to the primary antibody. Biotin has a very strong affinity for streptavidin and then binds strongly to a tertiary streptavidin-FITC conjugate. Streptavidin has an isoelectric point close to neutrality and contains no carbohydrate, making it less prone to non-specific binding (Amersham Pharmacia Biotech UK). A Digital camera connected to a fluorescence microscope was employed to capture the images, which were stored on the computer hardware for further quantitative analysis.

Immunohistochemistry has been extensively used in the study of the components in the basement membranes. Saylam et al (504) has demonstrated the dynamic relationship of FN, LN and collagen IV following conception in mice by employing immunohistochemical methods. Roach et al (302) successfully investigated the alterations in collagen IV by

immunohistochemistry in the basement membrane after skeletal muscle ischemia and reperfusion in rats. Moreover, immunohistochemistry has been employed to investigate the components in the basement membrane of the lungs, liver and kidney (505), (506), (507).

4.1.4 Enzyme-Linked Immunosorbent Assay (ELISA)

Enzyme immunoassays combine the specificity of antibodies with the sensitivity of simple spectrophotometric enzyme assays by using antibodies or antigen coupled to an easily assayed enzyme. In competitive ELISAS, a mixture of known amount of enzyme-labelled antigen and an unknown amount of unlabelled antigen is allowed to react with a specific antibody attached to a microtitre plate. After the complex has been washed with buffer, the enzyme substrate is added and the plate incubated for a certain period before the enzyme activity is measured. The difference between this value and that of a sample lacking unlabelled antigen is a measure of the concentration of unlabelled antigen. Under standard conditions, the enzyme activity measured is proportional to the proportion of labelled antigen in the mixture of labelled and unlabelled antigen. This method requires the preparation of a calibration curve during the assay (479). In the literature, ELISA has been widely employed to detect the concentration of pFN (508), (509), (510).

4.2 Materials and Methods

4.2.1 Quantitative Immunohistochemistry

4.2.1.1 Investigation of Alterations of Fibronectin and Laminin in the Basement membrane by Immunohistochemical Techniques

Frozen tissue samples obtained during I/R experiment were fixed to a cryostat chuck using Tissue-tek® OCT fixative. Sections were cut as follows: skeletal muscle 10 μm, lung, kidney and liver 5 μm and then applied to poly-L-lysine-coated slides. The slides were allowed to air dry, then immersed in 20 % acetone solution at –20 °C for 20 minutes and dried again. Tissue sections were circled with a PAP pen to create a well and then washed in 0.1 % BSA (bovine serum albumin)/PBS (2.3.1) solution for 3x5 minutes. Each slide was incubated with 100 μl of 1:200 anti fibronectin or anti laminin primary antibody (Rockland; Gilbertsville, PA, U.S.A) in a humidified chamber for 15 h at 4 °C. Following a further wash in 0.1 % BSA/PBS, the sections were incubated with 100 μl of 1:400 secondary antibody (anti-rabbit serum antibody) (Vector Laboratories; Burlingame, CA, U.S.A) in a humidified chamber at room temperature for 1 h. A third wash was performed prior to addition of 100 μl of 1: 200 streptavidin fluorescein label (Amersham Biosciences) and incubation for 1 $^{1}/_{2}$ hr at room temperature in the humidified chamber. A final wash preceded the addition of fluorescent mounting medium (DAKO, Australia) and the application of a cover slip.

Images of tissue sections were captured on an Olympus BH2 microscope with Reflected Light Fluoresecent Attachment (Olympus BHRFL-W) on maximum excitation wavelength of 494 nm and maximum emission wavelength of 518 nm. Colour images were then captured under a magnification of 200X. The pictures were then transmitted on a Panasonic Camera (WVCL 700) and saved as TIFF files. The images were analysed using a Video Pro 32 automated image analysis system (Leading Edge Pty Ltd, Marion, South Australia). In the previous studies conducted by Roach (511)), it was determined that the cumulative mean brightness

reached a steady state after 25 images had captured. This implied that after 25 images had been captured, any further images included would not change the arithmetic mean to be used in the statistical analysis. Therefore, for the immunohistochemical quantitation analyses, 25 images were collected for each rat in a standardised pattern through the whole experiment. This ensured that the number of images reached a normal statistical distribution. The level of brightness was chosen for quantitative comparisons analysis. The whole field brightness of each image was detected and the figure was recorded in tables of Appendix 6.5.

4.2.1.2 Descriptive Statistics

Each group contained 5 rats, 25 images were collected from each rat (125 images involved in each group). Brightness measurements representing quantity of fibronectin (or laminin), were analysed using Analysis of Variance (ANOVA) to study the difference between different treatment groups. Student-Newman-Keuls of Multiple Comparisons Test was used for comparison between the individual groups. $P < 0.05$ was considered as significant.

4.2.2 Plasma Fibronectin Analysis By ELISA Kit

The ELISA was carried out according to manufacturer's instruction. Briefly, the contents of a vial of Diluent Buffer Concentrate (BT-702) was transferred to a graduated cylinder and distilled water added to a volume of 150 ml before a set of working standards in the range of 25 ng/ml to 2000 ng/ml was prepared with working diluent buffer as shown in Table 4.2.1

Table 4.2.1

Dilution	Fibronectin Concentration
A. 100 ul stock + 4.9 ml diluent	2000 ng/ml
B. 1.0 ml Solution A+ 3.0 ml diluent	500 ng/ml
C. 1.0 ml Solution B + 1.0 ml diluent	250 ng/ml
D. 0.5 ml Solution B + 2.0 ml diluent	100 ng/ml
E. 0.1 ml Solution B + 0.9 ml diluent	50 ng/ml
F. 0.1 ml Solution C+ 0.9 ml diluent	25 ng/ml

Diluent buffer 150 µl was then pipetted into blank wells and 100µl of buffer into the Bmax wells. Subsequently, 100 µl of standards, controls or samples were added to appropriate wells.

To start detection, 50 µl of Fibronectin Antiserum (BT-703) was pipetted into all wells except blanks, followed by gentle mixing for 30 seconds. The wells were then covered tightly with parafilm and incubated at 37°C for 1 h, followed by the addition of 50 µl FN Tracer (BT-704) to all wells, further incubated at 37°C for 60 minutes. Wells were then aspirated, filled with diluent buffer and aspirated again. This process was repeated 3 times. The excess liquid was removed by gently tapping the empty plate on a paper towel. Prepared substrate solution (200 µl) was added to all wells, and incubated at 37°C. Measurement of absorbance was conducted at 400-410 nm in 5 minutes intervals until desired range was reached after 60 minutes incubation. Finally, 20 µl of Stop Solution (BT-707) was pipetted into all wells and the absorbance was measured within 1 h.

To obtain net mean absorbance, all duplicates and the blank was averaged. A standard curve was then constructed by plotting mean absorbance of each standard concentration or log concentration. The concentration of pFN was determined from this standard curve.

4.3. Results

As reported by D.Roach (D.Roach Thesis 2001, Adelaide University), the levels of collagen IV in basement membranes were not influenced by anesthesia. There were no significant differences in levels of collagen IV between different sham-operated groups (0/0/, 0/4, 0/24 or 0/72). Therefore, in this study the levels of fibronectin or laminin in the basement membranes following skeletal muscle ischemia with varying times of reperfusion were assessed using the same sham-group (0/24). Student-Newman-Keuls of Comparison Test was conducted for comparison between the I/R group and sham-operated group (0/24). $P < 0.05$ is considered as significant.

4.3.1 Elevation of FN in the basement membrane of skeletal muscle following I/R.

There was a significant accumulation of FN in the basement membrane of ischemic skeletal muscle following 4 h ischemia only ($P < 0.05$), when compared to sham-operated group. The level of FN was elevated throughout the time course of reperfusion, at least until 72 h ($P < 0.05$). The representative immunohistochemical pictures of fibronectin staining in skeletal muscle are shown in Figure 4.1, illustrating the trend of elevation in FN within different experimental groups.

The raw data of quantitative immunohistochemical analysis is shown in Appendix (6.4.1). The grouped descriptive statistical data for the analysis of brightness of FN staining is summarised in Table 4.3.1.

Table 4.3.1

SM FN	I/R 0/24	I/R 4/0	I/R 4/4	I/R 4/24	I/R 4/72
Mean Brightness	1551.9	2285.2	2512	2045.4	3612
SEM	163.1	251.5	204.8	171.7	386.5
St Dev	1823.4	2811.8	2290.3	1919.7	4321.4
P value		P<0.05	P<0.05	P<0.05	P<0.05

Figure 4.1 Representative immunohistochemistry images of skeletal muscle showing levels of fibronectin

Images were magified 200 X. The primary antibody was directed against fibronectin and secondary detection was carried out using biotin-labelled antibody and Streptavidin-Fluorescein Isothiocyanate. Images were captured on Olympus BH_2 microscope with Reflected Light Fluorescent Attachment.

I/R:0/24 Skeletal muscle from rats that have undergone 4 h anaesthesia followed by 24 h recovery, with no ischemia.

I/R:4/0 Skeletal muscle from rats following 4 h bilateral hindlimb ischemia, sacrificed before reperfusion.

I/R:4/4 Skeletal muscle from rats following 4 h bilateral hindlimb ischemia and 4 h reperfusion.

I/R:4/24 Skeletal muscle from rats following 4 h bilateral hindlimb ischemia and 24 h reperfusion.

I/R:4/72 Skeletal muscle from rats following 4 h bilateral hindlimb ischemia and 72 h reperfusion.

I/R : 0/24

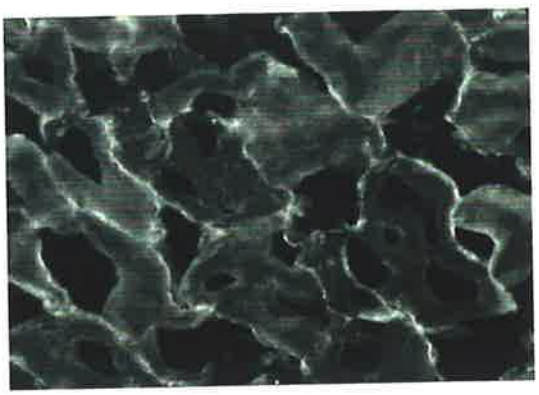

I/R : 4/0

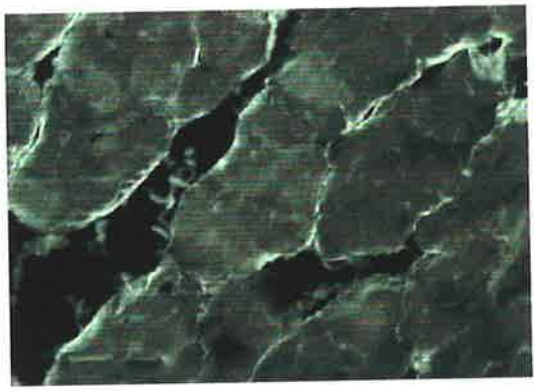

I/R : 4/4

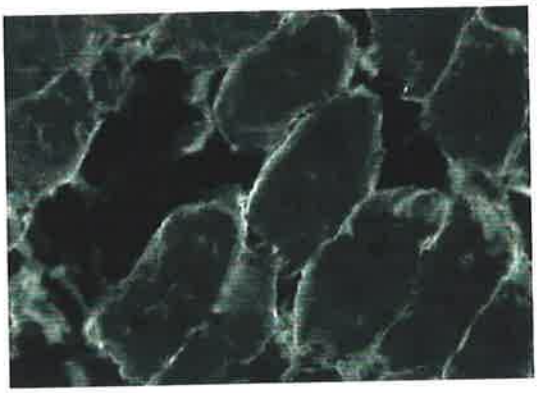

I/R : 4/24

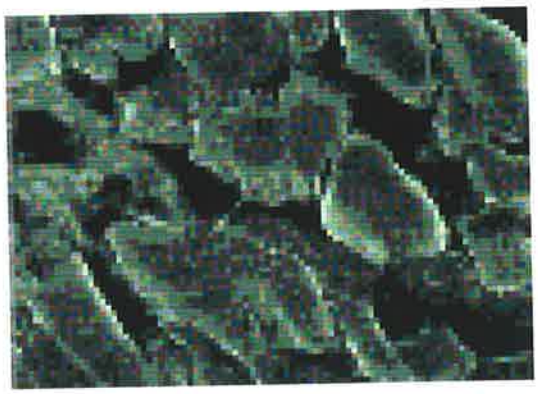

I/R : 4/72

SM FN: Fibronectin in the basement membrane of skeletal muscle

I/R 0/24: rats underwent 4 h anaesthesia with 24 h recovery, no ischemia.

I/R 4/0: rats underwent 4 h bilateral hindlimb ischemia only, with no reperfusion.

I/R 4/4: rats underwent 4 h bilateral hindlimb ischemia followed by 4 h reperfusion.

I/R 4/24: rats underwent 4 h bilateral hindlimb ischemia followed by 24 h reperfusion.

I/R 4/72: rats underwent 4 h bilateral hindlimb ischemia followed by 72 h reperfusion.

SEM: Standard error mean.

St Dev: Standard deviation.

4.3.2 Degradation of FN in the basement membrane of lung tissues following skeletal muscle I/R.

A significant degradation of FN was observed ($P < 0.05$) in the basement membrane of lung in rats following 4 h bilateral hindlimb ischemia only. Persistent degradation was found with increasing duration of reperfusion. Fibronectin was at its lowest level after 72 h of reperfusion. Representative pictures of FN staining in lung are shown in Figure 4.2, illustrating the trend of alterations in fibronectin of the lung within different experimental groups.

Raw data of quantitative immunohistochemical analysis is shown in Appendix (6.4.2). The grouped descriptive statistical data for the analysis of brightness of FN staining is summarised in Table 4.3.2.

Figure 4. 2. Representative immunohistochemistry images of lung tissues showing levels of fibronectin

Images were magified 200 X. The primary antibody was directed against fibronectin and secondary detection was carried out using biotin-labelled antibody and Streptavidin-Fluorescein Isothiocyanate. Images were captured on Olympus BH_2 microscope with Reflected Light Fluorescent Attachment.

I/R:0/24 Lung tissues from rats that have undergone 4 h anaesthesia followed by 24 h recovery, with no ischemia.

I/R:4/0 Lung tissues from rats following 4 h bilateral hindlimb ischemia, sacrificed before reperfusion.

I/R:4/4 Lung tissues from rats following 4 h bilateral hindlimb ischemia and 4 h reperfusion.

I/R:4/24 Lung tissues from rats following 4 h bilateral hindlimb ischemia and 24 h reperfusion.

I/R:4/72 Lung tissues from rats following 4 h bilateral hindlimb ischemia and 72 h reperfusion.

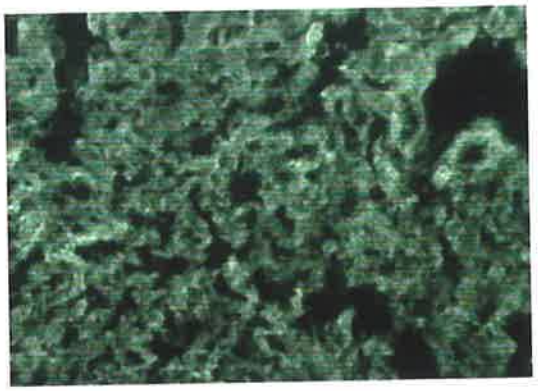

I/R : 0/24

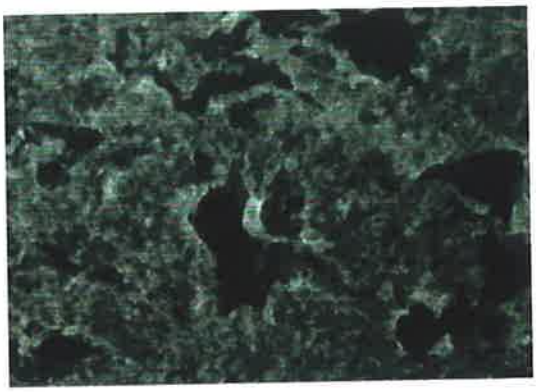

I/R : 4/0

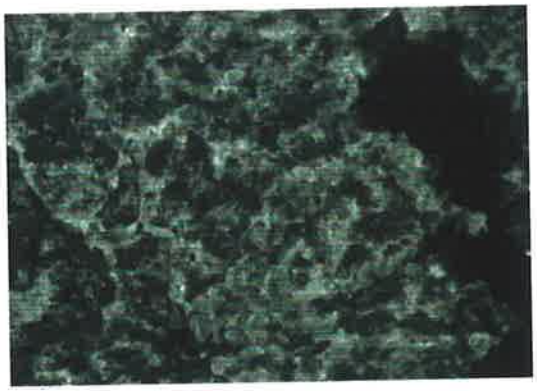

I/R : 4/4

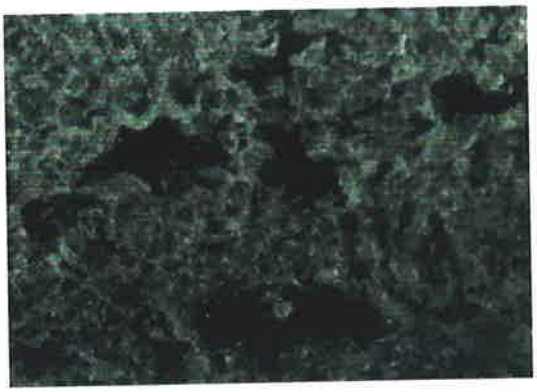

I/R : 4/24

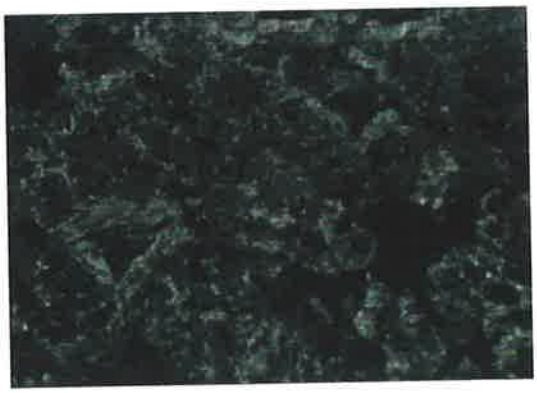

I/R : 4/72

Table 4.3.2

Lung FN	I/R 0/24	I/R 4/0	I/R 4/4	I/R 4/24	I/R 4/72
Mean Brightness	11727.7	3852.4	6086.2	2497.4	1541.5
SEM	869	366.6	613.7	437.6	204
St Dev	9716	4098.3	6861.3	4892.1	2280.7
P value		P<0.05	P<0.05	P<0.05	P<0.05

Lung FN: Fibronectin in the basement membrane of lung

I/R 0/24: rats underwent 4 h anaesthesia with 24 h recovery, with no ischemia.

I/R 4/0: rats underwent 4 h bilateral hindlimb ischemia only, with no reperfusion.

I/R 4/4: rats underwent 4 h bilateral hindlimb ischemia followed by 4 h reperfusion.

I/R 4/24: rats underwent 4 h bilateral hindlimb ischemia followed by 24 h reperfusion.

I/R 4/72: rats underwent 4 h bilateral hindlimb ischemia followed by 72 h reperfusion.

SEM: Standard error mean.

St Dev: Standard deviation.

4.3.3 FN in the basement membrane of renal tissues.

There was no clear evidence of degradation of FN in the basement membrane of kidneys following 4h bilateral hindlimb ischemia only ($P > 0.05$). Significant degradation occurred during reperfusion. Intensity of FN staining was lowest after 72 h of reperfusion. Representative immunohistochemical pictures of FN staining in kidney are shown in Figure 4.3, illustrating the degradation of FN in the kidney within different experimental groups.

Raw data of quantitative immunohistochemical analysis is shown in Appendix (6.4.3). The grouped descriptive statistical data for analysis of levels of fibronectin in kidney is summarised in the Table 4.3.3.

Figure 4. 3. Representative immunohistochemistry images of renal tissues showing levels of fibronectin in the kidney

Images were magified 200 X. The primary antibody was directed against fibronectin and secondary detection was carried out using biotin-labelled antibody and Streptavidin-Fluorescein Isothiocyanate. Images were captured on Olympus BH_2 microscope with Reflected Light Fluorescent Attachment.

I/R:0/24 Renal tissues from rats that have undergone 4 h anaesthesia followed by 24 h recovery, with no ischemia.

I/R:4/0 Renal tissues from rats following 4 h bilateral hindlimb ischemia, sacrificed before reperfusion.

I/R:4/4 Renal tissues from rats following 4 h bilateral hindlimb ischemia and 4 h reperfusion.

I/R:4/24 Renal tissues from rats following 4 h bilateral hindlimb ischemia and 24 h reperfusion.

I/R:4/72 Renal tissues from rats following 4 h bilateral hindlimb ischemia and 72 h reperfusion.

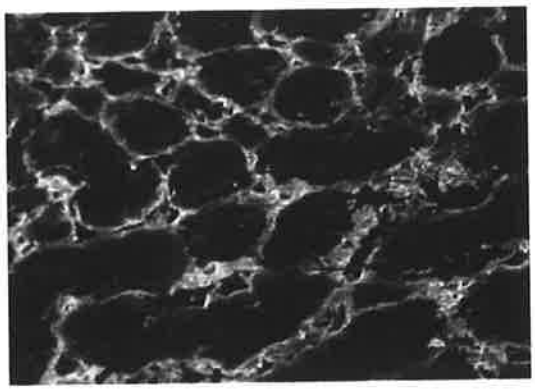

I/R : 0/24

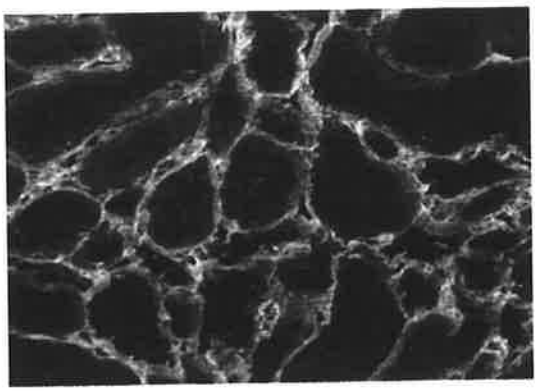

I/R : 4/0

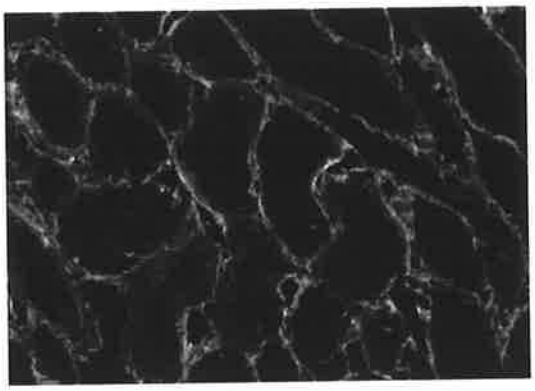

I/R : 4/4

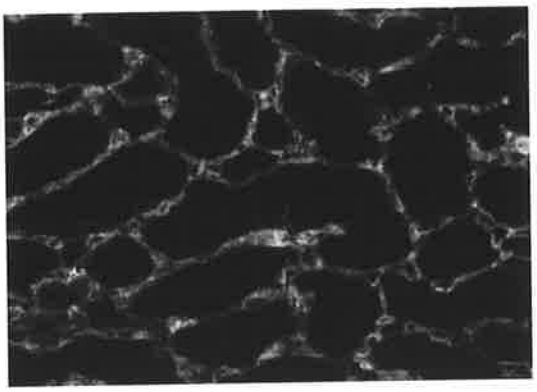

I/R : 4/24

I/R : 4/72

Table 4.3.3

Kidney FN	I/R 0/24	I/R 4/0	I/R 4/4	I/R 4/24	I/R 4/72
Mean Brightness	4550.4	4037.3	3174.2	2969.8	1556.1
SEM	338	244.1	230.2	249.8	137.7
St Dev	3778.9	2729.2	2573.3	2792.5	1540.1
P value		NS	P<0.05	P<0.05	P<0.05

Kidney FN: Fibronectin in the basement membrane of kidney

I/R 0/24: rats underwent 4 h anaesthesia with 24 h recovery, with no ischemia.

I/R 4/0: rats underwent 4 h bilateral hindlimb ischemia only, with no reperfusion.

I/R 4/4: rats underwent 4 h bilateral hindlimb ischemia followed by 4 h reperfusion.

I/R 4/24: rats underwent 4 h bilateral hindlimb ischemia followed by 24 h reperfusion.

I/R 4/72: rats underwent 4 h bilateral hindlimb ischemia followed by 72 h reperfusion.

SEM: Standard error mean.

St Dev: Standard deviation.

NS: No significance

4.3.4 Alterations of FN in the basement membrane of hepatic tissues. Quantitative immunohistochemistry for FN in the liver.

FN immunostaining was decreased markedly (P<0.05) in the liver immediately following skeletal muscle ischemia (4/0,4/4). It then increased with reperfusion, exceeding the baseline level after 24 h of reperfusion, reaching the highest level after 72 hours of reperfusion. Representative immunohistochemical pictures of FN staining in liver are shown in Figure 4.4, illustrating the elevation of FN in the liver following increasing duration of reperfusion.

Figure 4. 4. Representative immunohistochemistry images of hepatic tissues showing levels of fibronectin in the liver

Images were magified 200 X. The primary antibody was directed against fibronectin and secondary detection was carried out using biotin-labelled antibody and Streptavidin-Fluorescein Isothiocyanate. Images were captured on Olympus BH_2 microscope with Reflected Light Fluorescent Attachment.

I/R:0/24 Hepatic tissues from rats that have undergone 4 h anaesthesia followed by 24 h recovery, with no ischemia.

I/R:4/0 Hepatic tissues from rats following 4 h bilateral hindlimb ischemia, sacrificed before reperfusion.

I/R:4/4 Hepatic tissues from rats following 4 h bilateral hindlimb ischemia and 4 h reperfusion.

I/R:4/24 Hepatic tissues from rats following 4 h bilateral hindlimb ischemia and 24 h reperfusion.

I/R:4/72 Hepatic tissues from rats following 4 h bilateral hindlimb ischemia and 72 h reperfusion.

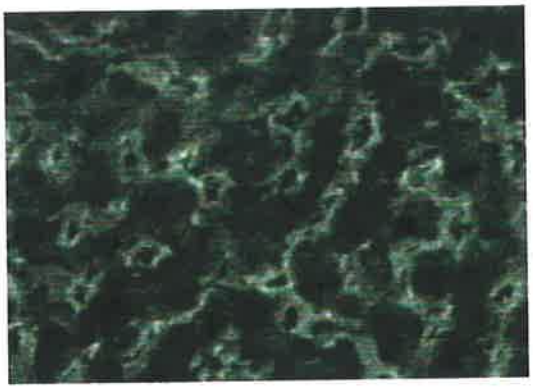

I/R : 0/24

I/R : 4/0

I/R : 4/4

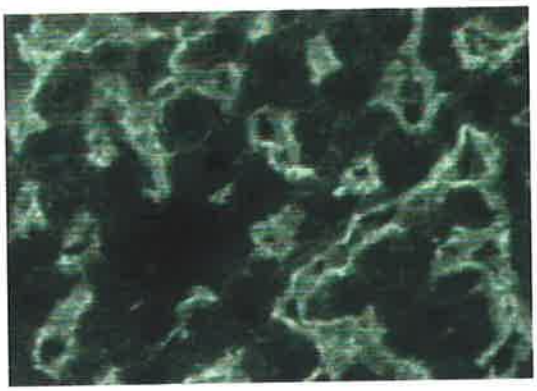

I/R : 4/24

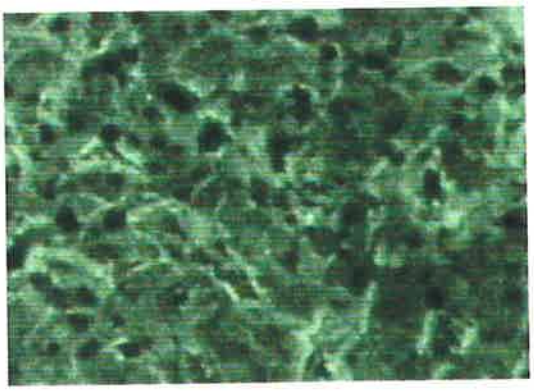

I/R : 4/72

Raw data of quantitative immunohistochemistry is shown in Appendix (6.4.4). The grouped descriptive statistical data for the analysis of levels of fibronectin in liver is summarised in the Table 4.3.4.

Table 4.3.4

Liver FN	I/R 0/24	I/R 4/0	I/R 4/4	I/R 4/24	I/R 4/72
Mean Brightness	693.8	159.5	199.4	1108.8	1919.7
SEM	69.2	26.4	41.4	196.9	305.5
St Dev	773.4	295	462.4	2201.6	3416.1
P value		P<0.05	P<0.05	P<0.05	P<0.05

Liver FN: Fibronectin in the basement membrane of liver

I/R 0/24: rats underwent 4 h anaesthesia with 24 h recovery, with no ischemia.

I/R 4/0: rats underwent 4 h bilateral hindlimb ischemia only, with no reperfusion.

I/R 4/4: rats underwent 4 h bilateral hindlimb ischemia followed by 4 h reperfusion.

I/R 4/24: rats underwent 4 h bilateral hindlimb ischemia followed by 24 h reperfusion.

I/R 4/72: rats underwent 4 h bilateral hindlimb ischemia followed by 72 h reperfusion.

SEM: Standard error mean.

St Dev: Standard deviation.

4.3.5 Summary of alterations of FN in the basement membranes of skeletal muscle, lung, kidney and liver of rats following 4 h bilateral hindlimb ischemia and increasing duration of reperfusion.

Figure 4.5 illustrates graphically the changes in FN level in basement membranes after skeletal muscle ischemia and reperfusion. As discussed above, there was a trend of accumulation of FN in skeletal muscle following I/R. In contrast, degradation of FN in lung and kidney was detected following skeletal muscle I/R. However, fibronectin initially

Figure 4.5. The graph showing alterations of fibronectin in the basement membrane of skeletal muscle, lung, kidney, and liver of rats following 4 h bilateral hindlimb ischemia with increasing duration of reperfusion

Tissue sections were labelled with fibronectin antibody, prepared and analysed as described in 4.2.1. Brightness refers to level of fibronectin detected with immunofluorescence.

Each column on the graph represents the mean brightness level of fibronectin in the basement membranes. Given five rats in each group, 25 images for each rat, 125 images were included in total. The standard deviation bars are shown on the graph.

IR 0/24 refers to rats that underwent a 4 h anaesthesia only, with no ischemia and were sacrificed after 24 h recovery.

IR 4/0 refers to rats that underwent a 4 h bilateral hindlimb ischemia and were sacrificed immediately after ischemia.

IR 4/4 refers to rats that underwent a 4 h bilateral hindlimb ischemia followed by 4 h of reperfusion.

IR 4/24 refers to rats that underwent a 4 h bilateral hindlimb ischemia followed by 24 h of reperfusion.

IR 4/72 refers to rats that underwent a 4 h bilateral hindlimb ischemia followed by 72 h of reperfusion.

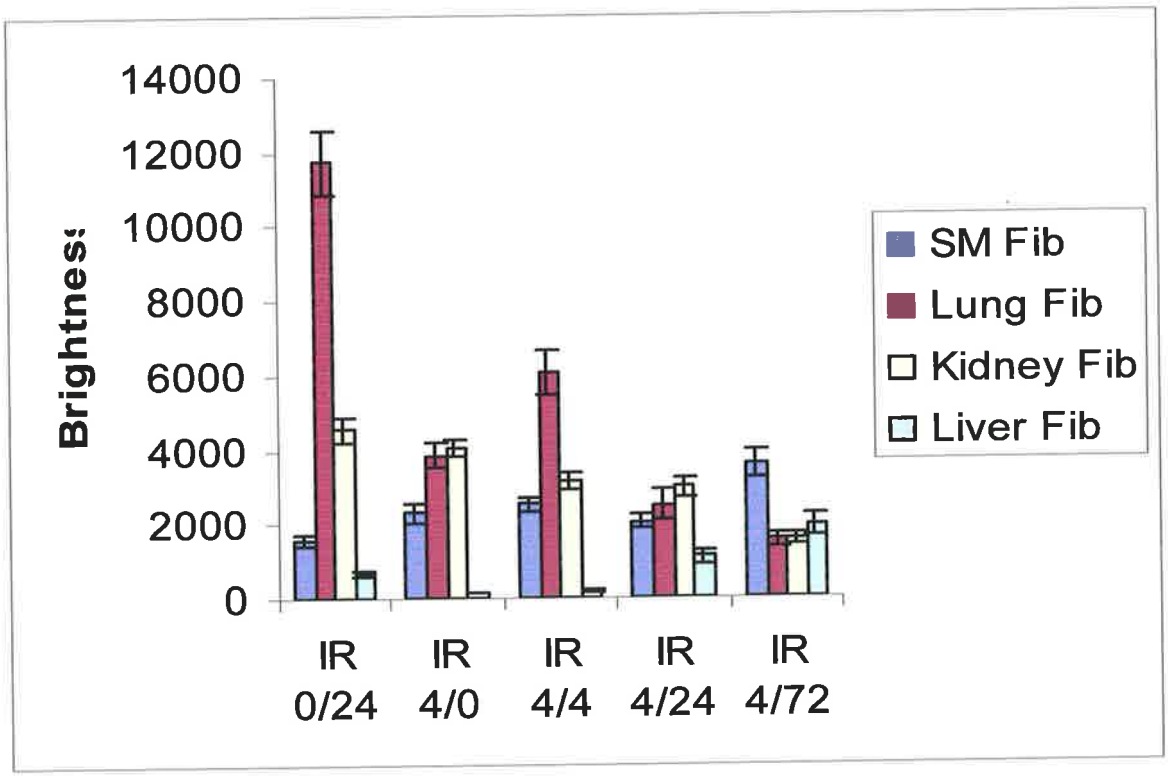
Brightness
14000
12000
10000
8000
6000
4000
2000
0
IR 0/24
IR 4/0
IR 4/4
IR 4/24
IR 4/72
SM Fib
Lung Fib
Kidney Fib
Liver Fib

decreased in the liver following skeletal muscle ischemia, then increasing with further reperfusion, exceeding the baseline level after 24 h of reperfusion. This change from baseline is significant ($P < 0.05$).

4.3.6 Alterations of LN in the basement membrane of skeletal muscle following I/R.

There was no clear change of Laminin in basement membrane of skeletal muscle immediately following 4 h of ischemic insult (4/0,4/4). LN levels were then slightly elevated in basement membrane with the further reperfusion, exceeding the baseline level after 24 h reperfusion ($P < 0.05$). Representative immunohistochemical pictures of LN staining in skeletal muscle are shown in Figure 4.6, illustrating the trend of changes for LN in the skeletal muscle within different experimental groups.

Raw data of quantitative immunohistochemistry is shown in Appendix (6.4.5). The grouped descriptive statistical data for the analysis of LN level in skeletal muscle is summarised in the Table 4.3.5.

Table 4.3.5

SM LN	I/R 0/24	I/R 4/0	I/R 4/4	I/R 4/24	I/R 4/72
Mean Brightness	21103.4	20074.9	21345.5	28041.4	27409.4
SEM	678.3	786.5	900.2	1423.4	891.8
St Dev	8308	9633.1	11025.7	17433.1	10922.2
P value		NS	NS	P<0.05	P<0.05

SM LN: Laminin in the basement membrane of skeletal muscle

I/R 0/24: rats underwent 4 h anaesthesia with 24 h recovery, with no ischemia.

I/R 4/0: rats underwent 4 h bilateral hindlimb ischemia only, with no reperfusion.

I/R 4/4: rats underwent 4 h bilateral hindlimb ischemia followed by 4 h reperfusion.

I/R 4/24: rats underwent 4 h bilateral hindlimb ischemia followed by 24 h reperfusion.

Figure 4.6. Representative immunohistochemistry images of skeletal muscle showing levels of laminin in skeletal muscle

Images were magified 200 X. The primary antibody was directed against laminin and secondary detection was carried out using biotin-labelled antibody and Streptavidin-Fluorescein Isothiocyanate. Images were captured on Olympus BH_2 microscope with Reflected Light Fluorescent Attachment.

I/R:0/24 Skeletal muscle from rats that have undergone 4 h anaesthesia followed by 24 h recovery, with no ischemia.

I/R:4/0 Skeletal muscle from rats following 4 h bilateral hindlimb ischemia, sacrificed before reperfusion.

I/R:4/4 Skeletal muscle from rats following 4 h bilateral hindlimb ischemia and 4 h of reperfusion.

I/R:4/24 Skeletal muscle from rats following 4 h bilateral hindlimb ischemia and 24 h of reperfusion.

I/R:4/72 Skeletal muscle from rats following 4 h bilateral hindlimb ischemia and 72 h of reperfusion.

I/R : 0/24

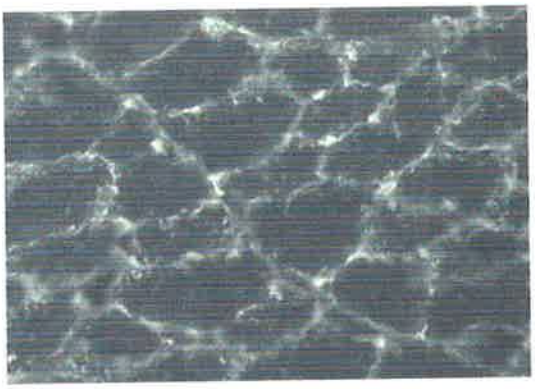

I/R : 4/0

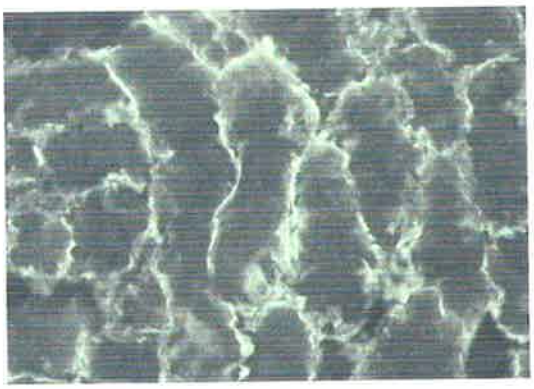

I/R : 4/4

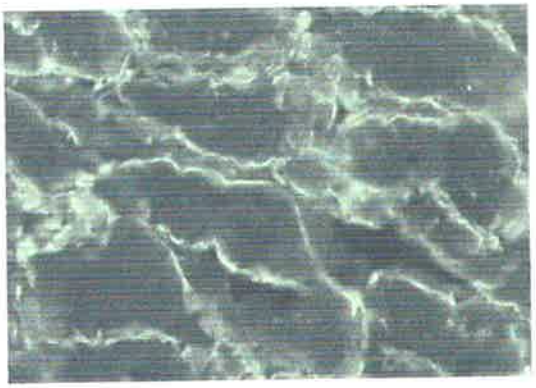

I/R : 4/24

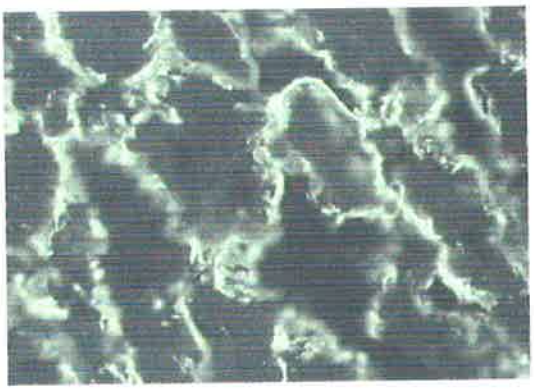

I/R : 4/72

I/R 4/72: rats underwent 4 h bilateral hindlimb ischemia followed by 72 h reperfusion.

SEM: Standard error mean.

St Dev: Standard deviation.

NS: No significance.

4.3.7 Alterations of LN in the basement membrane of renal tissues following skeletal muscle I/R.

LN was degraded significantly ($P < 0.05$) in basement membrane of the kidney after 4 h of skeletal muscle ischemia. The degradation was persistent in the early phase of reperfusion, reaching the lowest level after 4 h of reperfusion. LN levels then increased in basement membrane with the progression of reperfusion, returning to baseline level (sham 0/24) after 24 h reperfusion. There was no difference in LN level between group 4/24 and 0/24, but the change in LN level from time course 4/4 to 4/24 reached significance ($P<0.05$). Representative immunohistochemical pictures of LN staining in the kidney are shown in Figure 4.7, illustrating the trend of changes for LN in the renal tissues within different experimental groups.

Raw data of quantitative immunohistochemistry is shown in Appendix (6.4.6). The grouped descriptive statistical data for the analysis of LN levels in the kidney is summarised in the Table 4.3.6.

Figure 4. 7. Representative immunohistochemistry images of renal tissues showing levels of laminin in the kidney

Images were magified 200 X. The primary antibody was directed against laminin and secondary detection was carried out using biotin-labelled antibody and Streptavidin-Fluorescein Isothiocyanate. Images were captured on Olympus BH_2 microscope with Reflected Light Fluorescent Attachment.

I/R:0/24 Renal tissues from rats that have undergone 4 h anaesthesia followed by 24 h recovery, with no ischemia.

I/R:4/0 Renal tissues from rats following 4 h bilateral hindlimb ischemia, sacrificed before reperfusion.

I/R:4/4 Renal tissues from rats following 4 h bilateral hindlimb ischemia and 4 h of reperfusion.

I/R:4/24 Renal tissues from rats following 4 h bilateral hindlimb ischemia and 24 h of reperfusion.

I/R:4/72 Renal tissues from rats following 4 h bilateral hindlimb ischemia and 72 h of reperfusion.

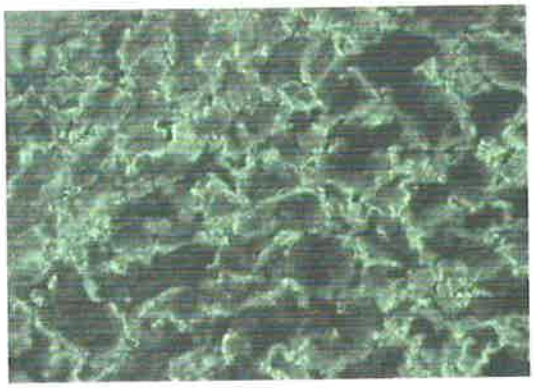

I/R : 0/24

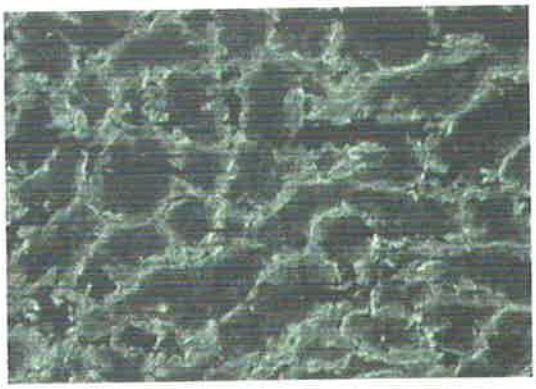

I/R : 4/0

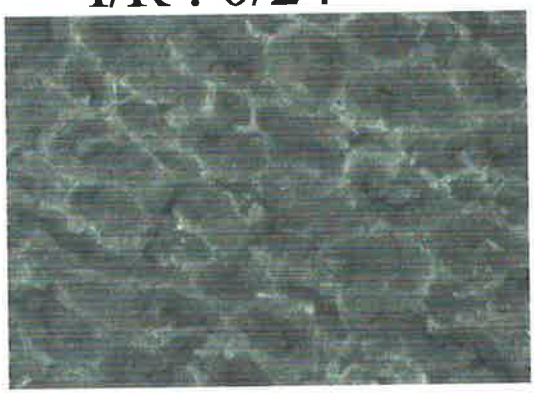

I/R : 4/4

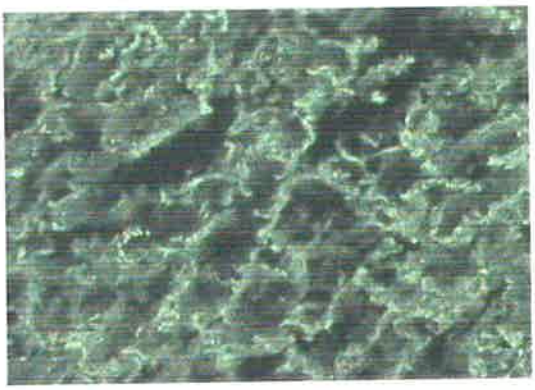

I/R : 4/24

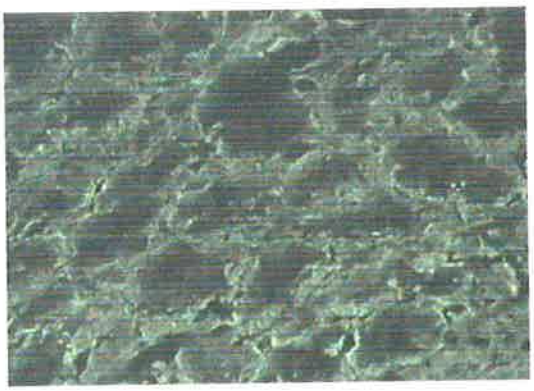

I/R : 4/72

Table 4.3.6

Kidney LN	I/R 0/24	I/R 4/0	I/R 4/4	I/R 4/24	I/R 4/72
Mean Brightness	43524.9	38004.4	18642.2	44648.1	34225.9
SEM	936.5	1120	1067.8	1294.5	1358.4
St Dev	11470.2	13717.2	13077.4	15854.7	16637.2
P value		P<0.05	P<0.05	NS	P<0.05

Kidney LN: Laminin in the basement membrane of kidney

I/R 0/24: rats underwent 4 h anaesthesia with 24 h recovery, with no ischemia.

I/R 4/0: rats underwent 4 h bilateral hindlimb ischemia only, with no reperfusion.

I/R 4/4: rats underwent 4 h bilateral hindlimb ischemia followed by 4 h reperfusion.

I/R 4/24: rats underwent 4 h bilateral hindlimb ischemia followed by 24 h reperfusion.

I/R 4/72: rats underwent 4 h bilateral hindlimb ischemia followed by 72 h reperfusion.

SEM: Standard error mean.

St Dev: Standard deviation.

NS: No significance.

4.3.8 Summary of alterations of LN in basement membranes of skeletal muscle and kidney of rats following 4 h bilateral hindlimb ischemia and increasing duration of reperfusion.

Figure 4.8 illustrates graphically the changes in LN level in basement membranes of skeletal muscle and kidney following bilateral hindlimb ischemia and reperfusion. There were no clear changes of LN level in skeletal muscle immediately following ischemia/reperfusion, but slightly elevation in LN level was detected with further reperfusion (4/24, 4/72), exceeding the baseline level after 24 h of reperfusion. A significant degradation of LN was observed in kidney following skeletal muscle ischemia. The LN level then returned to baseline after 24 h of reperfusion.

Figure 4.8 Changes in laminin patterns in the basement membranes of skeletal muscle and kidney of rats that had undergone 4 h of bilateral hindlimb ischemia with increasing duration of reperfusion

Tissue sections were labelled with laminin antibody, prepared and analysed as described in 4.2.1. Brightness refers to level of laminin detected with immunofluorescence.

Each column on the graph represents the mean brightness level of laminin in the basement membranes. Given five rats in each group, 25 images for each rat, 125 images were included in total. The standard deviation bars are shown on the graph.

IR 0/24 refers to rats that underwent a 4 h anaesthesia only, with no ischemia and were sacrificed after 24 h recovery.

IR 4/0 refers to rats that underwent a 4 h bilateral hindlimb ischemia and were sacrificed immediately after ischemia.

IR 4/4 refers to rats that underwent a 4 h bilateral hindlimb ischemia followed by 4 h of reperfusion.

IR 4/24 refers to rats that underwent a 4 h bilateral hindlimb ischemia followed by 24 h of reperfusion.

IR 4/72 refers to rats that underwent a 4 h bilateral hindlimb ischemia followed by 72 h of reperfusion.

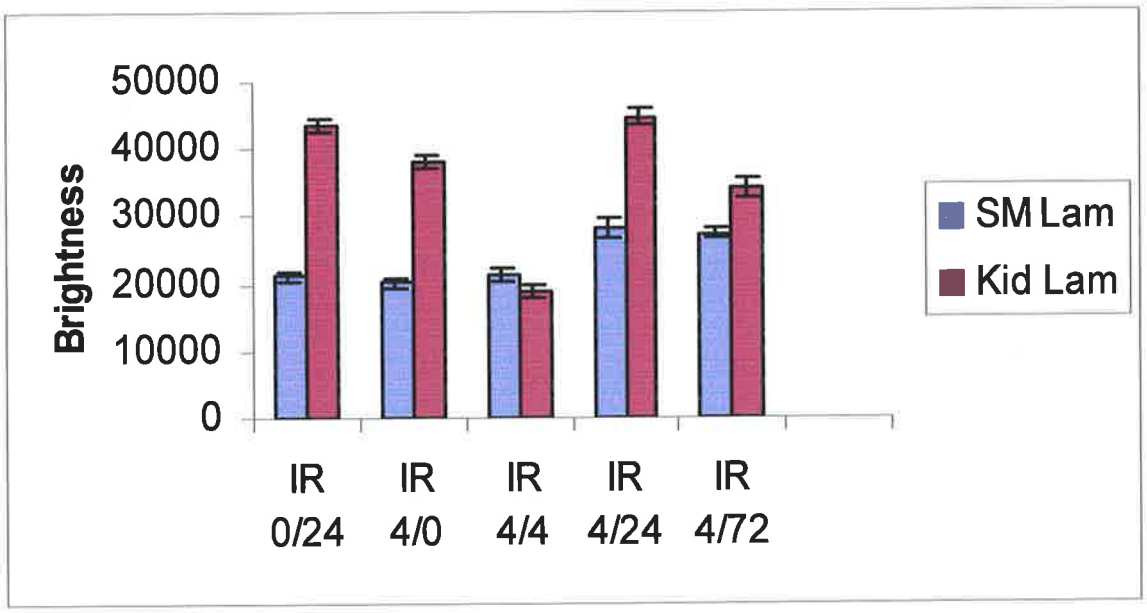
Brightness
50000
40000
30000
20000
10000
0
IR 0/24
IR 4/0
IR 4/4
IR 4/24
IR 4/72
SM Lam
Kid Lam

4.3.9 Alterations of LN in the basement membrane of lung tissues following skeletal muscle I/R.

A fluctuation in laminin level was observed in basement membrane of the lung following 4 h of skeletal muscle ischemia/reperfusion. The laminin level decreased initially after ischemia only, it then returning to baseline level after reperfusion (4/4, 4/24), decreasing subsequently with the further reperfusion. Finally, the laminin level reached the lowest level after 72 h of reperfusion ($P < 0.05$). The representative immunohistochemical pictures of laminin staining in the lung are shown in Figure 4.9, illustrating the wave of alterations of LN in the lung tissues within different experimental groups.

Raw data of quantitative immunohistochemistry is shown in Appendix (6.4.7). The grouped descriptive statistical data for the analysis of LN level in lung is summarised in the Table 4.3.7.

Table 4.3.7

Lung LN	I/R 0/24	I/R 4/0	I/R 4/4	I/R 4/24	I/R 4/72
Mean Brightness	494.6	229.3	521	445.1	129.6
SEM	100.2	38	90	88.2	23.4
St Dev	1120	425.3	1006.6	986	261.6
P value		NS	NS	NS	P<0.05

Lung LN: Laminin in the basement membrane of lung

I/R 0/24: rats underwent 4 h anaesthesia with 24 h recovery, with no ischemia.

I/R 4/0: rats underwent 4 h bilateral hindlimb ischemia only, with no reperfusion.

I/R 4/4: rats underwent 4 h bilateral hindlimb ischemia followed by 4 h reperfusion.

Figure 4. 9. Representative immunohistochemistry images of lung tissues showing levels of laminin in the lung

Images were magified 200 X. The primary antibody was directed against laminin and secondary detection was carried out using biotin-labelled antibody and Streptavidin-Fluorescein Isothiocyanate. Images were captured on Olympus BH_2 microscope with Reflected Light Fluorescent Attachment.

I/R:0/24 Lung tissues from rats that have undergone 4 h anaesthesia followed by 24 h recovery, with no ischemia.

I/R:4/0 Lung tissues from rats following 4 h bilateral hindlimb ischemia, sacrificed before reperfusion.

I/R:4/4 Lung tissues from rats following 4 h bilateral hindlimb ischemia and 4 h of reperfusion.

I/R:4/24 Lung tissues from rats following 4 h bilateral hindlimb ischemia and 24 h of reperfusion.

I/R:4/72 Lung tissues from rats following 4 h bilateral hindlimb ischemia and 72 h of reperfusion.

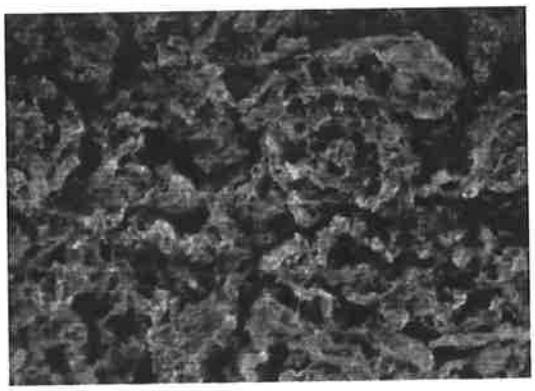

I/R : 0/24

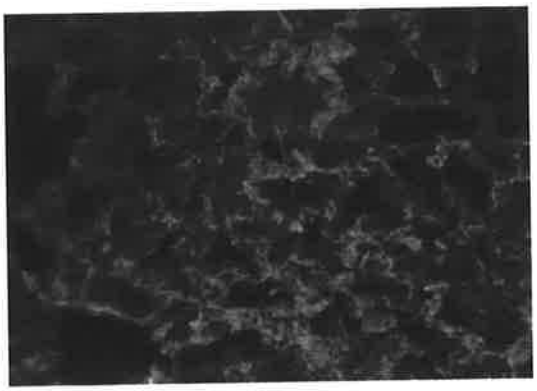

I/R : 4/0

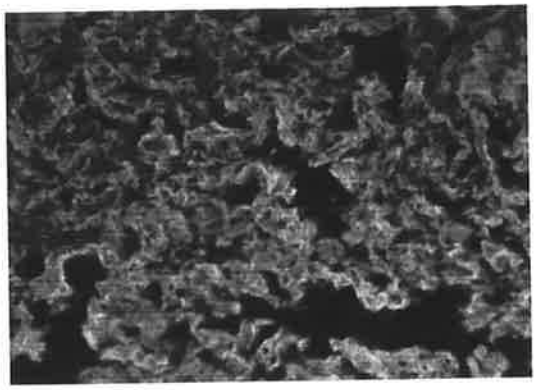

I/R : 4/4

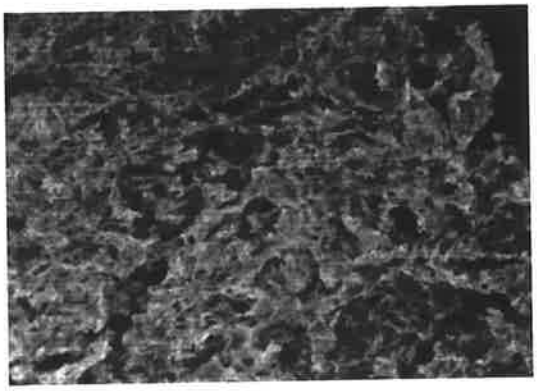

I/R : 4/24

I/R : 4/72

I/R 4/24: rats underwent 4 h bilateral hindlimb ischemia followed by 24 h reperfusion.

I/R 4/72: rats underwent 4 h bilateral hindlimb ischemia followed by 72 h reperfusion.

SEM: Standard error mean.

St Dev: Standard deviation.

NS: No significance.

4.3.10 Summary in graph showing change pattern of LN in basement membranes of the lung of rats following 4 h of bilateral hindlimb ischemia and increasing duration of reperfusion.

Figure 4.10 illustrates graphically the changes in LN levels in basement membrane of the lung following bilateral hindlimb I/R. A fluctuation in laminin level was observed in lung after skeletal muscle I/R. LN was initially degraded, then increasing with progression of reperfusion, returning to the baseline level after reperfusion (4/4, 4/24), decreasing again with further reperfusion, reaching the lowest level after 72 h of reperfusion.

4.3.11 The effects of doxycycline on the alterations of FN in the basement membrane of skeletal muscle following I/R. Quantitative immunohistochemistry for FN in skeletal muscle after doxycycline treatment

In following groups of experiment (4.3.11-4.3.19), doxycycline was administered in low dose and high dose respectively prior to 4 h of bilateral hindlimb ischemia followed by 24 h of reperfusion. Student-Newman-Keuls of Comparison Test was conducted for comparison between doxycycline treatment groups (I/R: 4/24 Doxy L.D and I/R: 4/24 Doxy H.D) and no treatment group (I/R: 4/24). $P < 0.05$ is considered as significant.

FN level in skeletal muscle increased following I/R (4/24). After administration of doxycycline, FN level was reduced slightly in the basement membranes of skeletal muscle,

Figure 4.10. Change patterns of laminin in the basement membrane of lung of rats that had undergone 4 hours of bilateral hindlimb ischemia with increasing duration of reperfusion

Tissue sections were labelled with laminin antibody, prepared and analysed as described in 4.2.1. Brightness refers to level of laminin detected with immunofluorescence.

Each column on the graph represents the mean brightness level of laminin in the basement membranes. Given five rats in each group, 25 images for each rat, 125 images were included in total. The standard deviation bars are shown on the graph.

IR 0/24 refers to rats that underwent a 4 h anaesthesia only, with no ischemia and were sacrificed after 24 h of recovery.

IR 4/0 refers to rats that underwent a 4 h bilateral hindlimb ischemia and were sacrificed immediately after ischemia.

IR 4/4 refers to rats that underwent a 4 h bilateral hindlimb ischemia followed by 4 h of reperfusion.

IR 4/24 refers to rats that underwent a 4 h bilateral hindlimb ischemia followed by 24 h of reperfusion.

IR 4/72 refers to rats that underwent a 4 h bilateral hindlimb ischemia followed by 72 h of reperfusion.

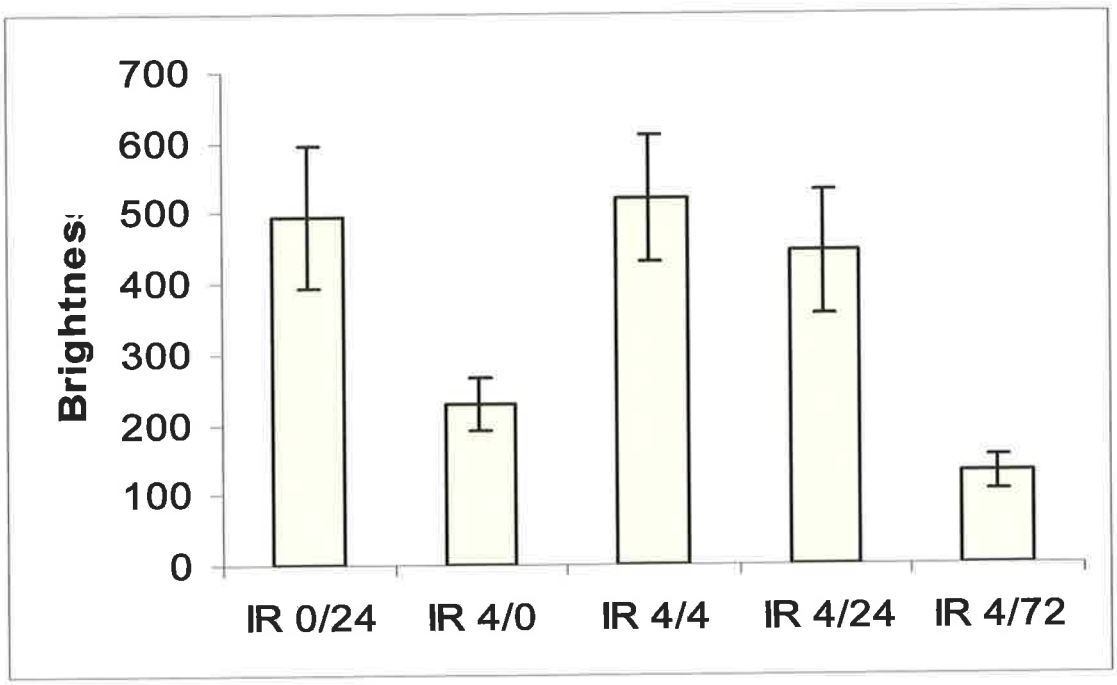
Brightnes
700
600
500
400
300
200
100
0
IR 0/24
IR 4/0
IR 4/4
IR 4/24
IR 4/72

Figure 4.11. Representative immunohistochemistry images of skeletal muscle showing levels of fibronectin after treatment of rats with various dose of doxycycline

I/R:0/24 Skeletal muscle from rats that have undergone 4 h anaesthesia followed by 24 h of recovery, with no ischemia, no doxycycline administration.

I/R:4/24 Skeletal muscle from rats that have undergone 4 h bilateral hindlimb ischemia, sacrificed after 24 h of reperfusion, no doxycycline treatment.

I/R:4/24 Doxy L.D Skeletal muscle from rats that were administered low dose of doxycycline prior to 4 h of bilateral hindlimb ischemia, sacrificed after 24 h of reperfusion.

I/R:4/24 Doxy H.D Skeletal muscle from rats that were administered high dose of doxycycline prior to 4 h of bilateral hindlimb ischemia, sacrificed after 24 h of reperfusion.

I/R : 0/24

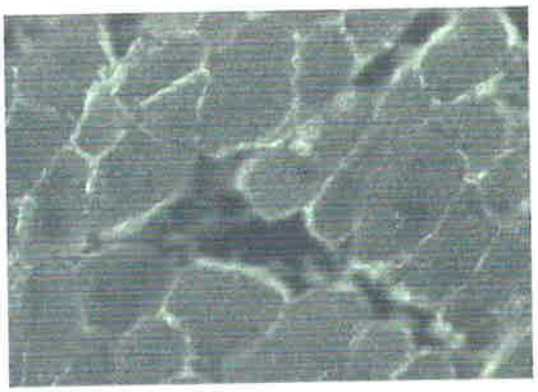

I/R : 4/24

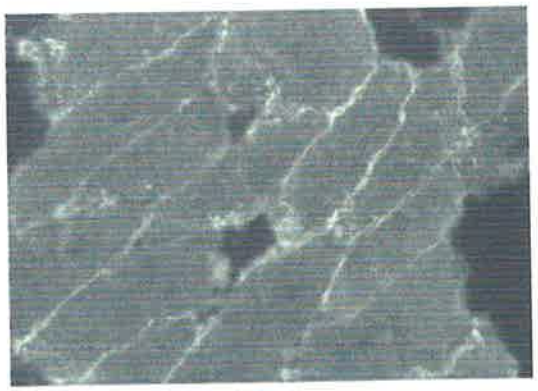

I/R : 4/24 Doxy L.D

I/R : 4/24 Doxy H.D

compared to no treatment group. Representative images of the immunohistochemical staining of skeletal muscle are shown in Figure 4.11, illustrating the alterations of FN after doxycycline treatment in immunostaining that occurred within the different experimental groups.

Raw data of quantitative immunohistochemistry is shown in Appendix (6.4.8). The grouped descriptive statistical data for analysis of FN levels in skeletal muscle is summarised in the Table 4.3.8. $P < 0.05$ was considered as significant.

Table 4.3.8

SM FN Doxy	IR 0/24	I/R: 4/24 No Doxy	I/R: 4/24 Doxy L.C	I/R: 4/24 Doxy H.D
Mean Brightness	5471.9	12987.2	11773.7	10524
SEM	450.1	1132	1176.6	1001.6
St Dev	5512.5	13863.9	14410.1	12267.6
P value			P<0.05	P<0.05

SM FN Doxy: Fibronectin in skeletal muscle after doxycycline treatment

I/R 0/24: Rats in Sham-group underwent 4 h anaesthesia followed by 24 h of recovery, with no ischemia.

I/R 4/24 no Doxy: Rats underwent 4 h bilateral hindlimb ischemia followed by 24 h of reperfusion, no doxycycline treatment.

I/R 4/24 Doxy L.D: Rats were administered low dose of doxycycline (50 mg/Kg, twice daily for 7 days) prior to 4 h of bilateral hindlimb ischemia followed by 24 h of reperfusion.

I/R 4/24 Doxy H.D: Rats were administered high dose of doxycycline (200 mg/Kg, twice daily for 7 days) prior to 4 h of bilateral hindlimb ischemia followed by 24 h of reperfusion.

SEM: Standard error mean.

St Dev: Standard deviation.

4.3.12 The effects of doxycycline on the alterations of FN in the basement membrane of lung tissues following skeletal muscle I/R.

The degradation of FN in the basement membrane of lung was inhibited significantly ($P < 0.05$) by administration of doxycycline, compared to no treatment group (I/R: 4/24 no Doxy) following skeletal muscle I/R. There was no significant difference between low dose and high dose of doxycycline. Representative images of the immunohistochemistry of the lung are shown in Figure 4.12, illustrating the alterations of FN in immunostaining that occurred within the different experimental groups after doxycycline treatment.

Raw data of quantitative immunohistochemistry is shown in Appendix (6.4.9). The grouped descriptive statistical data for the analysis of FN levels is summarised in the Table 4.3.9.

Table 4.3.9

Lung FN Doxy	I/R: 0/24	I/R: 4/24 No Doxy	I/R: 4/24 Doxy L.D	I/R: 4/24 Doxy H.D
Mean Brightness	5093.6	1304.7	5496	4180.9
SEM	465.8	198	545.6	405.9
St Dev	5207.7	2214.2	6099.8	4537.6
P value			P<0.05	P<0.05

Lung FN Doxy: Fibronectin in the lung of rats with doxycycline treatment

I/R 0/24: Rats in Sham-group underwent 4 hours anaesthesia followed by 24 h of recovery, with no ischemic insult.

I/R 4/24 no Doxy: Rats underwent 4 hours bilateral hindlimb ischemia followed by 24 h of reperfusion

Figure 4.12. Representative immunohistochemistry images of lung tissue showing levels of fibronectin following skeletal muscle ischemia/reperfusion with doxycycline treatment

I/R:0/24 Lung tissues from rats that have undergone 4 h anaesthesia followed by 24 h of recovery, with no ischemia, no doxycycline administration.

I/R:4/24 Lung tissues from rats that have undergone 4 h bilateral hindlimb ischemia, sacrificed after 24 h of reperfusion, no doxycycline treatment.

I/R:4/24 Doxy L.D Lung tissues from rats that were administered low dose of doxycycline prior to 4 h of bilateral hindlimb ischemia, sacrificed after 24 h of reperfusion.

I/R:4/24 Doxy H.D Lung tissues from rats that were administered high dose of doxycycline prior to 4 h of bilateral hindlimb ischemia, sacrificed after 24 h of reperfusion.

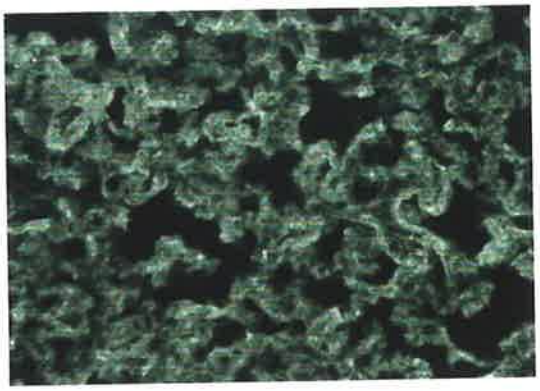

Sham I/R : 0/24

I/R : 4/24

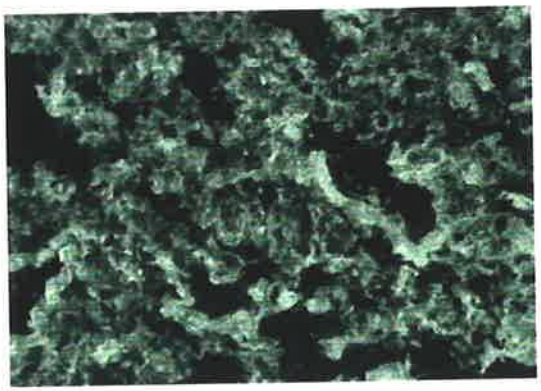

I/R : 4/24 Doxy L.D

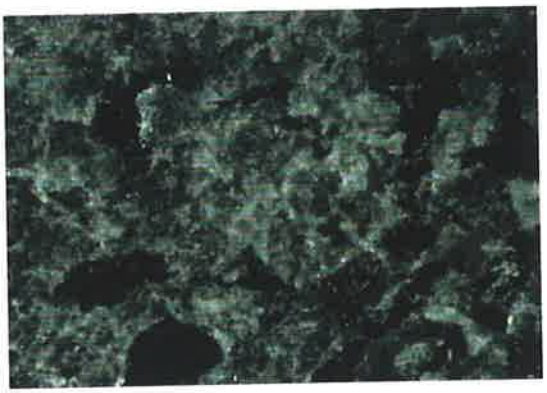

I/R : 4/24 Doxy H.D

I/R 4/24 Doxy L.D: Rats were administered low dose of doxycycline (50mg/Kg, twice daily for 7 days) prior to 4 h of bilateral hindlimb ischemia followed by 24 h of reperfusion.

I/R 4/24 Doxy H.D: Rats were administered high dose of doxycycline (200 mg/Kg, twice daily for 7 days) prior to 4 h of bilateral hindlimb ischemia followed by 24 h of reperfusion.

SEM: Standard error mean.

St Dev: Standard deviation.

4.3.13 The effects of doxycycline on the alterations of FN in the basement membrane of renal tissues following skeletal muscle I/R.

There was no change of FN in the kidney after skeletal muscle 4 h of ischemia followed by 24 h of reperfusion. The FN level in kidney was not elevated significantly ($P > 0.05$) by administration of doxycycline either with low dose or high dose. Representative images of the immunohistochemistry of the kidney are shown in Figure 4.13, illustrating the FN levels in kidney with doxycycline treatment in immunostaining that occurred within the different experimental groups.

Raw data of quantitative immunohistochemistry is shown in Appendix (6.4.10). The grouped descriptive statistical data for the analysis of FN level in kidney is summarised in the Table 4.3.10.

Figure 4.13. Representative immunohistochemistry images of renal tissues showing levels of fibronectin following skeletal muscle ischemia/reperfusion after treatment of rats with doxycycline

I/R:0/24 Renal tissues from rats that have undergone 4 h anaesthesia followed by 24 h of recovery, with no ischemia, no doxycycline administration.

I/R:4/24 Renal tissues from rats that have undergone 4 h bilateral hindlimb ischemia, sacrificed after 24 h of reperfusion, no doxycycline treatment.

I/R:4/24 Doxy L.D Renal tissues from rats that were administered low dose of doxycycline prior to 4 h of bilateral hindlimb ischemia, sacrificed after 24 h of reperfusion.

I/R:4/24 Doxy H.D Renal tissues from rats that were administered high dose of doxycycline prior to 4 h of bilateral hindlimb ischemia, sacrificed after 24 h of reperfusion.

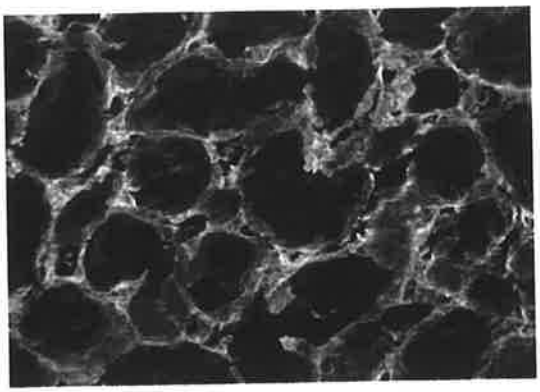

I/R : 0/24

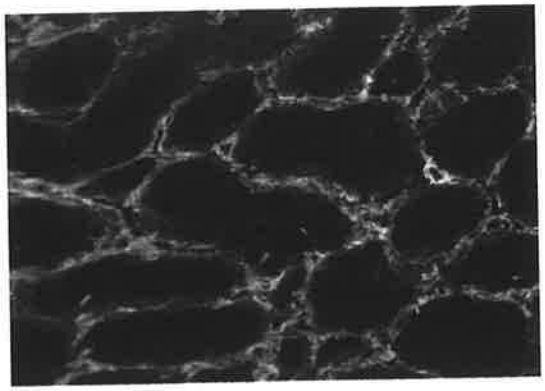

I/R : 4/24

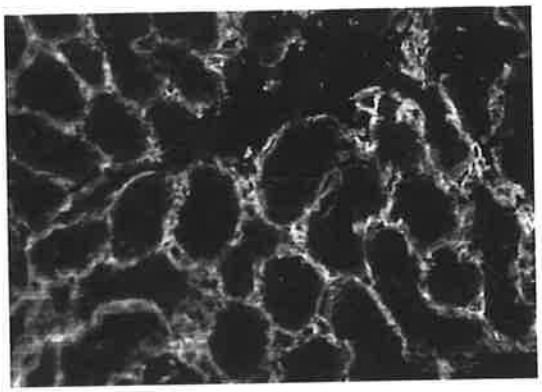

I/R : 4/24 Doxy L.D

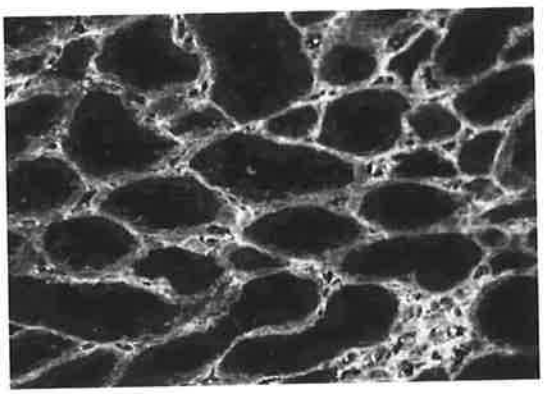

I/R : 4/24 Doxy H.D

Table 4.3.10

Kidney FN Doxy	I/R: 0/24	I/R: 4/24 No Doxy	I/R: 4/24 Doxy L.D	I/R: 4/24 Doxy H.D
Mean Brightness	6399.4	5980.7	6481.2	6655.2
SEM	350.5	380.1	435.3	530.3
St Dev	3919	4249.4	4866.5	5928.7
P value			NS	NS

Kidney FN Doxy: Fibronectin in the kidney of rats with doxycycline treatment.

I/R 0/24: Rats in Sham-group underwent 4 h anaesthesia followed by 24 h of recovery, with no ischemic insult.

I/R 4/24 No Doxy: Rats underwent 4 h bilateral hindlimb ischemia followed by 24 h of reperfusion

I/R 4/24 Doxy L.D: Rats were administered low dose of doxycycline (50 mg/Kg, twice daily for 7 days) prior to 4 h of bilateral hindlimb ischemia followed by 24 h of reperfusion.

I/R 4/24 Doxy H.D: Rats were administered high dose of doxycycline (200 mg/Kg, twice daily for 7 days) prior to 4 h of bilateral hindlimb ischemia followed by 24 h of reperfusion.

SEM: Standard error mean.

St Dev: Standard deviation

NS: No significance.

4.3.14 The effects of doxycycline on the alterations of FN in the basement membrane of hepatic tissue following skeletal muscle I/R.

There was an increase in FN in basement membrane of the liver after 4 h skeletal muscle ischemia followed by 24 h reperfusion. A further increase in FN was detected in the liver after treatment with doxycycline ($P < 0.05$). The further increase was also correlated to the dose of

doxycycline ($P < 0.05$). Representative images of the immunohistochemistry of the hepatic tissues are shown in Figure 4.14, illustrating FN level in the liver after doxycycline treatment.

Raw data of quantitative immunohistochemistry is shown in Appendix (6.4.11). The grouped descriptive statistical data for the analysis of FN level is summarised in the Table 4.3.11.

Table 4.3.11

Liver FN Doxy	I/R: 0/24	I/R: 4/24 No Doxy	I/R: 4/24 Doxy L.D	I/R: 4/24 Doxy H.D
Mean Brightness	13574.2	16652.8	24921.2	33519.1
SEM	513.5	706.8	781.5	966.1
St Dev	5740.8	7902.2	8737.5	10801.7
P value			P<0.05	P<0.05

Liver FN Doxy: Fibronectin in the liver after doxycycline treatment

I/R 0/24: Rats in Sham-group underwent 4 h anaesthesia followed by 24 h of recovery, with no ischemic insult.

I/R 4/24: Rats underwent 4 h bilateral hindlimb ischemia followed by 24 h of reperfusion.

I/R 4/24 Doxy L.D: Rats were administered low dose of doxycycline (50 mg/Kg, twice daily for 7 days) prior to 4 h of bilateral hindlimb ischemia followed by 24 h of reperfusion.

I/R 4/24 Doxy H.D: Rats were administered high dose of doxycycline (200 mg/Kg, twice daily for 7 days) prior to 4 h of bilateral hindlimb ischemia followed by 24 h of reperfusion.

SEM: Standard error mean.

St Dev: Standard deviation.

Figure 4.14. Representative immunohistochemistry images of hepatic tissues showing levels of fibronectin following skeletal muscle ischemia/reperfusion after treatment of rats with doxycycline

I/R:0/24 Renal tissues from rats that have undergone 4 h anaesthesia followed by 24 h of recovery, with no ischemia, no doxycycline administration.

I/R:4/24 Renal tissues from rats that have undergone 4 h bilateral hindlimb ischemia, sacrificed after 24 h of reperfusion, no doxycycline treatment.

I/R:4/24 Doxy L.D Renal tissues from rats that were administered low dose of doxycycline prior to 4 h of bilateral hindlimb ischemia, sacrificed after 24 h of reperfusion.

I/R:4/24 Doxy H.D Renal tissues from rats that were administered high dose of doxycycline prior to 4 h of bilateral hindlimb ischemia, sacrificed after 24 h of reperfusion.

I/R : 0/24

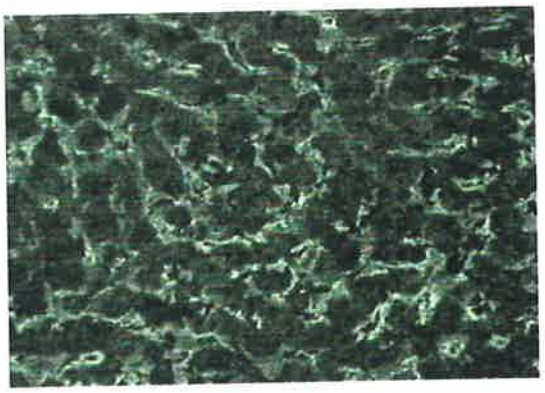

I/R : 4/24

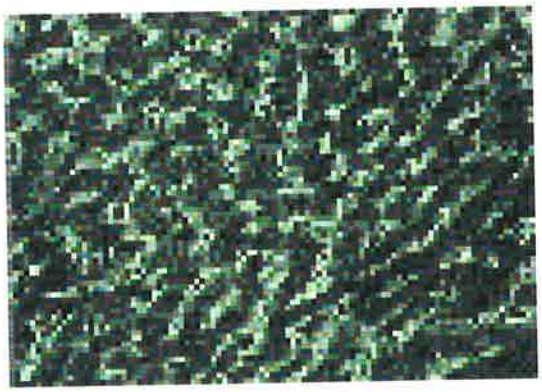

I/R : 4/24 Doxy L.D

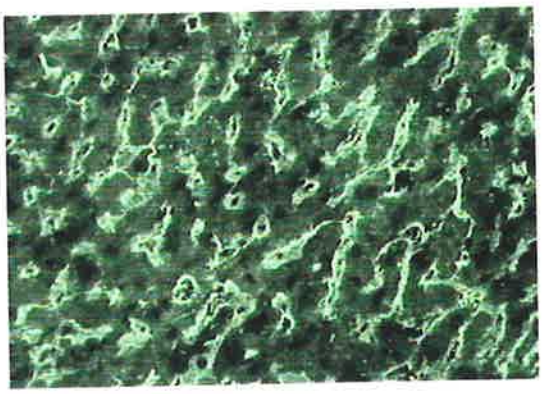

I/R : 4/24 Doxy H.D

4.3.15 Summary of effects of doxycycline on alterations of FN in basement membranes of skeletal muscle, lung, kidney and liver following 4 h of bilateral hindlimb ischemia and 24 h of reperfusion.

Figure 4.15 illustrates graphically the changes in FN levels in basement membranes following skeletal muscle ischemia and reperfusion after treatment of rats with doxycycline. FN level increased in basement membranes of skeletal muscle after 4 h of bilateral hindlimb ischemia and 24 h of reperfusion (I/R, 4/24). The increased FN level was reduced in basement membrane of skeletal muscle when rats were treated with doxycycline prior to I/R (4/24). The degradation of FN in lung was inhibited significantly after treatment of rats with doxycycline ($P < 0.05$). However, FN expression in kidney was not affected by doxycycline. In addition, a further increase in FN was detected in the liver after treatment of rats with doxycycline ($P<0.05$). The increase was also related to the dose of doxycycline.

4.3.16 The effects of doxycycline on degradation of LN in basement membrane of skeletal muscle following I/R.

There was a degradation of LN in basement membrane of skeletal muscle following 4 h of ischemia and 24 h of reperfusion. The degradation was inhibited significantly ($P<0.05$) when rats were treated with doxycycline prior to ischemic insult. There was no significance between low dose and high dose of doxycycline treatment. Representative images of the immunohistochemistry of skeletal muscle are shown in Figure 4.16, illustrating the LN level after doxycycline treatment.

Raw data of quantitative immunohistochemistry is shown in Appendix (6.4.12). The grouped descriptive statistical data for the analysis of LN level is summarised in the Table 4.3.12.

Figure 4.15. Analysis graph showing the effects of doxycycline on fibronectin in the basement membranes of skeletal muscle, lung, kidney and liver following bilateral hindlimb ischemia and reperfusion

Tissue sections were labelled with fibronectin antibody, prepared and analysed as described in 4.2.1. Brightness refers to level of fibronectin detected with immunofluorescence.

Each column on the graph represents the mean brightness level of fibronectin in the basement membranes. Given five rats in each group, 25 images for each rat, 125 images were included in total. The standard deviation bars are shown on the graph.

IR: 0/24 are rats that underwent 4 h anaesthesia only, and then sacrificed after 24 h of recovery.

IR: 4/24 are rats that underwent 4 h of bilateral hindlimb ischemia under anaesthesia followed by 24 h of reperfusion.

Doxy L.D are rats that had been administered low dose of doxycycline (50 mg/kg, twice daily for 7 days) orally before subjected to 4 h of bilateral hindlimb ischemia and 24 h of reperfusion.

Doxy H.D are rats that had been administered high dose of doxycycline (200 mg/kg, twice daily for 7 days) orally before subjected to 4 h of bilateral hindlimb ischemia followed by 24 h of reperfusion.

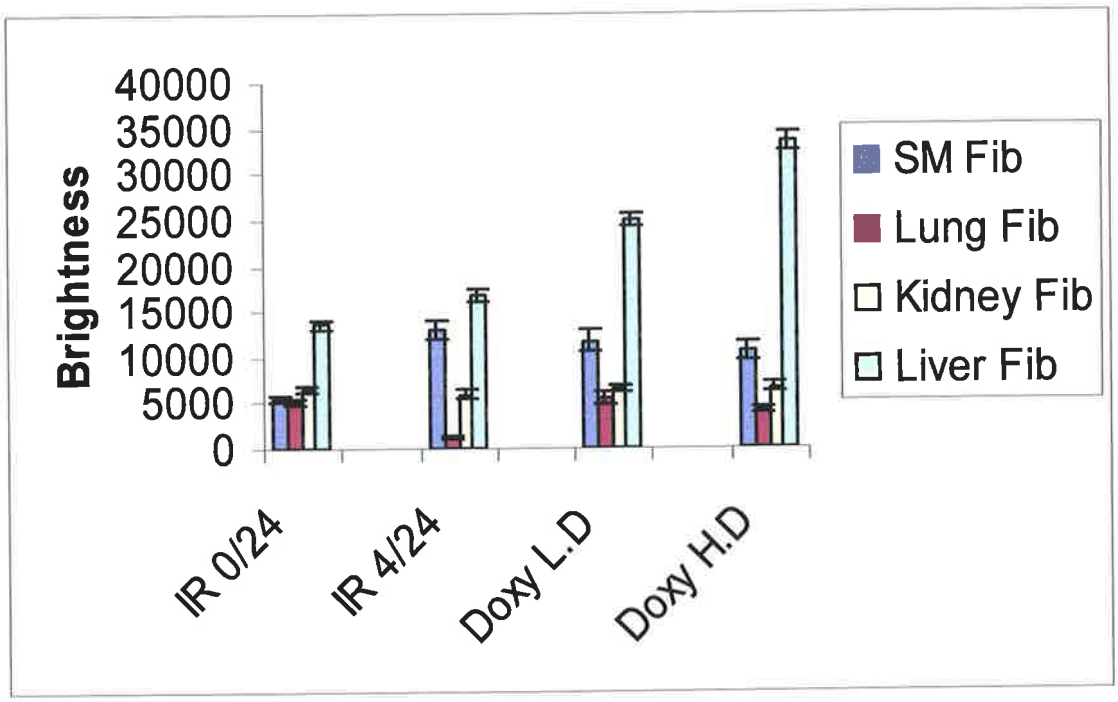
Brightness
40000
35000
30000
25000
20000
15000
10000
5000
0
IR 0/24
IR 4/24
Doxy L.D
Doxy H.D
SM Fib
Lung Fib
Kidney Fib
Liver Fib

Figure 4.16. Representative immunohistochemistry images of skeletal muscle showing levels of laminin after treatment of rats with doxycycline

I/R:0/24 Skeletal muscle from rats that have undergone 4 h anaesthesia followed by 24 h of recovery, with no ischemia, no doxycycline administration.

I/R:4/24 Skeletal muscle from rats that have undergone 4 h bilateral hindlimb ischemia, sacrificed after 24 h of reperfusion, no doxycycline treatment.

I/R:4/24 Doxy L.D Skeletal muscle from rats that were administered low dose of doxycycline prior to 4 h of bilateral hindlimb ischemia, sacrificed after 24 h of reperfusion.

I/R:4/24 Doxy H.D Skeletal muscle from rats that were administered high dose of doxycycline prior to 4 h of bilateral hindlimb ischemia, sacrificed after 24 h of reperfusion.

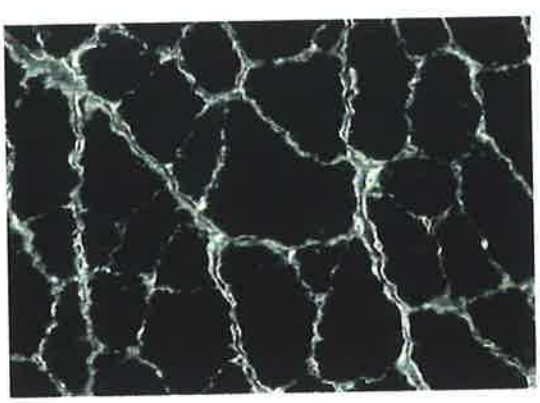

I/R : 0/24

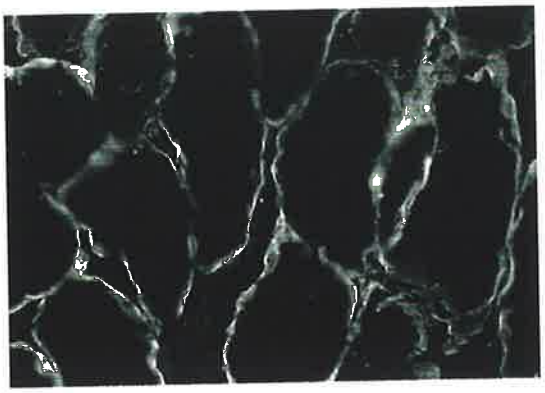

I/R : 4/24

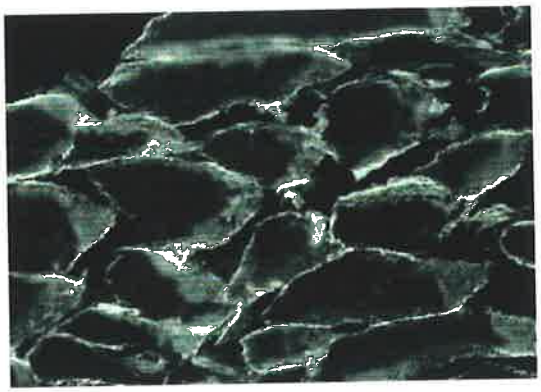

I/R : 4/24 Doxy L.D

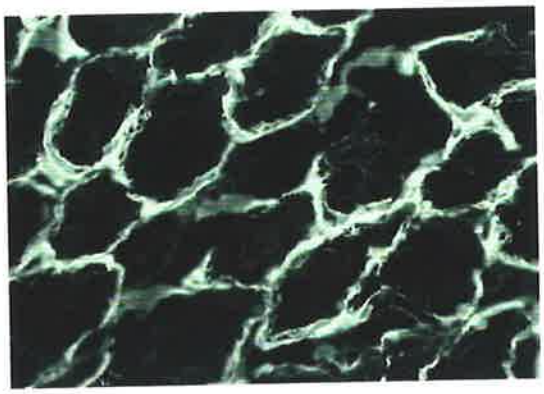

I/R : 4/24 Doxy H.D

Table 4.3.12

SM LN Doxy	I/R: 0/24	I/R: 4/24 No Doxy	I/R: 4/24 Doxy L.D	I/R: 4/24 Doxy H.D
Mean Brightness	11898.9	9425.7	13177	13665.5
SEM	423.2	469.5	640.7	751.1
St Dev	4731.9	5249.4	7163.1	8397.2
P value			P<0.05	P<0.05

SM LN Doxy: Laminin in skeletal muscle after doxycycline treatment.

I/R 0/24: Rats in Sham-group underwent 4 h anaesthesia followed by 24 h of recovery, with no ischemic insult.

I/R 4/24 No Doxy: Rats underwent 4 h of bilateral hindlimb ischemia followed by 24 h of reperfusion, no treatment with doxycycline.

I/R 4/24 Doxy L.D: Rats were administered low dose of doxycycline (50 mg/Kg, twice daily for 7 days) prior to 4 h of bilateral hindlimb ischemia followed by 24 h of reperfusion.

I/R 4/24 Doxy H.D: Rats were administered high dose of doxycycline (200 mg/Kg, twice daily for 7 days) prior to 4 h of bilateral hindlimb ischemia followed by 24 h of reperfusion.

SEM: Standard error mean.

St Dev: Standard deviation.

4.3.17 The effects of doxycycline on LN in basement membrane of lung tissues following skeletal muscle I/R.

LN level decreased in basement membrane of lung tissues following skeletal muscle 4 h of ischemia and 24 h of reperfusion (4/24). The decreased level of LN was elevated by administration of doxycycline either in low dose or high dose ($P < 0.05$). Representative

Figure 4.17. Representative immunohistochemistry images of lung tissue showing levels of laminin after treatment of rats with doxycycline

I/R:0/24 Lung tissues from rats that have undergone 4 h anaesthesia followed by 24 h of recovery, with no ischemia, no doxycycline administration.

I/R:4/24 Lung tissues from rats that have undergone 4 h bilateral hindlimb ischemia, sacrificed after 24 h of reperfusion, no doxycycline treatment.

I/R:4/24 Doxy L.D Lung tissues from rats that were administered low dose of doxycycline prior to 4 h of bilateral hindlimb ischemia, sacrificed after 24 h of reperfusion.

I/R:4/24 Doxy H.D Lung tissues from rats that were administered high dose of doxycycline prior to 4 h of bilateral hindlimb ischemia, sacrificed after 24 h of reperfusion.

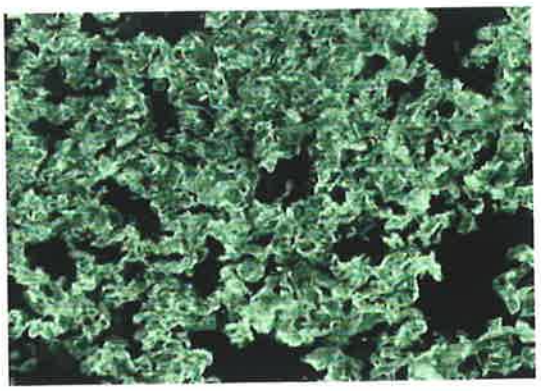

I/R : 0/24

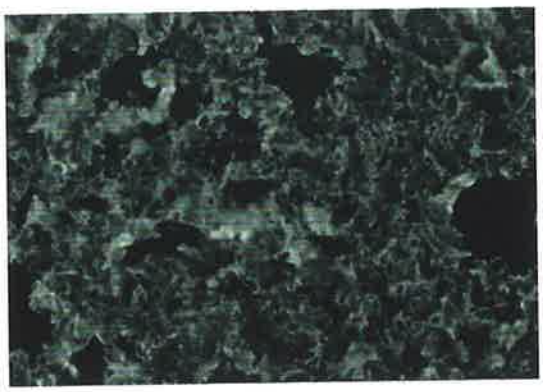

I/R : 4/24

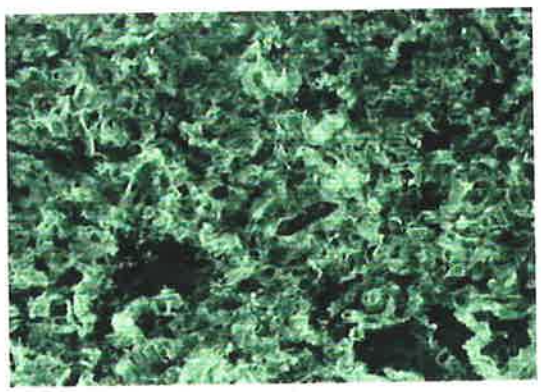

I/R : 4/24 Doxy L.D

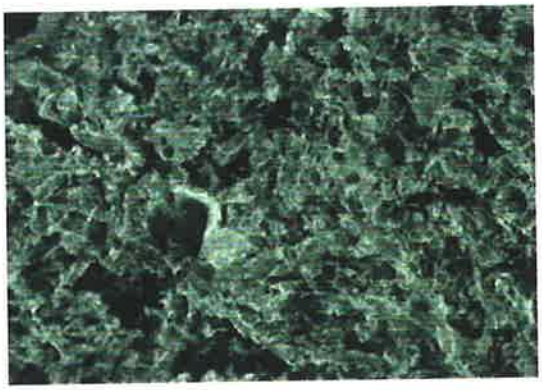

I/R : 4/24 Doxy H.D

images of the immunohistochemistry of the lung are shown in Figure 4.17, illustrating the LN staining in different experimental groups after doxycycline treatment.

Raw data of quantitative immunohistochemistry is shown in Appendix (6.4.13). The grouped descriptive statistical data for the analysis of LN level is summarised in the Table 4.3.13.

Table 4.3.13

Lung LN Doxy	I/R: 0/24	I/R: 4/24 No Doxy	I/R: 4/24 Doxy L.D	I/R: 4/24 Doxy H.D
Mean Brightness	25017.2	12852.2	24839.1	19675.2
SEM	1420.1	747.5	1136.8	1053.7
St Dev	15876.8	8357.8	12709.5	11780.2
P value			P<0.05	P<0.05

Lung LN Doxy: Laminin in the lung of rats after doxycycline treatment.

I/R 0/24: Rats in Sham-group underwent 4 h anaesthesia followed by 24 h of recovery, with no ischemic insult.

I/R 4/24 No Doxy: Rats underwent 4 h of bilateral hindlimb ischemia followed by 24 h of reperfusion, no treatment with doxycycline.

I/R 4/24 Doxy L.D: Rats were administered low dose of doxycycline (50 mg/Kg, twice daily for 7 days) prior to 4 h of bilateral hindlimb ischemia followed by 24 h of reperfusion.

I/R 4/24 Doxy H.D: Rats were administered high dose of doxycycline (200 mg/Kg, twice daily for 7 days) prior to 4 h of bilateral hindlimb ischemia followed by 24 h of reperfusion.

SEM: Standard error mean.

St Dev: Standard deviation.

4.3.18 The effects of doxycycline on LN in the basement membrane of renal tissues following skeletal muscle I/R.

LN level decreased in basement membrane of kidney following skeletal muscle 4h of ischemia and 24h of reperfusion (I/R, 4/24). After doxycycline treatment, LN level was then elevated either with low dose or high dose ($P < 0.05$). Representative images of the immunohistochemistry of renal tissue are shown in Figure 4.18, illustrating the LN staining in different experimental groups.

Raw data of quantitative immunohistochemistry is shown in Appendix (6.4.14). The grouped descriptive statistical data for the analysis of LN level is summarised in the Table 4.3.14.

Table 4.3.14

Kidney LN Doxy	I/R: 0/24	I/R: 4/24 No Doxy	I/R: 4/24 Doxy L.D	I/R: 4/24 Doxy H.D
Mean Brightness	9477.6	6140.5	8680.7	11106.5
SEM	517.3	323.1	501.1	583
St Dev	5783.7	3612.4	5602.1	6517.9
P value			P<0.05	P<0.05

Kidney LN Doxy: Laminin in the kidney after doxycycline treatment.

I/R 0/24: Rats in Sham-group underwent 4 h anaesthesia followed by 24 h of recovery, with no ischemic insult.

I/R 4/24 No Doxy: Rats underwent 4 h of bilateral hindlimb ischemia followed by 24 h of reperfusion

I/R 4/24 Doxy L.D: Rats were administered low dose of doxycycline (50 mg/Kg, twice daily for 7 days) prior to 4 h of bilateral hindlimb ischemia followed by 24 h of reperfusion.

I/R 4/24 Doxy H.D: Rats were administered high dose of doxycycline (200 mg/Kg, twice daily for 7 days) prior to 4 h of bilateral hindlimb ischemia followed by 24 h of reperfusion.

SEM: Standard error mean.

St Dev: Standard deviation.

Figure 4.18. Representative immunohistochemistry images of renal tissue showing levels of laminin after treatment of rats with doxycycline

I/R:0/24 Renal tissues from rats that have undergone 4 h anaesthesia followed by 24 h of recovery, with no ischemia, no doxycycline administration.

I/R:4/24 Renal tissues from rats that have undergone 4 h bilateral hindlimb ischemia, sacrificed after 24 h of reperfusion, no doxycycline treatment.

I/R:4/24 Doxy L.D Renal tissues from rats that were administered low dose of doxycycline prior to 4 h of bilateral hindlimb ischemia, sacrificed after 24 h of reperfusion.

I/R:4/24 Doxy H.D Renal tissues from rats that were administered high dose of doxycycline prior to 4 h of bilateral hindlimb ischemia, sacrificed after 24 h of reperfusion.

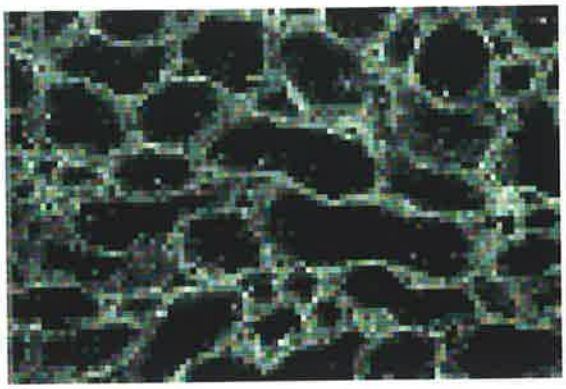

I/R : 0/24

I/R : 4/24

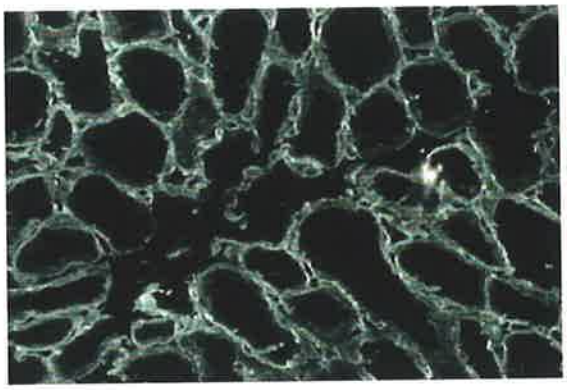

I/R : 4/24 Doxy L.D

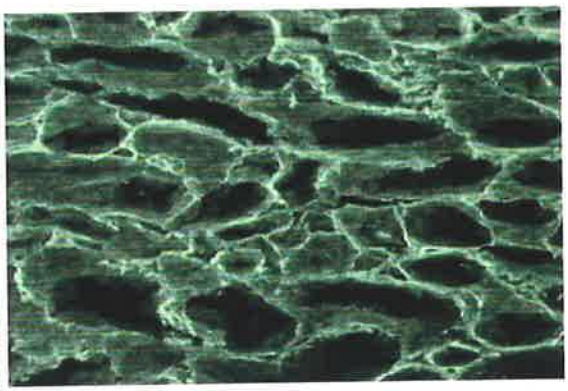

I/R : 4/24 Doxy H.D

4.3.19 Summary of effects of doxycycline on LN in basement membranes of skeletal muscle, lung and kidney following 4 h of bilateral hindlimb ischemia and 24 h of reperfusion.

Figure 4.19 illustrates graphically the change patterns of LN in basement membranes of skeletal muscle, lung and kidney following 4 h of bilateral hindlimb ischemia and 24 h of reperfusion (I/R, 4/24). LN level decreased in basement membranes of skeletal muscle, lung and kidney after I/R (4/24). After doxycycline treatment prior to I/R, LN level was elevated either in low dose or high dose. These results suggest that doxycycline is capable of inhibiting the degradation of LN in basement membranes of skeletal muscle, lung and kidney.

4.3.20. Alterations of FN in the plasma following skeletal muscle I/R.

In the immunohistochemical experiments, a rapid accumulation of FN was detected in basement membrane of the skeletal muscle subjected to I/R. The pattern of FN expression is different from those of collagen IV. Previous work from this laboratory demonstrated degradation of collagen IV in basement membrane following I/R (511). However, in the current experiments, FN was found to accumulate in basement membranes of skeletal muscle after I/R. Therefore, it was postulated that plasma FN may incorporate into the tissue FN following ischemic injury, leading to the accumulation in basement membrane observed on immunohistochemistry. Alterations of pFN have also been reported after tissue injury, such as burn. So changes in pFN may occur following bilateral hindlimb ischemia and reperfusion.

pFN was analysed using ELISA. It was rapidly depleted after 4 h of skeletal muscle ischemia (4/0) and during early reperfusion (4/4 h). FN then increased with the increasing periods of reperfusion, exceeding the normal baseline level compared to sham-group after 24 h of reperfusion. There was a trend for FN to recover to baseline level thereafter (Figure 4.20). The plasma protein concentration was also analysed using Bio-Rad Protein Assay and the relative pFN was calculated. The fraction of FN constituting plasma protein was increased immediately after skeletal muscle ischemia, and then decreased significantly with the

progressing of reperfusion. It was recovered to baseline level with the reperfusion up to 72 h (Figure 4.21 and 4.22).

Figure 4.19: Analysis graph showing effects of doxycycline on the degradation of laminin in the basement membranes of skeletal muscle, lung and kidney following bilateral hindlimb ischemia and reperfusion

Tissue sections were labelled with laminin antibody, prepared and analysed as described in 4.2.1. Brightness refers to level of laminin detected with immunofluorescence.

Each column on the graph represents the mean brightness level of laminin in the basement membranes. Given five rats in each group, 25 images for each rat, 125 images were included in total. The standard deviation bars are shown on the graph.

IR: 0/24 are rats that underwent 4 h anaesthesia only, and then sacrificed after 24 h of recovery.

IR: 4/24 No Doxy are rats that underwent 4 h of bilateral hindlimb ischemia under anaesthesia followed by 24 h of reperfusion, no doxycycline treatment.

Doxy L.D are rats that had been administered low dose of doxycycline (50 mg/kg, twice daily for 7 days) orally before subjected to 4 h of bilateral hindlimb ischemia and 24 h of reperfusion.

Doxy H.D are rats that had been administered high dose of doxycycline (200 mg/kg, twice daily for 7 days) orally before subjected to 4 h of bilateral hindlimb ischemia followed by 24 h of reperfusion.

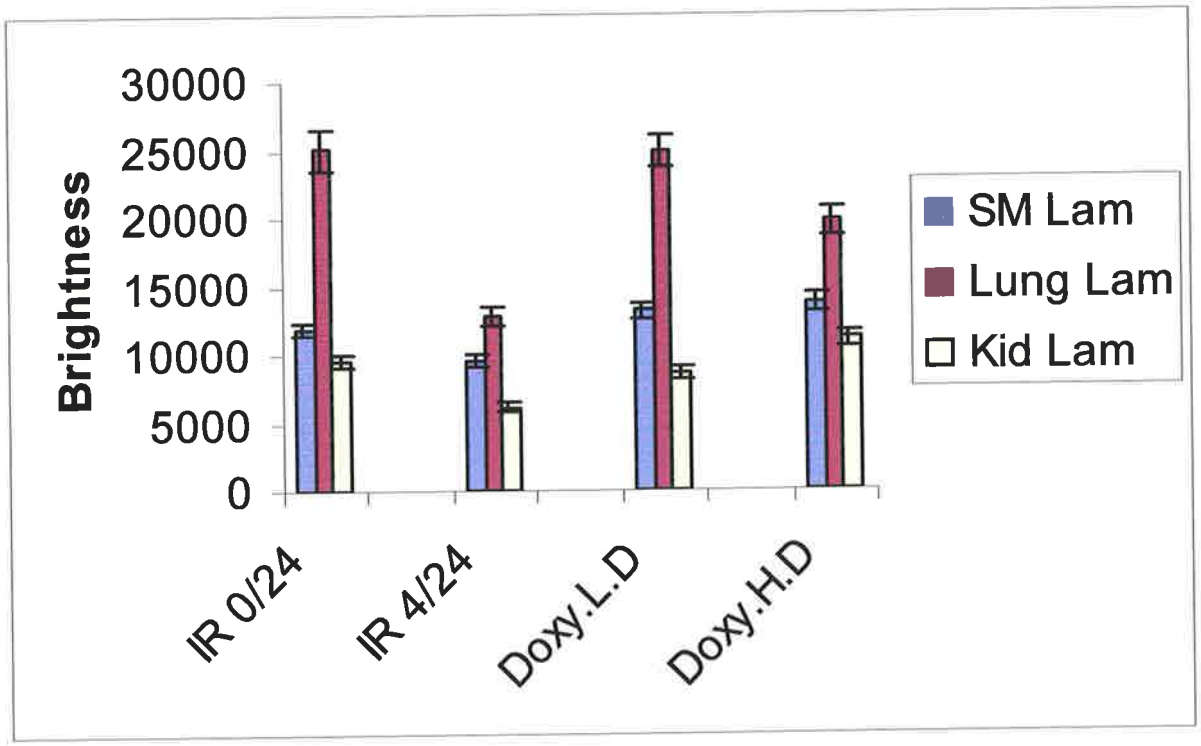
Brightness
30000
25000
20000
15000
10000
5000
0
IR 0/24
IR 4/24
Doxy.L.D
Doxy.H.D
SM Lam
Lung Lam
Kid Lam

Figure 4.20. Concentration of circulating plasma fibronectin of rats subjected to ischemia and reperfusion, compared with sham rats

Concentrations of circulating fibronectin were determined by competitive ELISA of sodium citrate-anticoagulated rat plasma collected by cardiac puncture on sacrifice. Values shown for each timepoint are the duplicate means ± SEM for each of five rats. Timepoints at which sham and ischemic values were significantly different are asterisked ($p \leq 0.05$, Tukey's HSD Post-hoc analysis).

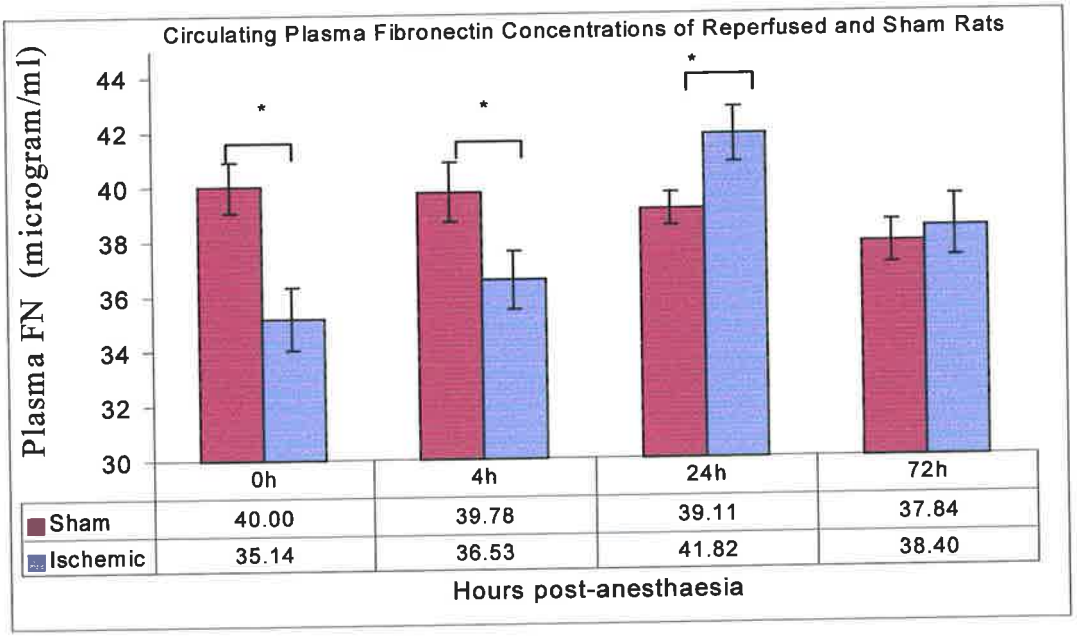
Circulating Plasma Fibronectin Concentrations of Reperfused and Sham Rats
Plasma FN (microgram/ml)
44
42
40
38
36
34
32
30
*
*
*
0h
4h
24h
72h
Sham
40.00
39.78
39.11
37.84
Ischemic
35.14
36.53
41.82
38.40
Hours post-anesthaesia

Figure 4.21: Plasma protein concentration

Total plasma protein was determined by the Bradford, Protein Assay, using BSA as a standard (1976). Values shown for each timepoint are the means of two determinations for each of five rats, ± SEM. Timepoints at which sham and ischemic values were significantly different are asterisked ($p \leq 0.05$, Tukey's HSD Post-hoc analysis).

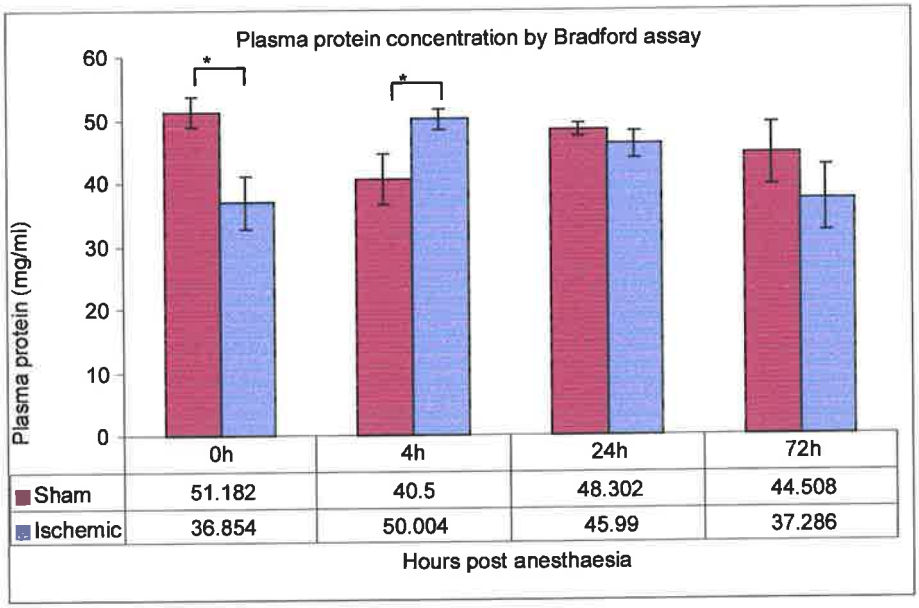
Plasma protein concentration by Bradford assay
Plasma protein (mg/ml)
60
50
40
30
20
10
0
*
*
0h
4h
24h
72h
Sham
51.182
40.5
48.302
44.508
Ischemic
36.854
50.004
45.99
37.286
Hours post anesthaesia

Figure 4.22: The relative concentration of plasma fibronectin

The fraction of total plasma protein comprising fibronectin was determined by dividing each of the ELISA duplicates by the corresponding plasma concentration; means and SEM's were then recalculated. This is an indication of changes in fibronectin release into plasma and sequestration from it. Means ± SEM are shown for each timepoint. Timepoints at which sham and ischemic values were significantly different are asterisked ($p \leq 0.05$, Tukey's HSD Post-hoc analysis).

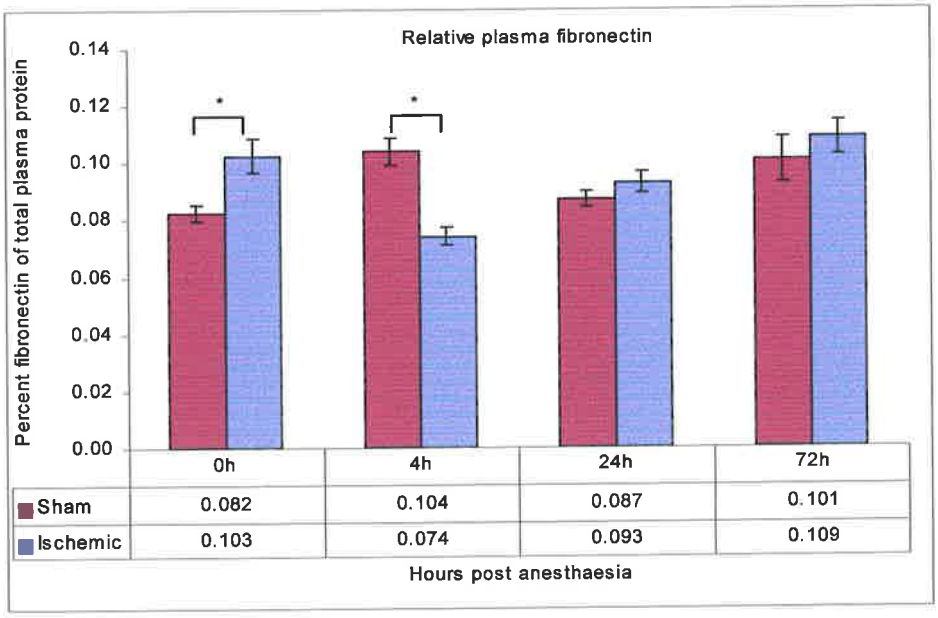
Relative plasma fibronectin
Percent fibronectin of total plasma protein
0.14
0.12
0.10
0.08
0.06
0.04
0.02
0.00
*
*
0h
4h
24h
72h
Sham
0.082
0.104
0.087
0.101
Ischemic
0.103
0.074
0.093
0.109
Hours post anesthaesia

4.4 Discussion

Fibronectins (FNs) are dimeric glycoproteins that exist both in blood, namely plasma fibronectin (pFN) and in tissue extracellular matrices-cellular fibronectin (cFN). Although both pFN and cFN are generated from a single gene, their isoforms differ due to alternative splicing (181). pFN is produced only by hepatocytes and is secreted in a soluble form into plasma where it has a half-life of two days, whereas cFN is expressed by a variety of cells such as endothelial cells and macrophages (171). Extensive studies indicate that fibronectins modulate cell proliferation, migration, survival and immunoreactivity (171) (184) (235) (221). Integrins serve as fibronectin receptors at the cell surface and this interaction is crucial for the ability of fibronectins to affect cellular activity (184), (512).

In the current study, we observed that the pFN was depleted immediately after 4 h bilateral hindlimb ischemia as compared with sham-operated group. Circulating pFN subsequently increased following reperfusion of ischemic skeletal muscle, exceeding levels of pFN in the sham group, reaching a maximum after 24 h of reperfusion and subsequently decreasing again. However, the fraction of FN in total plasma protein was elevated after 4 h ischemia of skeletal muscle, then dropped to a minimum level at 4 h of reperfusion, and consequently was enhanced with reperfusion.

Furthermore, a rapid accumulation of FN in the basement membrane of ischemic skeletal muscle was detected after 4 h of bilateral hind limb ischemia. This is the result of incorporation of FN from the plasma in retained blood into the basement membrane due to the increased vascular permeability during the period of ischemia. The binding of FN to the basement membrane continued with reperfusion at least until 72 h. Local endothelial cells newly synthesize another possible resource of accumulated FN. In contrast, FN was degraded in the basement membrane in remote organs (lung and kidney). The degradation persisted during the period of reperfusion. Moreover, FN was depleted markedly in the liver after

bilateral hind limb ischemia and during early reperfusion, then increased significantly with later periods of skeletal muscle reperfusion, exceeding the baseline level after 24 h of reperfusion.

Similar alterations have been observed by Thompson et al (188) in their study of tissue injury in a rat model. The ischemia of skeletal muscle was created by applying the tourniquet at upper thigh of hindlimb beneath the skin. They found that the rise of pFN was significantly greater at 22 h both in rats that underwent skeletal muscle ischemia/reperfusion and in sham-operated group compared to those in normal control group. The initial increase in pFN occurred after 2 hours of reperfusion, continued with the progressing of reperfusion. It has been concluded that prior pFN depletion is not required for this hyperfibronectinemic response and that it reflects a rather rapid increase in fibronectin synthesis. In addition, increased deposition of exogenous ^{125}I labelled fibronectin was detected at the site of injured muscle after release of the tourniquet. Its binding may form the provisional matrix for wound healing that is anticipated to occur following ischemic injury. Moreover, the liver and spleen were demonstrated greater FN deposition due to large populations of reticuloendothelial cells. Alterations in pFN were also observed in sublethal burn injury in a pattern of the depletion over 15-minute to 2-h period after burns, then normalisation by 4-8 h followed by a rebound hyper-fibronectinemia at 24 h (193), (190), (191).

pFN is an opsonic molecule that markedly enhances macrophage phagocytic clearance of blood-borne nonbacterial particulates (186). Clearance of such debris from blood by macrophages in the liver and spleen minimises deposition of the debris in extrahepatic beds such as the lung and kidney and is thought to ensure integrity of organ function by preventing micro-embolization of these particulates in vascular beds (187). It was suggested that the acute depletion of pFN might be attributed to its deposition at the site of injured tissue and its removal from the circulation by the liver (191)

The sequestration of pFN in areas of tissue injury reflects not only the affinity that FN may have for sites of tissue injury but also the increased vascular permeability at the site of injury. Incorporation of pFN into the tissue matrices was observed in a distribution pattern comparable to endogenous tissue fibronectin (513). Hayman and Ruoslahti demonstrated the patterns of incorporation of exogenously added pFN into the extracellular matrix of kidney cells in culture (514). It was considered that the deposition of pFN in the tissue matrix may play a crucial role in early tissue repair by improving fibroblast, epithelial and endothelial cell adhesion and migration, as well as regulating collagen matrix assembly (239). Moreover, the deposition of pFN was suggested to inhibit ischemia-induced tissue injury. Sakai et al (218) have found that there is a significant greater infarction volume in FN gene knockout mice than those in normal mice, accompanied by a lack of deposition of pFN in infarct area. Incidentally, an increased number of apoptotic cells were observed in infarct area in pFN-null mice with decreased number of Bcl-2 protein positive cells. These results indicate that the pFN interacts with the cells to inhibit apoptosis by inducing the expression of Bcl-2 protein. In addition, it has been demonstrated that interaction of pFN with $\alpha_5\beta_1$ integrin leads to an over expression of the anti-apoptotic protein Bcl-2 and this over expression of Bcl-2 may protect cells against ischemic damage (515) (516). Therefore, it was postulated that the rapid accumulation of FN in the basement membrane of ischemic skeletal muscle not only improves tissue repair but also protects the tissue against apoptosis.

Nevertheless, the mechanisms of degradation of FN in remote organ lung and kidney are not well characterised. A likely mechanism may involve the activation of neutrophils and their infiltration into the remote organ, releasing the enzymes such as MMPs and resulting in the degradation of extracellular matrix. Previous studies in our laboratory (302) have shown that there was an up-regulation of MMP-2 and MMP-9 accompanied by degradation of collagen IV in the basement membrane in both lung and kidney. Although the degradation of

extracellular matrix FN by MMPs may occur in ischemic skeletal muscle, the burst of deposition of FN in the injured tissue outweighed the degradation. As a result, a net accumulation of FN in the basement membrane of skeletal muscle was observed. The FN may possibly also be expressed by macrophages, which infiltrate into the tissue during I/R. The alterations of FN in liver observed in this study are consistent with the changes in FN levels in plasma, indicating that liver may be the source of pFN. This observation is in agreement with Thompson et al who demonstrated that the major source of rebound elevation of pFN after bilateral hind limb I/R was due to elevated synthesis of FN by the liver mediated by certain cytokines, such as TNF-α and IL-6 (188).

Furthermore, in a recent study, it was shown that intravenous administration of FN peptide V (FN-C/H-V) significantly diminished in a dose-dependent fashion, polymorphonuclear monocytes (PMN) accumulation in ischemic tissue, reducing the size of infarction, and improving neurological outcomes after transient focal cerebral ischemia in rats (220). Although the role of FN-C/H-V in mediating the adhesion of leukocytes is complex and poorly understood, FN-C/H-V may inhibit PMN accumulation directly via interaction with proteoglycans on the cell surface. It has also been hypothesised that cytokines or other cells that are related to fibronectin and PMN may play a role in the inhibition of PMN accumulation. Galkina and co-workers (517) observed that inhibition of neutrophil spreading during their adhesion to FN induced formation of long tubulovesicular cell extension (cytonemes). In addition, it is possible that FN-C/H-V could interact with a cell surface proteoglycan on effector cells and inhibits PMN accumulation, because proteoglycan interactions with selectins have been shown to facilitate leukocyte rolling (518). On the other hand, the adhesion of macrophages to FN may improve macrophage phagocytosis of apoptotic neutrophils at inflammatory sites, facilitating resolution of the inflammatory response (243).

Similarly, alterations of FN have been identified in the basement membrane of organ allografts that underwent I/R during transplant. In a small bowel transplant model, increased fibronectin levels were observed in the basement membrane within the villi cores and crypt areas after I/R (194). In heart allografts, it was found that the accumulation of FN in the cytoplasm was positively correlated with the degree of cardiomyocyte coagulation necrosis. Ischemia-induced damage of myocytes presents an intense FN cytoplasmic immunoreactivity that occurs before the morphological architectural changes observed on hematoxylin and eosin sections (519), Labarrere et al (195) have found that there was a correlation between the deposits of FN by immunohistochemistry on biopsy and the development of chronic rejection or graft failure during the follow-up of cardiac transplants. Similarly, the increased FN deposition found during biopsies of heart allograft predicted the high risk of graft failure (196).

In the kidney, it was shown that FN was markedly increased in the cortex, corticomedullary junction and glomeruli after ischemia and subsequent reperfusion. This deposition of FN was considered to originate from pFN (204). Kidney is unique in that after ischemic injury to the renal tubules, essentially complete regenerative repair can occur. In this respect, FN is suggested to be of potential importance in tubular regeneration after injury, as it contains multiple functional domains including cellular binding, spreading, proliferation and differentiation domains (215). It was postulated that FN might serve to organise the subsequent regeneration tubular epithelium. FN of the provisional matrix has been shown to promote the movement of fibroblast, macrophages and blood vessels into the wound space (520). Livant et al (521) observed that administration of the PHSRN polypeptide sequence of pFN appears to enhance the migration-dependent processes of re-epithelialization and neovascularization in the dermal wounds of healing-impaired mice. Therefore, pFN may be sources of a locally acting peptide chemotactic factor that function to attract the cells which

are crucial for tissue repair by inducing chemotaxis through the stroma and directional migration on the provisional matrix.

Furthermore, the accumulation of FN in the basement membrane after I/R may predispose the allograft to undergo fibrosis and lead to chronic allograft dysfunction. This was speculated to be the result of imbalance between the synthesis and degradation of extracellular matrix in favour of its accumulation. Both cytokines and MMPs are thought to be involved in this process. It has been demonstrated that chronic fibrosis in renal allograft is related to the up-regulation of expression of TGF-ß (522). Likewise, it has been shown that an increased infiltration of macrophages occurs with concomitant up-regulation of cytokines such as TGF-$ß_1$ and TGF-$ß_3$ and increased deposition of ECM during chronic lung rejection. These cytokines have an important role in stimulating fibroblasts to produce fibronectins, which are a major source of ECM (523).

FN is an active participant in the immune cascade in organ transplantation. (194), (221). In more recent studies, FN has been found to play a crucial role in allograft rejection. It was observed that intra-allografts EIII A^+ FN expression by macrophages is a critical feature of graft rejection versus tolerance. The lack of EIII A^+ FN expression by infiltrating macrophages in the tolerant state was associated with marked depression of IL-2 and IFN-r at both mRNA and protein levels. The expression of $EIIIA^+$ FN may amplify the rejection cascade via up-regulation of type 1 cytokines, IL-2 and IFN-r in allografts (221). The interaction between alpha-4-intergrin and FN may be important for leukocyte homing to the graft site (223). Pathologically, the most prominent feature of chronic rejection is expansion of extracellular matrix and widening of the basement membrane. FN is one of major constituent in basement membrane. Clinically, in patients with acute or chronic kidney allograft rejection, urinary FN levels are found to be significantly higher than those of patients

with stable graft function. This enhanced urinary FN is likely to arise from glomerular protein leakage and tubular cell secretion (224).

LN level remained unchanged in basement membrane of the skeletal muscle following bilateral hindlimb I/R, but it decreased in the remote organs (kidney and lung). The LN level increased subsequently in basement membrane with further reperfusion. This result is similar to the alterations of collagen IV in basement membrane following bilateral hindlimb I/R (302). It has been demonstrated that degradation of collagen IV was associated with the up-regulation of MMP-2 and MMP-9 (302). Therefore, it is postulated that degradation of LN observed in this study may be also related to the over-production of MMP-2 and MMP-9. LN could also be degraded by MMP-3 and/or MMP-7. So studies were carried out to investigate if MMP-3 and MMP-7 were produced in skeletal muscle by using casein gel zymography. However, there was no expression of MMP-3, nor MMP-7 in either healthy skeletal muscle, or after I/R (Chapter 3). Whether other MMPs are expressed following ischemia and reperfusion in the skeletal muscle remain unclear. Frisdal et al have also demonstrated that LN and collagen IV in the basement membrane of skeletal muscle were degraded after ischemia but without reperfusion. This degradation was closely correlated with the up-regulation of matrix metalloproteinases, MMP-2 and MMP-9 (271).

LN is a multifunctional glycoprotein and a major component of extracellular matrix that contributes to the architecture of the basement membrane. It plays significant roles in cellular adhesion, growth, migration and differentiation of several cell types (251). However, it has not been determined whether breakdown of LN may stimulate remodeling of the basement membrane and repair of skeletal muscle after I/R or if the alterations in LN are solely indicative of the degree of integrity of the basement membrane. Moreover, degradation of LN was observed in the basement membrane in cerebral and renal ischemia followed by reperfusion (269), (204). The loss of LN and other basement membrane components was

considered to be responsible for the disruption of microvascular integrity and increased vascular permeability.

LN may also contribute to muscle proliferation and fusion of satellite cells after injury (524). In addition, ECM proteins may serve as reservoir for various growth factors, which have beneficial effects on the control of muscle regeneration and angiogenesis (525). Furthermore, the changes of LN in the basement membrane during cold ischemia were more prominent than those after warm ischemia, suggesting these alterations were also potentiated by cold temperature (270).

Like FN, LN has also been found to participate in the immunoreactive cascade. It was observed that different isoforms of LN are able to improve PMN migration into the sites of inflammation and act as a signal to direct lymphocyte migration to the specific organs (261) (263). Administration of LN peptide could inhibit leukocyte accumulation and ameliorate brain injury in a rat model of transient focal cerebral ischemia (526). This result may offer a novel therapeutic approach to protect tissue against I/R-induced injury. In organ transplant, the elevation of LN in basement membrane may increase the risk of subsequent early allograft rejection (268). Therefore, the alterations of LN in the basement membrane after I/R may improve tissue repair by directing interactions between ECM-cells and cell-cytokines and the infiltration of inflammatory cells may exacerbate the existing injury. On the other hand, these alterations may change the expressions of major histocompatibility (MHC) and predispose the allograft to undergo immunoreactivity. Intervention in the changes of ECM will provide a new approach to attenuate the I/R injury and reduce allograft rejection.

Doxycycline belongs to the family of tetracyclines and is one of several chemically modified tetracyclines, which have been proven to have long-term safety and efficacy as antibiotics in the treatment of acne vulgaris (527). Recently, it has been shown that doxycycline is of

therapeutic benefit in several animal models of disease and in human abdominal aortic aneurysm, in which the activity of MMPs has been suggested to play a crucial role in the formation of lesions (528) (529) (377) (1) (475). In addition, a number of studies have demonstrated that doxycycline not only inhibits the expression and activity of MMPs (528) (475), but also modulates the expressions of cytokines, such as inducing up-regulation of protective cytokines TGF-ß$_3$ and down-regulating pro-inflammatory cytokines including IL-1α and IL-1ß (530). In this study, it was observed that the degradation of LN in the basement membrane was diminished by oral administration of doxycycline both in the ischemic/reperfused skeletal muscle and in the remote organs lung and kidney. Nevertheless, reduced degradation of FN following doxycycline treatment was only observed in the remote organs, lung, kidney and liver, but not in skeletal muscle itself. This observation implies that doxycycline may diminish the extent of degradation of LN and FN in basement membranes by inhibiting the activity of MMP-2 and/or MMP-9. Similarly, a previous study in our laboratory has determined that doxycycline could inhibit the activity of MMP-2 and MMP-9 after bilateral hind limb I/R, accompanied by reduced degradation of collagen IV in skeletal muscle (302). However, in the current study, doxycycline did not significantly reduce fibronectin loss from skeletal muscle when compared to placebo-treated reperfused controls. This may occur because the deposition of FN from the plasma into the basement membrane plays a major role in the accumulation of FN other than the possibility of reduced degradation of FN after doxycycline administration. It remains unclear why there was a further increase in FN in the liver after 4 h ischemia and 24 h reperfusion following administration of doxycycline. This increase may be associated with modulation of some cytokines after administration of doxycycline, except for the inhibition of FN degradation. As has been demonstrated the production of FN in the liver is increased by cytokines IL-6 and TNF-α after hind limb I/R (188). Therefore, doxycycline appears to inhibit basement membrane degradation after I/R, but it is not clear whether this effect is beneficial or harmful for tissue repair. Further studies are needed to investigate the effects of doxycycline in ischemia and

reperfusion injury. Hopefully, the administration of doxycycline will be a novel approach for reducing the severity of this injury.

In conclusion, the results of this study suggest that FN has an specific affinity to the injured tissue and may promote cell migration and tissue repair, as mirrored by rapid depletion of plasma FN. Interestingly, the changed patterns of FN in liver imply that pFN was secreted by the liver. Furthermore, we hypothesise that alterations of FN in lung and kidney and LN in all tissues are at least partially due to over-production of MMPs. Moreover, doxycycline was suggested to have an effect in reducing the extent of degradation of FN and LN by inhibiting the activity of MMPs. However, this effect was not shown in skeletal muscle and liver, because there was an over deposition of FN in skeletal muscle and the production of FN in the liver.

CHAPTER 5

SUMMARY,

FUTURE DIRECTIONS

AND

CONCLUSIONS

5.1 Summary of chapter 1

Ischemia and reperfusion is a common clinical event, that is encountered in ischemic heart disease, stroke, shock, following cardiopulmonary resuscitation, vascular surgery and in organ transplants. The morbidity and mortality of I/R-induced injury is very high, leading to ischemic tissue edema, or even necrosis, as well as remote organ injury such as pulmonary edema secondary to lower torso ischemia. A large number of studies have been conducted to explore the mechanisms of I/R.

During ischemia, the blood supply to the tissue is interrupted and oxygen is lacking. ATP is degraded, resulting in conversion of xanthine dehydrogenase to xanthine oxidase and hypoxanthine to xanthine within endothelial cells. Therefore, a burst of oxygen free radicals is produced following reperfusion. On the other hand, the depletion of ATP also causes elevation of intracellular calcium, leading to activation of proteases. The oxygen free radicals are highly reactive, initiating peroxidation of cellular lipid membranes and resulting in structural and functional cell damage. Lipid peroxidation induces the production of metabolites of arachidonic acid, thromboxane A2, leukotriene B4 (LTB4), platelet activating factor (PAF) and prostaglandins. All these metabolites are considered to contribute to the activation of neutrophils, release of cytokines and activation of complement. Activated neutrophils, with the help of adhesive molecules such as ICAM-1 and selectins, migrate across the capillary endothelium, leading to an increase in microvascular permeability and albumin extravasation. Plugging of neutrophils in capillaries, endothelial swelling, platelet aggregates, and compression by extravasated albumin combine to result in the "no flow" phenomena and tissue injury. In addition, activation of neutrophils also releases oxygen free radicals, cytokines and proteases. Moreover, nitric oxide (NO), a vasodilator and endothelin (ET), a vasoconstrictor are produced by endothelium, and are involved in I/R injury. The balance between NO and ET is tipped in favour of production of ET, improving neutrophil adhesion to the endothelium and increasing vascular constriction, thereby prolonging hypoxia.

Apoptosis also plays an important role in a variety of tissues following ischemia and reperfusion. The production of ROS, damage to mitochondria and activation of caspase family members all contribute to the process of apoptosis. The advantage of apoptosis is that it permits cell death without destruction of adjacent cells.

Alterations of fibronectin (FN) and laminin (LN) following ischemia/reperfusion imply that FN and LN play a role in I/R-induced injury. The rapid deposition of FN in the basement membrane during I/R is considered to attenuate tissue injury, as well to facilitate tissue repair. There are also complex interactions between FN and integrin family members on cell surface or cytokines by which cellular functions could be changed. Administration of FN and LN peptide has been suggested to ameliorate tissue injury.

MMPs are a family of zinc dependent enzymes that have been demonstrated to be able to degrade the extracellular matrix and to be involved in the multiple patho-physiological conditions. In recent studies, MMPs have been determined to play a crucial role in I/R injury. An elevation of MMP-9 and/or MMP-2 has been found in the brain, heart, kidney and lung tissues during ischemia and progressive reperfusion. The over-production of MMPs has been suggested to contribute to the disruption of basement membranes and increases in vascular permeability. Up-regulation of MMPs, combined with adhesive molecules, facilitates cell adhesion and migration through endothelial cells into the target site, improving tissue remodelling.

Based on understanding of the mechanisms of I/R injury, a number of therapeutic strategies have been employed to ameliorate the injury, which include antioxidation and scavenging of ROS, inhibition of proinflammatory cytokines, adhesive molecules, complements, and MMPs. A number of studies have been published to show that down-regulation of MMPs

either by MMP-antibodies or inhibitor, including doxycycline significantly decreases I/R organ injury.

The aims of this study were to investigate the alterations of fibronectin and laminin, major components of basement membrane and expression of potential caseinolytic MMPs involved in I/R. The effects of doxycycline on these substrates during ischemia/reperfusion injury were also explored.

5.2 Summary of chapter 2

The animal model for skeletal muscle ischemia and reperfusion was described in chapter 2. This animal model has been established in surgical laboratory at The Queen Elizabeth Hospital for study of I/R injury. The model mirrors the clinical procedure in repair of abdominal aortic aneurysm, in which the abdominal aortic is clamped and lower torso ischemia is created.

A tourniquet model of I/R injury has been used in many studies (531), (532), (533). These methods commonly apply a tape tourniquet or a rubber band above the level of greater trochanter of the rat. The advantages of this model are that it was easily established and reproduced. It also includes muscles of each fibre type in the ischaemic area and thus the overall effect of a mixture of fibre types was included in the element of reperfusion. This model corresponds to the human situation of ischaemic limbs arising due to trauma, embolism, thrombosis or in vascular surgery.

Vascular pedicle techniques have also been extensively employed in the studies of ischemic injury, such as canine gracilis muscle (534) Unlike the tourniquet model, this method involves isolating the selected muscle and compartment syndrome due to edema formation may have less pathogenic influences in this model since fascial planes are opened.

Samples were processed as follows. Two ml of blood were anticoagulated and centrifuged to obtain plasma. Both quadriceps muscles were harvested and divided into 3 parts, the upper part for histopathology, middle part for zymography and lower part for immunohistochemistry. The lung, kidney and liver were also retrieved and divided into 3 parts for histopathology, zymography and immunohistochemistry respectively.

In situ occlusion of artery with maintenance of venous outflow has also been utilized in the investigation of skeletal muscle I/R injury (535) This model needs surgical isolation of arterial vessels to the limbs and is more technically demanding than a tourniquet model. Nevertheless, it closely resembles clinical ischaemic events including thrombotic or embolic occlusions to the arterial vessels or aortic surgery.

A four-hour time course of ischemia was chosen in the current study. The length of ischaemia has been determined to be sufficientlly long to produce a histological damage to the skeletal muscle followed by reperfusion changes (511).

5.3 Summary of chapter 3

The proteolytic activity of MMPs has been investigated in various tissues following skeletal muscle ischemia and reperfusion in this chapter. The tissue samples were homogenised and dialysed for zymographic analysis. SDS-PAGE gels were embedded with gelatin or casein substrates for the detection of zymographic activity of MMPs. Western blots was also employed in these experiments for confirmation the identity of MMPs detected on zymograms.

A significant elevation of proMMP-2 and MMP-9 was observed in skeletal muscle following 4 h ischemia and reperfusion. MMP-9 was elevated only after 4 h of reperfusion. Elevation of MMP-9 and active MMP-2 were also detected in the lung tissue following skeletal muscle

ischemia and reperfusion. ProMMP-2 was detected at baseline level in renal tissue, while MMP-9 was not detected. proMMP-2 was present in the liver at low baseline levels, but no alterations of any MMP wwere detected in the liver following skeletal muscle ischemia and reperfusion. There was no caseinolytic MMP present in the skeletal muscle and liver on zymogram. Howerer, there were two proteolytically active bands observed in renal tissue but no changes in activity occurred following skeletal muscle ischemia and reperfusion. More significantly, a new active caseinolytic species was detected in lung tissues by zymography. It was a low molecular weight MMP (20 kDa), which was up-regulated in the lung immediately after hindlimb ischemia and early reperfusion. It then decreased following reperfusion, with the lowest level at 24 h reperfusion and recovery to baseline levels thereafter.

In the literature, it has been reported that there was an elevation of MMP-9 and / or MMP-2 in the brain, heart, kidney, and lung following ischemia and reperfusion. The elevation of MMP-9 and MMP-2 was suggested to be responsible for the disruption of basement membrane and tissue edema observed in reperfusion injury. In the current study, not only were MMP-9 and MMP-2 up-regulated both in ischemic skeletal muscle and in lung, but also a newly recognised caseinolytic MMP was elevated in lung tissue immediately after skeletal muscle ischemia. The over-production of multiple MMPs in the lung could explain why the lung is the most vulnerable target organ for injury following remote organ ischemia and reperfusion. Moreover, elevation of MMP-9 has been found in the lung tissues of patient with ARDS (301). It has also been determined that the production of MMPs was stimulated by some cytokines such as IL-1 (482).

5.4 Summary of chapter 4

Alterations of FN and LN were investigated in the basement membrane following skeletal muscle I/R injury. Immunohistochemical techniques were used to identify and quantify the

levels of FN and LN in the basement membrane. In addition, the pFN was analysed by ELISA.

There was a rapid depletion of pFN immediately after 4 h bilateral hindlimb ischemia and during early reperfusion. It was then elevated upon 24 h reprfusion, even exceeding the control levels, recovering to baseline levels after 72 h of reperfusion. Moreover, deposition of FN in the basement membrane of skeletal muscle was detected following ischaemia and the deposition of FN continued during reperfusion. In contrast, FN was degraded in the basement membrane of remote organs, lung and kidney. This degradation persisted in the period of reperfusion. Moreover, FN was decreased significantly in the liver after skeletal muscle ischemia and during early reperfusion, then increased markedly with the progression of reperfusion. LN was degraded in the basement membrane of skeletal muscle, as well as in remote organs, kidney and lung. It was then increased in the basement membrane with reperfusion. After administration of doxycycline, degradation of LN was inhibited in the basement membrane of skeletal muscle, lung and kidney. However, the degradation of FN was only inhibited by doxycycline in the basement membrane of lung and kidney.

The observations from this study support the hypothesis that FN has a specific affinity to injured tissues and promotes cell migration and tissue repair, as was mirrored by the depletion of pFN and accumulation of FN in the basement membrane of skeletal muscle. The liver was considered to produce the fibronectin under these conditions. The degradation of FN in the lung and kidney, and degradation of LN in all basement membranes is suggested to be the result of over-production of MMPs. Therefore, inhibition of MMP may be a new therapeutic approach to reduce I/R injury. Doxycycline, a broad–spectrum MMP inhibitor has been found to inhibit the degradation of FN in the lung and kidney and the degradation of LN in all basement membrane.

5.5 Future directions

As in chapter 1, the mechanism of I/R injury is very complicated and remains to be elucidated further. Our studies have found that alterations of MMP-2 and MMP-9 occurred both in the ischemic skeletal muscle and remote organ lung. In addition, another caseinolytic MMP was recognised in the lung tissue. This caseinolytic MMP was defined as low molecular MMP according to the standard molecular weight marker. However, It has not been identified to be which one of MMPs on western blots, because the suitable control MMP candidates such as MMP-7 and MMP-12 were not available in this experiment. Therefore, this newly detected caseinolytic MMP need to be identified on Western blotting in the near future.

MMPs have been emphasised to be involved in the I/R injury, degrading the extracellular matrix, participating the neutrophil extravasation and migration across basement membrane, enhancing tissue edema, shedding the molecules such as ICAM-1 and L-selectin from cell surface. The source of elevated MMPs has been studied in other studies. MMP-9 was suggested to be released by bronchial and type II alveolar epithelial cells and neutrophils that have infiltrated into the tissues, while MMP-2 was constitutively expressed by fibroblasts, endothelial cells, vascular smooth muscle cells and type II alveolar epithelial cells. MMP-7 was produced by type II epithelial cells in the lung. So the cellular source of this new caseinolytic MMP should be investigated in the future study.

In this study, it was found that MMPs play a role in remote organ lung injury after skeletal muscle ischemia and reperfusion. The mechanisms leading to elevation or suppression of MMP levels remains unclear. Elevation of MMP-9 was detected in parallel with the increase in proinflammatory cytokines such as IL-1 and TNF-α, in the lung of patients with ARDS (482). ROS was implicated to stimulate the production of MMPs. Therefore, exploration of the interactions between MMPs and cytokines and modulation of MMP expression by some agents could be the future direction in the area of ischemia and reperfusion injury.

5.6 Conclusions

A rat model for study of I/R injury has been established in Surgical Laboratory at The Queen Elizabeth Hospital, Adelaide University. In the current study, it was found that there was a rapid depletion of pFN immediately following skeletal muscle ischemia and during early period of reperfusion and then increased with reperfusion. This corresponded to the accumulation of FN in the basement membrane of ischemic muscle. Liver was induced to produce FN after depletion of fibronectin in plasma. Observation in this study supports the theory that FN has a specific affinity to ischemic tissue and facilitates tissue repair. The degradation of FN in the basement membrane of lung and kidney was detected after skeletal muscle I/R. Furthermore, the degradation of LN in the basement membrane of ischemic skeletal muscle, remote organ lung and kidney. This degradation of FN and LN was implicated to be the result of elevation of MMPs such as MMP-9 and MMP-2. Doxycycline, a broad-spectrum inhibitor of MMPs was found to be able to diminish the degradation of FN and LN occurred in the basement membrane.

Lung is vulnerable to organ damage following bilateral hindlimb I/R injury. Multiple MMPs have been detected in the lung tissues after skeletal muscle ischemia and reperfusion. MMP-2 and MMP-9 were increased in the lung of rats that have undergone 4 h bilateral hindlimb ischemia before, as well as after reperfusion. Moreover, a new caseinolytic MMP was detected in the normal lung tissue on zymogram. It was decreased in the lung following 4 h anesthesia by inhalation of oxygen, nitrous oxide and halothane and then increased with recovery. However, this caseinolytic MMP was increased significantly in the lung after skeletal muscle ischemia, and then decreased with the progression of reperfusion. This newly recognised caseinolytic MMP was defined as low molecular weight MMP, 20 kDa. Further studies are required to identify this MMP as one of the members of MMP family.

CHAPTER 6

APPENDICES

6.1 Abbreviations

AAA	abdominal aortic aneurysm
ADP	adenosine diphosphate
AMP	adenosine monophosphate
APMA	4-aminophenylmercuric acetate
APS	ammonium persulfate
ARDS	adult respiratory distress syndrome
ATP	adenosine triphosphate
BSA	bovine serum albumin
$CaCl_2$	calcium chloride dihydrate
CFN	Cellular fibronectin
cm	centimetres
DNA	deoxyribonucleic acid
EDTA	ethylenediamine tetraacetic acid
ELISA	enzyme-linked immunosorbent assay
ET	endothelin
FN	fibronectin
H_2O_2	hydrogen peroxide
HSP	heat shock protein
I/R	ischemia/reperfusion
ICAM	intercellular adhesion molecule
IL	interleukin
KDa	kilodaltons
LN	laminin
LTB4	leukotriene B4
M	molar
ml	millilitre

mm	millimetres
mM	millimolar
MMPs	matrix metalloproteinases
MQ H_2O	Milli Q plus H_2O (Ultra pure H_2O)
mRNA	messenger ribonucleic acid
NaCl	sodium chloride
NAD	nicotinamide adenine dinucleotide
NADPH	nicotinamide adenine dinucleotide phosphate
NF-KB	Nuclear factor [kappa]-B
nm	nanometres
NO	nitric oxide
PAF	platelet activating factor
PBS	phosphate buffered saline
PG	prostaglandin
PMN	polymorphonuclear cells
PMSF	phenylmethanesulfonyl fluoride α-toluenesulfonyl fluoride
RNA	ribonucleic acid
ROS	reactive oxygen species
rpm	revolutions per minute
SDS	sodium dodecyl sulfate
SM	skeletal muscle
St dev	standard deviation
TEMED	N, N, N', N'-tetramethylethylenediamine
TIMPs	tissue inhibitors of matrix metalloproteinases
TNF-α	tumor necrosis factor-α
Tris base	tris [hydroxymethyl] aminomethane
Tris HCl	tris [hydroxymethyl] aminomethane hydroxychloride

Tx A_2	thromboxane A_2
VCAM	vascular cell adhesion
W/V	weight per volume
µl	microlitre
µm	micrometre

6.2 Chemicals and Reagents

6.2.1 Sigma Chemical Co Ltd., St Louis MO USA, Supplied the chemicals and reagents.

Ammonium persulfate (APS)

Bovine serum albumin-Fraction V (BSA)

BriJ 35 solution 30% W/V. Brij is a registered trademark of ICI Americas, Incorporated

Casein

Coomassie Brilliant Blue-R

Ethylenediamine tetracetic acid (EDTA)

Gelatin (Type A from porcine skin)

Glycine

MMP control-1 (M2928)

Phenylmethanesulfonyl fluoride a – toluenesufonyl fluoride (PMSF)

N, N, N', N'-tetramethylethylenediamine (TEMED)

Tris [hydroxymethyl] aminomethane (Tris base)

Tris [hydroxymethyl] aminomethane hydroxychloride (Tris HCl)

Sodium dodecyl sulfate (SDS)

Urea

6.2.2 Ajax Chemicals, NSW, Australia supplied the chemicals and reagents.

Calcium chloride dihydrate ($CaCl_2$)

Glacial Acetic acid

Methanol

Sodium chloride (NaCl)

Triton-X 100

6.2.3 Other chemicals and reagents.

Acetone	Anala R MERCK 1td, Kilsyth, Vic, Australia
30% Acrylamide/Bis (37.5:1, 2.6%)	Bio-Rad Laboratories, Hercules, CA, USA
Biotinylated anti-rabbit IgG (H+L)	Vector Laboratories, Inc, Burlingame CA, USA
Bromophenol Blue	May + Baker Ltd, Pakenham, England
Affinity purified anti-fibronectin (Rabbit)	Rockland, Gilbersville, PA, USA
Affinity purified anti-laminin (Rabbit)	Rockland, Gilbersville, PA, USA
Dako fluorescent mounting medium	Dako Corporation, CA, USA

ECL	Amersham Pharmacia, Biotech UK Limited, Buckinghamshire, England
Foetal calf serum	Gibco BRL LIFE technologies
Glycerol	Merck Pty Ltd, Vic Australia
Milli Q Plus H_2O (MQ H_2O)	Millipore, Australia
Nitrocellulose membrane	Hybond ECL-Enhanced Chemiluminescence Amersham Pharmacia, Biotech UK Limited.
PAP Pen	Zymed Laboratories, Inc, San Francisco California, USA
Skim milk powder	Bonlac Food Pty, Melbourne
Tissue Tek OCT	Sakura Finetek, Torrance, CA, USA
Streptavidin-fluorescein (RPN 1232)	Amersham Pharmacia, Biotech UK Limited, Buckinghamshire, England
Tween 20	Bio-Rad Laboratories, Hercules, CA, USA
X-ray film Hyperfilm	Amersham Pharmacia, Biotech UK Limited, Buckinghamshire, England.

6.3 Equipment

Coverslips	Menzel GLASER, Gerhard Menzel, Glasbearbeitungswek, GmbH & Co.KG

Cryostat	Microm HM 505N, Microm Laborgerate GmbH, Walldorf
Doppler machine	Parks Medical Electronics Inc. Oregon, USA
Homogeniser	B.Braun. Melsungen AG
Rectal Probe	Kane-May Ltd, Welwyn Garden City, Herts
Spectrometer	Varian DMS 200, UV Visible Spectrometer

6.4 Raw Data of Quantitative Immunohistochemistry

For all tables in section 6.5, the figures of brightness represent the level of fibronectin (or laminin) detected in the basement membrane by fluorescent immunohistochemistry. IR 0/24 refers to rats in sham-operated group that have undergone 4 hours anaesthesia with 24 hours recovery, no ischemia created. IR 4/0 refers to the group in which rats have undergone 4 hours bilateral hindlimb ischemia, without progressing of reperfusion. . IR 4/4 refers to the group in which rats have undergone 4 hours bilateral hindlimb ischemia followed by 4 hours of reperfusion. IR 4/24 refers to the group in which rats have undergone 4 hours bilateral hindlimb ischemia followed by 24 hours of reperfusion. IR 4/72 refers to the group in which rats have undergone 4 hours bilateral hindlimb ischemia followed by 72 hours of reperfusion. There were five rats in each different group. Twenty-five individual figures were recorded for each tissue, 125 figures in total for each group, except in Table 6.5.5, Table 6.5.7, and Table 6.5.8 in which 30 figures were recorded for each tissue, 150 figures in total.

The mean refers to the arithmetic mean of all 125 figures (or 150 figures in Table 6.5.5, Table 6.5.7, and Table 6.5.8) representing the brightness for fibronectin (or laminin).

SEM refers to standard error mean.

St Dev refers to standard deviation

Table 6.4.1. Data for fibronectin quantitative immunohistochemistry in skeletal muscle

	IR 0/24	IR 4/0	IR 4/4	IR 4/24	IR 4/72
Brightness	2850.45	2306.46	512.43	4709.3	16236.05
	6040.26	3157.34	4389.49	2348.87	2785.88
	2018.58	6131.52	4779.59	800.03	1587.42
	1403.39	3155.68	7565.21	3380.61	9061.54
	1028.06	2898.87	3392.92	1509.86	4858.7
	824.99	6894.56	5368.27	2808.55	1604.82
	729.63	4459.26	1430.85	6014.44	1305.86
	1710.24	14534.43	539.75	722.78	1087.61
	661.22	10349.74	1188.05	3906.49	2014.17
	1915.52	1985.36	2553.02	2035.37	3529.6
	1492.75	2199.25	869.43	3241.95	7785.34
	931.52	1575.64	4549.99	2344.98	5452.09
	118.55	1410.66	2282.07	1699.19	23325.01
	10.85	1364.33	333.35	179.47	12896.83
	180.78	2730.2	1103.01	4286.48	2369.93
	1686.13	1824.43	223.49	4323.72	2547.8
	1790.9	3840.14	256.73	8455.35	3607.28
	700.89	1797.6	293.82	2054.29	18625.05
	668.09	6985.24	4065.16	777.98	850.24
	38.93	16196.68	2362.99	1557.42	1028.72
	1690.09	8843.55	688.74	774.07	261.82
	3362.29	6253.85	1091.43	1238.67	5805.35
	570.93	7353.94	530.85	2338.72	2033.69
	130.84	4096.9	696.67	298.1	3714.35
	2639.42	2439.72	95.81	154.23	3020.09
	868.81	5339.51	81.4	1771.48	1286.66
	465.73	2322.28	125.29	2741.39	4414.82
	319.91	3443.81	1621.08	790.13	1600.87
	1904.81	2903.77	343.72	1085.43	1725.84
	5956.66	1184.8	547.27	253.23	922.8
	3586.77	2450.74	1935.8	1339.52	3412.92
	1052.6	1092.73	2421.26	1571.92	2175.42
	468.63	872.92	1085.29	1429.16	958.8
	572.46	1639.18	466.99	486.65	2451.67
	783.63	631.13	540.73	114.96	1002.58
	77.02	3135.51	436.34	56.26	778.49
	314.08	1211.39	620.09	921.89	207.74
	379.17	1700.01	194.62	1556.53	117.65
	397.42	1265.49	1848.92	6728.81	1432.03
	310.19	1669.39	1805.86	4813.08	2914.11
	116.85	735.45	810.91	3618.79	231.2
	221.82	401.97	390.32	496.33	246.28
	225.96	1418.43	340.43	2223.98	43.04
	2197.74	1679.8	659.6	590.04	332.55
	2085.16	4970.82	948.53	3747.59	206.57
	5013.52	3612.79	1003	3485.53	167.56
	1572.11	10141.36	705.1	886.38	1210.56
	597.88	1799.44	402.24	2412.21	2902.5

	319.7	848.76	471.95	1034.35	1512.3
	184.08	1059.41	321.62	1128.6	1287.08
	958.72	1293.51	8936.85	1749.97	3375.11
	840.18	144.58	2050.21	392.89	4002.18
	674.36	48.54	3181.86	133.71	2474.86
	1019.98	32.25	2757.56	142.59	4517.66
	2114.93	165.98	6222.86	126.26	1098.26
	571.04	0.24	6459.76	169.13	3834.3
	100.6	341.97	3796.43	21.86	3687.88
	139.53	261.58	2778.92	29.6	2341.93
	2821.1	2755.29	1143.34	929.54	1624.18
	379.96	119.97	9156.65	93.04	2884.26
	373.41	10.45	7354.93	614.05	5728.43
	228.53	292.04	1981.95	2130.19	1805.2
	355.55	1265.24	6361.5	2729.11	2116.69
	181.37	90.11	7271.55	4537.04	1547.17
	254.44	42.19	4848.14	203.51	780.06
	154.5	25.87	3232.19	630.13	341.09
	1756.3	413.27	3982.85	1532.84	760.1
	178.17	38.39	2340.43	1976.34	872.55
	15.78	25.98	3730.61	3643.86	459.06
	74.63	272.99	2930.84	3430.23	760.35
	314.85	60.61	2319.21	708.16	6410.58
	127.18	3.95	3499.37	738.07	1809.02
	176.2	785.38	4570.8	175.5	629.38
	370.24	555.74	2750.13	253.31	3029.86
	558.35	576.1	1319.48	71.96	1149.85
	2132.01	3214.6	3631.83	6949.56	10062.6
	2261.31	1871.51	1758.24	1846.95	5290.47
	3384.25	5799.25	2151.67	1108.95	2941.13
	2034.34	5303.53	993.07	1178.68	3974.33
	1535.41	2187.96	856.18	1252.45	3748.08
	344.23	1623.55	2949.73	380.86	1876.43
	1342.67	1872.85	7478.51	1227.02	2811.35
	395.08	1371.45	3205.99	307.26	7695.2
	175.5	3622.04	850.55	1808.8	668.52
	528.64	3332.16	414.72	3302.43	289.53
	631.08	5375.42	2073.97	720.93	502.05
	416.91	4165.11	2863.25	358.73	186.38
	436.61	2771.63	702.48	3790.21	319.48
	818.26	2164.13	2602.08	1077.49	2330.48
	1047.34	4965.42	1681.84	2554.14	394.81
	1341.11	5782.6	270.48	2014.76	2754.04
	624.8	3998.93	830.45	853.76	8333.65
	69.8	8430.56	1310.92	1516.31	1459.61
	148.41	4949.92	3700.88	678.8	4990.41
	266.66	2871.64	356.54	1049.17	2449.16
	628.11	2224.31	1105.26	464.36	1725.05
	285.19	3830.54	1885.33	359.1	2209.31
	390.64	820.54	7643.59	3268.04	4261.01
	475.12	1101.02	4768.98	566.06	394.33
	108.51	1247.41	5547.71	2812.82	1048.62
	180.17	61.36	5216.82	5542.68	7764.51
	68.11	131.08	1708.33	2400.7	3526.32
	486.8	1333.92	2131.36	522.82	1510.81

	146.44	168.75	5214.64	669.32	2323.16
	7584.21	158.32	2144.52	657.13	214.48
	4764.29	240.81	2270.34	1559.46	802.23
	5794.57	174.81	4935.16	3714.2	463.41
	6952.32	499.26	1663.51	115.61	342.03
	3336.48	22.3	276.93	5850.11	757.89
	7227.25	55.31	2695.25	2579.33	3331.2
	2536.33	594.96	1759.68	2312.87	1019.53
	2627.08	289.91	2122.08	6147.13	13261.33
	5664.25	430.84	1065.13	2983.08	9079.99
	305.71	375.8	1222.68	4388.15	8758.3
	2399.23	782.1	10972.01	1286.15	10439.77
	4089.41	492.52	7229.72	1629.98	5787.59
	4924	73.53	83.24	5989.42	6565.72
	3679.34	309.65	849.02	858.67	6292.2
	4079.64	574.68	755.5	9213.24	4954.94
	3487.77	980.96	2945.03	6099.21	9948.63
	7463.19	108.45	3037.31	6345.74	3855.01
	5151.4	475.23	3106.36	3455.8	10254.84
	2776.78	57.91	7684.05	1894.8	25227.59
	4016.78	361.36	2066.47	558.89	3054.58
	2494.05	54.24	2945.03	3045.14	10270.5
Mean	1551.884	2285.157	2512.035	2045.403	3611.999
St Dev	1823.438	2811.821	2290.327	1919.696	4321.377
SEM	163.0932	251.4969	204.8531	171.7028	386.5157

Table 6.4.2. Data for fibronectin quantitative immunohistochemistry in lung tissues

	IR 0/24	IR 4/0	IR 4/4	IR 4/24	IR 4/72
Brightness	16540.44	12553.72	23107.44	35426.4	3955.47
	4888.88	13534.16	16333.22	1817.67	6386.87
	13348.29	7622.56	9653.08	391.28	1805.11
	7353.9	9603.88	12333.25	983.17	272.05
	4973.84	8924.6	8939.3	192.57	84.26
	18660.84	3401.62	6743.48	14792.87	262.39
	17204.23	9358.93	7045.88	23699.98	1446.97
	8570.38	5914.49	3769.86	17804.64	1273.16
	2252.52	8245.93	1769.56	1327.5	1715.06
	47079.35	2560.46	4304.01	1662.28	1152.96
	17196.2	5221	2319.58	1455.53	4458.8
	15560.65	10441.47	603.61	3691.67	11681.68
	9542.13	10175.75	206.9	595.53	4935.5
	19826.5	7875.6	11793.29	631.61	5084.83
	33942.53	17063.6	2300.98	384.25	1725.55
	17035.84	13283.63	1306.21	103.07	3358.57
	1816.84	2843.18	1447.73	8299.49	1892.73
	2393.04	7278.17	9576.37	2874.59	444.88
	437.28	6636.68	1536.88	1080.86	2360.99
	5400.26	8380.89	617.11	3736.01	315.51
	2925.2	1336.01	478.65	5199.68	7976.68
	485.58	1632.33	2559.81	5499.65	4212.45
	17473.64	8925.44	304.03	3480.18	838.09
	14712.2	13600.25	302.4	1263.2	402.98
	3863.66	22993.85	873.69	1114	105.99
	3890.54	2483.61	4551.8	1972.07	2020.2
	1022.99	5187.43	301.46	106.95	751.96
	1387.52	2198.22	60.22	84.74	1149.11
	3043.76	2114.92	37518.59	49.03	5367.22
	2113.58	3858.92	3447.21	50.16	2271.73
	764.37	208.2	7027.9	1046.03	1062.54
	6933.26	2045.27	1352.35	644.45	1812.93
	1145.9	6063.6	4900.38	4510.99	1893.5
	1120.53	327.63	1028.17	955.81	4953.45
	33904.06	1711.2	13601.72	1763.98	2443.1
	6546.76	1533.75	15838.72	862.64	906.02
	15307.58	2442.62	11415.71	306.9	114.39
	9283.97	4068.09	4555	3443.09	1573.53
	12081.52	4918.51	7693.3	521.68	4792.82
	8192.19	853	4820.04	13911.38	1607.6
	3540.81	998.58	4865.02	3636.48	921.07
	3200.54	2663.6	6265.06	184.33	86.61
	85.01	1232.68	2259.4	275.16	1121.01
	100.46	1748.35	4589.11	563.6	1117.45
	152.71	1339.85	4419.54	1967.58	464.22
	2795.99	208	4819.91	443.64	1536.08
	8200.63	144.37	2679.68	691.86	2982.43
	1071.75	70.3	1052.62	682.09	2008.26

	601.67	230.68	13684.55	153.05	2689.6
	6510.82	2687.47	12726.51	552.33	1159.36
	20987.02	7297.17	4433.95	18.21	7367.33
	8510.27	1809.05	723.76	80.98	2213.37
	5318.04	3348.44	393.93	579.21	1302.59
	2127.23	3001.19	3711.91	4692.86	2121.5
	942.92	2336.81	869.71	2695.65	2104.89
	9792.26	2258.24	4639.15	36.89	71.02
	15861.49	1814.81	4011.76	140.96	107.74
	11744.51	2705.6	661.04	616.45	1929.86
	7795.79	2941.82	2991.51	57.04	1013.23
	12893.56	5600.76	1037.55	2539.51	219.14
	10023.23	7505.38	1158.96	993.82	114.04
	8002.43	3061.97	1275.48	4634.82	339.78
	7649.5	4522.85	1303.59	6710.38	1252.64
	11386.36	3847.74	203.27	159.56	250.88
	13955.85	8310.83	240.19	110.37	264.82
	4320.28	5351.74	939.3	48.31	576.53
	10517.41	5134.15	2192.64	1177.47	1973.46
	41339.72	849.26	428.1	320.69	702.53
	26638.54	2407.35	1063.62	21.53	98.88
	11736.72	361.3	1484.77	37.73	42.33
	5236.05	592.15	530.71	88.44	5.92
	2732.11	1122.84	1828.02	32.9	29.76
	6800.86	7542.21	1578.15	43.74	16.83
	11378.49	3469.5	954.51	870.63	10.05
	15329.17	1640.69	161.38	77.73	12.93
	14996.49	1288.83	9050.22	21492.88	2853.62
	32544.18	775.54	3428.96	8373.63	6213.9
	17577.91	3864.07	8622.91	7836.43	3513.49
	22234.02	1371.46	3059.63	2463.57	12272.23
	23213.57	2116.78	7556.7	2500.95	10745.15
	23054.79	1631.59	4683.2	655.81	2171.11
	20682	583.63	4523.92	7798.91	54.88
	15643.82	685.75	12021.63	8469.74	5.94
	19519.46	1529.55	14720.8	2851.34	65.41
	14396	1646.52	16852.28	46.03	105.92
	10820.17	1741.57	3361.94	977.95	114.83
	18203.82	2443	1098.1	2192.34	1043.4
	8537.83	3062.12	1104.23	212.67	369.16
	23030.86	2106.64	2442.06	560.47	1676.31
	36313.4	9751.13	7503.71	1142.97	114.49
	17990.17	2400.94	4941.51	197.94	1008.19
	6878.89	8201.83	6627.51	271.03	355.4
	18238.41	6164.52	3682.09	56.59	1433.24
	30999.06	833.06	4491.03	955.77	795.97
	38354.48	361.3	6036.88	355.52	278.29
	26341.98	260.77	8497.93	423.77	102.83
	25054.39	3933.63	19763.25	91.67	73.54
	24653.9	601.49	28199.24	50.52	42.52
	11936.11	421.58	3272.71	91.8	40.8
	8715.89	579.71	3792.35	77.73	102.04
	10686.81	2789.71	18039.5	423.66	726.88
	13550.07	384.21	7199.7	433.41	291.61
	13108.15	448.06	3511.64	165.1	142.84

	2722.61	186.56	2468.43	1874.01	1712.59
	3405.52	174.35	4920.94	1214.68	110.01
	4826.24	88.38	7525.72	1342.41	18.61
	28749.75	554.69	16068.54	3308.33	13.43
	27092.73	293.6	18394.95	2440.63	84.64
	18748.88	405.85	5815.52	2159.68	15.62
	11972.46	861.67	2347.52	2931.3	6.42
	10448.64	1586.15	37325.83	495.75	14.42
	10189.56	276.62	17184.36	593.95	73.96
	5636.2	168.72	11573.75	2150.17	34.25
	10466	294.74	679.54	1668.43	36.69
	12060.05	569.21	3350.52	2437.89	163.17
	4911.19	1060.89	6312.75	2289.5	1099.27
	4318.31	479.09	9755.7	1747.14	1035.67
	1733.03	5687.56	13227.22	1261.36	1232.08
	6330.25	12030.88	18470.51	1082.72	127.38
	9201.63	6243.09	860.26	252.2	26.53
	2877.61	14671.36	496.79	1662.75	123.77
	4522.02	2708.2	2596.35	852.72	225.17
	5443.33	835.07	2362.73	4565.46	102.85
	8726.64	3159.9	6025.35	582.67	599.97
	4793.64	7657.84	10414.7	420.33	21.43
Mean	11727.65	3852.434	6086.247	2497.423	1541.518
St Dev	9715.963	4098.362	6861.315	4892.061	2280.74
SEM	869.0221	366.5687	613.6946	437.5592	203.9956

Table 6.4.3. Data for fibronectin quantitative immunohistochemistry in kidney

	IR 0/24	IR 4/0	IR 4/4	IR 4/24	IR 4/72
Brightness	12857.42	2520.23	124.39	4930.81	836.01
	7806.94	1021.47	335.5	4354.31	515.05
	16654.15	1558.24	749.91	2068.04	3673.76
	8073.43	816.16	430.06	2910.5	1396.55
	4458.24	11176.27	331.52	1730.57	4529.33
	4211.58	5702.89	1645.69	6966.78	1576.23
	3898.1	4556.66	4489.6	2832.32	662.24
	1133.9	4556.66	103.42	4138.65	641.63
	3517.11	13220.4	711.58	6885.99	6400.77
	2332.73	5875.37	365.42	7391.82	3642.03
	1710.38	2647.93	422.26	1178.67	3714.46
	6870.62	2322.92	6100.07	4734.6	3705.1
	7646.59	1772.76	2634.59	2168.03	4699.68
	4612.58	3424.73	623.52	341.47	2609.6
	1400.92	331.93	2206.61	6276.24	1595.66
	2188.76	1816.89	1296.85	2374.12	1442.37
	4686.74	3550.47	4391.2	2779.1	3233.16
	6435.05	5071.24	1840.2	6600.05	1956.47
	9246.01	5652.44	596.71	6972.88	2455.59
	6317.33	5557.23	297.66	4092.14	1156.32
	3858.07	2280.34	715.93	5141.61	3991.87
	915.55	2747.24	759.03	2629.38	6091.86
	1191.92	3569.48	739.12	6770.78	1280.61
	4092.43	1704.07	2172.28	3294.11	626.16
	1454.38	2843.36	2902.86	3930.21	1338.52
	4843.16	2682.64	4786.11	506.36	1850.91
	916.5	2770.69	3321.46	1200.13	1026.6
	7310.96	4837.52	1341.61	1786.72	620.69
	4567.18	1362.6	2840.36	1557.21	749.93
	1821.14	4476.01	1053.98	1792.75	772.2
	8999.31	2941.42	1083.92	4366.54	182.68
	294.11	3877.88	1382.61	521.25	559.61
	3017.09	2010.51	3647.35	1994.51	519.03
	543.5	2317.22	2282.46	3625.25	715.59
	1258.16	1975.33	1248.64	4288.17	467.89
	10335.79	3577.16	1672.29	6425.5	144.38
	3219.09	3671.04	5405.83	8173.11	124.87
	2427.13	4276.28	2800.89	2573.26	2055.76
	8782.2	3316.84	6782.53	4368.72	423.78
	14610.36	1390.65	9077	1038.36	866.32
	17467.31	2402.71	8865.71	1076.24	1224.07
	14955.97	1417.78	6757.56	263.71	285.05
	3589.12	1843.97	13368.7	980.08	219.08
	5377.35	2175.77	6822.66	1067.88	439.18
	7006.88	2265.04	6358.83	1086.13	629.66
	4925.62	2104.22	6366.02	2018.69	485
	1757.33	1595.84	8068.7	2730.13	275.36
	4271.15	2460.75	10350.63	1164.56	71.44

	7245.48	2011.46	8161.55	458.82	532.04
	4222.73	1285.75	4234.72	1303.15	541.6
	15255.92	7969.84	3126.5	1951.61	3539.4
	6876.91	5776.34	1141.06	1048.47	4087.59
	5628.54	2473.44	5513.53	872.12	3608.78
	6944.17	4921.1	5771.57	1282.67	3093.85
	4817.9	4741.43	5018.92	2210.88	1775.84
	3080.94	8876.86	2913.81	1553.72	1367.71
	3874.56	8169.47	6336.91	1197.72	572.24
	1678.52	5997.03	6281.18	639.68	527.53
	1315.97	6532.97	4301.46	734.81	2623.37
	883.59	5220.48	4143.82	755.13	2496.32
	1634.59	12612.03	3082.53	6702	3632.96
	2322.01	10420.43	2741.72	8065.12	3341.16
	555.7	9864.25	4273.2	8844.29	3291.75
	577.36	10457.83	2941.45	7471	639.34
	228.32	8133.24	2666.19	5996.13	2071.4
	1603.03	9331.31	1160.24	4758.86	727.3
	1143.01	9714.61	501.34	13748.42	571.13
	799.39	7338.87	1850.4	18555.75	1546.63
	1814.63	6548.53	2125.34	10684.09	377.02
	1055.58	5713.95	1654.34	6618.17	215.63
	845.26	1463.93	1402.27	1070.82	185.14
	3554.43	1308.26	1069.37	394.5	961.41
	2204.98	1097.67	2502.13	358.88	60.46
	618.82	1027.48	5785.03	320.07	1640.04
	1335.59	2761.67	5591.21	2009.1	1210.54
	1727.66	1808.84	2880.47	2707.61	7601.4
	1326.38	1642.26	1568.42	1116.61	2306.67
	4159.74	1289.28	1021.98	487.36	6958.96
	2263.63	2820.9	1454.28	1424.73	4604.66
	6839.62	470.93	2045.85	4154.43	2667.25
	3404.54	314.04	3032.36	1980.96	4230.17
	6961.11	2384.52	1015.31	2669.99	3377.54
	3157.55	4955.64	1170.44	472.98	1516.06
	2312.23	7959.68	1115.8	3668.66	2112.55
	867.76	8325.82	1127.7	6046.66	2744.43
	1197.95	6053.23	1137.56	2443.21	1449.73
	13222.55	7458.73	2498.98	5134.83	1438.16
	11879.79	4456.23	2876.99	2573.26	1324.62
	10261.68	5529.72	1671.34	2386.9	445.73
	5325.4	4375.88	3710.3	3986.5	1379.87
	8969.27	3923.6	2141.1	3986.5	1980.41
	6339.05	3167.76	2859.3	3559.51	2471.91
	3796.4	4768.7	3351.88	1772.7	2331.59
	10524.54	2884.31	3503.05	2331.69	1908.25
	3790.3	4531.4	2466.31	1289.97	190.2
	10096.5	7360.87	5680.72	665.51	320.16
	5288.8	5588.02	4652.56	2555.98	1086.53
	5124.41	4403.38	1880.45	1874.14	701.65
	3675.57	3206.24	728.54	1158.94	2683.11
	3472.27	2179.7	482.38	1533.94	871.42
	8381.13	1125.22	1872.35	565.72	867.64
	6765.31	5111.75	3195.2	399.01	409.13
	4333.35	4426.85	1398.75	321.78	552.02

	6786.78	4318.24	3278.57	356.86	655.19
	5500.28	7123.06	2021.55	105.03	107.37
	4434.21	1473.32	4940.02	981.02	135.77
	2367.01	1065.15	3885.66	845.91	293.56
	4803.56	1357.71	4087.99	836.58	434.91
	11662.66	3228.87	3752.39	902.79	136.38
	3781.33	2812.15	4771.34	3042.05	430.11
	2151.87	4117.35	9062.38	1575.82	393.82
	2464.28	7318.96	9581.27	3177.32	120.66
	2613.37	6271.89	7388.62	1809.87	691.92
	1220.93	6628.64	6271.81	1916.29	1082.12
	1198.99	3842.75	1440.48	1752.97	387.43
	7916.67	4695.39	1553.13	1735.77	436.28
	1674.55	3593.39	603.71	710.93	184.98
	1486.53	2919.68	234.76	3674.33	677.08
	1568.3	3282.85	496.41	3583.91	825.38
	2098.6	1792.13	469.72	2708.4	106.59
	2917.29	1226.83	173.83	3615.32	422.41
	1112.52	885.07	4864.58	1486.36	741.77
	523.79	842.73	5407.43	1078.24	896.91
	1287.79	1129.83	7345.74	1697.76	456.51
	1784.32	2401.27	3643.42	2659.94	634.63
Mean	4550.443	4037.346	3174.23	2969.824	1556.015
St Dev	3778.949	2729.25	2573.277	2792.486	1540.088
SEM	337.9994	244.1115	230.1609	249.7675	137.7497

Table 6.4.4. Data for fibronectin quantitative immunohistochemistry in liver

	IR 0/24	IR 4/0	IR 4/4	IR 4/24	IR 4/72
Brightness	981.45	238.57	105.33	510.79	339.63
	508.22	89.55	0	106.82	238.02
	853.99	1512.78	27.19	57.93	885.28
	208.11	709.57	0.24	8.82	68.9
	96.62	490.99	12.66	74.97	96.39
	108.83	376.68	18.94	215.7	603.32
	0	219.81	33.38	673.86	1149.71
	1.19	23.32	12.56	83.05	190.11
	27.77	830.25	0.49	1897.87	139.69
	26.95	1544.64	7.52	87.07	112.5
	70.79	86.91	22.37	1321.78	21.49
	589.55	14.53	54.93	1046.85	61.82
	181.64	23.64	5.37	475.88	391.08
	470.51	13.06	121.65	376.99	206.35
	66.3	26.14	59.12	4.44	792.14
	114.92	11.04	44.04	33.56	1133.34
	630.3	0	483.01	367.65	718.75
	549.98	0.99	127.87	922.47	670.67
	921.27	26.47	36.56	93.61	1279.54
	237.93	1414.46	164.29	78.87	1765.1
	154.2	1065.97	88.36	87.37	256.91
	216.29	131.62	1.3	1780.25	1191.04
	71.16	6.32	0	44.75	200.52
	137.86	0	0	66.56	32.23
	283.01	47.88	58.17	69.42	45.62
	248.65	18.82	356.26	0	435.83
	188.38	16.1	19.63	359.21	1112.69
	904.72	40.71	26.97	1.9	1223.56
	426.51	110.69	56.63	0	286.44
	349.68	142.89	16.6	11.4	373.7
	1541.09	633.26	3.85	12494.91	413.48
	142.98	64.05	1.43	78.22	122.22
	1328.56	419.81	27.85	2.29	572.73
	1622.17	106.74	20.63	515.4	12425.17
	841.41	29.49	201.73	1.53	21004.98
	5156.17	205.51	107.08	0.97	16560.42
	1775.74	192.8	182.14	1.71	12040.43
	1337.11	27.76	0	114.66	2158.74
	1607.28	116.34	0.47	35.01	3691.19
	1636.89	15	0	13.15	1923.77
	1178.3	11.04	0	8.49	488.96
	476.23	55.48	0.71	1.68	1467.56
	348.34	46.06	0	0	728.21
	112.18	24.4	105.84	0	1461.38
	816.2	76.54	44.44	1.69	412.31
	53.27	293.81	88.09	0.49	682.78
	847.39	576.66	14.17	2.42	627.41
	823.08	207.02	27.83	0.5	298.86

	252.29	3.5	56.62	23.3	50.69
	546.57	110.93	103.57	2.68	120.58
	1790.76	221.08	487.94	69.34	2787.66
	449.98	501.02	34.81	14.77	1798.87
	1230.64	55.53	50.08	2.49	5708.24
	1183.76	1112.04	24.28	109.23	2212.22
	1153.31	709.55	18.14	12.8	752.84
	2214.69	172.63	96.47	39.03	1575.33
	396.27	39.55	12.11	12.72	6939.85
	674.97	38	47.63	25.68	5058.21
	1132.04	101.69	210.98	1.25	8809.05
	1578.95	112.69	551.77	0	6116.37
	1631.6	14.25	109.06	0	11935.4
	311.75	368.8	91.43	1081.03	8545.65
	941.5	5.72	79.69	48.83	15807.22
	423.54	314.99	2812.5	5.04	1722.42
	695.37	219.49	1836.08	142.41	1433.01
	271.61	247.02	232.2	14.78	2368.56
	261.92	340.8	86.23	2.41	1239.1
	79.49	327.94	105.9	10.14	334.68
	307.38	188.39	119.38	167.04	1823.16
	811.43	23.9	113.69	312.12	1861.5
	517.99	52.18	1.74	8.14	582.94
	302.68	13.14	0	91.4	1009.43
	1047.86	62.44	0	28.04	949.08
	357.26	544.51	1.99	43.4	760.7
	147.04	19.99	9.58	36.31	893.58
	734.12	48.72	0.47	1300.03	347.06
	786.21	54.79	270.78	779.5	228.51
	359.11	44.76	56.46	6965.22	445.24
	608.5	1.98	1.71	1248.55	481.88
	2897.46	9.3	26.62	1374.41	452.53
	1915.12	158.98	41.92	1818.18	366.36
	1504.71	71.94	600.31	492.74	643.08
	1077.56	0	610.15	3219.25	136.62
	527.93	9.39	17.24	4030.55	751.53
	764.45	80.88	96.38	299.4	1715.26
	494.91	36.93	7.92	962.96	893.69
	3650.66	168.85	187.17	1699.09	1721.47
	1303.43	6.2	17.03	5895.94	887.7
	560.7	90.1	180.98	2208.09	843.79
	695.37	2.14	345.74	1907.92	582.09
	28.82	3.34	61.13	1642.69	507.44
	19.05	0	185.14	4338.4	1564.47
	123.57	4.83	68.69	33.81	2265.53
	40	22.08	322.36	5.93	1353.83
	5.38	0.47	621.38	11.28	659.43
	177.81	7.06	422.03	27.81	556.52
	68.65	39.06	13.78	164.82	377.02
	110.63	0	152.41	28.68	118.48
	305.92	0	155.61	31.56	76.61
	216.99	0.94	5.96	684.77	873.14
	908.25	24.48	192.22	491.48	2874.12
	626.08	8.72	117.15	7942.15	6813.33
	979.88	0	9	1629.17	885.33

	457.9	34.93	140.3	1076.01	469.05
	324.52	0	17.43	2559.67	726.66
	1830.17	0	62.49	7997.82	474.09
	193.19	0.5	676.17	9791.63	367.33
	383.31	0.24	64.86	10603.76	1691.33
	6.87	0	19.59	3617.72	678.44
	0	0	7.79	439.34	172.4
	11.01	11.58	217.04	129.06	126.67
	7.35	0.47	26.17	733.38	2000.44
	0.47	151.37	19.58	146.79	546.42
	89.85	32.9	89.36	329.54	1185.39
	1849.15	16.79	1.71	1897.94	67.96
	1167.16	22.18	70.66	2500.29	2220.97
	2062.86	313.57	278.67	1917.06	1496.59
	428.95	117.63	3220.69	1364.32	2901.88
	67.22	13.92	1600.63	591.42	295.08
	9.43	17.39	1531.84	2137.65	1398.06
	156.24	18.72	693.73	2558.55	3077.09
	2100.15	0	679.37	5146.39	1430.29
	1503.06	22.07	444.41	931.89	698.14
	153.89	0	22.15	4147.79	393.22
	445.39	4.16	170.07	315.18	1821.92
Mean	693.7858	159.4584	199.3922	1108.839	1919.686
St Dev	773.37	295.0202	462.4266	2201.648	3416.061
SEM	69.17232	26.38741	41.36069	196.9213	305.5418

Table 6.4. 5. Data for Laminin quantitative immunohistochemistry in skeletal muscle

	IR 0/24	IR 4/0	IR 4/4	IR 4/24	IR 4/72
Brightness	25756.15	31009.02	33444.27	37288.34	17845.23
	32347.71	42015.34	21257.15	25089.01	7904.09
	35700.5	24421.6	22297.62	70834.59	17375.94
	27126.42	22018.83	24753.49	45960.71	12101.9
	32576.73	21934.85	21093.11	27016.94	40893.48
	26262.3	20058.64	18751.56	12179.22	18299.64
	23908.37	21686.57	7294.37	39135.99	43353.74
	27451.02	26203.48	12457.37	66008.29	17215.18
	20941.65	37823.21	9785.73	38932.83	17351.04
	28163.44	30747.04	13166.84	29244.95	21004.15
	28533.67	22182.45	10283.35	32972.62	41534.54
	26713.17	18643.35	9091.35	49810.67	25728.41
	23960.8	16596.3	11239.3	46766.2	15742.99
	32866.32	11423.95	29351.84	26355.44	16904.7
	20606.21	22465.09	18555.31	50110.95	39677.47
	23068.33	18581.67	14178.61	31787.07	51860.78
	27399.46	21203.35	17251.82	71595.86	37003.93
	28082.89	26770.68	13779.37	42779.39	51161.88
	20710.41	32164.7	16628.53	80918.47	36161
	27940.49	26188.21	21055.75	68349.88	30369.9
	16333.03	19823.86	17079.17	43094.66	29530.77
	18078.61	21477.65	14221.14	19929.03	23523.94
	14634.28	16530.76	18007.9	16334.36	28717.56
	30959.24	20588.39	25127.1	27296.16	15313.66
	17966.27	16872.48	12185.47	7547.9	17816.28
	39782.3	20536.66	11610.68	80319.67	16821.11
	16546.41	35187.92	11645.17	35957.61	18617.68
	25015.73	24084.32	24526.38	63739.28	36582.39
	24660.01	31404.41	15059.82	33861.39	23488.69
	17412.13	23169.09	18974.18	42977.54	27251.04
	22283.59	23169.09	36271.65	25590.87	34102.67
	25989.18	19482.76	25295.67	48507.39	31062.8
	17377.31	16706.89	23635.39	27314.11	30464.73
	36709.31	12594.22	17640.53	34508.61	25577.24
	22455.67	12794.58	20245.59	16080.26	27796.48
	24186.97	9792.83	33484.42	11357.88	31083.23
	22415.25	11972.46	28951.99	28051.96	22998.16
	20769.97	13720.03	32750.97	26891.07	19659.06
	25254.25	10989.94	16536.28	23751.44	41711.9
	18156.63	10172.18	33441.84	14165.79	16657.12
	21461.78	17117.19	24834.29	27172.17	12715.67
	20673.18	21536.75	28073.93	32181.56	8415.82
	10191.91	18085.02	8407.05	20488.96	23738.07
	23871.61	16736.2	31517.67	41249.41	32250.9
	14815.07	13589.8	15406.64	29643.98	46154.73
	22691.99	17848.02	10272.19	31295.92	48675.61
	20753.36	16198.36	9221.91	61859.95	35731.28
	26725.67	16588.67	8850.7	28433.65	26905.02

	23511.22	17883.7	10275.81	13739.69	29897.01
	19414.59	9448.38	17550.94	9933.13	27784.4
	33685.72	13496.77	18460.1	15747.55	34950.83
	15030.79	13605.33	10789.18	19929.03	33230.46
	19950	19823.86	19410.6	36835.9	28463.74
	17013.36	9975.76	17552.27	29582.16	21194.79
	17219.92	8266.69	15815.77	21715.92	21913.34
	28369.91	11360.03	19071.5	17337.73	22742.73
	18709.4	6080.76	23888.11	19488.16	29368.76
	18000.6	8702.1	16507.79	12174.66	10738.86
	21394.68	10327.69	14056.24	15205.72	24575.78
	20683.74	7718.73	46596.81	13765.09	27316.22
	42611.08	7919.61	39052.84	984.69	53237.47
	27322.59	10629.34	30569.44	24340.85	33628.61
	30859.28	27331.15	36267.51	24772.92	25645.05
	33458.35	15688.75	49309.86	9916.27	22546.31
	33420.51	26238.57	35787.44	20769.3	25759.38
	41828.83	11425.53	56489.23	18086.79	23975.29
	34123.44	13460.63	39780.56	23311.85	27298.84
	43981.09	20356.11	48638.97	45461.83	15768.17
	23737.61	10543.29	14629.95	39309.32	30581.12
	40416.68	18666.43	20705.68	40135.54	26162.13
	24185.4	7875.46	23962.33	32516.26	33941.14
	25048.77	9179.14	31625.71	43069.72	24118.72
	33273.37	14818.13	31517.67	50668.4	34660.27
	37934.24	4529.63	29852.19	56014.32	25953.86
	38656.18	15577.99	29181.07	41537.05	65857.79
	18844.04	15913.09	52368.03	28472.02	35918.01
	10224.46	10696.21	28894.24	28938.16	22452.5
	18523.12	12988.2	34525.75	31038.21	25273.54
	19559.46	19238.94	26865.5	33389.31	19864.83
	22417.7	18666.43	34933.72	14975.41	21300.18
	16956.87	22663.73	40917.95	30986.61	13973.9
	17596.3	18666.43	38710.01	22431.78	17472.71
	14113.59	22663.73	38710.01	33614.91	15731.07
	17138.98	16378.29	49541.12	28816.35	11993.41
	15925.14	17318.21	41680.01	9839.2	61484.44
	13941.65	13634.03	27293.96	20935.36	32611.04
	23662.43	10693.1	23822.19	34300.51	15467.69
	25169.74	18556.87	34042.05	22824.96	27783.96
	31371.4	15516.28	29430.4	34247.55	33727.19
	29479.07	29557.97	19192.61	16731.28	25652.57
	23247.72	18733.1	23610.82	13229.36	13871.72
	21289.27	20509.48	24206.93	12559.47	6146.08
	13510.66	22928.08	27078.75	12822.55	23036.93
	10140.59	25582.17	14923.9	19861.07	29509.87
	26589.55	37894.04	11967.8	12507.13	34148.71
	22538.49	33134.55	16417.46	15635.67	11456.05
	16093.36	20446.76	11776.06	17243.64	14683.6
	8375.11	23777.16	10571.03	20597.61	22520.49
	13640.97	34174.63	17628.94	20619.08	9268.56
	14096.17	35885.54	14677.38	11726.33	52624.24
	17113.05	38152.78	19985.07	21960.89	31317.04
	19184.6	36009.48	27397.42	17677	17140
	11708.76	40010.28	38353.77	8837.74	20883.73

	32920.42	33947.33	24568.94	13867.03	25339.5
	13370.2	30915.12	10822.67	12573.59	15085.84
	18167.68	37776	8873.81	8480.15	9129.43
	20261.32	35434.1	4467.46	13542.4	12552.97
	13846.53	37127.92	7405.34	11144.35	33094.07
	14650.85	31439.61	4656.25	11071.83	40723.82
	19118.75	38726.56	17729.96	4551.44	25928.29
	14304.96	26402	19624.44	22600.76	47344.62
	20945.74	34342.17	11984.97	14701.78	57049.23
	12482.49	35287.9	30899.48	16846.2	31143.81
	12098.29	29425.05	19678.18	3847.86	12954.77
	5454.46	44268.35	23355.83	12737.41	22564.09
	25060.02	36882.69	18960.66	23155.3	21437.05
	22038.03	34551.91	18251.74	10304.47	21808.47
	18418.74	32521.15	12399.41	15632.37	8272.34
	19418.01	29653.96	44091.89	15358.96	31000.05
	31637.53	22534.84	26294.23	18719.25	25198.94
	17369.87	34062.91	16096.04	82764.77	30564.83
	21154.73	9197.69	8509.27	57511.96	22530.44
	18635.38	14581.55	6652.12	28793.83	34680.9
	15452.64	17907.01	23143.1	14607.05	23741.78
	23757.51	9714.32	7939.19	20023.19	23835.39
	20540.7	11693.65	10893.8	27058.78	24886.88
	18740.7	6681.72	5269.72	17129.58	19507.44
	21008.62	13811.1	7137.58	39779.4	33933.21
	11651.78	20137.65	7594.3	43156.61	32976.5
	16400.68	28722.48	10878.32	21666.02	32271.66
	14078.83	30961.92	7851.14	73191.66	31917.52
	9605.17	24893.69	8912.66	75997.95	35812.55
	16155.06	13367.15	9991.38	33818.22	37689.76
	10943.88	13610.25	15685.56	48083.68	40928.83
	13221.46	8429.62	18909.09	64137.99	32688.88
	16423	2743.39	18322.66	21304.74	28028.63
	12602.83	34308.29	13084.29	18235.37	29213.26
	14277.13	11241.87	9914.62	18145.73	19257.8
	11434.17	4628.65	5702.36	12614.28	39745.82
	9222.29	5081.71	10736.21	5396.08	34123.82
	8758.8	12625.9	26221.92	18352.62	34536.12
	6459.98	6724.4	21588.59	16443	33938.8
	4501.35	9284.23	25025.64	10149	32929.18
	2913.82	16915.95	22081.11	14260.64	28518.92
	6760.95	15892.85	25639.84	18688.78	38902.8
	13237.17	5027.8	29437.4	14532.12	30715.02
	8747.12	13699.31	30638.25	22438.35	33111.35
	12526.8	3930.16	26939.3	26065.1	26840.25
	8507.44	24707.68	10359.72	10994.38	25728.41
	31637.53	11187.84	10742.46	15829.26	15742.99
Mean	21103.35	20074.92	21345.49	28041.43	27409.37
St Dev	8308.033	9633.065	11025.67	17433.1	10922.24
SEM	678.348	786.5365	900.2425	1423.407	891.797

Table 6.4.6. Data for laminin quantitative immunohistochemistry in lungs

	IR 0/24	IR 4/0	IR 4/4	IR 4/24	IR 4/72
Brightness	9354	119.39	2.87	402.69	74.03
	268.09	152.09	0	9.72	236.74
	1657.02	86.59	1.48	83.35	16
	2507.32	511.65	14.93	4.11	25.73
	973.71	15.8	57.75	35.39	4.83
	87.18	34.15	0.72	0.96	35.22
	295.94	14.89	0	481.92	249.43
	163.93	624.19	1385.26	284.94	164.8
	440.14	146.61	133.03	1096.76	174.41
	2834.52	190.14	26.84	1388.35	167.77
	498.65	2.96	3.06	86.72	313.37
	155.79	0	13.18	1746.54	341.87
	111.69	0	0	360.84	472.52
	9.95	0.47	0	272.87	161.45
	773.83	122.39	9.08	146.25	132.02
	82.41	52.61	10.76	16.7	118.82
	415.69	48.33	100.23	24.97	90.66
	1296.6	3.59	57.73	156.94	7.96
	1366	6.09	893.5	59.86	119.41
	830.51	308.59	631.13	17.47	0
	21.35	479.89	100.68	38.18	37.69
	1689.28	146.81	284	258.32	13.4
	2722.7	221.95	609.87	240.99	1.34
	1507.01	124.77	8.23	322.59	4.83
	6303.46	0	1.49	205.41	40.48
	258.1	692.72	268.7	489.09	576.57
	21.44	652.25	77.76	180.98	188.44
	7.76	383.68	97.12	47.74	2.48
	11.87	537.22	182.06	50.07	1.69
	0	112.21	3.03	8.95	1.46
	15.66	37.44	47.9	9.4	0
	14.45	273.97	0.99	0	0
	0	3970.23	99.42	8.6	0
	4.83	141.35	22.99	11.42	0
	4.38	186.23	94.04	0	28.88
	12.3	24.2	128.66	3.28	538.29
	390.86	287.23	228.42	0	620.04
	10.25	193.39	68.34	0	138.51
	9.13	232.27	43.47	40.46	242.34
	1364.12	560.96	394.09	41.37	468.73
	176.53	467	568.41	2.21	21.54
	480.94	391.84	122.83	31.69	81.07
	484.7	475.98	180.81	52.3	0
	215.12	452.99	95.18	79.65	0.72
	11.44	443.05	75.37	0.24	682.15
	669.28	721.38	24.9	17.18	815.64
	677.18	1447.77	0.72	17.87	142.07
	0.24	1179.54	49.66	206.13	8.31

	0.24	659.9	6.68	363.37	91.47
	1.95	582.48	1816.28	1.71	21.23
	1191.92	279.71	568.41	3716.99	0
	1405.12	411.8	836.78	120.12	4.99
	1175.46	174.42	99.65	1403.84	1.04
	17.26	219.37	17.9	142.69	47.93
	71.14	129.18	28.81	1	10.15
	93.15	108.81	1061.12	0	0.71
	16.33	42.68	3245.11	1.11	0.24
	1952.11	37.73	1087.18	317.36	0.47
	73.52	26.47	579.35	737.82	6.81
	8.6	20.73	3291.95	168.13	95.07
	212.85	16.7	1588.35	495.73	0
	0.24	66.09	184.99	28.65	32.33
	945.94	304.18	346.49	322.3	7.51
	2.64	60.71	378.96	127.39	61.32
	16.79	17.94	36.41	2431.11	948.6
	421.82	45.25	756.55	4261.09	59.34
	676.65	60.87	318.27	3267.79	73.03
	408.07	93.49	43.12	6961.7	23.2
	1360.75	78.49	116.23	4591.25	41.19
	2.68	349.95	299.09	2365.99	1.24
	281.62	95.28	2951.33	42.9	18.86
	10.13	8.33	1326.58	0	0
	1.73	3.67	49.22	13.31	2.7
	0	2.22	12.49	5.57	2.03
	15.71	32.5	2.54	86.66	2.76
	572.07	4.45	399.12	1280.57	119.26
	236.79	1	2168.64	885.78	9.35
	32.93	0	4488.57	1094.18	0
	71.14	75.19	3447.56	571.73	1.96
	7.71	235.29	6661.36	543.56	24.09
	1308.84	76.05	1574.19	0	79.61
	364.41	186.11	3219.66	42.8	437.78
	28.29	34.47	192.11	991.78	0
	5.12	14.81	337.75	1037.15	226.64
	6.5	7.58	21.9	739.95	277.92
	4.42	5.37	307.37	644.31	366.04
	8.02	0.97	85.63	682.78	251.77
	4.61	0	1015.85	785.49	102.92
	2.64	0	105.99	103.86	37.99
	62.82	3.88	495.89	295.29	1968.46
	119.3	4.48	2841.89	12.71	141.66
	102.35	0	80.56	33.08	0.72
	171.57	1.71	64.03	7.39	576.93
	99.04	78.26	599.72	0	1185.5
	221.8	124.76	943.87	4.35	93.08
	131.48	9.08	2083.76	4.62	65.45
	85.46	111.97	37.06	0.5	184.98
	10.17	10.01	42.26	4.7	303.22
	6.79	52.57	733.39	6.36	54.38
	80.71	3.78	59.46	16.72	39.14
	213.15	302.65	1307.77	43.43	0.24
	360.97	1214.54	216.9	181.48	37.79
	34.81	55.71	14.01	269.64	0

	3.54	103.29	6.51	82.84	0
	89.52	107.11	3.17	663.82	3.15
	39.87	220.16	3.58	14.29	11.56
	2.82	447.12	0	85.64	2.76
	94.34	0	0	0	7.77
	36.76	673.41	4.32	0.72	16.91
	11.46	159.98	12.65	14.16	2.4
	20.87	713.24	64.11	427.53	104.6
	99.25	385.3	132.87	248.34	272.57
	14.66	320.8	224.18	43.48	0
	307.09	116.32	365.17	909.2	0
	90.51	28.13	323.96	529.2	7.81
	15.47	346.01	219.97	15.23	0
	1156	64.49	287.58	0	0
	245.74	151.68	720.43	0	0
	121.69	142.46	206.79	10.63	0
	339.1	234.07	132.39	478.49	0.47
	723.96	124.67	53.46	0.24	3.12
	469.16	458.35	262.91	102.31	49.12
	1129.4	36.68	200.07	140.84	0
	767.35	0	71.62	501.49	3.9
	120.2	0.94	6.53	62.3	10.05
Mean	494.5955	229.2536	520.9526	445.0561	129.608
St Dev	1120.024	425.3415	1006.612	985.9809	261.6027
SEM	100.178	38.0437	90.03407	88.18881	23.39846

Table 6.4.7. Data for laminin quantitative immunohistochemistry in kidney

	IR 0/24	IR 4/0	IR 4/4	IR 4/24	IR 4/72
Brightness	61273.97	56342.9	38680.79	42351.27	46175.08
	45346.53	52427.05	29169.14	31634.22	61518.03
	48879.17	43736.96	38897.03	46053.71	39808.43
	51421.93	37935.03	47569.4	41838.61	28337.82
	71268.29	29808.52	18755.59	35490.71	34633.85
	56251.77	26358.32	21370.92	24112.09	36095.71
	77728.01	31813.71	23465.2	32671.26	31326.25
	64122.41	28785.78	28890.6	29851.37	33674.26
	66549.17	16115.34	26943.28	29688.08	39917.49
	57660.27	24104.32	31135.5	35027.19	46928.13
	45412.38	39444.96	32491.39	27150.06	48515.2
	53926.48	36203.35	46406.87	24010.42	36961.32
	61339.77	25039.16	23509.14	42277.78	30086.26
	64261.1	25877.31	49958.88	31759.46	22717.1
	65341.14	30619.72	32323.45	37283.2	14684.88
	64754.81	23162.22	34328.88	40339.96	24483.23
	55152.34	32797.5	55205.05	28899.02	24049.3
	46369.49	30703.19	23736.46	34044.57	39576.64
	38605.42	16513.6	17698.67	17967.97	40669.09
	30519.22	20767.95	11312.66	19222.97	34924.25
	31883.98	26564.93	35549.18	24993.26	53243.58
	27817.78	28534.03	43025.72	55119.6	45213.29
	54219.02	22123.3	20372.42	44131.58	47005.12
	51045.99	18130.82	23431.59	44065.4	47964.6
	52556.03	40760.29	35910.12	33964.78	49644.09
	49048.52	23026.7	46172.7	26152.62	52562.63
	63775.27	26669.8	50597.48	36335.39	33804.02
	50310.05	43336.63	37343.75	33967.42	55089.35
	42579.97	17584.77	45553.78	51023.1	38845.4
	39555.3	23564.31	37891.97	43024.22	25383.67
	47596.23	27199.8	10700.38	69717.01	65486.31
	28891.18	39133	3493.69	45431.52	54626.24
	38677.22	31809.09	4247.53	46053.71	40785.1
	30722.01	21194.85	4332.76	41838.61	52083.63
	48813.57	37342.32	5010.02	43588.19	51102.63
	41853.29	20742.66	5420.41	35138.89	51088.11
	40609.19	21389.65	4848.18	41188.16	67319.67
	50483.57	18420.47	4177.71	34958.54	72466.55
	53214.77	12234.35	1530.9	33816.39	74037.86
	43319.71	17852.95	33059.88	41442.57	53403.32
	47014.5	23946.72	18658.13	43553.51	46928.19
	47536.54	24594.82	16020.24	63842.75	33227.05
	26200.46	15579.7	1822.63	67941.3	41355.7
	21490.75	17687.14	3142.62	63058.07	15220.98
	42789.25	23383.18	4763.82	70230.49	55051.14
	48786.29	42245.47	5863.79	56664.46	52686.88
	40654.64	40055.08	3244.72	49122.72	24029.58
	39474.69	27236.11	8888.03	45718.49	14410.64

	38327.93	32626.45	13674.62	61197.65	12975.97
	31765.62	21443.85	11347.27	42483.13	35418.7
	32741.81	16648.92	13688.34	38629.46	19424.48
	31830.79	14271.81	23024.3	34696.4	28794.1
	42174.64	14640.6	9900.23	28523.69	23202.13
	30038.85	21239.08	3759.29	27302.99	23202.13
	38457.73	24938.84	8940.55	33964.78	26116.87
	43945.12	30279.66	1752.64	26152.62	32075.85
	45622.92	48311.64	10407.19	35775.27	26866.77
	44054.03	34912.85	5267.03	41889.62	37941.89
	28100.47	53230.71	5091.08	28480.98	36875.2
	37584.41	44375.15	2081.79	37239.38	46921.76
	41318.91	65134.09	15055.23	70139.8	68211.21
	48247.68	35378.67	12266.54	38329.55	45169.74
	37480.17	47939.33	4202.3	32159.51	35868.28
	32172.94	34364.99	6861.38	36177.76	38486.39
	61132.62	26736.44	18768.03	21945.42	37004.98
	42558.11	42545.81	22068.75	21082.75	29714.63
	62463.28	45247.4	24616.89	13670.65	37354.79
	67201.74	45247.4	11133.44	44695.78	18529.02
	41576.04	62675.99	23751.47	30741.42	48645.04
	49597.96	42707.03	19667.99	45825.76	32399.92
	34222.97	41232.56	9507	42049.72	31299.07
	33059.48	44899.62	19031.42	32524.6	17936.58
	39716.05	44681.38	9287.14	60772.61	10915.56
	55404.81	32588.48	7628.19	63146.55	17224.27
	40612.82	38373.63	7196.59	36977.25	22045.76
	46028.11	31898.86	20285.38	40115.72	52686.88
	45732.27	34785.78	10011.51	38629.47	34408.39
	45549.18	51505.1	8940.82	36074.92	41530.62
	45985.05	47257.09	22337.08	26521.34	35458.59
	35826.69	40447.37	5571.99	33853.84	27241
	51023.42	48451.36	4972.81	21324.99	22169.53
	35915.31	31858.37	2063.5	23400.14	39981.81
	50658.04	26503.36	2321.37	24407.47	39420.13
	57053.96	41596.31	2327.27	52796.71	35581.49
	49885.78	31297.16	13434.3	51636.15	26516.37
	48275.92	51453.42	9085.61	36890.79	35414.41
	39195.08	55313.14	1852.39	42816.65	33819.64
	48442.18	44959.88	13155.6	44561.7	32428.65
	41206.5	30942.04	3493.1	20555.34	26654.76
	43899.99	42620.16	478.83	30423.17	25282.84
	47224.82	51099.5	22183.92	61138.55	71689.53
	42173.14	56419.01	14346.42	46696.37	57300.35
	37633.72	50173.59	13087.62	59262.99	47372.5
	48248.28	49741.04	8736.78	43700.17	46682.93
	55763.61	46862.96	14979.91	31613.5	45016.78
	48278.94	43320.01	10406.96	49027	52754.44
	35837.28	45754.11	12523.61	55267.83	61884.56
	41143.89	44278.16	1972.69	50476.85	56388.63
	46081.19	39251.23	4747.91	28715.26	45928.07
	28088.35	31432.46	5111.43	61389.76	49887.54
	59288.71	42685.36	1715.38	57193.55	43645.48
	71606.23	39511.93	40116.47	49116.42	43827.52
	52431.54	31382	38154.01	24386.5	45955.24

	54371.57	39018.27	36061.4	63146.55	48472.32
	27922.83	42877.11	19675.43	28659.27	32808
	33829.85	42452.69	24536.06	25156.8	38803.06
	26635.84	46484.07	37051.12	29995.24	14534.1
	44494.02	47010.55	37476.49	35930.05	17867.32
	52251.99	47257.09	31192.89	52859.17	12424.56
	49740.83	26257.36	33180.75	64707.81	73438.71
	56999.35	47119.83	17658.31	55151.81	48427.5
	36252.79	37697.3	25367.13	61638.84	30285.21
	22661.37	21480.57	19465.26	63465.42	34391.88
	7138.06	39101.27	21721.48	60948.67	42423.96
	34813.91	35008.49	11684.67	61886.23	36489.7
	37469.06	36314.79	38806.67	42560.99	59125.45
	35826.69	25061.71	31807.07	63620.55	35792.35
	44365.49	29444.04	35868.15	79005.73	38538.87
	43880.29	30269.15	23344.65	50658.14	46361.59
	50907.54	28086.71	21626.7	43267.91	1443.17
	48897.81	46827.05	26290.88	77235.14	986.48
	42555.03	27854.12	18248.06	74322.63	10097.29
	48316.42	60005.01	17489.93	61339.99	3892.12
	32286.94	29031.99	9803.11	49332.39	45016.78
	48436.64	39392.04	22074.15	46553.39	2901.85
	33645.19	50566.13	18563.73	55056.72	4075.08
	25430.56	59533.57	19117.7	65526.57	26449.56
	37549.77	44973.17	15985.49	72694.75	11105.25
	26017.7	39600.1	12315.28	81926.39	6408.16
	46186.06	39731.16	16710.33	69389.97	19019.2
	31367.06	79010.11	14644.05	52569.3	30280.73
	50695.39	68711.91	15432.59	49612.47	22680.04
	32799.89	46288.75	15597.76	58460.12	7356.74
	50171.6	66038.76	12970.37	60263.28	5981.88
	46139.1	44819.75	10230.64	78553.24	14683.68
	41216.75	41584.24	7394.47	76784.14	10605.1
	38884.83	70271.23	12062.51	102523.5	26559.03
	34444.5	54274.77	5581.94	75832.43	18244.46
	34042.57	56232.84	9909.29	57530.65	5390.75
	46122.59	57858.53	14752.78	49808	3220.72
	41563.79	47032.78	12122.35	47549.28	17299.39
	33565.43	52407.33	5147.62	46758.33	24834.41
	34727.16	56419.13	34541.26	45591.8	7392.08
	33859.95	25198.54	42783.14	35835.17	31581.29
	27024.84	74603.26	40072.8	30875.33	18538.1
	27849.33	70515.89	34104.48	34791.67	22443.33
	31661.49	43464	27770.48	56154.47	9557.63
	33605.83	42245.6	25316.95	36993.07	21358
	30948.33	61970.38	19344.04	31591.17	14795.54
	22172.93	32886.94	18112.1	26778.36	32808
Mean	43524.92	38004.42	18642.19	44648.12	34225.92
St Dev	11470.15	13717.23	13077.39	15854.69	16637.26
SEM	936.5339	1120.008	1067.764	1294.53	1358.427

Table 6.4.8. Data for fibronectin quantitative immunohistochemistry in skeletal muscle with doxycycline treatment

	IR 0/24	IR 4/24	Doxy L.D	Doxy H.D
Brightness	22462.63	18594.25	25315.03	11966.03
	11577.26	10789.83	4560.92	703.66
	13297.47	8968.23	31639.81	465.47
	5931.53	889.6	19005.69	688.09
	3190.03	142.33	7044.6	722.03
	25587.1	14333.42	41186.87	2193.38
	26699.48	29545.89	15886.47	574.92
	11470.42	1067.12	8715.36	2153.76
	1412.52	516.1	7806.7	1044
	13103.77	11497.87	10372.38	344.13
	8337.19	9668.6	3993.31	4428.39
	5293.6	5952.16	13274.51	4154.88
	10296.42	2482.03	3445.72	3961.4
	4413.2	7106.35	529.74	6082.13
	4004.66	1121.76	404.6	63.21
	1768	7806.35	90.89	393.53
	7928.39	2069.64	855.08	390.1
	1541.47	248.02	1642.82	1418.64
	1933.74	650.19	2109.73	51.14
	1224.05	18787.52	9764.87	1789.69
	4129.9	24730.25	6926.61	1007.2
	2172.59	9435.67	20288.66	333.36
	1406.02	9933.69	9501.81	109.53
	1337.94	44336.1	4535.11	405.36
	2390.93	5564	6376.44	573.4
	603.41	10113.66	61.38	673.24
	10760.72	3497.95	134.9	155.05
	8844.69	9222.71	135.27	622.95
	4734.36	25083.91	31639.81	1139.44
	778.53	8591.15	25629.22	1007.2
	5465.53	10682.6	22874.29	12300.03
	9294.46	8700.03	21014.58	700.5
	944.44	889.6	22311.51	11891.57
	4163.22	14445.3	13471.49	1752.09
	15367.71	3829.51	7401.17	2798.38
	256.6	7780.01	46102.26	20161.51
	27868.38	6362.82	12282.51	22714.94
	2107.88	6848.84	11974.31	6678.16
	5761.09	6791.98	8933.35	9525.69
	962.93	7736.12	9744.29	6278.73
	6320.77	5952.16	89063.31	7805.84
	15934.01	1061.61	2674.47	9721.71
	2591.88	7106.35	2604.61	4887.75
	1669.25	4160.73	62863.56	6308.01
	15356.3	4391.74	55485.38	3436.54
	1849.95	8478.4	41450.64	7556.59
	10168.96	4131.55	30993.94	21347.79
	10513.41	4375.96	59873.98	2275.72

	10211.84	14938.6	59585.54	4227.94
	1261.72	64383.56	27210.66	1672.56
	4152.27	43699.56	15308.78	498.04
	4043.14	60435.27	16961.51	1698.1
	4985.81	24989.23	27169.55	864.03
	5434.23	44336.1	7238.1	1775.56
	5966.35	25773.16	4064.16	912.25
	10117.76	43859.22	8279.82	277.64
	4282.23	7510.83	21503.55	269.97
	24110.12	3885.59	2424.1	1026.76
	8031.34	13535.13	13386.85	185.2
	2311.63	49406.88	3999.12	1033.92
	7248.89	20042.69	2180.62	13191.55
	1831.23	6026.47	2970.22	3515.75
	2973.69	31091.43	1771.7	3345.82
	1315.38	30282.24	4844.88	2895.28
	1211.44	41235.18	1491.26	17864.52
	686.53	6112.75	3239.94	12951.01
	243.7	15285.03	3206.36	17688.39
	3115.59	22027.96	1622.35	28095.34
	10365.7	14269.98	7629.96	18966.47
	3115.59	19807.38	1721.3	11235.54
	10268.12	7694.91	2496.06	2822.93
	9375.19	14604.68	3996.01	1755.27
	10937.06	20759.4	2127.12	1085.53
	6468.49	2658.94	530.84	830.93
	3614.74	17760.64	1978.07	11970.38
	1697.99	13282.68	841.8	3813.04
	6325.85	13456.29	2622.48	42703.4
	5922.54	9758.81	2302.79	42838.67
	8809.71	14676.97	430.07	18567.56
	2116.13	9037.18	159.46	9009.7
	8213.48	6931.36	171.11	2298.27
	10030.17	3726.34	434.5	4914.84
	5220.79	4638.31	7238.1	2179.85
	2483.74	4273.6	4417.51	2571.44
	1102.01	34014.07	6057.89	1361.22
	714.7	13155.96	5565.48	2545.4
	13157.95	6263.67	4923.5	153.46
	6168.66	64228.8	1536.25	1638.38
	6600.19	35221.48	434.5	251.23
	11444.07	6272.48	3092.31	4028.26
	7722.03	5843.49	1726.21	11227.09
	2678.34	21250.35	1080.37	6198.38
	1374.23	34485.88	7577.57	12530.01
	3571.14	39061.23	4193.55	2508.04
	1149.85	36300.54	5634.55	23788.06
	789.32	28860.53	1828.55	48056.55
	807.54	16396.59	34155.75	13772.88
	1049.83	14664.03	32252.63	17797.96
	15648.82	5233.49	11981.38	79408.06
	2359.23	5470.15	11974.97	20487.06
	7004.66	1995.37	1712.76	36906.99
	7543.73	2235.01	2625.68	33932.53
	3327.18	9480.33	306.47	24612.46

	6425.68	3366.55	2573.83	24055.56
	910.35	19218.28	3933.05	33179.45
	176.39	36037.91	12408.87	26795.05
	2384.66	15570.74	25118.98	21716.7
	237.43	7468.45	24395.88	31460.72
	30.08	4384.39	21630.02	32519.19
	2088.43	18586.47	6931.66	11436.23
	1463.23	11899.28	11560.19	12928.74
	2244.89	10807.79	2940.87	21816.64
	6221.41	1875.54	13547.23	18745.05
	89.9	621.67	3103.4	13042.48
	94.11	7775.69	5117.29	21902.52
	12992.69	9202.77	4085.69	14852.88
	12090.85	4065.68	6625.5	18337.74
	3253.86	5822.47	8490.39	8547.62
	2004.82	23084.53	9024.15	9631.46
	18268.89	62125.18	31869.91	13772.88
	11071.63	23356.24	39432.19	12831.1
	8650.02	22917.02	7103.44	52145.87
	7189.55	16329.36	4306.01	30942.68
	3510.92	6775.63	21939.79	34850.39
	6754.86	2385.16	16423.18	22517.7
	2373.2	3465.59	5448.5	13568.93
	3547.71	2034.42	11859.09	8475.6
	2644.62	4333.91	12442.93	8494.61
	3688.54	2953.75	8627.52	16286.42
	1108.76	11031.49	17288.92	17688.79
	1484.3	7544.71	16511.26	13477.08
	2174.24	3657.04	4213.45	7704.34
	1486.67	829.76	3623.63	9760.72
	1477.9	313.76	40575.98	13142.17
	1405.43	2680	17519.62	6500.83
	1495.43	933.76	7433.38	13271.5
	3949.54	745.44	12757.64	7121.14
	2489.39	6700.82	15466.69	7678.01
	1846.21	11795.15	5540.3	15907.23
	2053.97	1798.56	908.12	7311.64
	2018.26	1957.9	7381.06	11717.96
	3072.53	1571.77	8684.58	22175.07
	1959.01	3121.78	1702.38	7127.54
	696.39	6747.02	1827.97	2394.53
	2514.09	671.48	1886.79	721.79
	219.89	1016.08	1502.42	2106.92
	1615.86	7466.43	2749.16	2882.12
	4262.62	1798.56	19280.78	6119.98
	1153.43	1798.56	12602.73	20706.81
	3949.54	4333.91	5448.5	7704.34
Mean	5471.898	12987.19	11773.7	10523.93
St Dev	5512.496	13863.9	14410.06	12267.62
SEM	450.0934	1131.983	1176.576	1001.647

Table 6.4.9. Data for fibronectin quantitative immunohistochemistry in the lung with doxycycline treatment

	IR 0/24	IR 4/24	Doxy L.D	Doxy H.D
Brightness	7263.31	2620.75	15010.82	8526.53
	6979.41	2703.4	25194.63	10526.37
	1620.36	385.91	15550.9	5156.62
	23825.1	523.26	7310.07	8135.81
	9521.01	1009.91	9531.71	1841.91
	9474.81	711.61	6603.97	3395.6
	26374.78	376.36	10385.13	2259.35
	15916.22	316.52	10852.31	10854.11
	10666.79	2457.68	3839.33	984.66
	3767.34	767.98	7489.92	1100.43
	6800.68	257.74	1709.6	974.69
	5299.58	105.45	2177.96	473.96
	15791.14	1426.23	1646.33	482.5
	20809.92	1921.14	1261.1	264.6
	24162.09	4724.4	1838.59	505.41
	8014.5	1440.59	1624.04	2194.32
	2185.7	344.86	3441.07	1440.79
	9862.64	1830.94	849.7	1349.44
	2299.25	1682.78	8224.45	3970.74
	6362.59	150.41	9985.64	885.29
	3815.08	571.62	4573.7	5297.49
	18398.57	799.12	4027.26	4332.62
	818.74	756.42	3163.31	2840.76
	1570.05	252.9	5097.31	560.67
	5048.51	633.45	1592.68	154.68
	3379	851.16	19675.9	3383.9
	2781.56	493.99	19664.66	1139.81
	5025.09	1146.38	18890.24	743.19
	9875.27	1192.25	17264.02	552.97
	1485.9	251.88	19686.48	201.24
	1375.22	95.6	22398.05	1139.59
	3030.67	47.27	7348.72	2385.08
	1089.07	70.71	13186.2	2841.31
	316.8	299.82	15478.9	3234.66
	4557.59	2292.38	14394.11	3329.62
	2619.1	1567.46	5866.79	6204.49
	824.57	1359.95	2147.19	2341.84
	1039.34	151.17	15264.75	474.16
	8715.55	20.03	7757.05	2564.76
	959.68	381.32	2768.46	1614.04
	4301.11	219.11	3412.46	4296.44
	2899.75	982.79	3371.62	3093.49
	3006.75	34.73	1948.02	4444.3
	752.15	162.94	724.58	2092.74
	417.22	339.36	4295.03	256.37
	303.75	883.73	6670.82	1764.34
	4427.73	1567.92	10525.43	329.5
	7842.58	115.6	3561.69	6391.24

	3463.12	51.75	2943.18	855.98
	1301.7	2384.3	3529.12	380.09
	1798.34	2916.82	9737.26	14126.92
	7148	1320.07	9872.22	3157.28
	2005.75	847.15	20817.57	24508.53
	575.57	198.83	6673.23	11664.99
	3576.28	732.26	3918.05	9032.45
	4831.65	2762.45	18190.91	20159.62
	4338.13	1511.44	11285.09	22143.21
	5292.91	1946.16	8855.96	9970.79
	5108.83	5064.72	6033.18	2060.28
	7958.68	3349.87	6496.81	2626.62
	14017.8	2200.38	4973.44	2439.11
	2219.47	1308.26	1342.9	453.8
	5737.36	2505.39	413.85	1358.51
	1700.8	4038.34	700.5	390.49
	3749.1	1543.99	282.13	1754.13
	2608.12	307.75	1328.89	1224.99
	2286.52	1177.02	1929.07	3605.23
	3818.36	1151.83	305.78	4635.86
	1404.69	9945.97	754.76	1322.6
	7773.09	2704.7	2245.58	3543.87
	209.12	2152.01	8010.28	933.03
	372.58	275.91	916.76	2543.71
	241.72	217.5	85.27	2304.46
	170.01	70.93	77.57	447.07
	621.78	187.9	149.49	9926.67
	9988.13	7703.95	16531.6	717.42
	4514.81	3851.77	5182.33	1435.01
	12404.14	10954.47	14049.43	145.62
	3736.18	16362.34	24687.05	2216.83
	4790.77	3568.88	1769.53	2551.53
	2856.94	725.82	2233.54	1218.28
	4360.65	468.9	838.66	2308.1
	9424.22	6351.69	716.21	5622.61
	4431.94	1454.94	6986.98	11474.35
	3936.36	1101.46	2189	3508.63
	3502.8	116.1	8579.58	1163.69
	983.84	898.93	2578.49	558.84
	1548.34	11.31	3883.17	831.81
	2087.26	207.7	215	4398.83
	1137.22	264.46	3848.33	15644.94
	1701.53	252.55	2512.58	9981.24
	1586.39	76.99	2061.92	9448.94
	2691.02	257.86	1287.1	7151.02
	1482.53	445.14	389.99	6092
	2208.47	828.67	929.27	1022.7
	317.37	506.2	668.5	321.15
	6864.86	929.26	401.94	390.46
	9612.07	209.73	287.43	291.36
	1918.7	159.17	745.43	1875.88
	7507.04	170.4	382.97	1834.45
	11861.16	619.63	532.39	14293.11
	2690.65	88.45	870.86	11544.3
	12895.25	107.97	288.18	9108.84

	9530.15	80.95	123.62	5594.66
	7137.75	297.33	52.6	7997.02
	2077.49	209.01	46.47	5617.17
	4370.28	930.42	501.35	7194.84
	1504.31	416.02	97.81	4791.41
	5798.15	1414.91	443.34	1301.55
	19350.4	246.88	1451.91	1935.03
	5724.56	729.27	1937.13	5822.93
	4356.5	490.55	1230.57	7099.86
	3417.2	593.73	1186.97	6045.02
	1146.23	597.26	2684.98	8868.46
	4314.37	107.89	3305.99	3623.55
	6799.48	500.03	5809.75	5516.69
	2279.66	297.67	11394.5	9323.1
	614.45	140.66	33.22	6288.12
	1107.88	301.09	1778	690.8
	400.1	239.53	1778	2937.71
	792.29	58.4	5809.75	8148.4
	2949.92	27.43	3305.99	2003.42
	476.07	116.51	1186.97	832.73
	1573.26	215.21	2684.98	2102.69
	5941.19	213.96	3305.99	825.64
Mean	5093.643	1304.737	5495.591	4180.892
St Dev	5207.725	2214.163	6099.841	4537.585
SEM	465.7931	198.0408	545.5864	405.854

Table 6.4.10. Data for fibronectin quantitative immunohistochemistry in kidney with docycline treatment

	IR 0/24	IR 4/24	Doxy L.D	Doxy H.D
Brightness	2012.91	10316.48	6596.63	9659.19
	1858.32	9900.02	7698.8	2899.16
	6826.85	8227.54	5594.99	6591.96
	5332.52	9734.69	6781.73	7553.89
	2634	6554.52	4321.53	28303.03
	13080.7	16906.08	9016.05	19668.74
	15910.4	7197.42	12374.42	21094.53
	12458.54	10896.89	8827.31	11796.06
	6208.58	10636.22	10632.02	12188.09
	1893.11	5857.95	8641.98	19925.43
	5004.49	14512.64	7118.62	8609.16
	5776.74	6064.77	6436.06	15238.1
	16712.34	16958.24	8576.99	11963.33
	15024.68	5781.03	5886.1	14769.6
	9010.65	5521.79	6856.02	21085.58
	5932.69	8002.28	8612.2	8603.75
	6228.08	6348.41	8885.73	11641.07
	3297.75	13274.01	10893.24	8749.45
	1218.16	8987.71	16378.05	10827.89
	4036.74	7342.85	15622.99	4390.21
	903.23	5857.49	16774.9	3178.33
	1312.28	20580.14	13853.9	7464.7
	1594.03	18412.01	10001.82	6751.04
	6891.43	13640.48	4891.56	9458.67
	3066.22	13302.47	12998.01	1708.75
	5423.52	11621.9	10305.24	1632.62
	6861.94	11315.38	9865.3	2491.87
	5296.75	1136.01	18149	2076.97
	6575.93	10479.25	14421.17	6669.29
	6293.48	6153.5	37646.65	2417.63
	8565.21	3939.85	3620.85	11996.76
	8637.47	4578.05	9673.45	6502.41
	4496.36	3183.61	3553.38	9199.83
	4461.63	5011.54	4066.15	4570.86
	14365.77	4608.68	13324.53	10254.46
	13430.85	4197.06	19613.06	5583.11
	12427.82	2405.36	10826.52	13963.55
	9888.77	11059.55	9109.32	17400.04
	12628.29	8037.17	3430.02	9708.25
	4469.91	826.46	8189.57	5911.94
	3284.83	2400.96	11107.12	7384.64
	4197.65	7854.02	7952.07	7871.07
	8111.58	2286.32	7389.5	8389.9
	5827.33	1514.38	2489.09	1569.44
	7303.75	2242.12	7585.21	2498.21
	7130.02	1256.76	2127.65	3369.65
	5585.39	1251.67	3199.35	2504.87
	6891.41	1814.75	5158.85	2638.7

	7532.81	1599.62	2623.83	1912.86
	10712.48	1151.42	2070.96	4390.28
	9977.8	1402.53	5532.06	3328.76
	8994.2	3221.91	6413.76	3263.18
	10047.13	4089.69	4411.48	1381.51
	13125.84	1721.65	2994.38	1786.11
	18912.79	5181.47	3541.8	9061.67
	11587.53	2860.8	2874.74	3362.57
	11111.88	2644.41	4111.6	1380.08
	8815.85	15912.03	3694.78	956.9
	9063.81	13825.05	4931.11	3284.18
	5111.05	1307.52	3246.59	1510.43
	3875.69	1344.77	7377.15	1936.32
	4542.26	2132.92	3740.52	3591.36
	6295.1	1039.05	8777.86	1746.88
	8995.18	2946.08	7343.93	9708.25
	3902.4	2691.74	4649.15	1426.58
	2492.44	8396.89	4020.65	738.7
	7889.71	7064.67	1370.64	1627.89
	4835.57	4521.6	602.85	5994.35
	3434.17	5620.64	2303.54	1388.26
	3390.12	4804.76	3177.29	4597.08
	2439.74	11356.64	3044.68	1306.66
	1422.56	10668.7	3275.39	750.67
	3158.32	683.01	4307.18	284.62
	4820.39	125.16	1158.74	950.8
	8815.85	656.86	3244.11	1296.79
	2828.25	4071.02	1394.04	4651.13
	5453.36	4741.27	2370.66	2602.46
	2888.61	7325.12	3585.59	3787.5
	3845.88	4735.98	4244.23	3121.43
	1545.86	6337.69	3222.51	2405.86
	7234.73	5437.92	3086.66	249.17
	5737.85	12181.88	6472.03	272.37
	3489.91	5865.22	5282.08	244.85
	4372	7972.85	5754.11	14772.82
	8692.55	4588.39	2314.65	14213.56
	8957.31	5033.48	5036.73	24223.91
	2593.79	2756.96	5214.73	23537.75
	2391.53	7022.03	4440.06	22720.02
	1745.04	4361.15	4944.36	17645.8
	1873.54	4109.28	8786.99	8384.81
	7519.54	2539.49	6919.12	4268.21
	10260.83	4085.87	4300.34	1305.31
	13178.64	4343.43	1563.96	1905.78
	430.73	11921.65	3387.09	4849.85
	540.95	831.84	3837.02	2338.68
	7269.84	844.72	4592.05	899.19
	10121.46	2641.83	3262.31	3668.08
	13806.16	3797.38	3099.87	3503.38
	5228.15	4257.11	4122.27	1116.34
	7800.74	524.29	4769.7	1981.97
	4792.72	3559.52	12215.82	4443.59
	2560.24	6554.13	7476.27	3336.96
	6062.38	4068.48	5510.65	7040.27

	10357.76	2660.9	9647.61	15215.88
	1966.85	2782.75	7382.6	18086.72
	2470.75	6908.22	6033.08	3206.1
	1989.82	8630.72	5755.37	8830.42
	1520.73	11239.89	1797.53	5054.55
	6016.28	4763.57	3669.64	6226.61
	5140.65	8604.87	1457.57	7920.05
	8249.7	6155.87	2379.7	7892.33
	6817.58	3126.68	16646.76	6751.66
	15439.55	7625.43	12634.95	6035.85
	8365.11	10961.23	10206.66	6654
	10172.39	8547.3	6551.87	4361.47
	6698.21	10018.56	5325.64	5457.32
	4392.97	2985.16	4171.01	7808.1
	6873.12	2268.74	4044.39	9637.29
	7107.12	2895.68	2540.53	3693.21
	6278.89	3483.87	4961.05	5965.73
	3516.05	3016.62	2822.41	4697.4
	1972.54	4685.5	733.82	4215.85
	6249.64	4625.61	1940.96	3706.81
	1826.18	3307.6	1820.11	1435.56
	1593.5	2816.95	4502.5	1861.9
Mean	6399.374	5980.654	6481.177	6655.163
St Dev	3918.957	4249.361	4866.546	5928.708
SEM	350.5222	380.0744	435.2771	530.2798

Table 6.4.11. Data for fibronectin quantitative immunohistochemistry in liver with doxycycline treatment

	IR 0/24	IR 4/24	Doxy.L.D	Doxy.H.D
Brightness	13489.45	9538.32	44616.58	36698.73
	13744.56	11470.99	46801.87	33214.6
	8343.67	13166.63	31889.17	30861.88
	12677.53	28555.02	35364.97	29847.08
	13929.66	23695.23	33024.9	33457.35
	8756.25	22955.49	35423.59	34813.85
	13305.64	9876.83	38927.69	32210.16
	11632.16	11406.55	31015.7	32498.49
	8172.68	14479.19	23409.53	31481.98
	11739.81	12836.29	26033.12	31080.67
	8447.57	22015	43938.36	41648.36
	12815.73	31061.33	38857.75	29644.47
	13686.91	22855.7	34819.39	33285.15
	6664.93	15234.56	33894.92	29144.13
	14027.03	17957.76	29126.57	44102.07
	9368.23	15359.62	19726.27	43681.01
	6307.58	14008.74	26904.06	23979.46
	13279.67	17411.09	24037.23	33186.52
	13325.12	17186.88	27273.15	30613.81
	11083.55	19235.51	20016.69	24795.42
	11482.25	19073.58	20104.09	27864.27
	16957.99	9264.88	36926.56	18683.73
	11404.24	10340.39	30091.87	27806.25
	12771.7	8792.25	19035.82	33830.54
	16860.27	10715.57	15515.88	21956.98
	17825.78	20632.25	23305.09	12507.85
	10723.27	23954.72	23623.47	25496.95
	10323.09	14373.97	15043.72	37470.07
	8125.48	14217	15778.21	51194.03
	10332.41	10605.44	13637.01	57761.36
	5991.37	10904.8	13105.8	49564.4
	4677.63	8092.85	27816.71	48435.49
	3844.34	13520.42	32444.26	29437.13
	4400.82	6861.89	19744.52	35304.58
	6562.5	10175.3	27345.47	33824.42
	5290.03	15086.51	23480.67	21566.91
	9177.26	18402.23	22827.6	31730.96
	15587.1	17317.94	17856.53	32244.87
	9590.06	14170.73	22394.25	28901.65
	10788.35	14983.6	30913.82	42310.79
	10613.25	8585.42	15319.73	33103.45
	8569.12	9058.93	20746.7	23439.94
	11392.56	10995.78	31963.92	45285.87
	8622.03	14174.53	32603.35	44503.91
	4200.34	15744.74	15156.23	50249.68
	13510.52	17092.98	16456.76	38850.4
	14819.58	11197.42	9112.63	26816.06
	8406.91	9865.32	28035.08	26176.75

	4060	14311.94	26076.19	21545.68
	18134.38	7365.69	22395.22	28303.13
	27687.47	19485.62	11899.92	43277.13
	27721.44	12369.86	10124.39	37016.46
	16866.25	21111.76	15688.65	37235.64
	23647.67	27412.35	15236.4	36122
	22656.02	23498.11	16533.54	37963.87
	23164.87	12802.49	23519.09	36282.34
	15906.23	14001.92	13470.5	26251.27
	18623.53	12632.74	21076.98	43212.22
	15562.97	14976.01	20020.31	36568.32
	12990.12	11113.3	15188.09	35047.36
	8524.74	16505.39	31958.24	42238.09
	11131.9	19400.9	25552.23	46058.35
	10604.28	20247.42	25307.46	35387.15
	18644.73	13179.14	31156.44	45395.16
	13648.48	8811.13	23866.84	30934.56
	10756.16	10969.51	18740.31	41712.86
	20051.99	9829.95	21126.54	44777.46
	22249.94	8543.81	16682.56	35561.38
	20572.75	10056.34	15747.62	33194.72
	21771.33	16003.84	17303.91	31679.15
	21973.69	11177.28	16557.12	25217.99
	15027.12	6240.13	9681.76	30321.68
	24316.13	10294.85	14144.28	27768.52
	20044.58	4569.02	29110.43	26205.34
	19157.83	8453.95	33329.38	23051.49
	9026.03	20876.24	12476.93	46573.07
	10933.51	18677.02	24319.55	60819.07
	14473.1	25788.78	24401.23	50347.78
	10667.66	18619.7	17961.02	46669.99
	18596.82	26547.18	26642.76	43292.11
	22631.96	29384.02	28589.64	36023.44
	10603.86	29875.09	26145.28	34272.71
	20676.41	25575.16	19701.29	29007.14
	22433.66	35397.41	21017.29	29604.21
	15568.43	29465.17	21553.1	33543.68
	4366.99	36201.83	22250.46	37564.1
	7302.38	37194.84	30254.94	48323.07
	8627.77	29885.19	56769.84	42422.65
	3937.68	32973.76	20088.4	45041.52
	7905.13	20371	26732.32	37071.45
	14879.96	21116.72	25639.09	33797.52
	12844.04	27953.01	24827.55	39108.76
	16567.23	32707.19	13308.8	48895.73
	26129.44	33445.69	21521.31	49005.47
	27248.79	25329.83	25357.27	48247.81
	15830.99	27075.85	29260.1	43867.37
	4780.16	23074.62	32636.11	42856.08
	9470.83	29803.7	29182.79	51224
	19956.36	20481.65	25678.43	49788.09
	21788.57	33978.53	19463.81	36639.01
	13882.5	4894.69	13689.16	38221.53
	7898.93	14857.77	28276.13	29194.67
	17330.37	20320.94	22101.44	28788.16

	7724.39	21838.39	12416.15	28235.71
	16001.34	17031.37	7615.23	21638.37
	13397.87	9265.77	43898.14	32257.47
	7767.54	8745.68	40874.31	36996.98
	10046.99	19200.23	32536.84	25797.74
	8372.82	21653.1	22908.42	47681.49
	10784.51	12052.11	34553.45	34655.83
	6141.38	26435.49	28423.07	39011.78
	16134.66	9598.3	25059.06	7773.77
	20554.74	10677.18	32824.75	22789.5
	15681.87	12125.25	26877.75	20562.68
	21555.32	11939.44	29034.04	20104.7
	19982.22	3350.32	32692.34	20168.15
	20557.53	5493.05	41718.55	14168.82
	18109.97	5643.54	31401.28	18615.71
	13879.74	6436.59	27428.21	17233.56
	20514.56	10228.3	30676.13	10211.21
	12708.86	7515.29	22930.73	11693.23
	9225.57	11739.51	26097.51	10849.28
	9042.11	16153.57	8702.83	6949.88
	16515.03	7058.13	29100.66	17274
	12576.12	11675.63	30548.69	10107.31
Mean	13574.23	16652.81	24921.17	33519.05
St DEV	5740.801	7902.249	8737.464	10801.74
SEM	513.4728	706.7987	781.5026	966.1371

Table 6.4.12. Data for laminin quantitative immunohistochemistry in skeletal muscle with doxycycline treatment

	IR 0/24	IR 4/24	Doxy.L.D	Doxy.H.D
Brightness	5584.83	6765.91	7980.89	4009.61
	10245.95	5129.36	10473.99	8458.43
	10602.66	9585.54	6806.66	6792.57
	28038.78	10595.44	7399.18	1910.9
	15290.98	4109.02	20960.69	12501.16
	14152.52	6164.74	9382.97	7435.92
	17374.06	5793.76	16987.46	7314.65
	12629.36	14061.97	12655	2602.27
	12441.93	11052.54	6723.51	3138.97
	8811.05	4698.43	17047.96	4118.87
	14981.45	6617.33	13781.07	5188.32
	20891.65	9761.38	24576.74	5435.06
	15880.95	11018.37	20937.83	4842.87
	23192.54	13485.71	13085.61	5127.7
	14043.82	23005.24	10876.36	6345.44
	13747	14239.18	14988.84	5255.87
	10437.88	13262.84	9667.25	6996.88
	14308.53	3298.89	13417.85	6805.98
	14425.15	9406.75	16693.72	6378.13
	5039.41	13508.06	10582.02	2308.05
	6607.84	26615.72	11050.33	6216.36
	5227.32	24949.48	15883.24	3940.19
	21296.06	18106.01	16485.28	15163.7
	11133.98	22804.36	8750.87	13709.77
	11332.65	12768.77	9494.61	15136
	14462.4	11135.68	7519.19	8582.45
	7208.8	7525.23	19424.79	19747.18
	13288.98	5014.1	8369.19	4458.47
	14049.22	4175.7	6109.29	2292.6
	17490.93	3567.8	19212.33	2759.39
	16669.41	3278.07	25317.83	3867.19
	17118.82	15583.38	14345.31	7655.46
	21612.02	8754.21	13648.21	12091.56
	19621.05	5655.31	9963.85	5234.35
	15603.47	10947.02	17801.45	18353.54
	17536.66	10561.55	16543.33	21315.35
	17678.94	5954.77	22380.7	23631.09
	9871.62	6105.5	9002.25	21942.14
	12520.35	5921.79	28521.61	5783.14
	7557.92	13277.52	15285.11	6767.76
	15151.93	5353.88	21724.58	16178.13
	21753.56	23258.72	4031.31	8139.37
	22463.44	16985.53	18518.62	9056.7
	16188.03	5062.9	14042.65	13052.1
	12783.2	9422.6	12130.34	8009.99
	11193.68	7211.26	5585.84	5186.04
	4004.3	5692.81	8568.1	11762.74
	11618.19	6011.54	19836.43	5899.09

	10847.8	6935.28	24294.2	22614.56
	9459.43	5761.67	24533.3	17200.24
	16898.24	5999.92	21204.7	11307.27
	12417.44	7718.38	26076.87	30355.91
	12069.88	5262.28	24403.57	13662.54
	8739.78	7576.41	11753.94	10749.57
	13070.78	13945.38	16850.49	9972.21
	17588.82	14953.61	17946.01	6320.17
	12806.92	16985.13	25557.71	9402.68
	12092.4	13039.64	32290.53	5654.26
	14355.42	5265.51	18022.89	12878.43
	11472.07	17919.13	20120.53	24123.94
	12817.68	3524.1	32906.26	19047.14
	10284.91	5115.54	5229.93	26259.36
	12296.5	16366.29	16027.73	9287.28
	9237.96	9905.32	19805.87	7754.42
	12211.23	14818.49	20670.44	20821.73
	13577.43	20184.44	29657.77	10247.53
	11777.14	10509.21	25693.99	8701.94
	17146.95	12908.74	22992.89	19241.08
	10101.42	10353.48	26276.26	16629.81
	7385.78	5842.62	24244.54	47621.92
	9200.71	13102.69	24692.98	29409.31
	14933.5	8013.25	17388.93	29537.51
	7973.81	8872.75	24299.99	17105.06
	10915.28	9836.26	12206.12	12728.24
	10646.03	6055.35	11305.08	26901.63
	7628.11	22811.21	16755.18	19674.09
	6991.22	16704.01	14734.92	23947.64
	8669.33	15660.49	4970.69	28497.29
	16067.02	9696.95	7493.65	28889.51
	12205.76	7249.25	5767.36	25285.39
	15877.98	6745.79	7468.36	12445.86
	12456.14	7175.87	7253.11	10383.8
	2915.5	7766.95	11810.3	7078.28
	11694.72	3976.82	8549.93	7949.4
	8100.59	5208.7	7774.86	24455.82
	5751.27	5104.71	6248.14	25718.52
	4154.82	4909.48	9656.4	18316.95
	10717.98	9013.69	13632.57	22793.83
	3942.01	11333.29	7810.54	25054.45
	8503.49	11099.22	9899.97	26564.71
	7162.72	8902.22	6082.63	25401.44
	3945.86	7710.08	1690.87	31264.16
	4487.96	10240.72	10416.4	18240.73
	4119.15	13012.26	7494.15	33664.55
	9283.74	12392.52	20920.8	17780.43
	11148.53	8595.71	7060.36	13321.64
	11354.24	8651.1	11187.44	9104.83
	17545.3	17761.2	6709.28	18823.01
	12410.3	14535.98	5769.49	23946.83
	17345.99	15049.98	5172.57	18930.39
	7481.38	3838.33	7421.5	18101.16
	5345.11	2370.54	6972.55	8643.02
	5995.22	5041.04	5372.52	10219.33

	7126	5028.44	5501.43	9610.43
	18280.57	7153.88	10669.93	15938.74
	12622.4	3313.21	5491.63	12167.66
	13966.05	3284.98	7074.9	10212.58
	12240.29	1955.59	2480.84	16955.67
	16519.38	9183.17	2119.66	16617.46
	8039.79	5637.67	10301.03	14369.81
	15787.44	5471.17	10296.69	15662.59
	8028.42	1496.64	7025.43	7050.45
	4794.74	4775.64	6526.08	9923.92
	7122.61	14665.73	5349.93	5476.9
	13652.13	9946.69	5766.76	4684.8
	11869.12	6630.58	5875.03	7511.39
	13295.62	5708.93	9442.7	7705.87
	9248.39	6421.92	7409.57	8184.84
	15848.52	6399.19	2651.83	13165.97
	5479.48	4729.7	12133.93	13152.04
	3463.62	6626.85	10363.61	10703.43
	9643.18	3262.88	8244.21	13055.62
	10448.97	5994.79	9988.46	11719.73
	8184.96	8577.05	8991.64	21790.47
	10904.48	5356.75	10296.69	23594.82
Mean	11898.87	9425.697	13176.99	13665.5
St Dev	4731.909	5249.395	7163.141	8397.205
SEM	423.2348	469.5202	640.6908	751.0689

Table 6.4.13.Data for laminin quantitative immunohistochemistry in lung with doxycycline treatment

	IR 0/24	IR 4/24	Doxy.L.D	Doxy.H.D
Brightness	63372.57	15407.54	32829.08	39422.08
	36941.32	10818.23	31076.6	34084.91
	27117.99	14846.66	38273.1	15547.24
	56171.48	11215.44	20375.14	12429.74
	49405.88	12539.94	19636.54	17047.51
	47392.31	13445.47	24006.22	27700.32
	22642.28	16606.67	12831.99	11674.61
	80595.32	5364.93	47561.38	18870.53
	62322.98	13782.49	36951.78	6852.38
	44398.04	17666.83	39978.15	17516.03
	57885.33	1524.56	24656.55	14968.06
	45570.55	5345.34	17861.99	9094.77
	53926.46	41733.64	46995.13	17935.93
	90968.95	8960.82	41642.53	25264.68
	50292.09	1548.04	40602.65	17127.19
	52269.66	1473.22	38003.13	29869.29
	32746.93	977.1	32425.07	33957.56
	34765.86	1988.48	42029.34	37818.75
	12657.95	21393.49	22150.15	41085.09
	17539.71	14884.81	49844.09	22161.45
	12936.73	10240.87	39156.99	13518.19
	5457.58	10114.75	25806.23	17888.98
	7109.95	30374.33	38293.19	32263.09
	34102.69	32756.11	37116.01	17687.3
	46177.67	15950.99	32425.07	25284.69
	15563.46	13670.55	47776.88	19346.74
	11325.47	8621.66	32551.53	13561.02
	1256.91	10551.97	49615.58	22516.55
	21730.47	10071.83	39809.16	12764.87
	34846.14	6599.47	39553.98	12966.11
	29501.12	20398.98	52576.63	10152.37
	18806.34	16544.19	30540.3	14598.03
	12612.53	24439.67	32558.97	26741.33
	28503.29	17290.52	15891.14	18495.97
	13667.17	19971.21	23051.07	13643.56
	5068.15	24916.83	31693.43	8625.08
	7244.35	17419.49	38418.91	32397.63
	24418.54	1135.26	33639.66	22225.62
	32813.17	6987.03	23606.18	6572.2
	19675.55	4632.34	25056.6	5710.06
	20888.86	9703.42	11813.71	6601.93
	25816.68	5390.13	28408.58	33121.99
	20171.1	3523.58	6636.54	14355.11
	19670.26	4693.43	18574.39	21551.72
	31735.03	6917.42	11047.97	23972.86
	13214.62	10239.46	29426.75	17779.87
	49045.96	9725.15	9223.93	27994
	21779.94	5537.17	5344.39	20729.78

	11793.65	6848.86	5802.19	19657.68
	8661.93	14134.63	12065.15	10234.06
	20106.25	13015.96	21906.57	21215.83
	4509.42	28684.06	12309.19	25866.84
	2672.35	28837.89	29918.77	18340.03
	17869.84	22223.73	37890.73	25679.65
	35146.09	17490.17	35991.31	28158.22
	12045.36	31288.09	27892.57	19962.74
	21201.45	28559	4171.2	37595.17
	23100.33	387.28	5199.98	16879.07
	24931.39	9954.11	8608.82	48409.06
	18073.64	7082.19	6549.95	44154.59
	21105.88	3028.13	19953.88	35215.01
	15432.62	6132.18	2812.03	31059.55
	18754.24	9783.65	15033.64	43677.41
	7758.15	16085.1	10993.2	32015.23
	6395.65	7516.88	13287.12	42008.16
	9103.33	3652.4	25577.84	29418.45
	8323.75	3391.52	25259.45	31736.86
	8622.53	12605.99	16667	37914.28
	20092.11	7060.35	13530.95	26542.38
	26586.94	13947.94	7697.42	31757.8
	16253.56	16314.72	13444.29	39358.13
	17900.45	23089.7	14553.17	35949.85
	34907.86	17642.3	18818.39	35408.52
	23740.36	21168.21	18418.68	42472.12
	13621.58	16674.5	11768.62	35534.55
	22643.07	18260.09	33785.01	22155.66
	5119.3	12449.39	31460.8	26547.07
	2984.79	3133.96	20902.21	29551.69
	9113.76	6294.12	31299.8	23913.01
	20575.93	5730.77	10627.81	29251.68
	11390.93	2915.96	9198.54	13419.23
	8894.01	17149.36	2952.14	34146.17
	12755.65	13190.1	6860.69	31199.96
	17804.8	5974.65	12514.55	8735.67
	13647.22	29714.38	3073.58	10975.03
	35616.6	18740.62	13653.62	5419.17
	14560.83	16629.68	29119.07	15990.64
	15072.29	12274.92	22143.81	4744.47
	21937.33	8251.71	27703.62	9266.3
	21217.41	14664.01	26731.65	18860.91
	27684.57	5234.68	23174.31	2917.14
	20142.8	27567.56	16496.83	2941.9
	23936.35	11467.52	13094.23	1646.03
	20495.01	13740.57	13880.14	6634.43
	14099.44	34076.92	14583.5	3217.47
	12759.12	13794.74	22636.58	4489.44
	22259.74	19636.06	10137.59	2523.16
	37986.13	6115.06	6377.68	3964.02
	29869.33	13833.73	24216.03	21812.04
	22576.41	6926.14	25559.27	6204.65
	38358.19	28375.81	25153.07	45283.58
	26868.97	6481.98	25252.08	22130.42
	25619.99	19927.21	30513.23	6331.64

	4953.72	18422.92	31688.74	11415
	10713.38	27129.04	20917.63	6522.98
	28637.69	25143.81	40777.53	6423.72
	40260.96	15624.16	26407.21	26310.39
	30605.29	23190.35	30681.89	20783.35
	28663.67	3508.36	37075.32	6762.36
	23572.82	14154.01	37225.84	3174.35
	18046.39	10529.93	38813.22	9779.91
	19816.78	6362.07	33855.96	3386.74
	48430.55	5420.74	57043.43	4008.59
	30711.57	3229.23	59243.04	1586.51
	26364.18	9740.11	15617.1	13827.54
	30867.48	7355.18	20785.16	12488.95
	21260.37	8567.31	32197.37	4246.65
	20679.3	9050.63	25340.22	17239.9
	52407.21	10149.78	31206.05	6694.12
	40528.71	8333.09	34132.43	8951.99
	38496.83	8371.19	32439.46	6561.49
	33944.04	7969.03	17011.33	20767.81
	17262.49	2491	16254.61	11826.35
	8532.85	8662.78	6796.8	17275.27
	23572.82	4034.09	20811.05	15374.6
Mean	25017.23	12852.25	24839.11	19675.18
St Dev	15876.84	8357.804	12709.53	11780.24
SEM	1420.068	747.5447	1136.775	1053.657

Table 6.4.14.Data for laminin quantitative immunohistochemistry in kidney with docycycline treatment

	IR 0/24	IR 4/24	Doxy L.D	Doxy H.D
Brightness	10306.98	3511.2	17181.43	14840.76
	8271.35	5883.39	22124.71	18544.87
	10291.23	16146.21	17510.72	22370.13
	15900.47	8288.1	21707.85	23952.15
	19767.54	15357.67	5867.12	22151.21
	19811.23	10582.5	4825.98	10806.17
	21064.97	8026.34	13033.54	10730.89
	18926.72	17711.22	7617.62	14307.64
	12757.41	15222.79	9346.81	8474.33
	22154.41	6590.42	14732.24	13758.24
	13405.46	6226.63	11514.28	28287.96
	13115.21	7885.46	8081.86	38777.81
	10580.75	13182.7	8558.74	18340.8
	4553.28	9547.18	13815.16	9439.15
	10038.96	8709.94	8850.65	18767.06
	28874.22	22726.36	9193.56	6966.76
	12372.77	5897.61	5204.12	6448.57
	17936.46	10183.51	7828.41	10492.81
	16518.02	2532.7	7228.04	13834.91
	3714.5	2890.81	12782.98	19786
	4546.47	1460.54	7439.56	4599.24
	16249.34	5188.37	6413.63	7312.6
	6352.26	8449.97	5633.62	15165.21
	3482.96	6296.49	7912.14	14869.1
	4427.08	9157.01	4455.28	12460.3
	13804.9	7894.53	2121.39	13211.13
	14200.88	10096.37	2302.22	14014.9
	5617.66	10334.61	2985.66	7399.65
	12492.72	10955.67	3382.98	13700.62
	6938.13	11895.32	1484.48	5706.34
	12066.75	7701.84	2488.99	9966.76
	14687.39	6689.25	1403.67	19063.8
	23553.41	7557.58	3108.27	11960.19
	2626.33	9042.26	1935.03	19488.93
	11051.71	5460.15	2838.18	3590.14
	21083.82	3289.56	4671.56	3340
	12225.18	12433.72	5497.79	5013.24
	10853.17	4578.23	3185.15	8586.76
	8151.11	5269.26	2839.27	5146.07
	8646.58	3899.71	2011.71	8957.14
	12482.94	6559.11	10364.59	9880.77
	11918.55	5408.72	7557.14	10985.5
	1892.36	4119.48	2077.2	12366.47
	4596.72	3753.72	6305.19	7212.94
	6435.69	2621.64	4039.68	5585.75
	5001.89	5416.42	7464.64	6709.28
	4885.05	5642.43	6679.11	3344.59
	6314.18	4983.92	6248.32	3098.83

	4572.37	2930.2	9593.78	4620.85
	3465.94	1588.6	4459.95	3420.06
	13655	4011.82	10637.93	15718.53
	8179.78	743.57	8662.07	15199.05
	19087.95	3716.07	7285.2	15645.44
	10457	3345.1	7145.11	7118.84
	6431.5	5915.16	6690.52	5792.7
	9714.57	8840.03	3783.78	12278.05
	6377.89	10757.11	3532.8	11253.36
	6518.93	3319.51	4283	6410.08
	6657.96	2832.57	3581.41	6317.93
	4675.61	4729.79	2524.35	10028.33
	9179.05	6702.67	16033.44	11192.82
	10216.1	5343.26	12125.89	17591.06
	8408.53	4730.35	9559.13	5385.44
	7581.85	4732.16	8568.99	6178.83
	7049.74	6427.41	7296.13	7338.58
	4558.95	12128.72	7273.2	6723.66
	2678.2	2366.66	12877.06	5905.97
	6833.41	2353.6	6957.29	2897.26
	15572.31	2695.29	2466.36	4957.98
	7690.32	6705.68	11767.86	11090.85
	14366.47	11551.29	8558.33	15376.48
	7606.15	6580.65	3952.9	7001.01
	11619.2	4785.36	7181.88	2689.94
	14151.44	4844.55	7802.72	5568.53
	5333.77	6139.13	8792.07	2385.03
	35782.88	6108.17	6682.14	20971.71
	8746.43	4823.59	10333.51	19137.2
	6144.69	2726.2	9629.42	18679.4
	3537.92	3220.65	15083.35	14819.17
	6017.98	5771.24	6252.55	12714.21
	2279.45	3529.62	9154.72	13360.29
	4686.26	2114.12	9935.69	14491.93
	4129.04	4737.53	5867.16	7962.59
	8970.17	3938.17	10843.82	9475.78
	4798.94	3344.46	2769.06	27878.39
	4975.8	3182.12	2987.18	23740.25
	5548.46	2307.83	1888.77	18687.65
	8441.33	2843.79	3531.94	16675.4
	17396.59	2713.85	3048.52	15241.4
	18808.9	2736.76	16692.45	20566.39
	13125.86	3047.42	18970.14	16112.13
	5616.41	6662.6	25836.08	13876.8
	8154.17	3294.98	22779.45	20298.03
	13974.42	2971.8	10396.41	24794.32
	8013.49	3865.48	15978.49	21027.24
	2508.44	10170.21	6590.24	15649.35
	9530.58	3070.69	5650.25	9354.79
	13256.49	3400.01	4843.23	11804.58
	1900.14	3472.83	7802.72	8954.56
	6061.51	4615.82	19071.63	5556.06
	4729.41	5800.71	16777.95	8524.96
	11410.44	6100.52	19669.69	13897.05
	2600.53	4359.26	16370	11562.44

	2589.32	7426.01	13966.05	3509.37
	2984.89	9031.96	15845.91	4973.75
	5668.29	12026.29	10107.32	7728.96
	5240.22	6608.2	13772.29	5978.17
	8000.46	6524.38	8017.16	6785.51
	6508.75	7570.1	26878.78	6785.56
	4441.29	3530.95	19137.92	2544.88
	4543.16	5763.52	20307.74	7081.36
	5174.23	2748.05	13196.53	3402.19
	9067.23	3024.64	8940.41	2748.1
	12679.87	2248.26	9254.56	4322.46
	7405.71	4665.46	13390.11	5897.4
	9520.9	2498.28	7233.65	5791.59
	4992.67	5020.41	10012.33	13512.83
	9085.32	6831.85	3480.86	5749.35
	10943.37	4490.19	1950.98	6714.61
	14142.27	8321.75	1572.46	5358
	3358.94	6323.81	6047.85	7055.35
	2987.37	7340.62	4252.19	8341.71
	6069.75	6376.73	3626.86	6034.16
	10167.49	7690.25	8417.32	6443.8
	8389.79	2492.38	4995.5	5837.21
Mean	9477.561	6140.476	8680.694	11106.49
St Dev	5783.675	3612.404	5602.099	6517.85
SEM	517.3076	323.1032	501.067	582.9742

CHAPTER 7

BIBLIOGRAPHY

1. CurciJA, LiaoS, HuffmanMD, ShapiroSD, ThompsonRW. Expression and localization of macrophage elastase (matrix metalloproteinase-12) in abdominal aortic aneurysms. J Clin Invest 1998;102:1900-1910.

2. CeckaJM. The UNOS scientific renal transplant registry-2000. Clin Transpl 2000:1-18.

3. SmithCM, DaviesDB, McBrideMA. Liver transplantation in the United States: a report from the organ procurement and transplantation network. Clin Transpl 2000:19-30.

4. McCordJM, FridovichI. The reduction of cytochrome C by milk xanthine oxidase. J Biol Chem 1968;243:5753-5760.

5. FriedlHP, SmithDJ, TillGO, ThomsonPD, LouisDS, WardPA. Ischemia-reperfusion in humans. Am J Pathol 1990;136:491-495.

6. McCordJM. Oxygen-derived free radical in postischemic tissue injury. N Engl J Med 1985;312:159-163.

7. ParksDA, GrangerDN, BulkleyGB, ShahAK. Soybean trypsin inhibitor attenuates ischemia injury to the feline small intestine. Gastroenterology 1985;89:6-12.

8. GrangerDN. Role of xanthine oxidase and granulocytes in ischemia-reperfusion injury. Am J Physiol (Heart Circ Physiol 24) 1988;255:H1269-1375.

9. RoyRS, McCordJM. Superoxide and ischemia: conversion of xanthine dehydrogenase to xanthine oxidase. New York: Elsevier Science; 1983.

10. KellogEW. Superoxide, hydrogen peroxide and singlet oxygen in lipid peroxidation by a xanthine oxidase system. J Biol Chem 1975;250:8812-8817.

11. ErnsterL. Biochemistry of reoxygenation injury. Crit Care Med 1988;16:947-953.

12. KukrejaR, HessML. The oxygen free radical system: from equations through membrane-protein interactions to cardiovascular injury and protection. Cardiovasc Res 1992;26:641-655.

13. VaneJR, AnggardEK, BottingRM. Regulatory functions of the vascular endothelium. N Engl J Med 1990;323:27-36.

14. SpanguoloPJ, EllnerJJ, HasidA, DunnMJ. Thromboxane A2 mediates augmented polymorphonuclear leukocyte adhesiveness. J Clin Invest 1980;66:406-414.

15. WellesSL, SheproD, HechtmanHB. Eicosanoid modulation of stress fibres in cultured bovine endothelial cells. Inflammation 1985;9:549-556.

16. KonigW, SchonfeldW, RaulfM, KnollerM, KnollerJ, SchefferJ, et al. The neutrophil adn the leukotrienes-role in health and disease. Eicosanoids 1990;3:1-22.

17. Homer-VanniasinkamS, GoughMJ. Role of lipid mediators in the pathogenesis of skeletal muscle infarction and edema during reperfusion after ischemia. Br J Surg 1994;81:1500-1503.

18. IanSP, JosephMK, GideonG, LesterK, RichardW, RobertVC, et al. Thromboxane mediates the ischemia-induced neutrophil oxidative burst. Surgery 1989;106:224-229.

19. FiessingerJN, SchaferM. Trial of iloprost versus aspirin treatment for critical limb ischemia of thromboangitis obliterans. Lancet 1990;335:555-557.

20. Homer-VanniasinkamS, CrinnionJN, GoughMJ. Role of thromboxane A2 in muscle injury following ischemia. Br J Surg 1994;81:974-976.

21. HoballahJJ, MohanCR, SharpWJ, KresowikTF, CorsonJD. Lazaroid U 74389G attenuates skeletal muscle reperfusion injury in a canine model. Transplantation Proc 1995;27:2836-2839.

22. LewisMS, WhatleyRE, CainP, McIntyrePM, PrescottSM, ZimmermanGA. Hydrogen peroxide stimulates the synthesis of platelet-activating factor by endothelium and induces endothelial cell-dependent neutrophil adhesion. J Clin Invest 1988;82:2045-2055.

23. KubesP, SuzukiM, GrangerDN. Platelet activating factor induced microvascular dysfunction: the role of adherent leukocytes. Am J Physiol 1990;258:G158-163.

24. HouraniSM, CusackNJ. Pharmacological receptors on blood platelets. Pharmacol Rev 1991;43:243-298.

25. MarubayashiS, OshiroY, MaedaT, FukumaK, OkadaK, HinoiT, et al. Protective effects of monoclonal antibodies to adhesion molecules on rat liver ischemia-reperfusion injury. Surgery 1997;122:45-52.

26. GrangerDN. Physiology and pathophysiology of the microcirculation. Prog Cardiovasc Med 1998;3:123-140.

27. KorthiusRJ, GrishamMB, GrangerDN. Leukocyte depletion attenuates vascular injury in postischemic skeletal muscle. Am J Physiol (Heart Circ Physiol 23) 1988;254:H823-H827.

28. LinasSL, ShanleyPF, WhittenbergD, BergerE, RepineJE. Neutrophils accentuate ischemia-reperfusion injury in isolated perfused rat kidneys. Am J Physiol (Renal Fluid Electrolyte Physiol) 1988;255:F728-735.

29. SimpsonPJ, ToddRF3rd, FantoneJC, MickelsonJK, GriffinJD, LucchesiBR. Reduction of experimental canine myocardial reperfusion injury by a monoclonal antibody (anti-mol, anti-CD11 b) that inhibits leukocyte adhesion. J Clin Invest 1988;81:624-629.

30. KlausnerJM, PatersonIS, GoldmanG, KobzikL, ValeriCR, SheproD, et al. Thromboxane A2 mediates increased pulmonary microvascular permeability following limb ischemia. Circ Res 1989;64:1178-1189.

31. MiuraM, FuX, ZhangQW, RemickDG, FairchildRL. Neutralization of Gro-a and macrophage inflammatory protein-2 attenuates renal ischemia/reperfusion injury. Am J Pathol 2001;159:2137-2145.

32. GaoF, YueTL, ShiDW, ChristopherTA, LopezBL, OhlsteinEH, et al. P38 MAPK inhibition reduces myocardial reperfusion injury via inhibition of endothelial adhesion molecle expression and blockade of PMN accumulation. Cardiovasc Res 2002;53:414-22.

33. DavidLW, HaroldJM, ErikGE, JohnRS, PaulFS, OscarKR, et al. Neutrophil accumulate and contribute to skeletal muscle dysfunction after ischemia-reperfusion. Am J Physiol (Heart Circ Physiol 28) 1990;259:H1809-H1812.

34. BevilacquaMP, StengelinS, GimbroneMAJr, SeedB. Endothelial leukocyte adhesion molecule 1: an inducible receptor for neutrophils related to complement regulatory proteins and lectins. Science 1989;243:1160-1165.

35. LuscinskasFW, BrockAF, ArnaoutMA, GimbroneMAJr. Intercellular adhesion molecule-1 dependent and leucocyte (CD11/CD18) dependent mechanisms contribute to polymorphonuclear leukocyte adhesion to cytokine activated human vascular endothelium. J Immunol 1989;142:2257-2263.

36. ConnollyESJr, WinfreeCJ, SpringerTA, NakaY, LiaoH, YanSD, et al. Cerebral protection in homozygous null ICAM-1 mice after middle cerebral artery occlusion. Role of neutrophil adhesion in the pathogenesis of stroke. J Clin Invest 1996;97:209-216.

37. SpringerTA. Adhesion receptors of the immune system. Nature 1990;346:425-434.

38. CharlesJP, KimSC, ConnollyESJr, LiaoH, YanXF, PinskyDJ. CD18-mediated neutrophil recruitment contributes to the pathogenesis of reperfused but not nonreperfused stroke. Stroke 1999;30:1110-1117.

39. MatsuoY, OnoderaH, ShigaY, ShozuharaH, NinomiyaM, KiharaT, et al. Role of cell adhesion molecules in brain injury after transient middle cerebral artery occlusion in the rat. Brain Res 1994;656:344-352.

40. LindsbergPJ, SirenAL, FeuersteinGZ, HallenbeckJM. Antagonism of neutrophil adherence in the deteriorating stroke model in rabbits. J Neurosurg 1995;82:269-277.

41. IchikawaH, FloresS, KvietysPR, WolfRE, YoshikawaT, GrangerDN, et al. Molecular mechanisms of anoxia/reoxygenation-induce neutrophil adherence to cultured endothelial cells. Circ Res 1997;81:922-931.

42. HorganMJ, WrightSD, MalikAB. Antibody against leukocyte integrin (CD18) prevents reperfusion-induced lung vascular injury. Am J Physiol 1990;259 (4 Pt 1):L315-319.

43. CardenDL, SmithJK, KorthuisRJ. Neutrophil-mediated microvascular dysfunction in the post-ischemic canine skeletal muscle. Circ Res 1990;66:1436-1444.

44. NathanC, SrimalS, FarberC, SanchezE, KabbashL, AschA, et al. Cytokine-induced respiratory burst of human neutrophils: dependence on extracellular matrix proteins and CD11/CD18 integrins. J Cell Biol 1989;109:1341-1349.

45. LawrenceMB, BaintonDF, SpringerTA. Neutrophil tethering to and rolling on E-selectin are separable by requirement for L-selectin. Immunology 1994;1:137-141.

46. LawrenceMB, SpringerTA. Leukocytes roll on a selectin at physiologic flow rates: distinction from and prerequisite for adhesion through integrins. Cell 1991;65:859-873.

47. SmithCW, KishimotoTK, AbbassiO, HughesB, RothleinR, McIntireLV, et al. Chemotactic factors regulate lectin adhesion molecule-1 (LECAM-1) dependent neutrophil adhesion to cytokine stimulated endothelial cells in vitro. J Clin Invest 1991;87:609-618.

48. LozanoDD, KahlEA, WongHP, StephensonLL, ZamboniWA. L-selectin and leukocyte function in skeletal muscle reperfusion injury. Arch Surg 1999;134:1079-1081.

49. IwaoK, DonaldCA, MasayukiM, TakuyaT, JamesCP, RobertFT, et al. Molecular determinants of reperfusion-induced leukocyte adhesion and vascular protein leakage. Circ Res 1994;74:336-343.

50. ConnollyESJr, WinfreeCJ, PrestigiacomoCJ, KimSC, ChoudhriTF, HohBL, et al. Exacerbation of cerebral injury in mice that express P-selectin gene: identification of P-selectin blockade as a new target for the treatment of stroke. Circ Res 1997;81:304-310.

51. HuangJ, ChoudhriTF, WinfreeCJ, McTaggartRA. Postischemic cerebrovascular E-selectin expression mediates tissues injury in murine stroke. Stroke 2000;31:3047-3053.

52. RiceGE, BevilacquaMP. An inducible endothelial cell surface glycoprotein mediates melanoma adhesion. Science 1989;246:1303-1306.

53. WellerA, IsenmannS, VestweberD. Cloning of the mouse endothelial selectins: expression of both E- and P-selectin is inducible by tumor necrosis factor alpha. J Biol Chem 1992;267:15176-15183.

54. BuerkeM, WeyrichAS, ZhengZ, GaetaFC, ForrestMJ, LeferAM. Sialyl Lewis-containing oligosaccharide attenuates myocardial reperfusion injury in cats. J Clin Invest 1994;98:1140-1148.

55. SteinbergJB, MaoHZ, NilesSD, JutilaMA, KapelanskiDP. Survival in lung reperfusion injury is improved by an antibody that binds and inhibits L- and E- selectin. J Heart Lung Transplant 1994;13:306-318.

56. TakadaM, NadeauKC, ShawGD, TilneyNL. Prevention of late renal changes after initial ischemia/reperfusion injury by blocking early selectin binding. Transplantation 1997;64:1520-1525.

57. ChamounF, BurneM, O'DonnellM, RabbH. Pathophysiologic role of selectins and their ligands in ischemia reperfusion injury. Front Biosci 2000;5:E103-109.

58. BaldwinWM, PruittSK, BrauerRB, DahaMR, SangilippoF. Complement in organ transplantation. Transplantation 1995;59:797-808.

59. KilgoreKS, ParkJL, TanhehcoEJ, BoothEA, MarksRM, LucchesiBR. Attenuation of interleukin-8 in C6-deficient rabbits after myocardial ischemia/reperfusion. J Mol Cell Cardiol 1998;30:75-85.

60. ZhouW, FarrarCA, AbeK, PrattJR, MarshJE, WangY, et al. Predominant role for C5b-9 in renal ischemia/reperfusion injury. J Clin Invest 2000;105:1363-1371.

61. WeismanHR, BartowT, LeppoMK, MarshHCJr, CarsonGR, ConcinoMF, et al. Soluble human complement receptor type 1: in vivo inhibitor of complement suppressing post-ischemic myocardial inflammation and necrosis. Science 1990;249:146-151.

62. VakevaAP, AgahA, RollinsSA, MatisLA, LiL, StahlGL. Myocardial infarction and apoptosis after myocardial ischemia and reperfusion: role of the terminal complement components and inhibition by anti-C5 therapy. Circulation 1998;97:2259-2267.

63. BuerkeM, SchwertzH, SeitzW, MeyerJ, DariusH. Novel small molecule inhibitor of C1s exerts cardioprotective effects in ischemia-reperfusion injury in rabbits. J Immunol 2001;167:5375-5380.

64. LeferDJ. Pharmacology of selectin inhibitors in ischemia/reperfusion states. Annu Rev Pharmacol Toxicol 2000;40:283-294.

65. WelbournCR, GoldmanG, O'RiordainM, LindsayTF, PatersonIS, KobzikL, et al. Role for tumor necrosis factor as mediator of lung injury following lower torso ischemia. J Appl Physiol 1991;70:2645-2649.

66. KlausnerJM, PatersonIS, KobzikL, ValeriCR, SheproD, HechtmanHB. Oxygen free radicals mediate ischemia-induced lung injury. Surgery 1989;105:192-199.

67. HansenPR. Role of neutrophils in myocardial ischemia and reperfusion. Circulation 1995;91:1872-1885.

68. WybleCW, DesaiTR, ClarkET, HynesKL, GewertzBL. Physiologic concentrations of TNF-alpha and IL-1beta released from human intestine upregualte E-selectin and ICAM-1. J Surg Res 1996;63:333-338.

69. SeekampA, WarrenJS, RemickDG, TillGO, WardPA. Requirements of tumor necrosis factor-alpha and interleukin-1 in limb ischemia/reperfusion injury associated with lung injury. Am J Pathol 1993;143:453-463.

70. BassengeE. Clinical relevance of endothelium-derived relaxing factor (EDRF). Br J Pharmacol 1992;34:37-42S.

71. CardenDL, GrangerDN. Pathophysiology of ischaemia-reperfusion injury. J Pathol 2000;190:255-266.

72. EnglerR. Symposium: Granulocytes and oxidative injury in myocardial ischemia and reperfusion. Fed Proc 1987;46:2395-2433.

73. FengLJ, BergerBE, LyszTW, ShawWW. Vasoactive prostaglandins in the impending no-reflow state: evidence for a primary disturbance in microvascular tone. Plast Reconstr Surg 1988;81:755-64.

74. GidlofA, LewisDH, HammersenF. The effect of prolonged total ischemia on the ultrastructure of human skeletal muscle capillaries-a mophometric analysis. Int J Microcirc Clin Exp 1987;7:67-86.

75. HardySC, Homer-VanniasinkamS, GoughMJ. Effect of free radical scavenging on skeletal muscle blood flow during postischemic reperfusion. Br J Surg 1992;79:1289-1292.

76. KellyKJ, WilliamsWW, ColvinRB, BonventreJV. Antibody to intercellular adhsion molecule 1 protects the kidney against ischemic injury. Proc Natl Acad Sci USA 1994;91:812-816.

77. HallerH, DragunD, MiethkeA, ParkJK, WeisA, LippoldtA, et al. Antisense oligonucleotides for ICAM-1 attenuate reperfusion injury and renal failure in the rat. Kidney Int 1996;50:473-480.

78. FruchgottRF, ZawadzkiJV. The obligatory role of endothelial cells in the relaxation of arterial smooth muscle by acetylcholine. Nature 1980;288:373-376.

79. PalmerRMJ, FerrigeAG, MoncadaS. Nitric oxide release accounts for the biological activity of endothelium-derived relaxing factor. Nature 1987;327:524-526.

80. BilliarTR. Nitric oxide. novel biology with clinical relevance. Ann Surg 1995;221:339-349.

81. LowensteinCJ, SnyderSH. Nitric oxide, a novel biologic messenger. Cell 1992;70:705-707.

82. BusseR, LuckhoffA, BassengeE. Endothelium-derived relaxant factor inhibits platelet activation. Naunyn Schmiedebergs Arch Pharmacol 1987;336:556-571.

83. LuscherTF, YangZ, TschudiM, vonSesserL, StulzP, BoulangerC, et al. Interaction between endothelin-1 and endothelium-derived relaxing factor in human arteries and veins. Circ Res 1990;66:1088-1094.

84. SalazarFJ, PinillaJM, LopezF, RomeroJC, QuesadaT. Renal effects of prolonged synthesis inhibition of endothelium-derived nitric oxide. Hypertension 1992;20:113-117.

85. HukI, NanobashviliJ, NeumayerC, PunzA, MuellerM, AfkhampourK, et al. L-arginine treatment alters the kinetics of nitric oxide and superoxide release and reduce ischemia/reperfusion injury in skeletal muscle. Circulation 1997;96:667-682.

86. Fox-RobichaudA, PayneD, HasanSU, OstrovskyL, FairheadT, ReinhardtP, et al. Inhaled NO as a viable antiadhesive therapy for ischemia/reperfusion injury of distal microvascular beds. J Clin Invest 1998;101:2497-2505.

87. IWaoK, RobertW, MatthewBG, GrangerDN. Modulation of ischemia/reperfusion-induced microvascular dysfunction by nitric oxide. Circ Res 1994;74:376-382.

88. BeckmanJS, BeckmanTW, ChenJ, MarshallPA, FreemanBA. Apparent hydroxyl radical production by peroxynitrite: implications for endothelial injury from nitric oxide and superoxide. Proc Natl Acad Sci USA 1990;87:1620-1624.

89. RadiR, BeckmanJS, BushKM, FreemanBA. Peroxynitrite-induced membrane peroxidation: the cytotoxic potential of superoxide and nitric oxide. Arch Biochem Biophys 1991;288:481-487.

90. NielsenVG, TanS, BairdMS, McCammonAT, ParksDA. Gastric intramucosal pH and multiple organ injury: impact of ischemia-reperfusion and xanthine oxidase. Crit Care Med 1996;24:1339-1344.

91. WeinbroumAA, NielsonVG, TanS. Liver ischemia-reperfusion increases pulmonary permeability in rat: role of circulating xanthine-oxidase. Am J Physiol 1995;268:G988-996.

92. TeradaLS, DormishJJ, ShanleyPF, LeffJA, AndersonBO, RepineJE. Circulation xanthine oxidase mediates lung neutrophil sequestration after intestinal ischemia-reperfusion. Am J Physiol 1992;263:L394-401.

93. GrangerDN. Ischemia-reperfusion: mechanisms of microvascular dysfuction and the influence of risk factors for cardiovascular disease. Microcirculation 1999;6:167-178.

94. YanagisawaM, KuriharaH, KimuraS, TomobeY, KobayashiM, MitsuiY, et al. A novel potent vasoconstrictor peptide produced by vascular endothelial cells. Nature 1988;332:411-415.

95. FirthJD, RatcliffePJ, AEG R, LedinghamJGG. Endothelin: An important factor in acute renal failure. Lancet 2000;2:1179-1181.

96. WilhelmS, SimonsonMS, RobinsonAV, StoweNT, SchulakJA. Endothelin up-regulation and localization following renal ischemia and reperfusion. Kidney Int 1999;55:1011-1018.

97. MillerLW, RedfieldMM, BurnettJCJr. Integrated cardiac, renal and endocrine action of endothelin. J Clin Invest 1989;83:317-320.

98. MasakiT. The discovery, the present state and the future prospects of endothelin. J Cardiovasc Pharmacol 1989;13 (Suppl 5):1-4.

99. YanagisawaM, InoueA, TakuwaY, MitsuiY, KobayashiM, MasakiT. The human preproendothelin-1 gene: possible regulation by endothelial phosphoinositide turnover signaling. J Cardiovasc Pharmacol 1989;13 (Suppl 5):13-17.

100. BialeckiRA, IzzoNJJr, ColucciWS. Endothelin-1 increases intracellular calcium mobilization but not calcium uptake in rabbit vascular smooth muscle cells. Biochem Biophys Res Commun 1989;164:474-479.

101. KarmazynM. Mechanisms of protection of the ischemia and reperfused myocardium by sodium-hydrogen exchange inhibition. Thromb Thrombolysis 1999;8:33-38.

102. HirataY, TakagiY, FukudaY, MarumoF. Endothelin is a potent mitogen for rat vascular smooth muscle cells. Atherosclerosis 1989;78:225-228.

103. Lopez-FarreA, FiescoA, EspinosaG, DigiuniE, CernadasMR, AlvarezV, et al. Effect of endothelin-1 on neutrophil adhesion to endothelial cells and perfused heart. Circulation 1993;88:1166-1171.

104. KonV, YoshiokaT, FogoA, IchikawaI. Glomerular actions of endothelin in vivo. J Clin Invest 1989;83:1762-1767.

105. KaretFE, DavenportAP. Localization of endothelin peptides in human kidney. Kidney Int 1996;49:382-387.

106. GellaiM, JugusM, FletcherT, DewoflR, NambiP. Reversal of postischemic acute renal failure with a selective endothelin A receptor antagonist in the rat. J Clin Invest 1994;93:900-906.

107. ChanL, ChittinandanaA, ShapiroJI, DhanleyPF, SchrierRW. Effect os an endothelin-receptor antagonist on ischemia acute renal failure. Am J Physiol 1994;266 (Renal Fluid Electrolyte Physiol 35):F135-F138.

108. NambiP, PullenM, JugusM, GellaiM. Rat kidney endothelin receptors in ischemia-induced acute renal failure. J Pharmacol Exp Ther 1993;264:345-348.

109. MitsuokaH, SuzukiS, SakaguchiT, BabaS, MiwaM, KonnoH, et al. Contribution of endothelin-1 to microcirculation impairment in total hepatic ischemia and reperfusion injury. Transplantation 1999;67:514-520.

110. HughesAK, StricklettPK, PeterK, PadillaE, KohanDE. Effect of reactive oxygen species on endothelin-1 production by human mesangial cells. Kidney Int 1996;49:181-189.

111. ZojaCSO, PericoN, BenigniA, MorigiM, BenattiL, RambaldiA, et al. Constitutive expression of endothelin gene in cultured human mesengial cells and its modulation by transforming growth factor-beta, thrombin, and a thromboxane A2 analogue. Lab Invest 1991;64:16-20.

112. MaruiN, OffermannMK, SwerlickR, KunschC, RosenCA, AhmadM, et al. Vascular cell adhesion molecule-1 (VCAM-1) gene transcription and expression are regulated through an antioxidant-sensitive mechanism in human vascular endothelial cells. J Clin Invest 1993;92:1866-1874.

113. LermanA, BurnettJC. Intact and altered endothelium in regulation of vasomotion. Circulation 1992;86 (Suppl 3):12-19.

114. ShengH, ShaoJ, MorrowJD, BeauchampRD, DuboisRN. Modulation of apoptosis and Bcl-2 expression by prostaglandin E2 in human colon cancer cells. Cancer Res 1998;58:362-366.

115. StauntonMJ, GaffneyEF. Apoptosis: basic concepts and potential significance in human cancer. Arch Pathol Lab Med 1998;122:310-319.

116. ChungJH, KwonOS, EunHC, YounJI, SongYW, KimJG, et al. Apoptosis in the pathogenesis of cutaneous lupus erythematosus. Am J Dermatopathol 1998;20:233-241.

117. BeutlerB, BazzoniF. TNF, apoptosis and autoimmunity: a common thread ? Blood Cells Mol Dis 1998;24:216-230.

118. MallatZ, TedguiA, FontaliranFetal. Evidence of apoptosis in arrhythemogenic right ventricular dysplasia. N Engl J Med 1996;335:1190-1196.

119. WooD. Apoptosis and loss of renal tissue in polycystic kidney disease. N Engl J Med 1995;333:18-25.

120. LiY, ChoppM, JiangN, ZhangZG, ZalogaC. Induction of DNA fragmentation after 10-120 minutes of focal cerebral ischemia in rats. Stroke 1995;26:1252-1258.

121. FlissH, GattingerD. Apoptosis in ischemic and reperfused rat myocardium. Circ Res 1996;79:949-956.

122. FischerS, CassiviSD, XavierAM, CardellaJA, CutzE, EdwardsV, et al. Cell death in human lung transplantation: apoptosis induction in human lungs during ischemia and after transplantation. Ann Surg 2000;231:424-431.

123. SalahudenAK, JoshiM, JohnK. Apoptosis versus necrosis during cold storage and rewarming of human renal proximal tubular cells. Transplantation 2001;72:798-804.

124. DaemenMA, Van'tVeerC, DeneckerG, HeemskerkVH, WolfsTG, ClaussM, et al. Inhibition of apoptosis induced by ischemia-reperfusion prevents inflammation. J Clin Invest 1999;104:541-549.

125. SchierleGS, HanssonO, LeistM, NicoteraP, WidnerH, BrundinP. Caspase inhibition reduces apoptosis and increase survival of nigral transplants. Nat Med 1999;5:97-100.

126. YaoitaH, OgawaK, MaeharaK, MaruyamaY. Attenuation of ischemia/reperfusion injury in rats by a caspase inhibitor. Circulation 1998;97:276-281.

127. FischerS, MacleanAA, LiuM, CardellaJA, SlutskyAS, SugaM, et al. Dynamic changes in apoptotic and necrotic cell death correlate with severity of ischemia-reperfusion injury in lung transplantation. Am J Respir Crit Care Med 2000;162:1932-1939.

128. LieberthalW, MenzaSA, LevineJS. Graded ATP depletion can cause necrosis or apoptosis of cultured mouse proximal tubular cells. Am J Physiol 1998;274:F315--327.

129. KerrJFR, WyllieAH, CurrieAR. Apoptosis: a basic biological phenomenon with wide-ranging implications in tissue kinetics. Br J Cancer 1972;26:239-257.

130. MajnoG, JorisI. Apoptosis, oncosis and necrosis. An overview of cell death. Am J Pathol 1995;146:3-15.

131. LieberthalW, TriacaV, LevineJ. Mechanisms of death induced by cisplatin in proximal tubular epithelial cells: Apoptosis vs necrosis. Am J Physiol 1996;270 (4 Pt 2):F700-708.

132. UedaN, ShahSV. Tubular cell damage in acute renal failure-apoptosis, necrosis or both. Nephrol Dial Transplant 2000;15:318-323.

133. ChangSH, PhelpsPC, BerezeskyIK, EbersbergerML, TrumpBF. Studies on the mechanisms and kinetics of apoptosis induced by microinjection of cytochrome c in rat kidney tubule epithelial cells (NRK-52E). Am J Pathol 2000;156:637-649.

134. ScarabelliTM, StephanouA, PasiniE, CominiL, RaddinoR, RichardA, et al. Different signaling pathways induce apoptosis in endothelial cells and cardiac myocytes during ischemia/reperfusion injury. Circ Res 2002;90:745-748.

135. CohenGM. Caspases: the executioners of apoptosis. Biochem J 1997;326:1-16.

136. ThornberryN, LazebnikY. Caspase: enemies within. Science 1998;281:1312-1316.

137. SalvesenGS, DixitVM. Caspases: intracellular signaling by proteolysis. Cell 1997;91:443-446.

138. WallachE, VarfolomeevEE, MalininNL, GoltsevYV, KovalenkoAV, BoldinMP. Tumor necrosis factor receptor and Fas signaling mechanisms. Annu Rev Immunol 1999;17:331-367.

139. GreenDR, ReedJC. Mitochondria and apoptosis. Science 1998;281:1309-1312.

140. KaushalGP, UedaN, ShahSV. Role of caspase (ICE/CED3 proteases) in DNA damage and cell death in response to a mitochondrial inhibitor, antimycin A. Kidney Int 1997;52:438-445.

141. KaushalGP, SinghAB, ShanSV. Identification of caspase(ICE-like protease) gene family in rat kidney and altered expression in ischemia/reperfusion injury. Am J Physiol 1998;274:F587-595.

142. RouslinW. Mitochondrial complexs I, II, III, IV and V in myocardial ischemia and autolysis. Am J Physiol 1983;244:H743-738.

143. JaeschkeH, MitchellJR. Mitochondrial and xanthine oxidase both generate reactive oxygen species in isolated perfused rat liver after hypoxic injury. Biochem Biophys Res Commun 1989;160:140-147.

144. KowaltowskiAJ, CastihoRF, GrijalbaMT, BecharaEJ, VercesiAE. Effect of inorganic phosphate concentration of nature of inner mitochondrial membrane alterations mediated by Ca2+ ions. J Biol Chem 1996;271:2929-2934.

145. BakerJE, KalyanaramqanB. Ischemia-induced changes in myocardial paramagnetic metabolites: implications for intracellualr oxy-radical generation. FEBS Lett 1989;244:311.

146. ArduiniA, MezzettiA, PorrecaE, LapennaD, DeJuliaJ, MarzioL, et al. Effect of ischemia and reperfusion on antioxidant enzymes and mitochondrial inner membrane proteins in perfused rat heart. Biochem Biophys Acta 1988;970:113-121.

147. KurokawaT, KobayashiH, NonamiT, HaradaA, NakaoA, TakagiH. Mitochondrial glutathione redox and energy producing function during liver ischemia and reperfusion. J Surg Res 1996;66:1-5.

148. JassemW, RoakeJA. The molecular and cellular basis of reperfusion injury following organ transplantation. Transplant Rev 1998;12:14.

149. ShigenagaMK, HagenTM, AmesBN. Oxidative damage and mitochondrial decay in aging. Proc Natl Acad Sci USA 1994;91:10771-10778.

150. KroemerG, PetitP, ZamzamiN, VayssiereJL, MignotteB. The biochemistry of programmed cell death. J FASEB 1995;9:1277-1287.

151. KroemerG, DallaportaB, Resche-RigonM. The mitochondrial death/life regulation in apoptosis and necrosis. Annu Rev Physiol 1998;60:619-642.

152. HockenberyDM, OltaviZN, YinXM, MillimanCL, KorsmeyerSJ. Bcl-2 functions in an antioxidant pathway to prevent apoptosis. Cell 1993;75:241-251.

153. ReedJC, JurgensmeierJM, MatsuyamaS. Bcl-2 family proteins and mitochondria. Biochem Biophys Acta 1998;1366:127.

154. LiuX, KimCN, YangJ, JemmersonR, WangX. Induction of apoptosis program in cell-free extracts: requirement of dATP and cytochrome C. Cell 1996;86:147-157.

155. KluchRM, Bossy-WetzelE, GreenDR, NewmeyerDD. The release of cytochrome C from mitochondria: a primary site for Bcl-2 regulation of apoptosis. Science 1997;275:1132-1136.

156. LiF, SrinivasanA, WangY, ArmstrongRC, TomaselliKJ, FritzLC. Cell-specific induction of apoptosis by microinjection of cytochrome C. J Biol Chem 1997;272:30299-30305.

157. ButtleTM, SandstromPA. Oxidative stress as a mediator of apoptosis. Immunol Today 1994;15:7-10.

158. CluttonS. The importance of oxidative stress in apoptosis. Br Med Bull 1997;53:662-668.

159. UedaN, ShahSV. Endonuclease-induced DNA damage and cell death in oxidant injury to renal tubular epithelial cells. J Clin Invest 1992;90:2593-2597.

160. UedaN, WalkerPD, HsuS-M, ShahSV. Activation of a 15-kDa endonuclease in hypoxia/reoxygenation injury without morphologic feathres of apoptosis. Proc Natl Acad Sci USA 1995;92:7202-7206.

161. UedaN, KaushalGP, ShahSV. Recent advances in understanding mechanisms of renal tubular injury. Adv Renal Replace Ther 1997;4:1-8.

162. FeldenbergLR, ThevanantherS, RioM D, LeonMD, DevarajanP. Partial ATP depletion induces Fas-and Caspase-mediated apoptosis in MDCK cells. Am J Physiol 1999;276:F837-846.

163. EguchiY, ShimizuS, TsujimotoY. Intracellular ATP levels determine cell death fate by apoptosis or necrosis. Cancer Res 1997;57:1835-1840.

164. LeistM, SinsleB, CastoldiAF, KuhnleS, NicoteraP. Intracellular adenosine triphosphate (ATP) concentration: a switch in the decision between apoptosis and necrosis. J Exp Med 1997;185:1481-1486.

165. JoSK, YunSY, ChangKH, ChaDR, ChoWY, KimHK, et al. A-MSH decrease apoptosis in ischemic acute renal failure in rats: possible mechanism of this beneficial effect. Nephrol Dial Transplant 2001;16:1583-1591.

166. SuzukiK, MurtuzaB, SmolenskiRT, SammutIA, SuzukiN, KanedaY, et al. Overexpression of interleukin-1 receptor antagonist provides cardioprotection against ischemia-reperfusion injury associated with reduction in apoptosis. Circulation 2001;104 (Suppl 1):I308-313.

167. Borghi-ScoazecG, ScoazecJY, DurandF, BernuauJ, BelghitiJ, FeldmannG, et al. Apotosis after ischemia-reperfusion in human liver allografts. Liver Transpl Surg 1997;3:407-415.

168. ShahKA, ShureyS, GreenCJ. Characterization of apoptosis in intestinal ischemia-reperfusion injury - a light and electron microscopic study. Int J Exp Pathol 1997;78:355-363.

169. CowledPA, LeonardosL, MillardSH, FitridgeRA. Apoptotic cell death makes minor contribution to reperfusion injury in skeletal muscle in the rat. Eur J Vasc Endovasc Surg 2001;21:28-34.

170. KnightKR, MessinaA, HurleyJV, ZhangB, MorrisonWA, StewartAG. Muscle cells become necrotic rather than apoptotic during reperfusion of ischemic skeletal muscle. Int J Exp Pathol 1999;80:169-175.

171. HynesRO. Fibronectins. New York: Springer-Verlag; 1990.

172. YamadaKM, AotaS, AkiyamaSK, LaFlammeSE. Mechanisms of fibronectin and integrin function during cell adhesion and migration. Cold Spring Harb Symp Quant Biol 1992;57:203.

173. HynesRO. Cell adhesion and human disease. Chairman's introduction. Ciba Found Symp 1995;189:1.

174. WaynerEA, Garcia-PardoA, HumphriesMJ, McDonaldJA, CarterWG. Identification and characterization of the T lymphocyte adhesion receptor for an alternative cell attachment domain (CS-1) in plasma fibronectin. J Cell Biol 1989;109:1321-1330.

175. VartioT, LaitinenL, NarvanenO, CutoloM, ThorhellLE, ZardiL, et al. Differential expression of the ED sequence-containing form of cellular fibronectin in embronic and adult human tissues. J Cell Sci (Pt 4) 1987;88:419-430.

176. CarnemollaB, BalzaE, SiriA, ZardiL, NicotraMR, BigottiA, et al. A tumor-associated fibronectin isoform generated by alternative splicing of messenger RNA precursors. J Cell Biol 1989;108:1139-1148.

177. BrownLF, DubinD, LavigneL, LoganB, DvorakHF, VanDeWaterL. Macrophages and fibroblasts express embryonic fibronectin during cutaneous wound healing. Am J Pathol 1993;142:793-801.

178. French-ConstantC, DeWaterLV, DvorakHF, HynesRO. Reappearance of an embryonic pattern of fibroncetin splicing during wound healing in the adult rat. J Cell Biol 1989;109:903-914.

179. KnowltonAA, ConnellyCM, RomoGM, MamuyaW, ApsteinCS, BrecherP. Rapid expression of fibronectin in the rabbit heart after myocardial infarction with and without reperfusion. J Clin Invest 1992;89:1060-1068.

180. MamuyaWS, BrecherP. Fibronectin expression in the normal and hypertrophic rat heart. J Clin Invest 1992;89:392-401.

181. SchwartzbauerJE. Fibronectin: from gene to protein. Curr Opin Cell Biol 1991;3:786-791.

182. HauzenbergerD, KlominekJ, SundqvistKG. Functional specialization of fibronectin-binding beta 1-integrins in T lymphocyte migration. J Immunol 1994;153:960-971.

183. OstergaardHL, MaEA. Fibronectin induce phosphorylation of 120-kDa protein and synergizes with the T cell receptor to activate cytotoxic T cell clones. Eur J Immunol 1995;25:252-256.

184. GiancottiFG, E R. Integrin signaling. Science 1999;285:1028-1032.

185. GeorgeEL, Georges-LabouesseEN, Patel-KineRS, RayburnH, HynesRO. Defects of mesoderm, neural tube and vascular development in mouse embryos lacking fibronectin. Development 1993;119:1079-1091.

186. BlumenstockF, SabaTM, RoccarioE, ChoE, KaplanJE. Opaonic fibronectin after trauma and particle injection as determined by a peritoneal macrophage monolayer assay. J Reticuloencothel Soc 1981;30:61-71.

187. SabaTM. Fibronectin: relevance to phagocytic host response to injury. Circ Shock 1989;29:257-278.

188. ThompsonPN, BlumenstockFA, ShahDM, SabaTM. Rebound elevation of fibronectin after tissue injury and ischemia: role of fibronectin synthesis. Am J Physiol 1992;263:G437-G445.

189. SabaTM, JaffeE. Plasma fibronectin (opsonic glycoprotein): Its synthesis by vascular endothelial cells and role in cardiopulmonary integrity after trauma as related to reticuloendothelial function. Am J Med 1980;68:577-582.

190. LancerME, SabaTM, ScovillWA. Opsonic glycoprotein (plasma fibronectin) levels after burn injury. Ann Surg 1980;192:776-782.

191. DenoDC, McCaffertyMH, SabaTM, BlumenstockFA. Mechanism of acute depletion of plasma fibronectin following thermal injury in rats-appearance of a gelatinlike ligand in plasma. J Clin Invest 1984;73:20-34.

192. RichardsWO, ScovillWA, ShinB. Opsonic fibronectin deficiency in patients with intra-abdominal infection. Surgery St. Louis 1983;94:210-217.

193. CellePL, BlumenstockFA, MckinleyC, SabaTM, VincentPA, GrayV. Blood-Borne collagenous debris complexes with plasma fibronectin after thermal injury. Blood 1990;75:470-479.

194. MuellerAR, PlatzKP, HeckertC, HauslerM, GuckelbergerO, SchuppanD, et al. The extracellular matrix: an early target of preservation/reperfusion injury and acute rejection after small bowel transplantation. Transplantation 1998;65:770-776.

195. LabarrereCA, DR N, WP F. Myocardial fibrin deposits in the first month after transplantation predict subsequent coronary artery disease and graft failure in cardiac allograft recipients. Am J Med 1998;105:207.

196. SchachererC, KoopsD, WiemerJ, HartmannA, WeisM, KlepzigH, et al. Extracellular matrix structure after heart transplantation. Int J Cardio 1999;68:115-20.

197. WardC, HidenaoK, JulianAS, YuZX, VictorJF. Immunohistochemical study of fibronectin in experimental myocardial infarction. Am J Pathol 1990;137:801-810.

198. KentSP. Diffusion of plasma proteins into cells: a manifestation of cell injury in human myocardial ischemia. Am J Pahtol 1967;50:632-637.

199. PlowEF, GinsbergMH, MarquerieGA. Biochemistry of Platelets. In: InphillipsDR, ShumanMA, editors. Expression and function of adhesive proteins on the platelet surface. New York: Academic Press; 1986. p. P226-256.

200. GinsbergMH, PlowEF. Fibronectin. In: DF M, editor. Fibronectin: A contender in platelet adhesive functions. San Diego: Academic Press; 1989. p. 273-293.

201. SpornMB, RobertsAB, WakefieldLM, DeCrombruggheB. Some recent advances in the chemistry and biology of transforming growth factor-beta. J Cell Biol 1987;105:1039-1045.

202. IshikawaF, MiyazonoK, HellmanU, DrexlerH, WernstedtC, UsukiK, et al. Identification of biologic activity and the cloning and expression of platelet-derived endothelial cell growth factor. Nature 1989;338:557-562.

203. CarlyleWC, JacobsonAW, JuddDL, TianB, ChuC, HauerKM, et al. Delayed reperfusion alters matrix metalloproteinase activity and fibronectin mRNA expression in the infarct zone of the ligated rat heart. J Mol Cell Cardiol 1997;29:2451-2463.

204. WalkerPD. Alterations in renal tubular extracellular matrix components after ischemia-reperfusion injury to the kidney. Lab Invest 1994;70:339-346.

205. ZukA, BonventreJV, BrownD, MatlinKD. Polarity, integrin, and extracellular matrix dynamics in the postidchemic rat kidney. Am J Physiol 1998;275 (3 Pt 1):C711-731.

206. FujikawaLS, FosterCS, HarristTJ, LaniganJM, ColvinRB. Fibronectin in healing rabbit corneal wounds. Lab Invest 1981;45:120-129.

207. GokeM, ZukA, PodolskyDK. Regulation and function of extracellular matrix in intestinal epithelial restitution in vitro. Am J Physiol (Gastrointest Liver Physiol) 1996;34:G729-740.

208. CharashWE, VincentPA, McKeown-LongoPJ, SabaTM, LewisE, LewisMA. Kinetics of plasma fibronectin: increased lung tissue incorporation after postoperative bacteremia. Am J Physiol 1991;260 (Regulatory Integrative Comp. Physiol. 29):R 553-R 562.

209. TorikataC, VilligerD, KihnC, McDonaldJA. Ultrastructural distribution of fibronectin in normal and fibrotic human lung. Lab Invest 1985;52:399-408.

210. KowalczykAP, TullohRH, McKeown-LongoPJ. Polarized fibronectin secretion and localized matrix assembly sites correlate with subendothelial matrix formation. Blood 1990;75:2335-2342.

211. WheatleyEM, VincentPA, McKeown-LongoPJ, SabaTM. Effect of fibronectin on permeability of normal and TNF-treated lung endothelial cell monolayers. Am J Physiol 1993;264 (Regulatory Integrative Comp. Physiol. 33):R 90-96.

212. AoshibaK, RennardSI, SpurzemJR. Fibronectin supports bronchial epithelial cell adhesion and survival in the absence of growth factors. Am J Physiol 1997;273:L684-693.

213. ManiscalcoWM, WatkinsRH, CampbellMH. Expression of fibronectin mRNA splice variants by rabbit lung in vivo and by alveolar type II cells in vitro. Am J Physiol 1996;271 (6 Pt 1):L 972-980.

214. CharashWE, VincentPA, SabaTM, MinnearFL, McKeown-LongoPJ, MigliozziJA, et al. Immunofluorescent analysis of plasma fibronectin incorporation into the lung during acute inflammatory vascular injury. Am Rev Respir Dis 1993;148:467-476.

215. LimperAH, RomanJ. A versatile matrix protein with roles in thoracic development, repair and infection. Chest 1992;101:1663-73.

216. ResnikoffM, BrienT, VincentPA, RotundoRF, LewisE, Mckeown-LongoPJ, et al. Lung matrix incorporation of plasma fibronectin reduces vascular permeability in postsurgical bacteremia. Am J Physiol 1999;277:L749-759.

217. CurtisTM, McKeown-LongoPJ, VincentPA, HomanSM, WheatleyEM, SabaTM. Fibronectin attenuates increased endothelial monolayer permeability after RGD peptide, anti-alpha 5 beta 1, or TNF-alpha exposure. Am J Physiol 1995;269 (2 Pt 1):L 248-260.

218. SakaiT, JohnsonKJ, MurozonoM, SakaiK, MA M, WielochT, et al. Plasma fibronectin supports neuronal survival and reduces brain injury following transient focal cerebral ischemia but is not essential for skin-wound healing and hemostasis. Nature Med 2001;7:324-330.

219. YanakaK, CamarataPJ, SpellmanSR, McCarthyJB, FurchtLT, LowWC, et al. Synthetic fibronectin peptides and ischemic brain injury after transient middle cerebral artery occlusion in rats. J Neurosurg 1996;85:125-130.

220. YanakaK, CamarataPJ, SpellmanSR, McCarthyJB, FurchtLT, LowWC. Antagonism of leukocyte adherence by synthetic fibronectin peptide V in a rat model of transient focal cerebral ischemia. Neurosurgery 1997;40:557-564.

221. CoitoAJ, Kupiec-WeglinskiJW. Extracellular matrix proteins in organ transplantation. Transplantation 2000;69:2465-2473.

222. CoitoAJ, KatoH, AzimiR, Kupiec-WeglinskiJW. Chronic allograft rejection versus tolerance: a critical role for EIIIA+ fibronectin. Transplantation Proc 2001;33:526-527.

223. StegallMD, ElicesM, PietraW, ShepardG, GupC, GillRG. Different roles of a4-integrin/VCAM-1 and a4/fibronectin interactions in allograft rejection. Transplantation Proc 1999;31:786.

224. PaczekL, PazikJ, BartlomiejczykI, GradowskaL, M L, RowinskiW, et al. Chronic kidney allograft rejection is accompanied by increased urinary excretion of fibronectin. Transplantation Proc 2000;32:1333-1334.

225. JulianoRL, HaskillS. Signal transduction from the extracellular matrix. J Cell Biol 1993;120:577-585.

226. BearzA, G T, S F, S M, A C. Adhesion to fibronectin promotes the activation of the p125 FAK/Zap-70 complex in human T cells. Immunol 1999;98:564-568.

227. MatsuyamaT, YamadaA, KayJ, YamadaKM, AkiyamaSK, SchlossmanSF, et al. Activation of CD4 cells by fibronectin and anti-CD3 antibody: a synergistic effect mediated by VLA-5 fibronectin receptor complex. J Exp Med 1989;170:1133-1148.

228. YamadaA, NikaidoT, NojimaY, SchlossmanSF, MorimotoC. Activatio of human CD4 T lymphocytes: interaction of fibronectin with VLA-5 receptor on CD4 cells induces the AP-1 transcription factor. J Immunol 1991;146:53-56.

229. HershkovizR, GilatD, MironS, MekoriYA, AderkaD, WallachD, et al. Extracellular matrix induces tumor necrosis factor-a secretion by an interaction between resting CD4+ Tcells and macrophages. Immunology 1993;78:50-57.

230. CoitoAJ, BrownLF, PetersJH, Kupiec-WeglinskiJW, L V. Expression of fibronectin splicing variants in organ transplantation: a differential pattern between rat cardiac allograft and isografts. Am J Pathol 1997;150:1757-1772.

231. CoitoAJ, BinderJ, BrownLF, deSousaM, VanDeWaterL, Kupiec-WeglinskeJW. Anti-TNF-a treatment down-regulates the expression of fibronectin and decreases cellular infiltration of cardiac allografts in rats. J Immunol 1995;154:2949-2958.

232. CoitoAJ, KoromS, GraserE, VolkHD, VanDeWaterL, Kupiec-WeglinskiJW. Blockade of very late antigen-4 integrin binding to fibronectin in allograft recipients: I. Treatment with concecting segment-1 peptides prevents acute rejection by suppressing intragraft mononuclear cell accumulation, endothelial activation, and cytokine expression. Transplantation 1998;65:699-706.

233. KoromS, HancockWW, CoitoAJ, Kupiec-WeglinskiJW. Blockade of very late antigen-4 integrin binding to fibronectin in allograft recipients. II. Treatment with connecting segment-1 peptides prevents chronic rejection by attenuating arteriosclerotic development and suppressing intragraft T cell and macrophage activation. Transplantation 1998;65:854-859.

234. CoitoAJ, OnoderaK, KatoH, BusuttilRW, Kupiec-WeglinskiJW. Fibronectin-mononuclear cell interactions regulate type 1 helper T cell cytokine net work in tolerant transplant recipients. Am J Pathol 2000;157:1207-1218.

235. BrunmarkA, RourkeAM O. Augmentation of mature CD4+ T cell response to isolated antigenic class II proteins by fibronectin and intercellular adhesion molecule-1. J Immunol 1997;159:1676-1685.

236. WahlSM, AllenJB, HinesKL, ImamichiT, WahlAM, FurchtLT, et al. Synthetic fibronectin peptides suppress arthritis in rats by interrupting leukocyte adhesion and recruitment. J Clin Invest 1994;94:655-662.

237. FergusonTA, MizutaniH, KupperTS. Two integrin-binding peptides abrogate Tcell-mediated immune responses in vivo. Proc Natl Acad Sci USA 1991;88:8072-8076.

238. EsparzaJ, VilardellC, CalvoJ, JuanM, VivesJ, Urbano-MarquezA, et al. Fibronectin upregulates gelatinase B (MMP-9) and induces coordinated expression of gelatinase A (MMP-2) and its activator MT1-MMP (MMP-14) by humanTlymphocyte cell lines. A process repressed through RAS/MAP kinase signaling pathways. Blood 1999;94:2754-2766.

239. ClarkRA. Fibronectin matrix deposition and fibronectin receptor expression in healing and normal skin. J Invest Dermatol 1990;94:128S-134S.

240. GrinnellF. Fibronectin and wound healing. J Cell Biochem 1984;26:107-116.

241. JoannT, RobertEB, JamesNW, BradleyWM, HollyHB, KeithAY, et al. Fibronectin fragments modulate monocyte VLA-5 expression and monocyte migration. J Clin Invest 1999;104:419-430.

242. SugaharaH. Induction of programmed cell death in human hematopoietic cell lines by fibronectin via its interaction with very late antigen 5. J Exp Med 1994;179:1757-1766.

243. McCutcheonJC, HartSP, CanningM, RossK, HumphriesMJ, DransfiedI. Regulation of macrophage phagocytosis of apoptotic neutrophils by adhesion to fibronectin. Journal of Leukocyte Biology 1998;64:600-607.

244. HaddenHL, HenkeCA. Induction of lung fibroblast apoptosis by soluble fibronectin peptides. Am J Respir & Criti Care Med 2000;162 (4pt1):1553-1560.

245. ChappellVL, LaGroneL, MileskiWJ. Inhibition of leukocyte-mediated tissue destruction by synthetic fibronectin peptide (Trp-9-Tyr). J Burn Care & Rehabilitation 1999;20:505-510.

246. VadayGG, HershkovizR, RahatMA, LahatN, CahalonL, LiderO. Fibronectin-bound TNF-alpha stimulates monocyte matrix metalloproteinase-9 expression and regulates chemotaxis. J Leukocyte Biology 2000;68:737-747.

247. JacobsM, StaufenbergerS, GergsU, MeuterK, BrandstatterK, HafnerM, et al. Tumor necrosis factor-alpha at acute myocardial infarction in rats and effects on cardiac fibroblasts. J Mol Cell Cardiol 1999;31:1949-1959.

248. ManiscalcoWM, SinkinRA, WatkinsRH, CampbellMH. transforming growth factor-beta 1 modulates type II cell fibronectin and surfactant protein C expression. Am J Physiol 1994;267 (5 Pt 1):L 569-577.

249. NickeleitV, ZagachinL, NishikawaK, PetersJH, HynesRO, CovinRB. Embryonic fibronectin isoforms are synthesized in cresents in experimental autoimmune glomerulonephritis. Am J Pathol 1995;147:965-978.

250. TimplR, RohdeH, GehronRP, RennardSI, FoidartJM, MartinGR. Laminin-a glycoprotein from basement membranes. J Biol Chem 1979;254:9933-9937.

251. ColognatoH, YurchencoPD. Form and function: the laminin family of heterotrimers. Dev Dyn 2000;218:213-234.

252. FrieserM, NockerH, PauschF, FoderC, HahnA, DeutzmannR, et al. Cloning of the mouse laminin alpha 4 gene: expression in a subset of endothelium. Eur J Biochem 1997;246:727-735.

253. SorokinLM, FrieserM, PauschF, KrogerS, OhageE, NewbyAC. Developmental regulation of laminin alpha 5 suggests a role in epithelial and endothelial cell maturation. Dev Biol 1997;189:285-300.

254. BreesDK, OgleRC, WilliamsJCJr. Laminin and firbronectin content of mouse glomerular and tubular basement membrane. Renal Physiology & Biochemistry 1995;18:1-11.

255. Peutz-KootstraCJ, HansenK, DeHeerE, AbrassCK, BruijnJA. Differential expression of laminin chains and anti-laminin autoantibodies in experimental lupus nephritis. J Pathol 2000;192:404-412.

256. MooneyA, JacksonK, BaconR, StreuliC, EdwardsG, BassukJ, et al. Type IV collagen and laminin regulate glomerular mesangial cell susceptibility to apoptosis via beta(1)-mediated survival signals. Am J Pathol 1999;155:599-606.

257. AumailleyM, SmythN. The role of laminins in basement membrane function. J Anat 1998;193:1-21.

258. GullbergD, TigerCF, VellingT. Laminins during muscle development and in muscular dystrophies. Cellular and Molecular Life Sciences 1999;56:442-460.

259. KreifergJA, DonovanMJ, GoldsteinSL, RennkeH, ShepherdK, JonesRC, et al. a3beta-1 integrin has a crucial role in kidney and lung organogenesis. Development 1996;122:3537-3547.

260. LaurentGP, MarylineA, FlaviaS, OlivierP, ChristineR, Jean-paulO, et al. The short arm of the laminin 2 chain plays a pivotal role in the incorporation of laminin 5 into the extracellular matrix and in cell adhesion. J Cell Biol 2001;153:835-850.

261. GeberhiwotT, AssefaD, KortesmaaJ, IngerpuuS, PedrazaC, WondimuZ, et al. Laminin-8 (alpha4gamma1) is synthesized by lymphoid cells, promotes lymphocyte migration and costimulates T cell proliferatiojn. J Cell Sci 2001;114 (Pt 2):423-33.

262. SixtM, EngelhardtB, PauschF, HallmannR, WendlerO, SorokinLM. Endothelial cell laminin isoforms, laminin 8 and 10, play decisive roles in T cell recruitment across the blood-brain barrier in experimental autoimmune. J Cell Biol 2001;153:933-946.

263. Kupiec-WeglinskiJW, DESousaM. Lymphocyte traffic is modified in vivo by anti-laminin antibody. Immunol 1991;72:312-313.

264. Silva-BarbosaSD, Cotta-deAlmeidaV, RiedererI, DeMeisJ, DardenneM, BonomoA, et al. Involvement of laminin and its receptor in abrogation of heart graft rejection by autoreactive T cell from Trypanosoma cruzi-infected mice. J Immunol 1997;159:997-1003.

265. QuondamatteoF, MichalskiS, WeslingF, MiosgeN, SchlemmingerR, HerkenR. Laminin localization in enterocytic basement membrane of rat small bowel grafts. A light and electron microscopic study. Matrix Biology 1998;17:647-655.

266. Lannes-VieiraJ, ChammasR, Villa-VerdeDM, Vannier-dos-SantosMA, MellocoelhoV, deSouzaSJ, et al. Extracellular matrix components of the mouse thymic microenvironment. III. Thymic epithelial cells express the VLA6 complex that is involved in laminin-mediated interactions with thymocytes. Int Immunol 1993;5:1421-1430.

267. ImhofBA, RuizP, HesseB, PalaciosR, DunonD. EA-1, a novel adhesion molecule involved in the homing of progenitor T lymphocytes to the thymus. J Cell Biol 1991;114:1069-1078.

268. MuellerAR, PlatzKP, HaakM, UndiH, MullerC, KottgenE, et al. the release of cytokines, adhesion molecules, and extracellular matrix parameters during and after reperfusion in human liver transplantation. Transplantation 1996;62:1118-1126.

269. HamannGF, OkadaY, FitridgeR, delZoppoGJ. Microvascular basal lamina antigens disappear during cerebral ischemia and reperfusion. Stroke 1995;26:2120-6.

270. PlatzKP, HahnP, SchirmeierA, LangM, StangeB, RayesN, et al. Basement membrane changes associated with cold temperature. Transplantation Proceedings 2000;32:1258-1260.

271. FrisdalE, TeigerE, LefaucheurJP, AdnotS, PlanusE, LafumaC, et al. Increased expression of gelatinases and alteration of basement membrane in rat soleus muscle following femoral artery ligation. Neuropathology and Applied Neuropathology 2000;26:11-21.

272. HershkovizR, GoldkornI, LiderO. Tumor necrosis factor-a interacts with laminin and function as a pro-adhesive cytokine. Immunol 1995;85:125-130.

273. FantiniGA, ConteMS. Pulmonary failure following lower torso ischemia: clinical evidence for a remote effect of reperfusion injury. American Surgeon 1995;61:316-319.

274. AdamDJ, MohanIV, StuartWPetal. Community and hospital outcome from ruptured abdominal aortic aneurysm within the catchment area of a regional vascular surgical service. J Vasc Surg 1999;30:922-928.

275. HuberTS, HarwardTR, FlynnTCetal. Operative mortality rates after elective infrarenal aortic reconstructions. J Vasc Surg 1995;22:287-293.

276. WelbournCR, GoldmanG, KobzikL, PatersonIS, ValeriCR, SheproD, et al. Role of neutrophil adherence receptors (CD18) in lung permeability following lower torso ischemia. Cir Res 1992;71:82-86.

277. KlausnerJM, AnnerH, PatersonIS, KobzikL, ValeriCR, SheproD, et al. Lower torso ischemia-induced lung injury is leukocyte dependent. Ann Surg 1988;208:761-767.

278. WelbournCR, GoldmanG, PatersonIS, ValeriCR, SheproG, HechtmanHB. Pathophsiology of ischemia reperfusion injury: central role of the neutrophil. Br J Surg 1991;78:651-655.

279. KlausnerJM, PatersonIS, ValeriCR. Limb ischemia-induced increase in permeability is mediated by leukocytes and leukotrienes. Ann Surg 1988;208:755-760.

280. KyriakidesC, AustenWGJr, WangY, FavuzzaJ, MooreFDJr, HechtmanHB. Neutrophil mediated remote organ injury after lower torso ischemia and reperfusion is selectin and completment dependent. J Trauma 2000;48:32-38.

281. HattoriR, HamiltonKK, FugateRD, McEverRP, SimsPJ. Stimulated secretion of endothelial von Willebrand factor is accompanied by rapid redistribution to the cell surface of the intracellular granule membrane protein GMP-140. J Bio Chem 1989;264:7768-7771.

282. WalcheckB, KhanJ, FisherJM, WangBB, FiskRS, PayanDG, et al. Neutrophil rolling altered by inhibition of L-selectin shedding in vitro. Nature 1996;380:720-723.

283. KyriakidesC, FavuzzaJ, WangY, AustenWGJr, MooreFDJr, HechtmanHB. Recombinant soluble P-selectin glycoprotein ligand 1 moderates local and remote injuries following experiment lower-torso ischemia. Br J Surg 2001;88:825-830.

284. DiamondMS, SpringerTA. A subpopulation of Mac-1 (CD11b/CD11 8) molecules mediates neutrophil adhesion to ICAM-1 and fibronogen. J Cell Biol 1993;120:545-556.

285. LindsayTF, HillJ, OrtizF, RudolphAL, ValeriCR, HechtmanHB, et al. Blockade of complement activation prevents local and pulmonary albumin leak after lower torso ischemia-reperfusion. Ann Surg 1992;216:677-683.

286. HillJ, LindsayTF, OrtizF, YehCG, HechtmanHB, MooreFDJr. Soluble complement receptor type 1 ameliorates the local and remote organ injury after intestinal ischemia-reperfusion in the rat. J Immunol 1992;149:1723-1728.

287. SeekampA, TillGO, MulliganMS, PaulsonJC, AndersonDC, MiyasakaM, et al. Role of selectins in local and remote tissue injury following ischemia and reperfusion. Am J Pathol 1994;144:592-598.

288. HarkinDW, BarrosD'SaAAB, McCallionK, HoperM, HallidayMI, CampbellFC. Bactericidal/permeability-increasing protein attenuates systemic inflammation and acute lung injury in porcine lower limb ischemia reperfusion injury. Ann Surg 2001;234:233-244.

289. SoccalPM, GascheY, PacheJC, SchneuwlyO, SlosmanDO, MorelDR, et al. Matrix metalloproteinase correlate with alveolar-capillary permeability alteration in lung ischemia-reperfusion injury. Transplantation 2000;70:998-1005.

290. McCannUG2nd, GottoLA, SearlesB, CarneyDE, LutzCJ, PiconeAL, et al. Matrix metalloproteinase inhibitor: differential effects on pulmonary neutrophil and monocyte sequestration following cardiopulmonary bypass. J Extra Corpor Technol 1999;31:67-75.

291. FusekM, VetuickaV. Aspartic proteinases: physiology and pathology. CRC Press Boca Roca Raton 1995:FL 1-35.

292. HayashiT, RushWL, TravisWD, LiottaLA, Steler-StevensonWG, FerransVJ. Immunohistochemical study of matrix metalloproteinases and their tissue inhibitors in pulmonary Langerhan's cell granulomatosis. Arch Pathol Lab Med 1997;121:930-937.

293. YanoM, OmotoY, YamakawaY, NakashimaY, KiriyamaM, SaitoY, et al. Increased matrix metalloproteinase 9 activity and mRNA expression in lung ischemi-reperfusion injury. J Heart Lung Transplant 2001;20:679-686.

294. RicouB, NicodL, LacrazS, WelgusHG, SuterPM, DayerJM. Matrix metalloproteinases and TIMP in acute respiratory distress syndrome. Am J Respir Crit Care Med 1996;154:346-352.

295. MautinoG, OliverN, ChanezP, BousquetJ, CaponyF. Increased release of matrix metalloprotinase-9 in bronchoalveolar lavage fluid and by alveolar macrophages of asthmatics. Am J Respir Cell Mo Biol 1997;17:583-591.

296. ParksWC, Lopez-BoadoYS, WilsonCL. Matrilysin in epithelial repair and defense. Chest 2001;120:Suppl 36s-41s.

297. TorriK, IidaKI, MiyazakiY, SagaS, KonkohY, TaniguchiH, et al. Higher concentration of matrix metalloproteinases in bronchoalveolar lavage fluid of patients with adult respiratory distress syndrome. Am J Respir Crit Care Med 1997;155:43-46.

298. CarneyDE, LutzCJ, PiconeAL, GattoLA, RamamurthyNS, GolubLM, et al. Matrix metalloproteinase inhibitor prevents acute lung injury after cardiopulmonary bypass. Circulation 1999;100:400-406.

299. TobiasKJH, BalcomV, CarlosFernandez-Del, BozenaAA, AndrewLW. Matrix metalloproteinase-9 promotes neutrophil migration and alveolar capillary leakage in pancreatitis-associated lung injury in the rat. Gastroenterology 2002;122:188-201.

300. BrigitteN, NikoZ, AndreasV, KlausP, Claus-DieterH, BernhardH. Mechanisms of acute inflammatory lung injury induced by abdominal sepsis. Int Immunol 1999;11:217-227.

301. PuginJ, VerghsesG, WidmerMC, MatthayMA. The alveolar space is the site of intense inflammatory and profibrotic reactions in the early phase of acute respiratory distress syndrome. Crit Care Med 1999;27:304-312.

302. RoachDM, FitridgeRA, LawPE, MillardSH, VareliasA, CowledPA. Up-regulation of MMP-2 and MMP-9 leads to degradation of type IV collagen during skeletal muscle reperfusion injury, protection by MMP inhibitor, doxycycline. Eur J Vasc Endovasc Surg 2002;23:260-9.

303. EnricoA, JudithNH, WangC, AnilH, MarcelS. Glycine preserves function and decreases necrosis in skeletal muscle undergoing ischemia and reperfusion injury. Surgery 2001;129:231-235.

304. ManginoMJ, MurphyMK, GrabauGG, AndersonCB. Protective effects of glycine during hypotheric renal ischemia-reperfusion injury. Am J Physiol 1991;261:F841-848.

305. YinM, ZhongZ, ConnorHD, BunzendahlH, FinnWF, RusynI, et al. Protective effect of glycine on renal injury induced by ischemia/reperfusion in vivo. Am J Physiol Renal Physiol 2002;282:F417-423.

306. PapanastasiouS, EstsaleSE, Homer-VanniasinkamS, MathieRT. Protective effect of preconditioning and adenosine pretreatment in experimental skeletal muscle reperfusion injury. Br J Surg 1999;86:916-922.

307. SalvatoreC, EmanuelaM, LauraD, AchillePC, KarlA, DennisPR, et al. Protective effects of a new stable, highly active SOD mimetic, M40401 in splanchnic artery occlusion and reperfusion. Br J Pharmaco 2001;132:19-29.

308. HukI, BrovkovychV, ViliJN, WeigelG, NeumayerC, PartykaL, et al. Bioflavonoid quercetin scavenges superoxide and increase nitric oxide concentration in ischemia-reperfusion injury: an experimental study. Br J Surg 1998;85:1080-1085.

309. ZughaibME, TangXL, SchlemanM, JeroudiMO, BolliR. Beneficial effects of MDL 74405 a cardioselective water soluble alpha-tocopherol analogue, on the recovery of function of stunned myocardium in intact dogs. Cardiovasc Res 1994;28:235-241.

310. FerreiraRF, MileiJ, LiesuyS. Antioxidant action of vitamins A and E in patients submitted to coronary artery bypass surgery. Vasc Surg 1991;25:191-195.

311. MurphyME, KolvenbachR, AleksisM, HansenR, SiesH. Antioxidant depletion in aortic cross-clamping ischemia: increase of the plasma alpha-tocopheryl quinone/alpha-tocopherol ration. Free Rad Biol Med 1992;13:95-100.

312. NovelliGP, AdembriC, GandiniE, OrlandiniSZ, PapucciL, formigliL, et al. Vitamin E protects human skeletal muscle from damage during surgical ischemia-reperfusion. Am J Surg 1997;173:206-209.

313. GurkeL, MarxA, SutterP-M, SeeligJ, HarderF, HebererM. Allopurinol improves postischemia skeletal muscle performance and endurance but not high-energy phosphate levels. Transplantation Proc 1995;27:2840-2841.

314. SalahudenAK, ClarkEC, NathKA. Hydrogen peroxide-induced renal injury: a protective role for pyruvate in vitro and in vivo. J Clin Invest 1991;88:1886-1893.

315. CicaleseL, LeeK, SchrautW, WatkinsS, BorleA, StankoR. Pyruvate prevents ischemia-reperfusion mucosal injury of rat small intestine. Am J Surg 1996;171:97-100.

316. CicaleseL, YacoubW, SubbotinV, KuddusR, FungJJ, StankOR, et al. Pyruvate inhibits the chronic damage which ensues after ishemia/reperfusion injury of kidneys. Transplantation Proc 1999;31:1033.

317. SileriP, SchenaS, MoriniS, RastelliniC, PhamS, BenedettiE, et al. Pyruvate inhibits hepatic ischemia-reperfusion injury in rats. Transplantation 2001;72:27-30.

318. MisterM, NorisM, SzymczukJ, AzzolliniN, AielloS, AbbateM, et al. Propionyl-L-carnitine prevents renal function deterioration due to ischemia/reperfusion. Kidney Int 2002;61:1064-1078.

319. KellyKJ, PlotkinZ, DagherPC. Guanosine supplementation reduces apoptosis and protects renal function in the setting of ischemic injury. J Clin Invest 2001;108:1291-1298.

320. LassA, SuessenbacherA, WolkartG, MayerB, BrunnerF. Functional and analytical evidence for scavenging of oxygen radicals by L-arginine. Mol Pharmacol 2002;61:1081-1088.

321. GaoF, YaoCL, GaoE, MoQZ, YanWL, McLanughlinR, et al. Enhancement of glutathione cardioprotection by ascorbic acid in myocardial reperfusion injury. J Pharmacol Exp Ther 2002;301:543-550.

322. MelinJ, HellbergO, LarssonE, ZezinaL, FellstromBC. Protective effect of insulin on ischemic renal injury in diabetes mellitus. Kidney Int 2002;61:1383-1392.

323. ArumuganTV, ShielsIA, WoodruffTM, ReidRC, FairlieDP, TaylorSM. Protective effect of a new C5a receptor antagonist against ischemia-reperfusion injury in the rat small intestine. J Surg Res 2002;103:260-267.

324. RuehlML, OrozcoJA, StolerMB, McDonaghPF, CoullBM, RitterLS. Protective effects of inhibiting both blood and vascular selectins after stroke and reperfusion. Neurol Res 2002;24:226-232.

325. EppingerMJ, WardPA, BollingSF, DeebGM. Regulatory effects of interleukin-10 on lung ischemia-reperfusion injury. J Thorac Cardiovasc Surg 1996;112:1301-1305.

326. EnglesRE, HuberTS, ZanderDS, HessPJ, WelbornMB, MoldawerLL, et al. Exogenous human recombinant interleukin-10 attenuates hindlimb ischemia-reperfusion. J Surg Res 1997;69:425-428.

327. DengJP, KohdaY, ChiaoH, WangY, HuX, HewittSM, et al. Interleukin-10 inhibits ischemic and cisplatin-induced acute renal injury. Kidney Int 2001;60:2118-2128.

328. HaywardR, NossuliTO, ScaliaR. Cardioprotective effects of interleukin-10 in murine ischemia-reperfusion. Eur J Pharmacol 1997;334:157-163.

329. GrunenfelderJ, MiniatiDN, MurataS, FalkV, HoytEG, KownM, et al. Upregulation of Bcl-2 through caspase-3 inhibition ameliorate ischemia/reperfusion injury in rat cardiac allograft. Circulation 2001;104:202-206.

330. KrishnadasanB, NaiduB, RosengartM, FarrAL, BarnesA, VerrierED, et al. Decreased lung ischemia-reperfusion injury in rats after preoperation administration of cyclosporine and tacrolimus. Thorac Cardiovasc Surg 2002;123:756-767.

331. YangCW, AhnHJ, HanHJ, KimWY, LiC, ShinMJ, et al. Pharmacological preconditioning with low-dose cyclosporine or FK 506 reduces subsequent ischemia/reperfusion injury in rat kidney. Transplantation 2001;72:1753-1759.

332. CurdioR, MariB, LouisK, RostagnoP, Saint-PaulMC, GiudicelliJ, et al. Rat liver injury after normothermic ischemia is prevented by a phophinic matrix metalloproteinase inhibitor. FASEB 2002;16:93-95.

333. CheungPY, SawickiG, WozniakM, WangW, RadomskiMW, SchulzR. Matrix metalloproteinase-2 contributes to ischemia-reperfusion injury in the heart. Circulation 2000;101:1833-1839.

334. NagaseH, WoessnerJ. Matrix metalloproteinase. J Biol Chem 1999;274:21491-21494.

335. DavisV, PersidskaiaR, Baca-RegenL, ItohY, NagaseH, PersidskyY, et al. Matrix metalloproteinase-2 production and its binding to the matrix are increased in abdominal aortic aneurysms. Arterioscler Thromb Biol 1998;18:1625-1633.

336. MatrisianLM. The matrix-degrading metalloproteinases. BioEssays 1992;14:455-463.

337. GearingAJH, BeckettP, ChristodoulouM, ChurchillM, ClementsJ, DavidsonAH, et al. Processing of tumor necrosis factor-a precursor by metalloproteinases. Nature 1994;370:555-557.

338. Ben-YosefY, LahatN, ShapiroS, BittermanH, MillerA. Regulation of endothelial matrix metalloproteinase-2 by hypoxia/reoxygenation. Circ Res 2002;90:784-791.

339. FujimuraM, GascheY, Morita-FujimuraY, MassengaleJ, KawaseM, ChanPH. Early appearance of activated matrix metalloproteinase-9 and blood-brain barrier disruption in mice after focal cerebral ischemia and reperfusion. Brain Res 1999;842:92-100.

340. PlanasAM, SoleS, JusticiaC. Expression and activation of matrix metalloproteinase-2 and -9 in rat brain after transient focal cerebral ischemia. Neurobiol Dis 2001;8:834-846.

341. HeoJH, LuceroJ, AbumiyaT, KoziolJA, CopelandBR, delZoppoGJ. Matrix metalloproteinases increase very early during experimental focal cerebral ischemia. J Cereb Blood Flow Metab 1999;19:624-633.

342. GascheY, CopinJC, SugawaraT, FujimuraM, ChanPH. Matrix metalloproteinase inhibition prevents oxidative stress-associated blood-brain barrier disruption after transient focal cerebral ischemia. J Cereb Blood Flow Metab 2001;21:1393-1400.

343. GascheY, FujimuraM, Morita-FujimuraY, CopinJ-P, KawaseM, MassengaleJ, et al. Early appearance of activated matrix metalloproteinase-9 after focal cerebral ischemia in mice: a possible role in blood-brain barrier dysfunction. J Cereb Blood Flow Metab 1999;19:1020-1028.

344. RosenbergGA, CunninghamLA, WallaceJ, AlexanderS, EstradaEY, GrosseteteM, et al. Immunohistochemistry of matrix metalloproteinases in reperfusion injury to rat brain: activation of MMP-9 linked to stromelysin-1 and microglia in cell cultures. Brain Res 2001;893:104-112.

345. Gursoy-OzdemirY, BolayH, SarigasO, DalkaraT. Role of endothelial nitric oxide generation and peroxynitrite formation in reperfusion injury after focal cerebral ischemia. Stroke 2000;31:1974-1981.

346. Steler-StevensonWG. Matrix metalloproteinase in angiogenesis: a moving target for therapeutic intervention. J Clin Invest 1999;103:1237-1241.

347. TakahashiS, BarryAC, FactorSM. Collagen degradation in ischemic rat hearts. Biochem J 1990;265:233-241.

348. DanielsenCC, WiggersH, AndersenHR. Increased amounts of collagenase and gelatinase in porcine myocardium following ischemia and reperfusion. J Mol Cell Cardiol 1998;30:1431-1442.

349. RobertHC, ShizukoT, ZhaoM, EdmundHS, CalvinE. Collagen loss in the stunned myocardium. Circulation 1992;85:1483-1490.

350. EtohT, JoffsC, DeschampsAM, DavisJ, DowdyK, HendrickJ, et al. Myocardial and interstitial matrix metalloproteinase activity after acute myocardial infarction in pigs. Am J Physiol Heart Circ Physiol 2001;281:H987-994.

351. RajagopalanS, MengXP, RamasamyS, HarrisonDG, GalisZS. Reactive oxygen species produced by macrophage-derived foam cells regulate the activity of vascular matrix metalloproteinases in vitro: implications for atherosclerotic plaque stability. J Clin Invest 1996;98:2572-2579.

352. FrearsER, ZhangZ, BlakeDR, O'ConnellJP, WinyardPG. Inactivation of tissue inhibitor of metalloproteinase-1 by peroxynitrite. FEBS Lett 1996;381:21-24.

353. YasminW, StrynadkaKD, SchulzR. Generation of peroxynitrite contributes to ischemia/reperfusion injury in isolated rat hearts. Cardiovasc Res 1997;33:422-432.

354. BaghelaiK, MarktannerR, DattiloJB, DattiloMP, JakoiER, YagerDR, et al. Decreased expression of tissue inhibitor of metalloproteinase 1 in stunned myocardium. J Surg Res 1998;77:35-39.

355. LindseyM, WedinK, BrownMD, KellerC, EvansAJ, SmolenJ, et al. Matrix-dependent mechanism of neutrophil-mediated release and activation of matrix metalloproteinase 9 in myocardial ischemia/reperfusion. Circulation 2001;103:2181-2187.

356. Gallea-RobacheS, MorandV, MilletS, BrunearJM, BhatnaagarN, ChouaibS, et al. A metalloproteinase inhibitor blocks the shedding of soluble cytokine receptors and processing of transmembrane cytokine precursor in human monocytic cells. Cytokine 1997;9:340-346.

357. LombardMA, WallaceTL, KubicekMF, PetzoldGL, MitchellMA, HendgesSK, et al. Synthetic matrix metalloproteinase inhibitor and tissue inhibitor of metalloproteinase (TIMP)-

2 but not TIMP-1, inhibit shedding of tumor necrosis factor-alpha receptor in a human colon adenocarcinoma (Colo 205) cell line. Cancer Res 1998;58:4001-4007.

358. SchonbeckU, MachF, LibbyP. Generation of biologically active IL-1 beta by matrix metalloproteinase: a novel caspase-1-independent pathway of IL-1 beta processing. J Immunol 1998;161:3340-3346.

359. OpdenakkerG. On the roles of extracellular matrix remodeling by gelatinase B. Verh K Acad Geneeskd Belg 1997;59:489-514.

360. O'ConnorCM, FitzGeraldMX. Matrix metalloproteases and lung disease. Thorax 1994;49:602-609.

361. ShapiroSD, SeniorRM. Matrix metalloproteinases (matrix degradation and more). Am J Respir Cell Mol Biol 1999;20:1100-1102.

362. YaoPM, BuhlerJM, d'OrthoMP, LebargyF, DelclauxC, HarfA, et al. Expression of matrix metalloproteinase gelatinase A and B by cultured epithelial cells from human bronchial explants. J Biol Chem 1996;26:15580-15589.

363. GottschallPE, YuX. Cytokines regulate gelatinase A and B (Matrix metalloproteinase2 and 9) activity in cultured rat astrocytes. J Neurochem 1995;64:1513-20.

364. LyonsPD, BenvenisteEN. Cleavage of membrane-associated ICAM-1 from astrocytes: involvement of a metalloproteinase. Glia 1998;22:103-112.

365. PreeceG, MurphyG, AgersA. Metalloproteinase-mediated regulation of L-selectin levels on leukocytes. J Biol Chem 1996;271:11634-11640.

366. JainS, BicknellGR, NicholsonML. Molecular changes in extracellular matrix turnover after renal ischemia-reperfusion injury. Br J Surg 2000;87:1188-1192.

367. WalkerPD, KaushalGP, ShahSV. Meprin A, the major matrix degrading enzyme in renal tubules, produces a novel nidogen fragment in vitro and vivo. Kidney Int 1998;53:1673-1680.

368. TrachtmanH, ValderramaE, DietrichJM, BondJS. The role of meprin A in the pathogenesis of acute renal failure. Biochem Biophys Res Commun 1995;208:498-505.

369. HibbsMS. Expression of 92 kDa phagocyte gelatinase by inflammatory and connective tissue cells. Matrix Suppl 1992;1:51-57.

370. GuerinCW, HollandPC. Synthesis and secretion of matrix-degrading metalloproteinases by human skeletal muscle satellite cells. Dev Dyn 1995;202:91-99.

371. BaxterBT, McGeeGS, ShivelyVP, DrummondIA, DixitSN, YamauchiM, et al. Elastin content, cross-links and mRNA in normal and aneurysmal human aorta. J Vasc Surg 1992;16:192-200.

372. BrophyCM, ReillyJM, SmithGJW, TilsonMD. The role of inflammation in nonspecific abdominal aortic aneurysm disease. Ann Vasc Surg 1991;5:229-233.

373. VineN, PowellJT. Metalloproteinases in the degenerative aortic disease. Clin Sci 1991;81:233-239.

374. NewmanKM, Jean-ClaudeJ, LiH, ScholesJV, OgataY, NagaseH. Cellular localization of matrix metalloproteinases in the abdominal aneurysm wall. J Vasc Surg 1994;20:814-820.

375. NewmanKM, MalonAM, ShinRD, ScholesJV, RameyWG, TilsonMD. Matrix metalloproteinases in abdominal aortic aneurysm: characterization, purification and their possible sources. Connect Tissue Res 1994;30:265-276.

376. NataliaAT, WilliamDM, VeraPS, WilliamHP. Expression of matrix metalloproteinases and their inhibitors in aneurysms and normal aorta. Surgery 1997;122:264-272.

377. SakalihasanN, DelvenneP, NusgensBV, LimetR, LapiereCM. Activated forms of MMP2 and MMP-9 in abdominal aortic aneurysms. J Vasc Surg 1996;24:127-33.

378. YamashitaA, NomaT, NakazawaA, SaitoS, FujiokaK, ZempoN, et al. Enhanced expression of matrix metalloproteinase-9 in abdominal aortic aneurysms. World J Surg 2001;25:259-265.

379. GoodallS, CrowtherM, HemingwayDM, BellPR, ThompsonMM. Ubiquitous elevation of matrix metalloproteinase-2 expression in the vasculature of patients with abdominal aneurysma. Circulation 2001;104:304-309.

380. TakinoT, SatoH, ShinagawaA, SeikiM. Identification of the second membrane-type matrix metalloproteinase (MT-MMP-2) gene from a human placenta cDNA library: MT-MMPs form a unique membrane-type subclass in the MMP family. J Biol Chem 1995;270:23013-23020.

381. CrabbeT, O'ConnellJP, SmithBJ, DochertyAJ. Reciprocated matrix metalloproteinase activation: a process performed by interstitial collagenase and progelatinase A. Biochemistry 1994;33:14419-14425.

382. LohiJ, LehtiK, WestermarckJ, KahariVM, Keski-OjaJ. Regulation of membrane-type matrix metalloproteinase-1 expression by growth factors and phorbol 12-myristate 13-acetate. Eur J Biochem 1996;239:239-247.

383. CrowtherM, GoodallS, JonesJL, BellPRF, ThompsonMM. Localization of matrix metalloproteinase 2 within the aneurysmal and normal aortic wall. Bri J Surg 2000;87:1391-1400.

384. NollendorfsA, GreinerTC, NagaseH, BaxterBT. The expression and localization of membrane type-1 matrix metalloproteinase in human abdominal aortic aneurysms. J Vasc Surg 2001;34:316-322.

385. ThompsonRW, HolmesDR, MertensRA, LiaoS, BotneyMD, MechamRP, et al. Production and localization of 92-kilodalton gelatinase in abdominal aortic aneurysms: an elastolytic metalloproteinase expressed by aneurysm-infiltrating macrophages. J Clin Invest 1995;96:318-326.

386. McMillanWD, PattersonBK, KeenRR, PearceWH. In situ localization and quantification of seventy-two kilodalton type IV collagenase in aneurysmal, occlusive and normal aorta. J Vasc Surg 1995;22:295-305.

387. PatelMI, MelroseJ, GhoshP, ApplebergM. Increased synthesis of matrix metalloproteinases by aortic smooth muscle cells is implicated in the etiopathogenesis of abdominal aortic aneurysms. J Vasc Surg 1996;24:82-92.

388. GalisZS, MuszynskiM, SukhovaGK, Simon-MorrisseyE, UnemoriEN, LarkMW, et al. Cytokine-stimulated human vascular smooth muscle cells synthesize a complement of enzymes required for extracellular matrix digestion. Circ Res 1994;75:181-189.

389. NewmanKM, Jean-ClaudeJ, LiH, RameyWG, TilsonMD. Cytokines that activate proteolysis are increased in abdominal aortic aneurysms. Circulation 1994;90 (Part II):II 224-227.

390. MurphyG, CockettMI, WardRV, DochertyAJ. Matrix metalloproteinase degradation of elastin, type IV collagen and proteoglycan: a quantitative comparison of the activities of 95 kDa gelatinases, stromelysin-1 and -2 and punctuated metalloproteinase (PUMP). J Biochem 1991;277:277-279.

391. AnnabiB, ShedidD, GhosnP, KenigsbergRL, DesrosiersRR, BojanowskiMW, et al. Differential regulation of matrix metalloproteinase activities in abdominal aortic aneurysms. J Vasc Surg 2002;35:539-46.

392. CarrellTW, BurnandKG, WellsGM, ClementsJM, SmithA. Stromelysin-1 (MMP-3) and tissue inhibitor of metalloproteinase-3 are overexpressed in the wall of abdominal aortic aneurysms. Circulation 2002;105:477-482.

393. Wojtowicz-PragaSM, DicksonRB, HawkinsMJ. Matrix metalloproteinase inhibitors. Invest New Drugs 1997;15:61-75.

394. TreharneGD, BoyleJR, GoodallS, LoftusIM, BellPRF, TohmpsonMM. Marimastat inhibits elastin degradation and matrix metalloproteinase-2 activity in a model of aneurysm disease. Br J Surg 1999;86:1053-1058.

395. BigatelDA, ElmoreJR, CareyDJ, Cizmeci-SmithG, FranklinDP, YoukeyJR. The matrix metalloproteinase inhibitor BB-94 limits expansion of experimental abdominal aortic aneurysms. J Vasc Surg 1999;29:130-138.

396. MosorinM, JuvonenJ, BiancariF, SattaJ, SurcelHM, LeinonenM, et al. Use of doxycycline to decrease the growth rate of abdominal aortic aneurysms: a randomized, double-blind, placebo-controlled pilot study. J Vasc Surg 2001;34:606-610.

397. HenneyAM, WakeleyPR, DaviesMJ, FosterK, HembryR, MurphyG, et al. Localization of stromelysin gene expression in atherosclerotic plaques by in situ hybridization. Proc Natl Acad Sci USA 1991;88:8154-8158.

398. WelgusHG, CampbellEJ, CurryJD, EisenAZ, SeniorRM, WilhelmSM, et al. Neutral metalloproteinase produced by human mononuclear phagoctyes: enzyme profile, regulation and cellular defferentiation. J Clin Invest 1990;86:1496-1502.

399. SukhovaGK, SchonbeckU, RabkinE, ChoenFJ, PooleAR, BillinghurstRC, et al. Evidence for increased collagenolysis by interstitial collagenase-1 and -3 in vulnerable atheromatous plaques. Circulation 1999;99:2503-2509.

400. DaviesMJ, ThomasAC. The cause of acute myocardial infarction, sudden ischemic death and cresendo angina. Br Heart J 1985;53:363-373.

401. DavisMJ, RichardsonPD, WoolfN, KatzDR, MannJ. Risk of thrombosis in human atherosclerotic plaques: role of extracellular lipid, macrophage, and smooth muscle cell content. Br Heart J 1993;69:377-381.

402. VanderWalAC, BeckerAE, VanderLoosCM, DasPK. Site of intimal rupture or erosion of thrombosed coronary atherosclerotic plaques is characterized by an inflammatory process irrespective of the dominant plaque morphology. Circulation 1994;89:36-44.

403. NikkariTS, O'BrienKD, FergusonM, HatsukamiT, WelgusHG, AlpersCE, et al. Interstitial collagenase (MMP-1) expression in human carotid atherosclerosis. Circulation 1995;92:1393-1398.

404. LoftusIM, NaylorAR, GooddallS, CrowtherM, JonesL, BellPRF, et al. Increased matrix metalloproteinase-9 activity in unstable carotid plaques: A potential role in acute plaque disruption. Stroke 2000;31:40-47.

405. KaiH, IkedaH, YasukawaH, KaiM, SekiY, KuwaharaF, et al. Peripheral blod levels of matrix metalloproteinase-2 and -9 are elevated in patients with acute coronary syndromes. J Am Coll Cardiol 1998;32:368-372.

406. HermanMP, SukhovaGK, LibbyP, GerdesN, TangN, HortonDB, et al. Expression of neutrophil collagenase (Matrix metalloproteinase-8) in human atheroma: a novel collagenolytic pathway suggested by transcriptional profiling. Circulation 2001;16:1899-1904.

407. FuX, KassimSY, ParksWC, HeineckeJW. Hypochlorous acid oxygenates the cysteine switch domain of pro-matrilysin (MMP-7). A mechanism of matrix metalloproteinase activation and atherosclerotic plaque rupture by myeloperoxidase. J Bilo Chem 2001;276:41279-41287.

408. GeorgeSJ, ZaltsmanAB, NewbyAC. Surgical preparative injury and neointima formation increase MMP-9 expression and MMP-2 activation in human saphenous vein. Cardiovasc Res 1997;33:447-459.

409. ZempoN, KoyamaN, KenagyRD, LeaHJ, ClowesAW. Regulation of vascular smooth muscle cell migration and proliferation in vitro and in injured rat arteries by a synthetic matrix metalloproteinase inhibitor. Arterioscler Thromb Vasc Biol 1996;16:28-33.

410. KranzhoferA, BakerAH, GeorgeSJ, NewbyAC. Expression of tissue inhibitor of metalloproteinase-1, -2, and -3 during neointima formation in organ cultures of human saphenous vein. Arterioscler Thromb Vasc Bio 1999;19:255-265.

411. BakerAH, ZaltsmanAB, GeorgeSJ, NewbyAC. Divergent effects of tissue inhibitor of metalloproteinase-1,-2 or -3 over expression on rat vascular smooth muscle cell invasion, proliferation, and death in vitro: TIMP-3 promotes apoptosis. J Clin Invest 1998;101:1478-1487.

412. GeorgeSJ, JohnsonJL, AngeliniGD, NewbyAC, BakerAH. Adenovirus-mediated gene transfer of the human TIMP-1 gene inhibits smooth muscle cell migration and neointimal formation in human saphenous vein. Hum Gene Ther 1998;9:867-877.

413. JamesTW, WagnerR, WhiteLA, ZwolakRM, BrinkerhoffCE. Induction of collagenase and stromelysin gene expression by mechanical injury in vascular smooth muscle-derived cell line. J Cell Physiol 1993;157:426-437.

414. SouthgateKM, BanningAP, GrovesPH, CheadleH, NewbyAC. Upregulation of basement membrane-degrading metalloproteinases by balloon angioplasty in pigs. Br Heart J 1994;71 (suppl 5):65.

415. StraussBH, RobinsonR, BatchelorWB, ChisholmRJ, RaviG, NatarajanMK, et al. In vivo collagen turnover following experimental balloon angioplasty injury and the role of matrix metalloproteinase. Circ Res 1996;79:541-550.

416. BendeckMP, IrvinC, ReifyMA. Inhibition of matrix metalloproteinase activity inhibits smooth muscle cell migration but not neointimal thickening after arterial injury. Circ Res 1996;78:38-43.

417. DeSmetBJGL, KleijinD d, HanemaaijerR, VerheijenJH, RobertusL, van-der-HelmYJM, et al. Metalloproteinase inhibition reduces constrictive arterial remodeling after balloon angioplasty: A study in the atherosclerotic yucatan micropig. Circulation 2000;101:2962-2967.

418. WoessnerJF. Regulation of matrilysin in the rat uterus. Bio Cell Biol 1996;74:777-784.

419. WilsonCL, MatrisianLM. Matrilysin an epithelial matrix metalloproteinase with potentially novel functions. Int J Biochem & Cell Biol 1996;28:123-136.

420. VonBredowDC, NagleRB, BowdenGT, CressAE. Degradation of fibronectin and characterization of the degradation products. Experimental Cell Research 1995;221:83-91.

421. Saarialho-kereUK, CrouchEC, ParksWC. Matrix metalloproteinase matrilysin is constitutively expressed in adult human exocrine epithelium. J Invest Dermatol 1995;105:190-196.

422. WilsonCL, HeppnerKJ, RudolphLA, MatrisianLM. The metalloproteinase matrilysin if preferentially expressed by epithelial cells in a tissue-restricted pattern in mouse. Mol Biol Cell 1995;6:851-869.

423. DonaldFB, VijaykumarB, LeslieCN, WilliamCP, HowardGW. Matrilysin expression by hyuman mononuclear phagocytes and its regulation by cytokines and hormones. J Immunol 1995;154:6484-6491.

424. WolfC, RouyerN, LutzY, AdidaC, LoriotM, BellocqJP, et al. Stromelysin-3 belongs to a subgroup of proteinases expressed in breast carcinoma fibroblastic cells and possibly implicated in tumor progression. Pro Natl Acad Sci USA 1993;90:1843.

425. PajouhMS, NagleRB, BreathnachR, FinchJS, BrawerMK, BowdenGT. Expression of metalloproteinase genes in human prostate cancer. J Cancer Res Clin Oncol 1991;117:144-150.

426. RodgersWH, OsteenKG, MatrisianLM, NavreM, GiudiceLC, GorsteinF. Expression and localization of matrilysin, a matrix metalloproteinase, in human endometrium during the reproductive cycle. Am J Obstri Gynecol 1993;168 (1 Pt 1):253-260.

427. BarilleS, BataillerR, RappMJ, HarousseauJL, AmiotM. Production of metalloproteinase-7 (matrilysin) by human myeloma cells and its potential involvement in metalloproteinase-2 activation. J Immunol 1999;163:5723-5728.

428. SenotaA, ItohF, YamamotoH, AdachiY, HinodaY, ImaiK. Relation of matrilysin messenger RNA expression with invasive activity in human gastric cancer. Clinical & Experimental Metastasis 1998;16:313-321.

429. YamashitaK, AzumanoI, MaiM, OkadaY. Expression and tissue localization of matrix metalloproteinase 7 (Matrilysin) in human gastric carcinoma. Implications for vessel invasion and metastasis. Int J Cancer 1998;79:187-194.

430. HondaM, MoriM, UeoH, SugimachiK, AkiyoshiT. Matirx metalloproteinase-7 expression in gastric carcinoma. Gut 1996;39:444-448.

431. ItohF, YamamotoH, HinodaY, ImaiK. Enhanced secretion and activation of matrilysin during malignant conversion of human colorectal epithelium and its relationship with invasive potential of colon cancer cells. Cancer 1996;77:1717-1721.

432. YamamotoH, ItohF, HinodaY, ImaiK. Suppression of matrilysin inhibits colon cancer cell invasion in vitro. Int J cancer 1995;61:218-222.

433. IchikawaY, IshikawaT, MomiyamaN, YamaguchiS, MasuiH, HasegawaS, et al. Detection of regional lymph node metastases in colon cancer by using RT-PCR for matrix metalloproteinase-7, matrilysin. Clinical & Experimental Metastasis 1998;16:3-8.

434. NagashimaY, HasegawaS, KoshikawaN, TakiA, IchikawaY, KitamuraH, et al. Expression of matrilysin in vascular endothelial cells adjacent to matrilysin-producing tumors. Int J Cancer 1997;72:441-445.

435. MoriM, BarnardGF, MimoriK, UeoH, AkiyoshiT, SugimachiK. Overexpression of matrix metalloproteinase-7 mRNA in human colon carcinomas. Cancer 1995;75:1516-1519.

436. BolonI, DevouassouxM, RobertC, MoroD, BrambillaC, BrambillaE. Expression of urokinase-type plasminogen activator, stromelysin 1, stromelysin 3, and matrilysin genes in lung carcinomas. Am J Pathol 1997;150:1619-1629.

437. KnoxJD, WolfC, McDanielK, ClarkV, LoriotM, BowdenGT, et al. Matrilysin expression in human prostate carcinoma. Molecular Carcinogenesis 1996;15:57-63.

438. LynchCC, McdonnellS. The role of matrilysin (MM-7) in leukaemia cell invasion. Clinical & Experimental Metastasis 2000;18:401-406.

439. Rudolph-OwenLA, CannonP, MatrisianLM. Overexpression of the matrix metalloproteinase matrilysin results in premature mammary gland differentiation and male infertiligy. Molecular Biology of the Cell 1998;9:421-435.

440. Lopez-BoadoYS, WilsonCL, HooperLV, GordonJI, HultgrenSJ, ParksWC. Bacterial exposure induced and activates matrilysin in mucosal epithelial cells. J Cell Bio 2000;148:1305-1315.

441. WilsonCL, OuelletteAJ, SatchellDP, AyabeT, Lopez-BoadoYS, StratmanJL, et al. Regulation of intestinal (alpha)-defensin activation by the metalloproteinase matrilysin in innate host defense. Science 1999;286:113-117.

442. LehrerRI, GanzT. Endogenous vertebrate antibiotics: defensins, protegrins, and other cysteine-rich antimicrobial peptides. Ann NY Acad Sci 1996;797:228-239.

443. DunsmoreSE, Saarialho-KereUK, RobyID, WilsonCL, MatrisianLM, WelgusHG, et al. Matrilysin expression and function in airway epithelium. J Clin Invest 1998;102:1321-1331.

444. SuWY, RichardHJ, JudyR, SusanRA, Frederick-WoessnerJ, WH Y, et al. Induction of pulmonary matrilysin expression by conbustion and ambient air particles. Am J Physiol Lung Cell Mol Physiol 2000;279:L152-L160.

445. StrieterRM. Mechanisms of pulmonary fibrosis: Conference summary. Chest 2001;120:77S-86S.

446. AnthonyDC, FergusonB, Matyzak, MillerKM, EsiriMM, PerryVH. Differential matrix metalloproteinase expression in cases of multiple sclerosis and stroke. Neuropathology & Applied Neurobiology 1997;23:406-415.

447. KleinRD, BorchersAH, SundareshanP, BougeletC, BerkmanMR, NagleRB, et al. Interleukin-1 beta secreted from monocytic cells induces the expression of matrilysin in the prostatic cell line LNCap. J Bio Chem 1997;272:14188-14192.

448. ShapiroSD, KobayashiD, TimothyJ. Cloning and characterization of a unique elastolytic metalloproteinase produced by human alveolar macrophages. J Biol Chem 1993;268:23824-23829.

449. GronskiTJJr, MartinRL, KobayashiKD, WalshBC, HolmanMC, HuberM, et al. Hydrolysis of a broad spectrum of extracellular matrix proteins by human macrophage metalloelastase. J Biol Chem 1997;272:12189-12194.

450. GibbsDF, WarnerRL, WeissSJ, JohnsonKJ, VaraniJ. Characterization of matrix metalloproteinases produced by rat alveolar macrophages. Am J Respir Cell Mol Biol 1999;20:1136-1144.

451. FuJY, LygaA, ShiH, BlueML, DixonB, ChenD. Cloning, expression, purification, and characterization of rat MMP-12. Protein Expr Purif 2001;21:268-74.

452. LangR, KocourekA, BraunM, TschescheH, HuberR, BodeW, et al. Substrated specificity determinants of human macrophage elastase (MMP-12) based on the 1.1 A crystal structure. J Mol Biol 2001;312:731-42.

453. PrescottMF, SawyerWK, Linden-ReedJV, JeuneM, ChouM, CaplanSL, et al. Effect of matrix metalloproteinase inhibition on progression of atherosclerosis and aneurysm in LDL receptor-deficient mice overexpression MMP-3, MMP-12, and MMP-13 and on restenosis in rats after balloon injury. Annals of the New York Academy of Sciences 1999;878:179-190.

454. GalisZS, SukhovaGK, LarkMW, LibbyP. Increased expression of matrix metalloproteinases and matrix degrading activity in vulnerable regions of human atherosclerotic plaques. J Clin Invest 1994;94:2493-2503.

455. MatsumotoS, KobayashiT, KatohM, SaitoS, IkedaY, KoboriM, et al. Expression and localization of matrix metalloproteinase-12 in the aorta of cholesterol-fed rabbits. Am J Pathol 1998;153:109-119.

456. FeinbergMW, JainMK, WernerF, SibingaNES, WieselP, WangH, et al. Transforming growth factor-beta1 inhibits cytokine-mediated induction of human metalloelastase in macrophages. J Biol Chem 2000;275:25766-25773.

457. WuL, FanJ, MatsumotoS, WatanabeT. Induction and regulation of matrix metalloproteinase-12 by cytokines and CD40 signaling in monocyte/macrophages. Biochem Biophys Res Commun 2000;269:808-15.

458. CorneliusLA, NehringLC, HardingE, BolanowskiM, WelgusHG, KobayashiDK, et al. Matrix metalloproteinase generate angiostatin: effects on neovascularization. J Immunol 1998;161:6845-6852.

459. PowellWC, MatrisianLM. Complex roles of matrix metalloproteinase in tumor progression. Curr Top Microbiol Immunol 1996;213:1.

460. DongZ, KumarR, YangX, FidlerIJ. Macrophage-derived metalloelastase is responsible for the generation of angiostatin in Lewis lung carcinoma. Cell 1997;88:801-810.

461. Gorrin-RivasMJ, Arii, FurutainM. Mouse macrophage metalloelastase gene transfer into a murine melanoma suppresses primary tumor growth by halting angiogenesis. Clin Cancer Res 2000;6:1647-1654.

462. HartzellW, ShapiroSD. Macrophage elastase prevents Gemella morbillorum infection and improves outcome following murine bone marrow transplantation. Chest 1999;116:31s-32s.

463. ShapiroSD. Elastolytic metalloproteinases produced by human mononuclear phagocytes: potential roles in destructive lung disease. Am J Respir Crit Care Med 1994;150:S160-S164.

464. HautamakiRD, KobayashiDK, SeniorRM, ShapiroSD. Requirement for macrophage elastase for cigarette smoke-induced emphysema in mice. Science 1997;277:2002-2004.

465. WarnerRL, LewisCS, BeltranL, YounkinEM, VaraniJ, JohnsonKJ. The role of metalloelastase in immune complex-induced acute lung injury. Am J Pathol 2001;158:2139-44.

466. TraskBC, MaloneMJ, LumEH, WelgusHG, CrouchEC, ShapiroSD. Induction of marophage matrix metalloproteinase biosynthesis by surgactant protein D. J Biol Chem 2001;276:37846-37852.

467. SwaisgoodCM, FrenchEL, NogaC, SimonRH, PloplisVA. The development of bleomycin-induced pulmonary fibrosis in mice deficient for components of fibrinolytic system. Am J Pathol 2000;157:177-187.

468. ShipleyJM, WesselschmidtRL, KobayashiDK, LeyTJ, ShapiroSD. Metalloelastase is required for macrophage-mediated proteolysis and matrix invasion in mice. Proc Natl Acad Sci USA 1996;93:3942-3946.

469. Saarialho-KereUK, VaalamoM, PuolakkainenP, AirolaK, ParksWC, Karjalainen-LindsbergML. Enhanced expression of matrilysin, collagenase, and stromelysin-1 in gastrointestinal ulcers. Am J Pathol 1996;148:519-526.

470. VaalamoM, Karjalainen-LindsberyM-L, PuolakkainenP, KereJ, Saarialho-KereU. Distinct expression profiles of stromelysin-2 (MMP-10), Collagenase-3 (MMP-13), Macrophage metalloelastase (MMP-12), and tissue inhibitor of metalloproteinases-3 (TIMP-3) in intestinal ulcerations. Am J Pathol 1998;152:1005-1014.

471. RiesC, PetridesPE. Cytokine regulation of matrix metalloproteinase activity and its regulatory dysfunction in disease. Biol Chem Hoppe Seyler 1995;376:345-355.

472. WoessnerJF. Matrix metalloproteinases and TIMPs. New York: Oxford University Press; 2000.

473. ParsonsSL, WatsonSA, BrownPD, CollinsHM, SteeleRJC. Matrix metalloproteinases. Bri J Surg 1997;84:160-166.

474. AshleyRA. Clinical trials of a matrix metalloproteinase inhibitor in human periodontal disease. SDD Clinical Research Team. Ann NY Acad Sci 1999;878:335-346.

475. CurciJA, MaoD, BohnerDG, AllenBT, RubinBG, ReillyJM, et al. Preoperative treatment with doxycycline reduces aortic wall expression and activation of matrix metalloproteinases in patients with abdominal aortic aneurysm. J Vasc Surg 2000;31:325-42.

476. SorsaT, DingY, SaloT, LauhioA, TeronenO, IngmanT, et al. Effects of tetracyclines on neutrophil, gingival, and salivary collagenases. A functional and western-blot assessment with special reference to their cellular source in periodontal disease. Ann NY Acad Sci 1994;732:112-131.

477. ZhangX, SakamotoT, HataY, KubotaT, HisatomiT, MurataT, et al. Expression of matrix metalloproteinases and their inhibitors in experimental retinal ischemia-reperfusion injury in rats. Exp Eye Res 2002;74:577-584.

478. RomanicAM, HarrisonSM, BaoW, Burns-KurtisCL, PickeringS, GuJ, et al. Myocardial protection from ischemia/reperfusion injury by targeted deletion of matrix metalloproteinase-9. Cardiovasc Res 2002;54:549-558.

479. WilsonK, WalkerJM. Principles and techniques of practical biochemistry. Fourth edition ed. Cambridge: Cambridge University Press; 1994.

480. CokerML, ThomasCV, ClairMJ, HendrickJW, KrombachRS, GalisZS, et al. Myocardial matrix metalloproteinase activity and abundance with congestive heart failure. AJP-Heart and Circulatory Physiology 1998;274: H1516-H1523.

481. HashimotoK, KihiraY, MatuoY, UsuiT. Expression of matrix metalloproteinase-7 and tissue inhibitor of metalloproteinase-1 in human prostate. J Urol 1998;160:1872-1876.

482. ChangYC, YangSF, HsiehYS. Regulation of matrix metalloproteinase-2 production by cytokines and pharmacological agents in human pulp cell cultures. J Endod 2001;27:679-682.

483. AnnerH, KaufmanRPJr, ValeriCR, SheproD, HechtmanHB. Reperfusion of ischemic lower limbs increases pulmonary microvascular permeability. J Trauma 1988;28:607-610.

484. AndersonBO, BrownJM, BensardDD, GrossoMA, BanerjeeA, PattA, et al. Reversible lung neutrophil accumulation can cause lung injury by elastase-mediated mechanisms. Surgery 1990;108:262-268.

485. MatsubaraO, TamuraA, OhdamaS, MarkEJ. Alveolar basement membrane breaks down in diffuse alveolar damage: an immunohitochemical study. Pathol Int 1995;45:473-482.

486. WarnerRL, BeltranL, YounkinEM, LewisCS, VaraniJ, JohnsonKJ. Role of stromelysin and gelatinase B in experimental acute lung injury. Am J Respir Cell Mol Biol 2001;24:1-8.

487. PardoA, BarriosR, MaldonadoV, MelendezJ, PerezJ, RuizV, et al. Gelatinases A and B are up-regulated in rat lungs by subactue hyperoxia. Am J Pathol 1998;153:833-844.

488. PardoA, SelmanM, RidgeK, BarriosR, SznajderJI. Increased expression of gelatinases and collagenases in rat lungs exposed to 100% oxygen. Am J Respir Crit Care Med 1996;154:1067-1075.

489. YuLPJr, SmithGNJr, HastyKA, BrandtKD. Doxycycline inhibits type XI collagenolytic activity in human osteoarthritic cartilage. J Rheumatol 1991;18:1450-1452.

490. NipLH, UittoV-J, GolubLM. Inhibition of epithelial cell matrix metalloproteinases by tetracyclines. J Periodontal Res 1993;28:379-385.

491. LiderO, HershkovizR, KachalskySG. Interactions of migrating T lymphocytes, inflammatory mediators, and the extracellular matrix. Crit Rev Immunol 1995;15:271-283.

492. NerlichA. Morphology of basement membrane and associated matrix proteins in normal and pathological tissues. Veroff Pathol 1995;145:1-139.

493. MiosgeN. The ultrastructural composition of basement membranes in vivo. Histol Histopathol 2001;16:1239-1248.

494. OgawaS, OtaZ, ShikataK, HironakaK, HayashiY, OtaK, et al. High-resolution ultrastructural comparison of renal glomerular and tubular basement membranes. Am J Nephrol 1999;19:686-93.

495. EngvallE. Structure and function of basement membranes. Int J Dev Biol 1995;39:781-787.

496. vanderpijiJW, DahaMR, VandenBornJ, VerhagenNA, LemkesHH, BucalaR, et al. Extracellular matrix in human diabetic nephropathy: reduced expression of heparan sulphate in skin basement membrane. Diabetologia 1998;41:791-798.

497. GelbmannCM, MestermannS, GrossV, KollingerM, ScholmerichJ, FalkW. Strictures in Crohn's disease are characterised by an accumulation of mast cells colocalised with laminin but not with fibronectin or vitronectin. Gut 1999;45:210-217.

498. ZaouiP, BarroC, MaynardC, DescotesJL, Maurizi-BalzanJ, CordonnierDJ. Inter-regulated balance between gelatinase and tissue inhibitor (TIMP-1) in isolated human glomeruli. Ren Fail 1998;20:201-209.

499. OremC, CelikS, OremA, CalapogluM, ErdolC. Increased plasma fibronectin levels in patients with acute myocardial infarction complicated with left ventricular thrombus. Thromb Res 2002;105:37-41.

500. SongKS, KimHK, ShimW, JeeSH. Plasma fibronectin levels in ischemic heart disease. Atherosclerosis 2001;154:449-453.

501. vanVlietAI, vanAlderwegenIE, BaeldeHJ, deHeerE, BruijnJA. Fibronectin accumulation in glomerulosclerotic lesions: self-assembly sites and the heparin II binding domain. Kindney Int 2002;61:481-489.

502. ZukA, BonventreJV, MatlinKS. Expression of fibronectin splice variants in the postischemic rat kidney. Am J Physiol Renal Physiol 2001;280:F1037-1053.

503. SternbergerL. Immunocytochemistry. Third ed ed. New York: John Wiley & Sons; 1986.

504. SaylamC, OzdemirN, ItilIM, SendagF, TerekMC. Distribution of fibronectin, laminin and collagen type IV in the maternofetal boundary zone of the developing mouse placenta. Experimental study. Arch Gynecol Obstet 2002;266:83-85.

505. MaruyamaH. Morphological study of the basement membrane of the developing lung in rats. Nihon Kyobu Shikkan Gakkai Zasshi 1989;27:1173-1183.

506. RescanPY, ClementB, GrimaudJA, GuilloisB, StrainA, GuillouzoA. Participation of hepatocytes in the production of basement membrane components in human and rat liver during the perinatal period. Cell Differ Dev 1989;26:131-144.

507. ChibaN. Immunohistochemical study on the extracellular matrix components in various renal diseases. Nippon Jinzo Gakkai Shi 1991;33:925-938.

508. KowalczynskaHM, Nowak-WyrzykowskaM, DobkowskiJ, KolosR, KaminskiJ, Makowska-CynkaA. Absorption characteristics of human plasma fibronectin in relationship to cell adhesion. J Biomed Mater Res 2002;61:260-269.

509. SudSS, GuptaI, DhaliwalLK, KaurB, GangulyNK. Serial plasma fibronectin levels in pre-eclamptic and normotensive women. Int J Gynacol Obstet 1999;66:123-128.

510. DigirolamoN, UnderwoodA, McCluskeyPJ, WakefieldD. Functional activity of plasma fibronectin in patients with diabetes mellitus. Diabetes 1993;42:1606-1613.

511. RoachDM. Upregulation of matrix metalloproteinases-2 and -9 and type IV collagen degradation in skeletal muscle reperfusion injury [Medical science]. Adelaide: Adelaide University; 2002.

512. YamadaKM. Fibronectin peptides in cell migration and wound repair. J Clin Invest 2000;105:1507-1509.

513. OhE, PierschbacherM, RuoslahtiE. Deposition of plasma fibronectin in tissues. Proc Natl Acad Sci USA 1981;78:3218-3221.

514. HaymanEG, RuoslahtiE. distribution of fetal bovine serum fibronectin and endogenous rat cell fibronectin in extracellular matrix. J Cell Biol 1979;83:255-259.

515. ZhangZ, VuoriK, ReedJC, RuoslahtiE. The a5ß1 integrin supports survival of cells on fibronectin and up-regulates Bcl-2 expression. Proc Natl Acad Sci USA 1995;92:6161-6165.

516. MartinouJC. Overexpression of Bcl-2 in transgenic mice protects neurons from naturally occurring cell death and experimental ishemia. Neuron 1994;13:1017-1030.

517. GalkinaSI, Sud'inaGF, UllrichV. Inhibition of neutrophil spreading during adhesion to fibronectin reveals formation of long tubulovesicular cell extensions (cytonenes). Experimental Cell Research 2001;266:222-8.

518. Norgard-SumnichitKE, VarkiNM, VarkiaA. Calcium-dependent heparin-like ligands for L-selectin in nonlymphoid endothelial cells. Science 1993;261:480-483.

519. PanizoA, PardoFJ, LozanoMD, AlavaE d, SolaI, IdoateMA. Ischemic injury in posttransplant endomyocardial biopsies: immunohistochemical study of fibronectin. Transplantation Proc 1999;31:2550-2551.

520. ClarkRAF. Wound repair: overview and general consideration. In the molecular and cellular biology of wound repair. 2nd edition ed. New York, USA: Plenum press; 1996.

521. LivantDL, BrabecRK, KurachiK, AllenDL, WuYL, HaasethR, et al. The PHSRH sequence induces extracellular matrix invasion and accelerates wound healing in obese diabetic mice. J Clin Invest 2000;105:1537-1545.

522. ViklickyO, MatlI, HeemannUW. Chronic rejection of renal allograft . Part 1. Present knowledge of etiopathogenesis. Cas Lek Cesk 1999;138:711-5.

523. HirabayashiT, DemertzisS, SchafersJ, HoshinoK, NashanB. Chrionic rejection in lung allografts: immunohistological analysis of fibrogenesis. Transpl Int 1996;9 (Suppl 1):S293-5.

524. OcalanM, GoodmanSL, KuhlU, HauschkaSD, VanDerMarkK. Laminin alters cell shape and stimulates mobility and proliferation of murine skeletal myoblasts. Dev Biol 1988;125:158-67.

525. TaipaleJ, Keski-OjaJ. Growth factors in the extracellular matrix. FASEB 1997;11:51-9.

526. YanakaK, CamarataPJ, SpellmanSR, SkubitzAP, FurchtLT, LowWC. Laminin peptide ameliorate brain injury by inhibiting leukocyte accumulation in a rat model of transient focal cerebral ischemia. J Cereb Blood Flow Metab 1997;17:605-11.

527. HarrisonPV. A comparison of doxycycline and minocycline in the treatment of acne vulgaris. Clin Exp Dermatol 1988;13:242-4.

528. BoyleJR, McDermottE, CrowtherM, WillsAD, BellPRF, ThompsonMW. Doxycycline inhibits elastin degradation and reduces metalloproteinase activity in a model of aneurysmal disease. J Vasc Surg 1998;27:354--61.

529. PetrinecD, LiaoS, HolmesDR, ReillyJM, ParksWC, ThompsonRW. Doxycycline inhibition of aneurysmal degeneration in an elastase-induced rat moel of abdominal aortic aneurysm: preservation of aortic elastin associated with suppressed production of 92 kD gelatinase. J Vasc Surg 1996;23:336-46.

530. ShlopovBV, StuartJM, GumanovskayaML, HastyKA. Regulation of cartilage collagenase by doxycycline. J Rheumatol 2001;28:835-842.

531. CrinnionJN, Homer-VanniasinkamS, ParkinSM, GoughMJ. Role of neutrophil-endothelial adhesion in skeletal muscle reperfusion injury. Br J Surg 1996;83:251-254.

532. GustafssonU, GidlofA, PovlsenB, SirsjoA. Skeletal muscle tissue oxygen pressure distribution during early reperfusion after prolonged ischemia. Eur J Vasc Endovasc Surg 1999;17:41-46.

533. McCutchanHJ, SchwappachJR, EnquistEG, WaldenDL, TeradaLS, ReissOK, et al. Xanthine oxidase-derived H2O2 contributes to reperfusion injury of ischemic skeletal muscle. Am J Physiol 1990;258:H 1415-1419.

534. SabidoF, MilazzoVJ, HobsonRW, DuranWN. Skeletal muscle ischemia reperfusion injury: a review of endothelial cell-leukocyte interactions. J invest Surg 1994;7:39-47.

535. PetrasekPF, WalkerPM. A clinically relevant small-animal model of skeletal muscle ischemia-reperfusion injury. J Invest Surg 1994;7:27-38.